POLITECHNIKA KRAKOWSKA
im. Tadeusza Kościuszki

WYDZIAŁ INŻYNIERII I TECHNOLOGII CHEMICZNEJ

PRACA DOKTORSKA

mgr inż. Agnieszka Kącka-Zych

Teoretyczne studia nad mechanizmem eliminacji kwasów karboksylowych z estrów nitroalkoholi

Promotor:
dr hab. inż. Radomir Jasiński, prof. nadzw. PK

– Kraków 2017 –

„Cokolwiek robisz lub marzysz, że możesz to zrobić - zacznij tylko.

W zdecydowaniu drzemie geniusz, siła i magia.

Zacznij teraz.”

J. W. Goethe

Składam serdeczne podziękowania:

Najserdeczniejsze podziękowania pragnę złożyć

dr hab. inż. Radomirowi Jasińskiemu, prof. PK

za poświęcony czas, cenne uwagi i nieocenioną pomoc w opracowaniu niniejszej pracy.

Szczególne podziękowania składam również ***Mężowi***, ***Rodzicom*** *i* ***Przyjaciołom***

za motywację, cierpliwość oraz wsparcie w trudnych momentach.

Pragnę również podziękować pracownikom ***Akademickiemu Centrum Komputerowemu „CYFRONET”*** *za udostępnienie mocy obliczeniowej oraz pomoc techniczną w obliczeniach na klastrach Zeus i Prometheus.*

SPIS TREŚCI

I. WSTĘP

Chemia związków nitrowych nieustająco wzbudza zainteresowanie chemików organików ze względu na szerokie spektrum zastosowań tych połączeń jako prekursorów w syntezie organicznej [1-9]. Współczesne zastosowania nitrozwiązków związane są również z produkcją środków biologicznie aktywnych [9-11], bakteriobójczych [12-14] czy produktów leczniczych [15]. W grupie tej istotne miejsce zajmują sprzężone nitroalkeny.

Najbardziej uniwersalną, a zarazem najpopularniejszą metodą syntezy sprzężonych nitroalkenów jest termiczna dekompozycja odpowiednich estrów nitroalkilowych [16]. Do tej pory sugerowano, iż wszystkie reakcje termicznej dekompozycji estrów kwasów karboksylowych zachodzą według mechanizmu jednoetapowego, idealnie pericyklicznego [17-20], niezależnie od natury związku wyjściowego. Jednakże pogląd ten w moim przekonaniu jest błędny, i nie powinniśmy a priori odnosić go do wszystkich reakcji tej grupy. Należy zaznaczyć, w tym miejscu, że w ostatnich latach zakwestionowano mechanizm pericykliczny w wielu reakcjach z udziałem nitrozwiązków, w których był on uważany za słuszny. Są to między innymi reakcje Dielsa-Aldera 4,6-dinitrobenzofuroksanu z 1,1,1-trimetylosiloksy-1,3-butadienem [21], czy reakcje dekompozycji fluoronitroazoksyzwiązków [22,23]. Dlatego też, natura reakcji dekompozycji estrów kwasów karboksylowych i nitroalkoholi wymaga głębszego poznania.

Niniejsza praca stanowi owoc kwantowo-chemicznych studiów procesów dekompozycji estrów kwasów karboksylowych i nitroalkoholi. W szczególności, w jej ramach postanowiłam zbadać mechanistyczne aspekty reakcji rozkładu estrów nitroalkilowych prowadzonych w warunkach termicznych oraz podobnych procesów katalizowanych kwasami Lewisa oraz kationami cieczy jonowych.

Praca składa się z dwóch części. W pierwszej przeanalizowałam dostępne strategie syntezy sprzężonych nitroalkenów, ukazując na tym tle znaczenie procesu dekompozycji estrów. Z kolei, w drugiej części zebrałam zestawienie wyników badań własnych w postaci monotematycznego cyklu siedmiu recenzowanych publikacji naukowych.

II. CZĘŚĆ LITERATUROWA

1. Sprzężone nitroalkeny – wprowadzenie

Sprzężone nitroalkeny (*conjugated nitroalkenes* – CNA) stanowią wyjątkowo cenny i uniwersalny surowiec w syntezie organicznej [3, 4, 24-27].

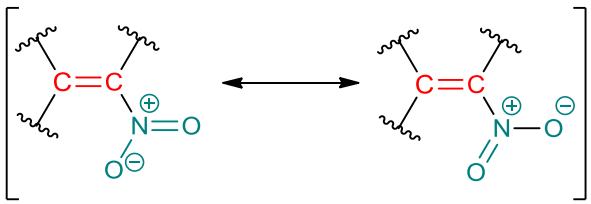

Ze względu na łatwą konwersję grupy nitrowej do różnorodnych grup funkcyjnych, nitroalkeny są prekursorami w preparatyce m.in. nitroparafin, amin, hydroksyloamin, oksymów, związków karbonylowych oraz wielu innych połączeń (Schemat 1) [9, 28-34].

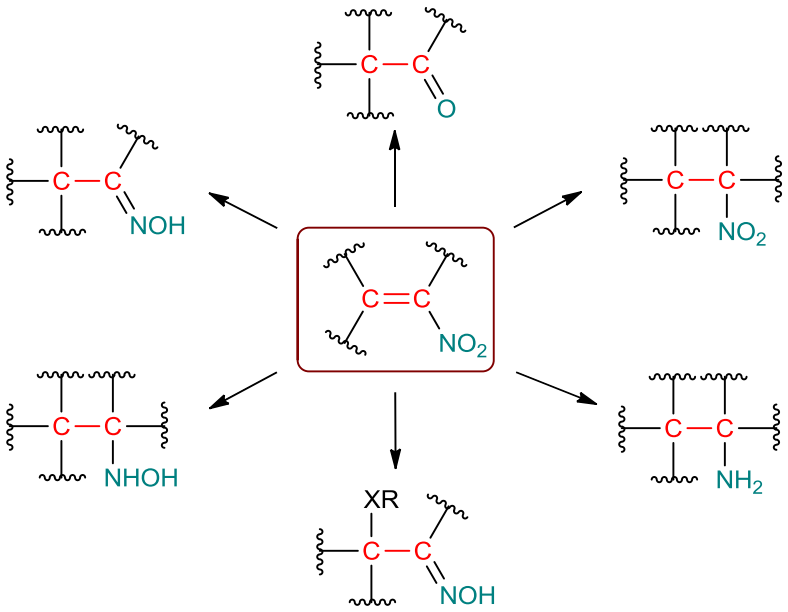

Schemat 1. Przykładowe kierunki transformacji nitroalkenów w syntezie organicznej [9, 28-34].

Nitroalkeny powszechnie stosowane są jako substraty w dużej grupie różnych popularnych chemicznych transformacji, między innymi w reakcjachy Michaela [35, 36] czy Friedla-Craftsa [37, 38]. Ponadto, ze względu na wysoką aktywność w reakcjach z komponentami nukleofilowymi [5, 39-48], nitroalkeny są uniwersalnymi prekursorami

w syntezie (również stereokontrolowanej) 4-, 5-, 6- i 7-członowych związków karbo- i heterocyklicznych [49-57].

Z uwagi na zarysowane wyżej uwarunkowania, nitroalkeny stanowią wyjątkowo cenny surowiec do syntezy produktów naturalnych [58, 59]. Łatwo ulegają ponadto polimeryzacji, dając użyteczne w technice militarnej związki wielkocząsteczkowe polinitrowe [60-62].

Sprzężone nitroalkeny wykazują godną uwagi aktywność biologiczną. Stosowane są jako prekursory wielu środków leczniczych posiadających działanie bakteriobójcze [10, 11, 63]. Są również stosowane jako prekursory substancji bioaktywnych wykazujących aktywność przeciwnowotworową i przeciwgruźliczą [10, 11, 64-66]. Wykazano ponadto szkodliwe działanie tych związków na owady [13, 14, 67] oraz grzyby [68-70].

2. Metody syntezy sprzężonych nitroalkenów

Wśród metod otrzymywania nienasyconych nitrozwiązków możemy wyróżnić dwie grupy:

- ✓ reakcje otrzymywania nitroalkenów polegające na wprowadzeniu grupy nitrowej do układu zawierającego już wiązanie podwójne,

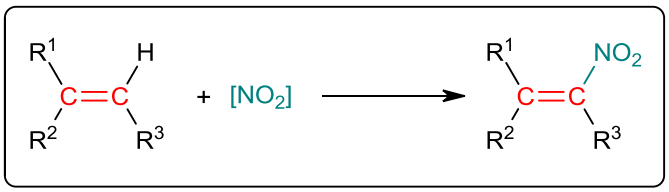

- ✓ oraz reakcje w których następuje tworzenie wiązania podwójnego w nasyconych układach zawierających grupę nitrową.

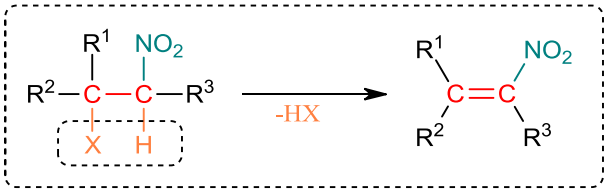

2.1. Metody syntezy nitroalkenów polegające na wprowadzeniu grupy nitrowej do związków nienasyconych

Pierwsze doniesienia dotyczące reakcji nitrowania nienasyconych węglowodorów pochodzą już z XIX wieku. I tak *Bouis* w 1855 roku [71], w reakcji okt-1-enu (**1**) z kwasem azotowym (V) uzyskał produkt, któremu przypisał strukturę 2-nitrookt-1-enu (**2**). Niestety praca nie zawiera żadnych doniesień na temat wydajności reakcji [71]. Nie wiadomo również czy zsyntezowany produkt jest w istocie indywidualnym połączeniem.

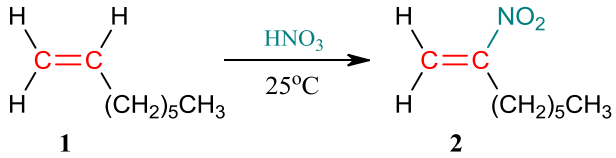

1 **2**

Należy w tym miejscu zaznaczyć, że kilkanaście lat później, *Konovalov* [72], badał syntezę nitroalkenów na drodze reakcji różnych alkenów ze stężonym kwasem azotowym (V). Reakcje te realizują się z niską, nie przekraczającą 30% wydajnością i prowadzą do mieszanin izomerów trudnych do jednoznacznej identyfikacji.

Z kolei zespół *Gupta* w 1987 roku [73], w swoich badaniach nad otrzymywaniem nitroalkenów zastosował dymiący kwas azotowy (V) w obecności azotanu (III) sodu i środowisku lodowatego kwasu octowego. Okazało się, że reakcja konwersji octanu dek-9-enu (**3**) w tych warunkach prowadzi do trzech produktów: dwóch nitroalkenów ((**6**) - 27% i (**7**) - 9%) oraz nitroalkoholu (**5**) (60%). Zidentyfikowany w masie poreakcyjnej nitroalkohol (**5**) powstaje najprawdopodobniej w wyniku spontanicznej hydrolizy tworzącego się pierwotnie estru kwasu azotowego (III) (**4**).

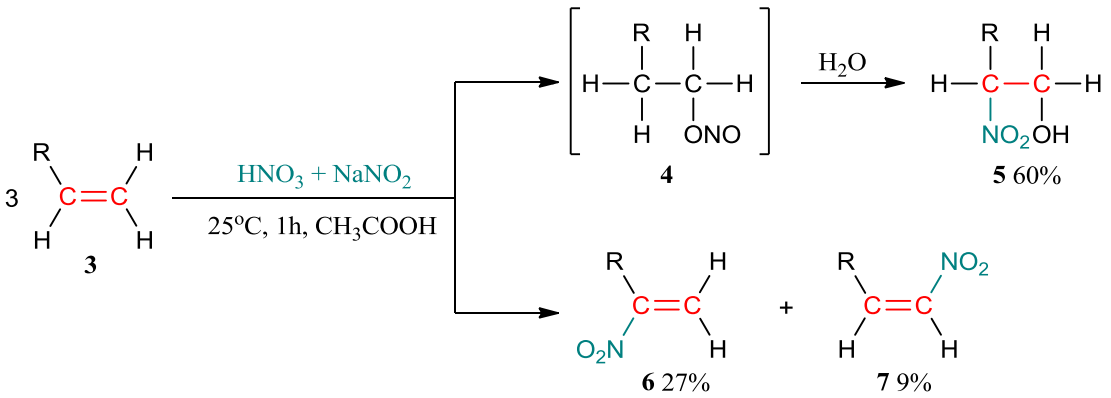

3 **4** **5** 60%

6 27% **7** 9%

3-7: R=$(CH_2)_8COOCH_3$.

W 1988 roku *McMurray* wraz z zespołem [74] opisali syntezę 3-nitroalkrylanu metylu (**9**). Reakcja ta realizuje się z udziałem tetratlenku diazotu, jodu oraz octanu sodu i prowadzi do produktu z wydajnością 78%.

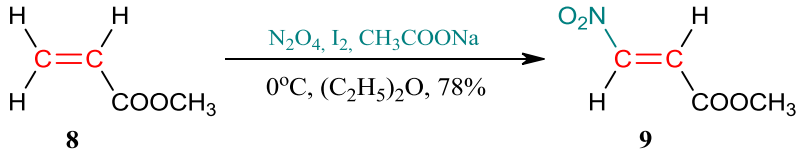

8 **9**

Z kolei *Andrews* i *Kelly* w 1981 roku [75] w roli czynnika nitrującego zastosowali kompleks palladu (II) ($Pd(CH_3CN)_2(NO_2)_2$). W tak realizowanej syntezie uzyskali oni 2-nitrodec-1-en (**11**) z wydajnością zaledwie 13%.

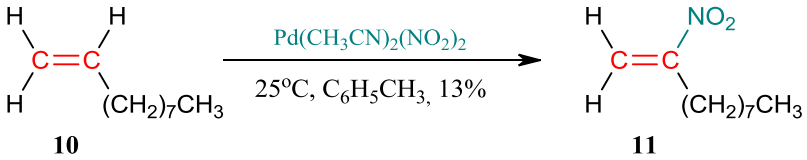

10 **11**

Wyższe wydajności nitroalkenów otrzymali *Corey* i *Estreicher* [24] stosując w roli odczynnika nitrującego chlorek rtęci (II) i azotan (III) sodu w obecności trietyloaminy. Zespół ten zsyntezował 2-nitroheks-1-en (**14a**) oraz 3-nitroheks-3-en (**14b**) z wydajnościami odpowiednio 70% i 65%. Z kolei *Pecunioso* i *Menicagli* [76] w analogiczny sposób uzyskali 5-nitroheks-5-en-2-on (**14c**) z wydajnością 40%.

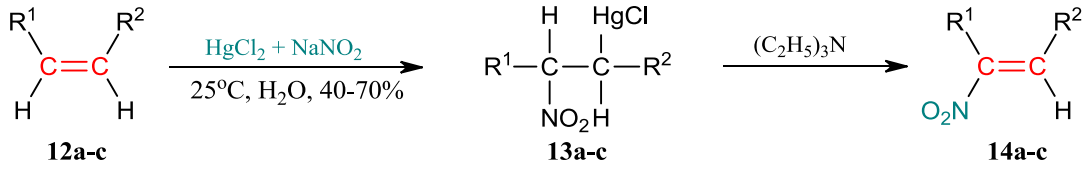

12a-c **13a-c** **14a-c**

12-14: **a)**$R^1=C_4H_9$, $R^2=H$, **b)**$R^1=R^2=C_2H_5$, **c)**$R^1=(CH_2)_2C(O)CH_3$, $R^2=H$.

W 1994 roku *Hwu*, *Chen* i *Ananthan* [77] podobnie jak *Gupta* [73] przedstawili doniesienia na temat reakcji syntezy 2-alkilo i 2-arylonitroetenów (**16a-d**) przy użyciu mieszaniny azotanu amonowo-cerowego (IV) i azotanu (III) sodu jako odczynnika nitrującego. Syntezy te prowadzą do 2-alkilo i 2-arylonitroetenów (**16a-d**) z wysokimi wydajnościami (Tabela 1).

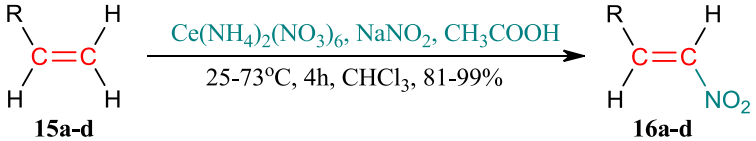

15a-d **16a-d**

15,**16**: **a)**R=C_6H_{13}, **b)**R=C_6H_5, **c)**R=$CH_2Si(C_3H_7)_3$, **d)**R=$CH_2Si(C_4H_9)_3$.

Tabela 1. Synteza 2-alkilo i 2-arylonitroetenów **(16a-d)** przy użyciu mieszaniny azotanu amonowo-cerowego (IV) i azotanu (III) sodu [77].

2-alkilo, 2-aryloeteny	Produkt	Wydajność [%]
15a	**16a**	99
15b	**16b**	82
15c	**16c**	81
15d	**16d**	86

W 2013 roku *Maity* oraz współpracownicy, przeprowadzili szereg reakcji nitrowania olefin (**15a-b**, **17a-h**) wykorzystując azotyn tertbutylu ($(CH_3)_3CONO$) oraz N-tlenek 2,2,6,6-tetrametylopiperydyny (TEMPO) jako katalizator [78]. Reakcje te dają możliwość syntezy 2-alkilo i 2-arylonitroetenów (**16a-b**, **18a-h**) z wydajnościami 74-85%.

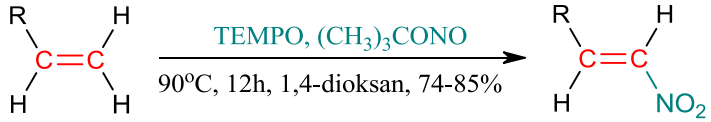

15a-b, 17a-h **16a-b, 18a-h**

15,**16**: **a)**R=C_6H_{13}, **b)**R=C_6H_5.

17,**18**: **a)**R=C_6H_{11}, **b)**R=$C_8H_{16}Br$, **c)**R=4-CH_3-C_6H_4, **d)**R=4-CH_3O-C_6H_4, **e)**R=2-Cl-C_6H_4, **f)**R=2-CH_3O-C_6H_4, **g)**R=3-NO_2-C_6H_4, **h)**R=4-CN-C_6H_4.

Tabela 2. Synteza 2-alkilo i 2-arylonitroetenów **(16a-b**, **18a-h)** w obecności TEMPO i $(CH_3)_3CONO$ [78].

2-alkilo, 2-aryloeteny	Produkt	Wydajność [%]
15a	**16a**	82
15b	**16b**	85
17a	**18a**	82
17b	**18b**	80
17c	**18c**	80
17d	**18d**	79
17e	**18e**	84
17f	**18f**	74
17g	**18g**	82
17h	**18h**	84

2.2.Metody syntezy nitroalkenów polegające na utworzeniu wiązania podwójnego w układach zawierających grupę nitrową

2.2.1. Reakcje otrzymywania nitroalkenów oparte na konwersji 2-nitroetanoli

Spośród wielu metod syntezy sprzężonych nitroalkenów polegających na utworzeniu wiązania podwójnego w układach nasyconych zawierających grupę nitrową, największe zastosowanie znalazły procedury oparte na konwersji nitroalkoholi.

Doniesienia na temat dehydratacji nitroalkoholi przebiegające w fazie gazowej, przedstawił między innymi *Hasche* w 1942 roku [79]. Uzyskał on 1-fenylonitroeten (**20**) na drodze dehydratacji 2-fenylo-2-nitroetanolu (**19**). Reakcja ta przebiega w temperaturze 250-350˚C i obecności tlenku chromu (VI) jako katalizatora. Niestety Autor nie podaje informacji na temat wydajności otrzymanego produktu [79].

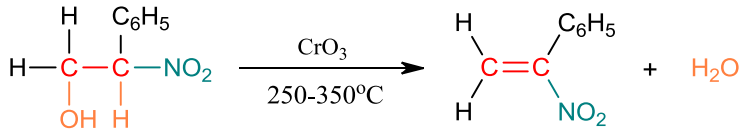

19 **20** **21**

Bachman i *Standisch* w 1961 roku [80], w reakcjach dehydratacji 2-alkilonitroetanoli (**22a-c**), zastosowali inny katalizator – siarczan (VI) magnezu. Reakcja prowadzi do 1-alkilonitroetenów (**23a-c**) z wydajnościami 15-40%. Nieco wyższe wydajności otrzymał w 1966 roku *Abbott* [81] stosując w roli katalizatora tlenek niobu (V). Reakcje przebiegające w obecności tlenku niobu (V) realizują się już w temperaturach 180-190˚C i prowadzą do 1-alkilonitroetenów (**23a-b**), z wydajnościami 51-73%.

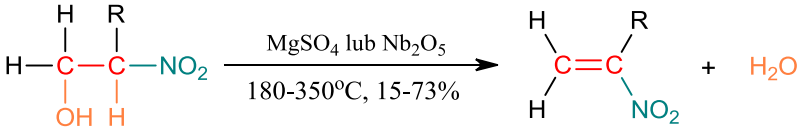

22a-c **23a-c** **21**

22,**23**: **a)**R=CH_3, **b)**R=C_2H_5, **c)**R=C_3H_7.

Tabela 3. Synteza 1-alkilonitroetenów **(23a-c)** przy użyciu katalizatorów $MgSO_4$ [80] i Nb_2O_5 [81].

Nitroalkohol	Katalizator	Temperatura [˚C]	Produkt	Wydajność [%]
22a	$MgSO_4$	290-350	**23a**	15
22b	$MgSO_4$	290-350	**23b**	40
22c	$MgSO_4$	290-350	**23c**	35
22a	Nb_2O_5	180	**23a**	51
22b	Nb_2O_5	180	**23b**	73

Bachman i *Standisch* [80] podobnie jak *Chattaway* i *Witherington* [82] oraz *Chattaway*, *Dewitt* i *Perkes* [83] zajmowali się otrzymywaniem 2-(trichlorometylo)-1-alkilo-1-nitroetenów (**25a-c**) na podobnej drodze. Reakcje te realizują się w obecności siarczanu (VI) magnezu, temperaturze 360°C i prowadzą do produktów (**25a-c**) z wydajnościami nie przekraczającymi 9%.

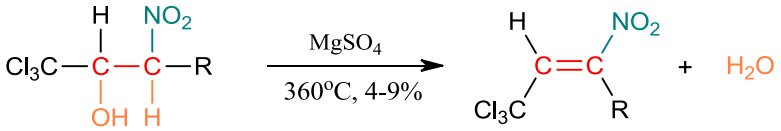

24a-c **25a-c** **21**

24,**25**: **a)**R=H, **b)**R=CH_3, **c)**R=C_2H_5.

Tabela 4. Synteza 2-(trichlorometylo)-1-nitro-1-alkiloetenów (**25a-c**) w obecności $MgSO_4$ [80].

Nitroalkohol	Produkt	Wydajność [%]
24a	**25a**	Śladowe ilości
24b	**25b**	9
24c	**25c**	4

Ballini, *Castagnani* i *Petrini* [84] w 1991 roku do dehydratacji 1-alkilo i 1,2-dialkilonitroetanoli (**26a-g**) zastosowali tlenek glinu (III). Na tej drodze autorzy otrzymali 1-alkilo i 1,2-dialkilonitroeteny (**16a**, **27a-f**) z wydajnościami sięgającymi 77%.

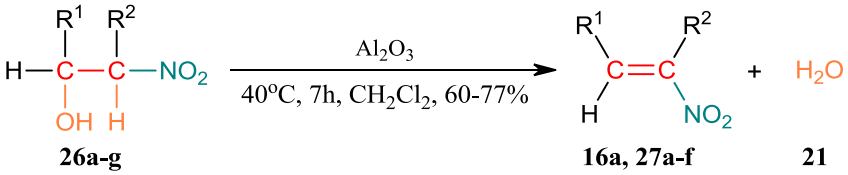

26a-g **16a, 27a-f** **21**

16: **a)**$R^1=C_6H_{13}$, $R^2=H$.

26: **a)**$R^1=C_6H_{13}$, $R^2=H$, **b)**$R^1=R^2=CH_3$, **c)**$R^1=CH_3$, $R^2=C_2H_5$, **d)**$R^1=CH_3$, $R^2=(CH_2)_4COOCH_3$, **e)**$R^1=C_2H_5$, $R^2=H$, **f)**$R^1=C_2H_5$, $R^2=CH_2OH$, **g)**$R^1=C_2H_5$, $R^2=CH_3$.

27: **a)**$R^1=R^2=CH_3$, **b)**$R^1=CH_3$, $R^2=C_2H_5$, **c)**$R^1=CH_3$, $R^2=(CH_2)_4COOCH_3$, **d)**$R^1=C_2H_5$, $R^2=H$, **e)**$R^1=C_2H_5$, $R^2=CH_2OH$, **f)**$R^1=C_2H_5$, $R^2=CH_3$.

Tabela 5. Synteza 1-alkilo i 1,2-dialkilonitroetenów (**16a**, **27a-f**) w obecności Al_2O_3 [84].

Nitroalkohol	Produkt	Wydajność [%]
26a	**16a**	61
26b	**27a**	75
26c	**27b**	77
26d	**27c**	76
26e	**27d**	60
26f	**27e**	64
26g	**27f**	64

Podobne podejście dotyczące dehydratacji 2-bromo-2-nitroetanolu (**28**) zastosowali *Sopova* wraz z współpracownikami [85]. Autorzy stosując silnie hydrofilowy tlenek fosforu (V) w temperaturze 180˚C, otrzymali 1-bromonitroeten (**29**) z wydajnością zaledwie 11%.

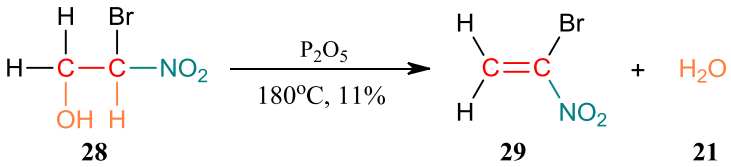

28 **29** **21**

Według podobnej procedury, *Wilkendorf* i *Trenel* w 1924 roku [86] zsyntezowali 1-chloronitroeten (**31**). Jednakże, autorzy nie podają wydajności otrzymanego produktu.

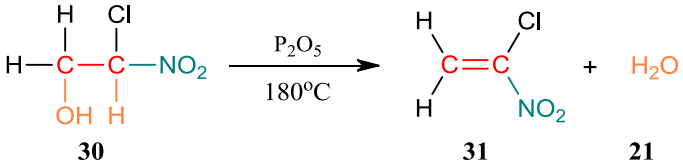

30 **31** **21**

W 2006 roku *Molteni* wraz ze współpracownikami [87], stosując również tlenek fosforu (V), zsyntezowali 3-fluorometylo-1-nitroeteny (**33a-c**) oraz 3-chloro-3,3-

difluorometylo-1-nitroeten (**33d**). Reakcje prowadzone w temperaturze 80-132˚C, prowadzą do produktów (**33a-d**) z wydajnościami 37-48%.

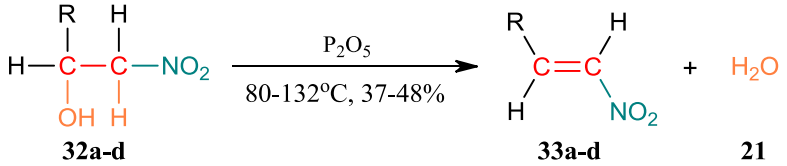

32a-d **33a-d** **21**

32,**33**: **a)**R=CF_3, **b)**R= C_2F_5, **c)**R=CHF_2, **d)**R= $CClF_2$.

Tabela 6. Synteza 3-fluorometylo-1-nitroetenów (**33a-c**) oraz 3-chloro-3,3-difluorometylo-1-nitroetenu (**33d**) [87].

Nitroalkohol	Temperatura [°C]	Produkt	Wydajność [%]
32a	132	**33a**	48
32b	80-90	**33b**	37
32c	80-90	**33c**	40
32d	103-105	**33d**	39

Z literatury wynika natomiast, że powyższa metoda nie ma zastosowania do syntezy nitroetenu [60].

Melton i *McMurry* w 1975 roku [88], przedstawili studia dotyczące reakcji dehydratacji 1-nitropropan-2-olu (**34a**) oraz 1,2-dialkilonitroetanoli (**26a**, **26g**, **34b-c**). Reakcje te prowadzone były w obecności chlorku metanosulfonylu (CH_3SO_2Cl) oraz trietyloaminy ($(C_2H_5)_3N$). Autorzy otrzymali związki (**27a**, **27g**, **35b-c**) z wydajnością sięgającą 80%. Z kolei dehydratacja 1-nitropropan-2-olu (**34a**) prowadzi do produktu z wydajnością jedynie 30%, ponieważ obecna w reakcji trietyloamina sprzyja polimeryzacji 1-nitropropenu (**35a**) [89, 90].

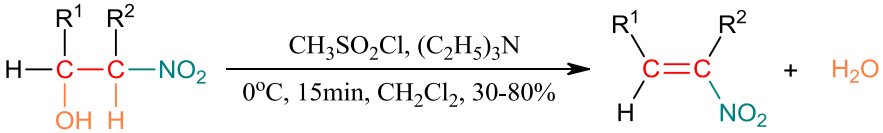

26a, 26g, 34a-c **27a, 27g, 35a-c** **21**

26,**27**: **a)**R^1=R^2=CH_3, **g)**R^1=C_2H_5, R^2=CH_3.

34,**35**: **a)**R^1=CH_3, R^2=H, **b)**R^1=R^2=C_2H_5, **c)**R^1=C_3H_7, R^2=C_2H_5.

Tabela 7. Synteza 1-nitropropenu (**35a**) oraz 1,2-dialkilonitroetenów **(27a, 27g, 35b-c)** w obecności CH_3SO_2Cl i $(C_2H_5)_3N$ [88].

Nitroalkohol	Produkt	Wydajność [%]
26a	**27a**	67
26g	**27g**	80
34a	**35a**	30
34b	**35b**	70
34c	**35c**	78

Zespół *Gingras* [91] w odniesieniu do dehydratacji 1-metylo-2-alkilonitroetanoli (**36a-e**) zastosowali trifenylofosfinę ($(C_6H_5)_3P$) w obecności trietyloaminy $(C_2H_5)_3N$.

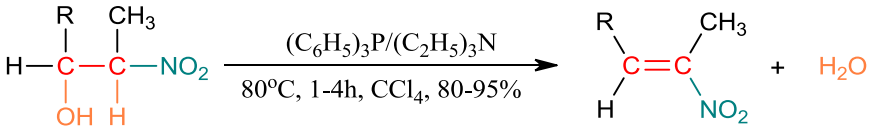

36a-e **37a-e** **21**

36,**37**: **a)**R=4-CH_3O-C_6H_4, **b)**R=4-Cl-C_6H_4, **c)**R=$(CH_3)_2C=CH(CH_2)_2CH(CH_3)CH_2$, **d)**R=$CH_3(CH_2)_{15}CH_2$, **e)**R=$C_3H_7$.

Tabela 8. Synteza 1-metylo-2-alkilonitroetenów **(37a-e)** w obecności $(C_6H_5)_3P/(C_2H_5)_3N$ [91].

Nitroalkohol	Czas [h]	Produkt	Wydajność [%]
36a	1	**37a**	90
36b	2	**37b**	95
36c	2	**37c**	95
36d	4	**37d**	80
36e	3,5	**37e**	90

Przeprowadzone eksperymenty wykazały, że reakcje te charakteryzują się wydajnością na poziomie 80-95%.

Reakcjami dehydratacji nitroalkoholi zajmowali się również *Rokhum* i *Bez* [92]. Autorzy zaproponowali otrzymywanie 1,2-dialkilo i 2-alkilonitroetenów (**37a**, **39a**) wobec trifenylofosfiny, jodu i imidazolu na nośniku polimerowym (PBTPP).

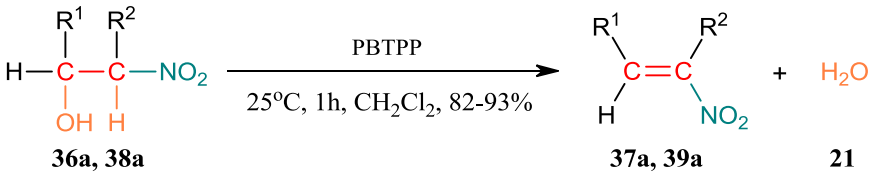

36a, 38a **37a, 39a** **21**

36,**37**: **a)** R^1=4-CH_3O-C_6H_4, R^2=H.

38,**39**: **a)**R^1=3-Br-C_6H_4, R^2= CH_3.

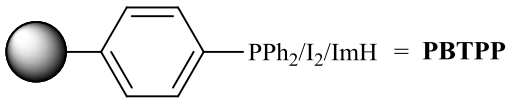

Tabela 9. Synteza 1,2-dialkilo i 2-alkilonitroetenów (**37a, 39a**) wobec trifenylofosfiny, jodu i imidazolu na PBTPP [92].

Nitroalkohol	Produkt	Wydajność [%]
36a	**37a**	93
38a	**39a**	89

Knochel i *Seebach* [93], podobnie jak *Gingras* oraz jego współpracownicy [91], zajmowali się reakcjami dehydratacji 1-alkilo, 2-alkilo, 1,2-dialkilonitroetanoli (**22a**, **26a**, **40a-c**) w obecności N,N'-dicykloheksylokarboimidu (DCC) stosując chlorek miedzi (I) jako katalizator. Autorzy w tych warunkach otrzymali 1-alkilo, 2-alkilo oraz 1,2-dialkilonitroeteny (**23a**, **27a**, **41a-c**) z wydajnościami sięgającymi 90%.

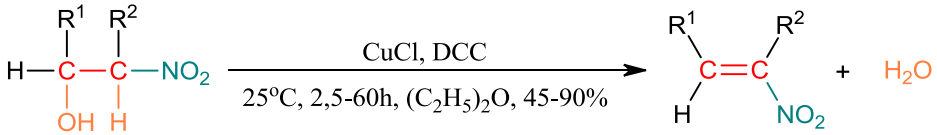

22a, 26a, 40a-c **23a, 27a, 41a-c** **21**

22,**23**: **a)**R^1=H, R^2=CH_3.

26,**27**: **a)**R^1=R^2=CH_3.

40,**41**: **a)**R^1=H, R^2=C_4H_9, **b)**R^1=H, R^2=C_6H_{13}, **c)**R^1=CH_3-CH=CH-, R^2=H.

Tabela 10. Synteza 1-alkilo, 2-alkilo i 1,2-dialkilonitroetenów **(23a, 27a, 41a-c)** w obecności CuCl i DCC [93].

Nitroalkohol	Czas [h]	Produkt	Wydajność [%]
22a	3,5	**23a**	45
26a	17	**27a**	82
40a	10	**41a**	90
40b	2,5	**41b**	60
40c	60	**41c**	70

W 2012 roku *Karaoglu* i *Baykal* [94] przedstawili pierwsze doniesienia na temat syntezy 1-metylo-2-alkilonitroetenów (**27a**, **43a**) prowadzonych w obecności hybrydowego organiczno-nieorganicznego, heterogenicznego katalizatora – kwasu 4-pirydynokarboksylowego naniesionego na nanocząstki Fe_3O_4 (PPCA-Fe_3O_4). Reakcje te prowadzą do produktów (**27a**, **43a**) z wydajnościami 67-92% [94].

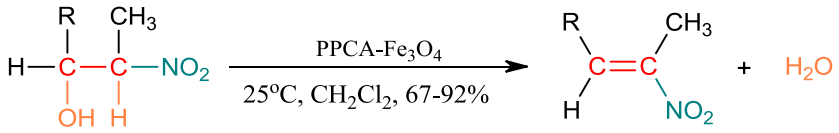

26a, 42a **27a, 43a** **21**

26,**27**: **a)**R=CH_3.

42,**43**: **a)**R=C_6H_{13}.

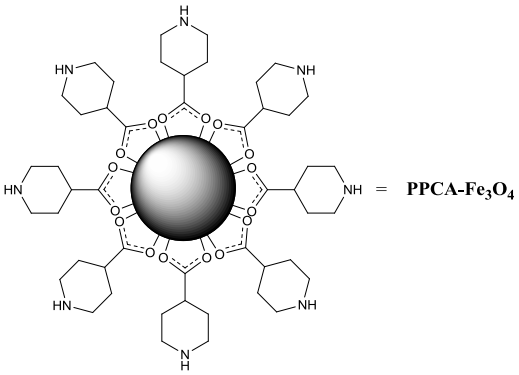

Tabela 11. Synteza 1-metylo-2-alkilonitroetenów (**27a**, **43a**) w obecności katalizatora PPCA-Fe_3O_4 [94].

Nitroalkohol	Produkt	Wydajność [%]
26a	**27a**	92
42a	**43a**	67

Zespół *Anbazhagana* w 1997 roku [95-98], w odniesieniu do konwersji nitroalkoholi z relatywnie dużymi podstawnikami alkilowymi w pozycji 2 (**44a-b**) zastosowali katalizatory zeolitowe oraz heterogeniczne warunki reakcji.

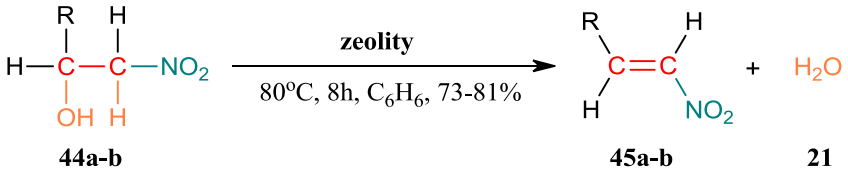

44a-b **45a-b** **21**

44,**45**: **a)**R=$CH(CH_3)_2$, **b)**R=C_6H_{11}.

Ustalili, że reakcje te prowadzą do 2-alkilonitroetenów (**45a-b**) z wydajnościami powyżej 73% (patrz Tabela 12).

Tabela 12. Synteza 2-arylonitroetenów **(45a-b)** w warunkach heterogenicznych i obecności katalizatora H-Y [95].

Nitroalkohol	Produkt	Wydajność [%]
44a	**45a**	73
44b	**45b**	81

Nitroalkohole można (jak wykazałam powyżej) poddać bezpośredniej dehydratacji. Jednak w praktyce znacznie lepiej jest przekształcić je w odpowiednie estry, i dopiero te połączenia przekształcić w odpowiednie nitroalkeny. Reakcje pirolizy estrów realizują się zazwyczaj w łagodniejszych warunkach, i bez konieczności operowania drogimi i/lub toksycznymi odczynnikami jak w przypadku bezpośredniej dehydratacji nitroalkoholi.

W 1945 roku *Blumquist*, *Tapp* i *Johnson* [90] zajmowali się pirolizą benzoesanu 2-nitropylu (**46b**). Reakcja ta przebiega w temperaturze 190-195˚C i prowadzi do 2-nitropropenu (**23a**) z wydajnością 84%. Kilka lat później *Hoff* i *Capaul* [99] otrzymali 2-nitroeten (**47**) w reakcji pirolizy benzoesanu 2-nitroetylu (**46c**). Reakcja realizuje się w temperaturze 260˚C i prowadzi do produktu z wydajnością 56%. Z 85% wydajnością *Leseticky* w 1973 roku [100] z beznoesanu 2-fenylo-2-nitoetylu (**46a**) w temperaturze 180-190˚C otrzymał 1-fenylonitroeten (**20**).

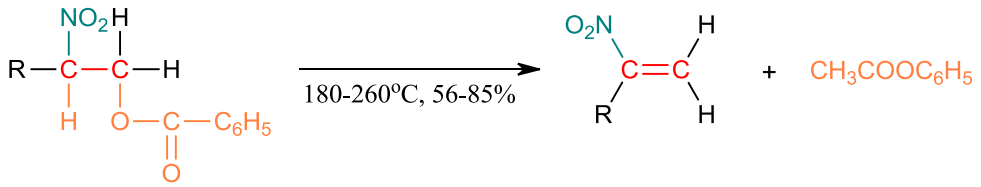

46a-c **20, 23a, 47** **48**

20: R=C_6H_5.

23: **a)**R=CH_3.

46: **a)**R=C_6H_5, **b)**R=CH_3, **c)**R=H.

47: R=H.

Tabela 13. Synteza 1-alkilonitroetenów **(20, 23a, 47)** [90, 99, 100].

Benzoesan 2-nitroalkilu	Temperatura [˚C]	Produkt	Wydajność [%]
46a	180-260	**20**	85
46b	190-195	**23a**	84
46c	260	**47**	56

Pirolizą ftalanów di(nitroalkilowych) zajmowało się wiele zespołów [80, 89, 101-105]. *Buckley* i *Scaife* w 1947 roku [89], otrzymali nitroeten (**47**) wychodząc z ftalanu di(nitroetylu) (**49a**) z wydajnością 66%. Piroliza ftalanu di(nitropropylu) (**49b**) prowadzona w temperaturze 175-190˚C, prowadzi do produktu (**23a**) z wydajnością 56-58% [89, 101]. Podobne reakcje w odniesieniu do ftalanu di(nitrobutylu) (**49c**) [89, 101, 102], prowadzą do 2-nitrobut-1-enu (**23b**) z wydajnościami sięgającymi 95%. Piroliza ftalanu di(nitropentylu) (**49d**) przebiega w takich samych warunkach temperaturowych i prowadzi do 2-nitropent-1-enu (**23c**) z wydajnością 30-50% [80, 89]. Z kolei 2-nitroheks-1-en (**14a**) otrzymywany jest z wydajnością 58% [102].

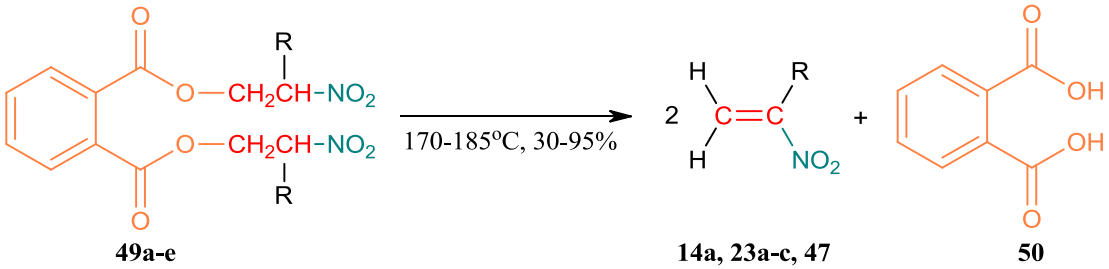

49a-e **14a, 23a-c, 47** **50**

14: **a)**R=C_4H_9.

23: **a)**R=CH_3, **b)**R=C_2H_5, **c)**R=C_3H_7.

47: R=H.

49: **a)**R=H, **b)**R=CH_3, **c)**R=C_2H_5, **d)**R=C_3H_7, **e)**R=C_4H_9.

Tabela 14. Synteza 1-alkilonitroetenów (**14a**, **23a-c**, **47)**.

Ftalan	Temperatura [˚C]	Produkt	Wydajność [%]
49a	170-185	**47**	66 [89]
49b	175-180	**23a**	56 [89]
49b	180-190	**23a**	58 [101]
49c	180-190	**23b**	95 [101]
49c	175-180	**23b**	71 [102]
49c	175-180	**23b**	37 [89]
49d	175-180	**23c**	50 [102]
49d	175-180	**23c**	30 [89]
49e	175-180	**14a**	58 [102]

Buckley i *Scaife* [89] w analogiczny sposób otrzymali również 1-nitroprop-1-en (**52**) z wydajnością 67%.

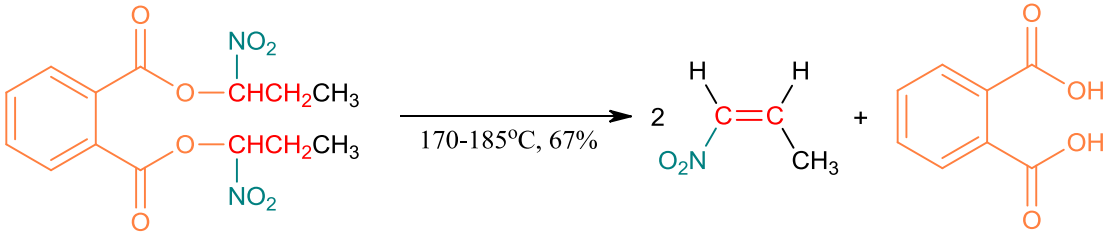

51 **52** **50**

Z kolei *Bachman* i *Standish* [80] wykorzystując pirolizę ftalanów di(trichloronitroalkanów) (**53a-d**) realizującą się w temperaturze 180-190°C, otrzymali 2-(trichlorometylo)-1-alkilonitroeteny (**25a-c**, **54**) z wydajnościami 5-17%.

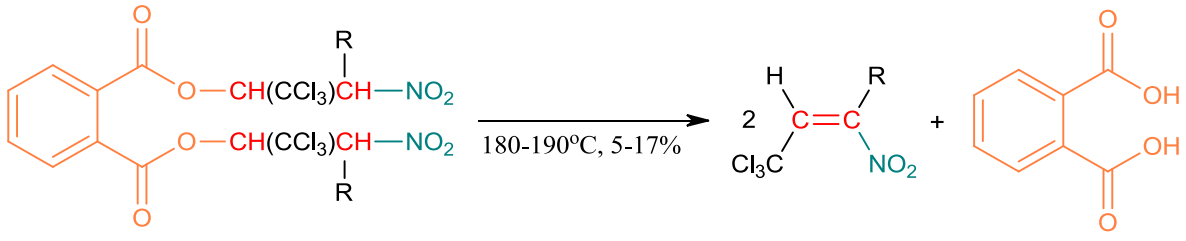

53a-d **25a-c, 54** **50**

25: **a)**R=H, **b)**R=CH_3, **c)**R=C_2H_5.

53: **a)**R=H, **b)**R=CH_3, **c)**R=C_2H_5, **d)**R=C_3H_7.

54: R=C_3H_7.

Tabela 15. Synteza 2-(trichlorometylo)-1-alkilonitroetenów (**25a-c**, **54)** [80].

Ftalany di(trichloronitroalkanów)	Produkt	Wydajność [%]
53a	**25a**	9
53b	**25b**	17
53c	**25c**	11
53d	**54**	5

Piroliza ftalanów di(nitroalkilowych) przebiega w nieco łagodniejszych warunkach niż benzoesanów nitroalkilowych, jednakże nie pozbawiona jest wad. Stosunkowo wysoka temperatura reakcji oraz postępująca w czasie reakcji powolna dehydratacja kwasu ftalowego powoduje powstanie wody, która z kolei sprzyja polimeryzacji niskocząsteczkowych nitroalkenów [89, 90].

Hoff i *Capaul* [99] w swoich badaniach zajmowali się termiczną dekompozycją octanu nitroetylu (**55**). Reakcja ta przebiega w temperaturze 240˚C prowadzi do nitroetenu (**47**) z wydajnością 61%.

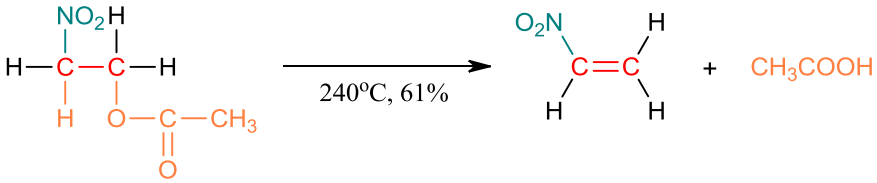

55 **47** **56**

Ci sami autorzy [99] analizowali również reakcje pirolizy propanianu (**57a**) i butylanu nitroetylu (**57b**). Reakcje te realizują się w temperaturze 240-250˚C i prowadzą do nitroetenu (**47**) z wydajnościami odpowiednio 60% i 55%.

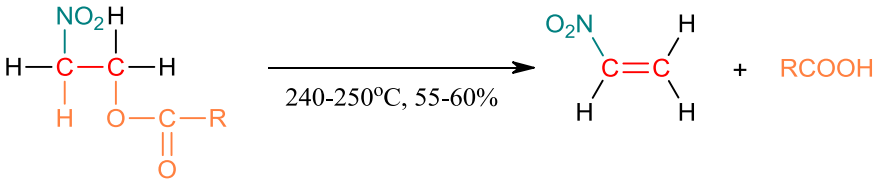

57a-b **47** **58a-b**

57,**58**: **a)**R=C_2H_5, **d)**R=C_3H_7.

Tabela 16. Synteza nitroetenu (**47**) w reakcji pirolizy propanianu (**57a**) i butylanu nitroetylu (**57b**) [99].

Propianian, butylan nitroetylu	Temperatura [°C]	Produkt	Wydajność [%]
57a	240	**47**	60
57b	250	**47**	55

W 1946 roku *Gold* [106], jak również *Hoff* i *Capaul* [99] przedstawił badania dotyczące syntezy 1-nitroprop-1-enu (**52**) oraz 2-alkilonitroetenów (**23a-b, 60**) w wyniku pirolizy octanów nitroalkilowych (**59a-d**), w obecności soli wapnia i magnezu ($Ca_3(PO_4)_2$+$Mg_3(PO_4)_2$) w temperaturze 180-375˚C, uzyskując produkty (**23a-b, 52, 60**) z wydajnościami sięgającymi 90%.

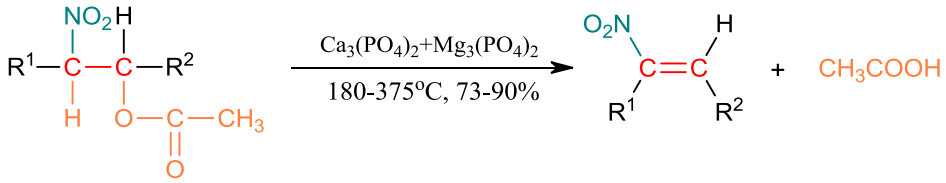

59a-d **23a-b, 52, 60** **56**

23: **a)**R^1=CH_3, R^2=H, **b)**R^1=C_2H_5, R^2=H.

52: R^1=H, R^2=CH_3.

59: **a)**R^1=CH_3, R^2=H, **b)**R^1=C_2H_5, R^2=H, **c)**R^1=H, R^2=CH_3, **d)**R^1=CH_2COOCH_3, R^2=H.

60: R^1=CH_2COOCH_3, R^2=H.

Tabela 17. Synteza 1-alkilo oraz 2-alkilonitroetenów (**23a-b, 52, 60**) [99, 106].

Octan nitralkilowy	Temperatura [˚C]	Produkt	Wydajność [%]
61a	285	**23a**	79
61b	275-375	**23b**	90
61c	285	**52**	85
61d	180	**60**	73

Z kolei *Hass*, *Susie* i *Heider* w 1949 roku [107] jak również w 1963 roku *Carroll*, *White* i *Wall* [108], przedstawili doniesienia na temat termicznej dekompozycji octanów nitroalkilowych (**61a-g**) katalizowanych węglanem sodu w środowisku wrzącego benzenu. Reakcje te prowadzą do 2-alkilo oraz 1,2-dialkilonitroetenów (**16a, 37e, 62a-e**) z wydajnościami 39-68%.

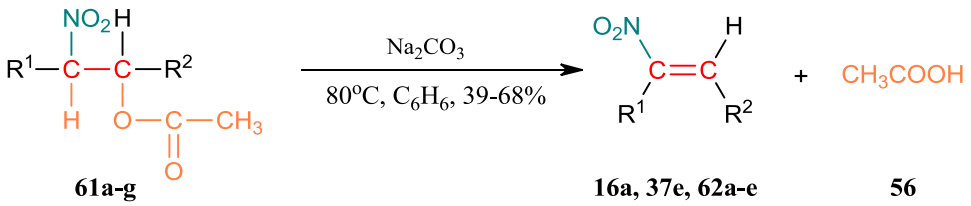

61a-g **16a, 37e, 62a-e** **56**

16: **a)**R^1=H, R^2=C_6H_{13}.

37: **e)**R^1=CH_3, R^2=C_3H_7.

61: **a)**R^1=H, R^2=C_3H_7, **b)**R^1=H, R^2=C_4H_9, **c)**R^1=H, R^2=C_5H_{11}, **d)**R^1=H, R^2=C_6H_{13}, **e)**R^1=H, R^2=C_7H_{15}, **f)**R^1=CH_3, R^2=C_3H_7, **g)**R^1=C_2H_5, R^2=C_3H_7.

62: **a)**R^1=H, R^2=C_3H_7, **b)**R^1=H, R^2=C_4H_9, **c)**R^1=H, R^2=C_5H_{11}, **d)**R^1=H, R^2=C_7H_{15}, **e)**R^1=C_2H_5, R^2=C_3H_7.

Tabela 18. Synteza 2-alkilo oraz 1,2-dialkilonitroetenów (**16a, 37e, 62a-e**) [107, 108].

Octan nitroalkilowy	Produkt	Wydajność [%]
61a	**62a**	68
61b	**62b**	43
61c	**62c**	65
61d	**16a**	49
61e	**62d**	61
61f	**37e**	55
61g	**62e**	39

Feuer [109], *Schwarz* [110], *Kędzierski* [111] i *Lampe* wraz z zespołem [112] do pirolizy octanów nitroalkilowych (**63a-i**) zastosowali octan sodu. Reakcje dekompozycji niskocząsteczkowych octanów zachodzą w temperaturach 48-50˚C, z kolei do octanów zawierających większą liczbę atomów węgla w podstawnikach niezbędna jest temperatura 130-160˚C. Nitroeten (**47**), 1-alkilo, 2-alkilo, 2,2-dialkilonitroeteny (**14a**, **23a-c**, **52**, **64a-c**) w tych reakcjach otrzymywane są z wydajnością 42-68%.

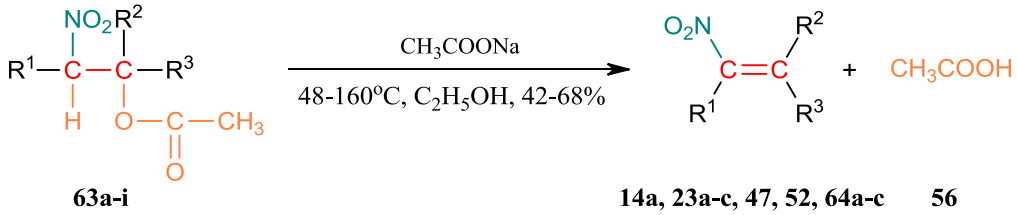

63a-i **14a, 23a-c, 47, 52, 64a-c** **56**

14: **a)** R^1=C_4H_9, R^2=R^3=H.

23: **a)** R^1=CH_3, R^2=R^3=H, **b)**R^1=C_2H_5, R^2=R^3=H **c)**R^1=C_3H_7, R^2=R^3=H.

47: $R^1=R^2=R^3=H$.

52: $R^1=R^2=H$, $R^3=CH_3$.

63: **a)**$R^1=R^2=R^3=H$, **b)** $R^1=R^2=H$, $R^3=CH_3$, **c)** $R^1=CH_3$, $R^2=R^3=H$, **d)** $R^1=R^2=H$, $R^3=C_2H_5$, **e)** $R^1=H$, $R^2=R^3=CH_3$, **f)**$R^1=C_2H_5$, $R^2=R^3=H$, **g)**$R^1=C_3H_7$, $R^2=R^3=H$, **h)**$R^1=CH(CH_3)CH_3$, $R^2=R^3=H$ **i)**$R^1=C(CH_3)_3$, $R^2=R^3=H$.

64: **a)** $R^1=R^2=H$, $R^3=C_2H_5$, **b)** $R^1=H$, $R^2=R^3=CH_3$, **c)**$R^1=CH(CH_3)CH_3$, $R^2=R^3=H$.

Tabela 19. Synteza nitroetenu (**47**), 1-alkilo, 2-alkilo, 2,2-dialkilonitroetenów (**14a**, **23a-c**, **52**, **64a-c**) [109-112].

Octan nitroalkilowy	Temperatura [˚C]	Produkt	Wydajność [%]
63a	115-120	**47**	42
63b	115-120	**52**	60
63c	115-120	**23a**	58
63d	115-120	**64a**	66
63e	115-120	**64b**	62
63f	48-50	**23b**	68
63g	48-50	**23c**	43
63h	130-150	**64c**	65
63i	150-160	**14a**	49

Podobne podejście w odniesieniu do pirolizy octanu 2-fluoro-2-nitroetylu (**65**) zastosowali *Eremenko* i *Oreshko* w 1969 roku [113], stosując jako katalizator octan sodu i temperaturę 130-140°C. Uzyskali 1-fluoro-1-nitroeten (**66**), jednakże praca nie zawiera żadnych doniesień na temat wydajności otrzymanego produktu.

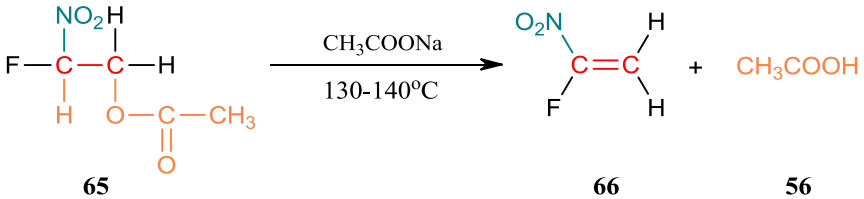

65 **66** **56**

Reakcjami otrzymywania 1,2-dialkilonitroetenów (**68a-e**) z octanów nitroalkilowych (**67a-e**) zajmowali się również *Ferrand*, *Schneider*, *Gerardin* i *Liubinoux* [114]. Reakcje te realizowane w obecności metanolanu potasu, prowadzą do produktów (**68a-e**) z wydajnościami 8-69%.

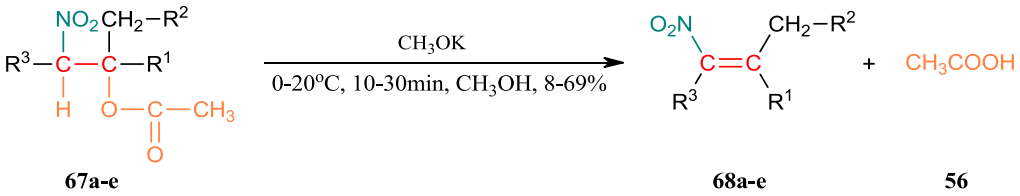

67a-e **68a-e** **56**

67,**68**: **a)**R^1=C_2H_5, R^2=CH_3, R^3=H, **b)**R^1=C_3H_7, R^2=C_2H_5, R^3=H, **c)**R^1=R^2=-$(CH_2)_4$-, R^3=CH_3, **d)**R^1=C_3H_7, R^2=R^3=C_2H_5, **e)**R^1=R^2=-$(CH_2)_4$-, R^3=C_2H_5.

Tabela 20. Synteza 1,2-dialkilonitroetenów **(68a-e)** z octanów nitroalkilowych (**67a-e**) [114].

Octan nitroalkilowy	Produkt	Wydajność [%]
67a	**68a**	69
67b	**68b**	60
67c	**68c**	8
67d	**68d**	53
67e	**68e**	64

Larkin, Cummings i *Kreuz* [115] wykazali, iż w roli prekursorów nitroalkenów wykorzystać można też estry kwasów nieorganicznych. W szczególności autorzy uzyskali 2-alkilo (**70a-d**) i 2,2-dialkilonitroeteny (**70e-f**) w reakcji pirolizy azotanów (V) nitroalkilowych (**69a-f**) z wydajnościami sięgającymi 90%.

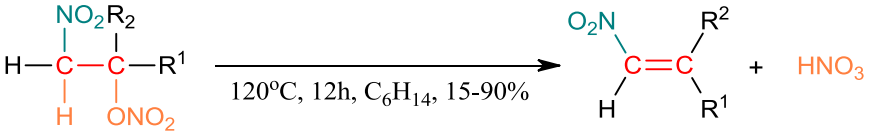

69a-f **70a-f** **71**

69,**70**: **a)**R^1=C_3H_7, R^2=H, **b)**R^1=C_4H_9, R^2=H, **c)**R^1=C_6H_{11}, R^2=H, **d)**R^1=C_8H_{11}, R^2=H, **e)**R^1=C_3H_7, R^2=CH_3, **f)**R^1=$CH_2C(CH_3)_2CH_3$, R^2=CH_3.

Tabela 21. Synteza 2-alkilo i 2,2-dialkilonitroetenów **(70a-f)** z azotanów (V) nitroalkilowych (**69a-f**) [115].

Azotan (V) nitroalkilowy	Produkt	Wydajność [%]
69a	**70a**	90
69b	**70b**	90
69c	**70c**	90
69d	**70d**	90
69e	**70e**	50
69f	**70f**	15

Z kolei *Wilkendorf* i *Trenel* w 1924 [116] otrzymali 1-chloronitroeten (**31**) w reakcji termicznej dekompozycji azotanu (V) 2-chloro-2-nitroetylu (**72**). Niestety autorzy nie podają wydajności uzyskanego produktu.

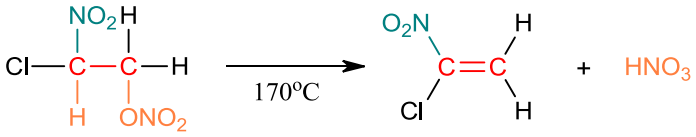

72 **31** **71**

2.2.2. Inne reakcje otrzymywania nitroalkenów z nitrozwiązków nasyconych

Oprócz wody i organicznych oraz mineralnych kwasów, także i inne cząsteczki mogą ulec eliminacji z nasyconych nitrozwiązków. I tak *Gold* [106, 117] 1947 roku przedstawił doniesienia na temat dehydrochlorowania 2-chloro-1-nitroetanu (**73**). Rekcje te realizują się w fazie gazowej, w temperaturze 250-450˚C, w obecności chlorku wapnia lub węglanu wapnia i prowadzą do produktu (**47**) z wydajnościami sięgającymi 30%.

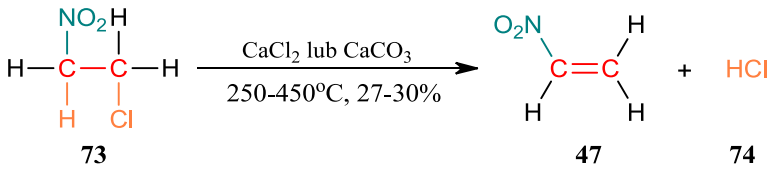

73 **47** **74**

Tabela 22. Synteza 1-nitroetenu **(47)** [117].

Katalizator	Temperatura [˚C]	Produkt	Wydajność [%]
$CaCl_2$	250	**47**	27
$CaCO_3$	275-450	**47**	30

Kilka lat później również *Viehe* [118, 119] zajmował się reakcjami dehydrochlorowania. Poddał on dehydrochlorowaniu eterowe roztwory 1,1-dichloronitroetanu (**75a**) i 1,2-dichloronitroetanu (**75b**) za pomocą bezwodnego octanu sodu w temperaturze 0˚C. Autor otrzymał 1-chloro-2-nitroeten (**76**) z wydajnością 46% oraz 1-chloro-1-nitroeten (**31**) (w tym przypadku Autor nie podaje wydajności otrzymanego produktu).

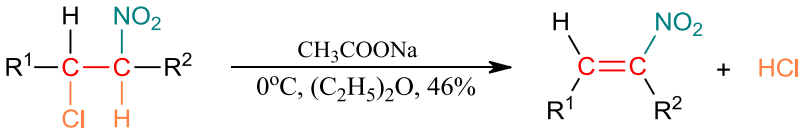

75a-b **31, 76** **74**

31: **b)**R^1=H, R^2=Cl.

75: **a)**R^1=Cl, R^2=H, **b)**R^1=H, R^2=Cl.

76: R^1=H, R^2=Cl.

Podobne podejście w odniesieniu do reakcji termicznego dehydrochlorowania kwasu 2-chloro-1-nitropropanowego (**77a**) oraz octanu 2-chloro-1-nitroetylu (**77b**) przedstawił *Shechter* wraz z zespołem [120]. Autorzy otrzymali produkty (**78a-b**) z wydajnościami 65% i 70% odpowiednio.

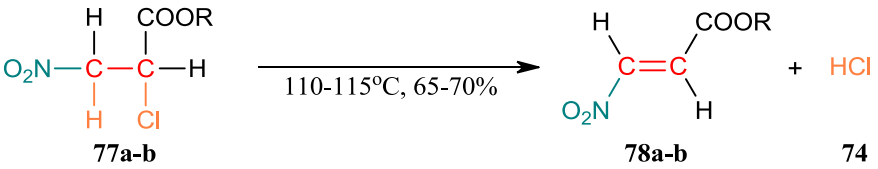

77a-b **78a-b** **74**

77,**78**: **a)**R=H, **b)**R=CH_3.

Tabela 23. Synteza estrów 3-nitroetenu (**78a-b**) [120].

Ester 2-chloro-3-nitroetanu	Temperatura [˚C]	Produkt	Wydajność [%]
77a	110	**78a**	65
77b	110-115	**78b**	70

Ci sami autorzy [120] analizowali również reakcje dehydrochlorowania eterowego roztworu 2-chloro-3-nitropropionitrylu (**79**) w obecności octanu sodu jako katalizatora. Uzyskali 3-nitroakrylonitryl (**80**) z wydajnością 79%.

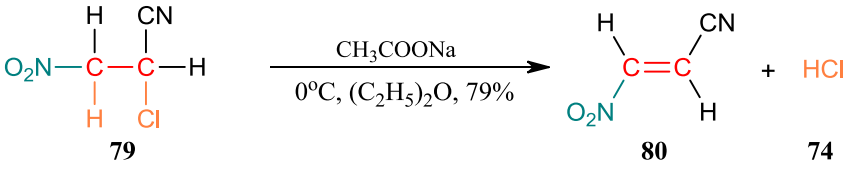

79 **80** **74**

Z kolei *Botata* wraz z zespołem [103, 104] w reakcjach dehydrobromowania otrzymali 1-chloro- (**82a**) oraz 1-bromo-1-nitrobut-1-en (**82b**) z wydajnościami odpowiednio 50% i 78%.

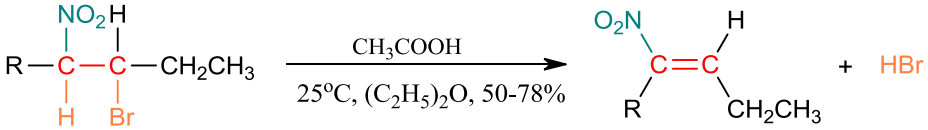

81a-b **82a-b** **83**

81,**82**: **a)**R=Cl, **b)**R=Br.

Syntezę nitroalkenów na drodze dehydrojodowania przedstawili w 1964 roku *Pietrov, Rail* i *Vildovskaya* [121]. Uzyskali oni 2-nitropent-1-en-3-yn (**85a**) oraz 2-nitroheks-1-en-3-yn (**85b**) z wydajnością 20%, stosując $(CH_3COO)_2Sn$ w roli akceptora jodowodoru.

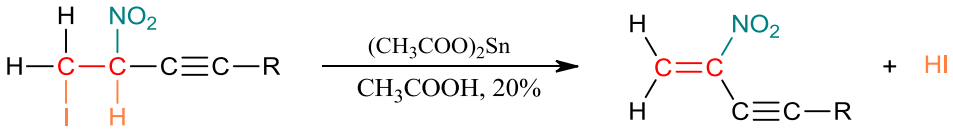

84a-b **85a-b** **86**

84,**85**: **a)**R=CH_3, **b)**R=C_2H_5.

W 1950 roku *Obenland* [122] do otrzymywania 2-nitrobut-1-enu (**23b**) zastosował dekompozycję N-(2-nitrobutylo)-dinitroetyloaminy (**87**). Reakcja realizuje się w temperaturze 118-125°C i prowadzi do produktu z 46-53% wydajnością.

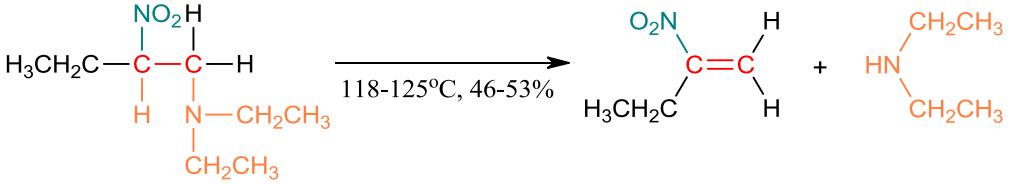

87 **23b** **88**

W 1948 roku *Blomquist* [123] otrzymał 1-alkilonitroeteny (**14a**, **23a-c**, **90**) stosując termiczną dekompozycję chlorowodorków amoniowych (**89a-e**). Reakcje przebiegające w temperaturze 100-175˚C prowadzą do produktów (**14a**, **23a-c**, **90**) z wydajnościami 50-75%.

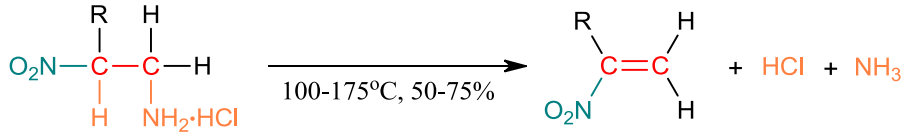

89a-e **14a, 23a-c, 90** **74** **91**

14: **a)**R=C_4H_9.

23: **a)**R=CH_3, **b)**R=C_2H_5, **c)**R=C_3H_7.

89: **a)**R=CH_3, **b)**R=C_2H_5, **c)**R=C_3H_7, **d)**R=C_4H_9, **e)**R=C_5H_{11}.

90: R=C_5H_{11}.

Tabela 24. Synteza 1-alkilonitroetenów **(14a, 23a-c, 90)** w reakcji termicznej dekompozycji chlorowodorków amoniowych (**89a-e**) [123].

Chlorowodorek amoniowy	Temperatura [˚C]	Produkt	Wydajność [%]
89a	105-160	**23a**	50
89b	100-175	**23b**	73
89c	110-115	**23c**	75
89d	105-165	**14a**	70
89e	110-150	**90**	70

Te same nitroalkeny uzyskali *Emmons*, *Cannon*, *Dawson* i *Ross* [124], na drodze termicznej dekompozycji trifluoroboranów amoniowych (**92a-c**). Otrzymali oni 1-alkilonitroeteny (**23a-c**) stosując nieco niższą temperaturę oraz z wydajnościami sięgającymi 90%.

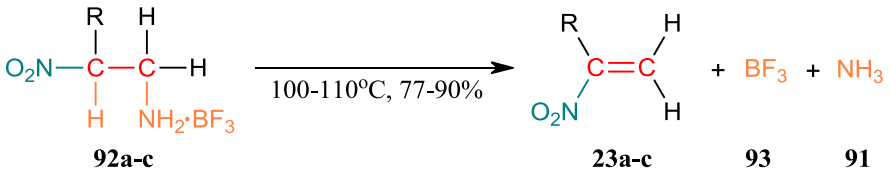

92a-c **23a-c** **93** **91**

23,**92**: **a)**R=CH_3, **b)**R=C_2H_5, **c)**R=C_3H_7.

Tabela 25. Synteza 1-alkilonitroetenów **(23a-c)** na drodze termicznej dekompozycji trifluoroboranów amoniowych (**92a-c**) [124].

Trifluoroborany amoniowe	Temperatura [˚C]	Produkt	Wydajność [%]
92a	105	**23a**	77
92b	100	**23b**	86
92c	110	**23c**	90

Z kolei *Ranaganathan* wraz z zespołem [125] przedstawili otrzymanie nitroetenu (**47**) z fenylosulfotlenku (**94**). Niestety Autorzy nie przedstawiają wydajności otrzymanego produktu.

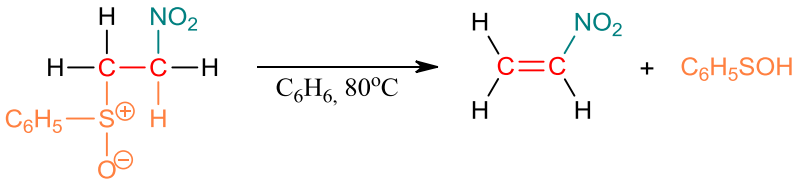

94 **47** **95**

Barton, *Togo* i *Zard* w 1985 roku [126] przeprowadzili pirolizę 1,3-ditiofenylo-2-nitropropanu (**96**) w obecności miedzi uzyskując 1-tiofenylometylonitroeten (**97**) z wydajnością 86%.

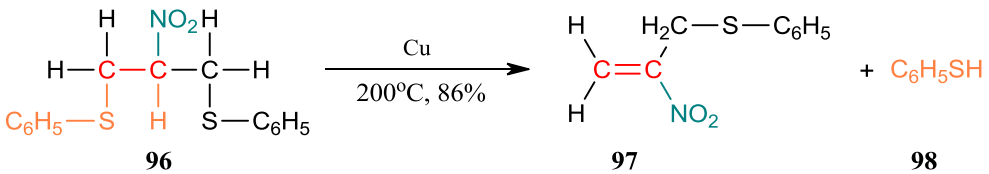

96 **97** **98**

Jang, *Lin* i współpracownicy w 2003 roku [127], zaproponowali otrzymywanie 2,2-dialkilonitroetenów (**64b, 68a, 101a-i**) z 2-nitromarkeptanów (**99a-k**). Związki te utleniane kwasem metachloroperoksybenzoesowym (**m-CPBA**) lub nadtlenkiem wodoru tworzą 2-nitroalkilosulfotlenki (**100a-k**), które ulegają konwersji do 2,2-dialkilonitroetenów (**64b, 68a, 101a-i**) [127].

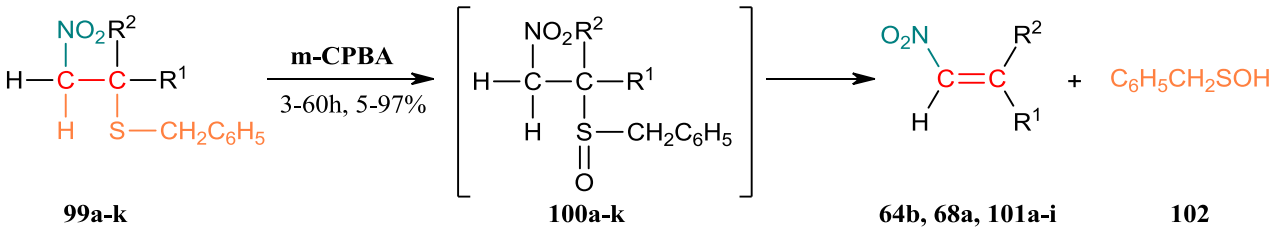

64: **b)**R^1=R^2=CH_3.

68: **a)**R^1=R^2=C_2H_5.

99-100: **a)**R^1=R^2=CH_3, **b)**R^1=CH_3, R^2=C_2H_5, **c)**R^1=R^2=C_2H_5, **d)**R^1=CH_3, R^2=$CH_2CH(CH_3)_2$, **e)**R^1=CH_3, R^2=$(CH_2)_3CH_3$, **f)**R^1+R^2=$(CH_2)_4$, **g)**R^1+R^2=$(CH_2)_5$, **h)**R^1+R^2=$(CH_2)_6$, **i)**R^1+R^2=$(CH_2)_7$, **j)**R^1=CH_3, R^2=$(CH_2)_2C_6H_4$, **k)**R^1=CH_3, R^2=C_6H_5.

101: **a)**R^1=CH_3, R^2=C_2H_5, **b)**R^1=CH_3, R^2=$CH_2CH(CH_3)_2$, **c)**R^1=CH_3, R^2=$(CH_2)_3CH_3$, **d)**R^1+R^2=$(CH_2)_4$, **e)**R^1+R^2=$(CH_2)_5$, **f)**R^1+R^2=$(CH_2)_6$, **g)**R^1+R^2=$(CH_2)_7$, **h)**R^1=CH_3, R^2=$(CH_2)_2C_6H_4$, **i)**R^1=CH_3, R^2=C_6H_5.

Tabela 26. Synteza 2,2-dialkilonitroetenów **(64b**, **68a**, **101a-i)** z 2-nitromarkeptanów (**99a-k**) [127].

2-nitromarkeptany	Rozpuszczalnik	Czas [h]	Produkt	Wydajność [%]
99a	THF	12	**64b**	96
99b	THF	18	**101a**	82
99c	THF	60	**68a**	42
99d	CH_3CN	13	**101b**	59
99e	CH_3CN	14	**101c**	95
99f	DMF	3	**101d**	43
99f	DMF	8	**101d**	~5
99g	THF	12	**101e**	71
99h	THF	15	**101f**	68
99h	CH_3CN	12	**101f**	83
99i	CH_3CN	8	**101g**	51
99j	THF	24	**101h**	97
99k	THF	60	**101i**	5
99k	CH_3CN	12	**101i**	23

W 1984 *Grebennikov* wraz z zespołem [22] ustalili, iż otrzymywanie nitroalkenów jest również możliwe na drodze pirolizy fluoroazoksyzwiązków. W swoich badaniach autorzy przedstawili otrzymywanie 2-nitropropenu (**23a**) na drodze pirolizy fluoroazoksydimetylonitrometanu (**103**), jednak nie podają oni wydajności otrzymanego nitroalkenu. Molekularny mechanizm tej reakcji był również w ostatnich latach obiektem szczegółowych badań [23].

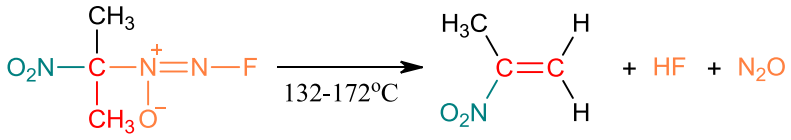

103 **23a** **104** **105**

W 1989 roku *Lee* i *Oh* [128], przedstawili studia dotyczące zastosowania 2-trimetylosiloksy nitroalkanów (**106a-g**) w roli prekursorów nitroalkenów. Okazało się, że związki te w obecności wodorku sodu konwertują się do 1,2-dialkilonitroetenów (**107a-g**) z wydajnościami sięgającymi 82%.

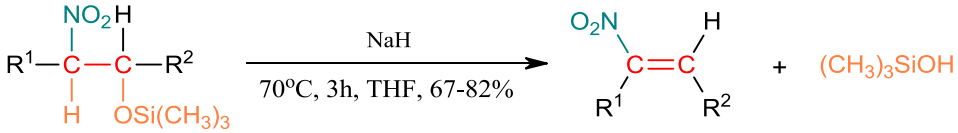

106a-g **107a-g** **108**

106,**107**: **a)**R^1=C_2H_5, R^2=4-CH_3O-C_6H_4, **b)**R^1=C_2H_5, R^2=CH_3, **c)**R^1=C_2H_5, R^2=$(CH_2)_5CH_3$, **d)**R^1=$(CH_2)_4CH_3$, R^2=4-NO_2-C_6H_4, **e)**R^1=$(CH_2)_4CH_3$, R^2=C_4H_4O, **f)**R^1=$(CH_2)_4CH_3$, R^2=4-CH_3O-C_6H_4, **g)**R^1=CH_3, R^2=$(CH_2)_5CH_3$.

Tabela 27. Synteza 1,2-dialkilonitroetenów **(107a-g)** z 2-trimetylosiloksy nitroalkanów (**106a-g**) [128].

2-trimetylosiloksy nitroalkany	Produkt	Wydajność [%]
106a	**107a**	76
106b	**107b**	67
106c	**107c**	82
106d	**107d**	82
106e	**107e**	76
106f	**107f**	70
106g	**107g**	78

Syntezę nitroalkenów z halogeno N,N-di(trimetylosiloksy)enamin (**109a-e**) w obecności octanu tetrabutyloamoniowego ($(C_4H_9)_4NOCOCH_3$) przedstawił w 2005 roku

Kunetsky wraz z zespołem [129]. Autorzy otrzymali nitroeten (**47**), 1-alkilo oraz 2-alkilonitroeteny (**23a**, **52**, **110a-b**) z wydajnościami sięgającymi 82%.

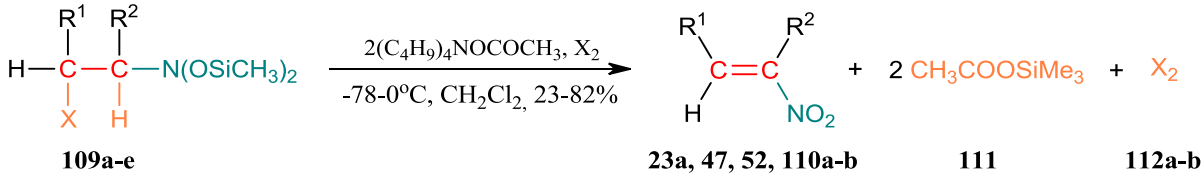

109a-e **23a, 47, 52, 110a-b** **111** **112a-b**

23: **a)**R^1=H, R^2=CH_3.

47: R^1=R^2=H.

52: R^1=CH_3, R^2=H.

109: **a)**R^1=H, R^2=$(CH_2)_2COOCH_3$, **b)**R^1=H, R^2=CH_3, **c)**R^1=R^2=H, **d)**R^1=C_5H_{11}, R^2=H, **e)**R^1=CH_3, R^2=H.

110: **a)**R^1=H, R^2=$(CH_2)_2COOCH_3$, **b)**R^1=C_5H_{11}, R^2=H.

112: **a)**Br_2 **b)**I_2.

Tabela 28. Synteza nitroetenu (**47**), 1-alkilo oraz 2-alkilonitroetenów (**23a**, **52**, **110a-b**) z halogeno N,N-di(trimetylosiloksy)enamin (**109a-e**) [129].

halogeno N,N-di(trimetylosiloksy)enamina	X_2	Produkt	Wydajność [%]
109a	**112a**	**110a**	82
109b	**112a**	**23a**	71
109c	**112a**	**47**	82
109d	**112b**	**110b**	76
109e	**112b**	**52**	23

Na podstawie przeprowadzonego studium literaturowego można stwierdzić, iż metody syntezy nitroalkenów polegające na wprowadzeniu grupy nitrowej do związków nienasyconych realizują się z małą selektywnością oraz konieczne jest zastosowanie drogich i/lub toksycznych odczynników takich jak związków ceru [130-133], rtęci [130, 134-139] czy palladu [130, 138-140]. Z kolei bezpośrednia dehydratacja nitroalkoholi wymaga wysokich temperatur i/lub toksycznych związków jak na przykład tlenek fosforu (V). Jest to metoda mało uniwersalna i dedykowana do wąskich grup konkretnych połączeń. Przeprowadzona analiza literaturowa wskazuje, że najbardziej uniwersalną metodą syntezy nitroalkenów są reakcje termicznej dekompozycji estrów kwasów karboksylowych i nitroalkoholi oraz reakcje katalizowane zasadami. Procesy te mogą realizować się w warunkach bez katalitycznych, lub

jako reakcje katalityczne. Podobne reakcje katalizowane kwasami Lewisa nie były jak dotąd obiektem badań.

III. OMÓWIENIE WYNIKÓW BADAŃ WŁASNYCH

1. Cel i zakres pracy

Celem niniejszej pracy było zbadanie molekularnego mechanizmu reakcji dekompozycji estrów kwasów karboksylowych i nitroalkoholi prowadzonych w warunkach termicznych jak również w obecności kwasów Lewisa oraz kationów cieczy jonowych. Do tej pory sugerowano, iż reakcje dekompozycji estrów (niezależnie od ich budowy) przebiegają według mechanizmu jednoetapowego, idealnie pericyklicznego [141-144]. Jednakże, w mojej opinii, w przypadku reakcji dekompozycji estrów z mechanizmem uzgodnionym (idealnie pericyklicznym (**I**)) konkurować mogą mechanizmy asynchroniczne (E1-like (**II)** i E1-cb like (**III)**) oraz czysto jonowe (**IV** i **V**) (Schemat 2).

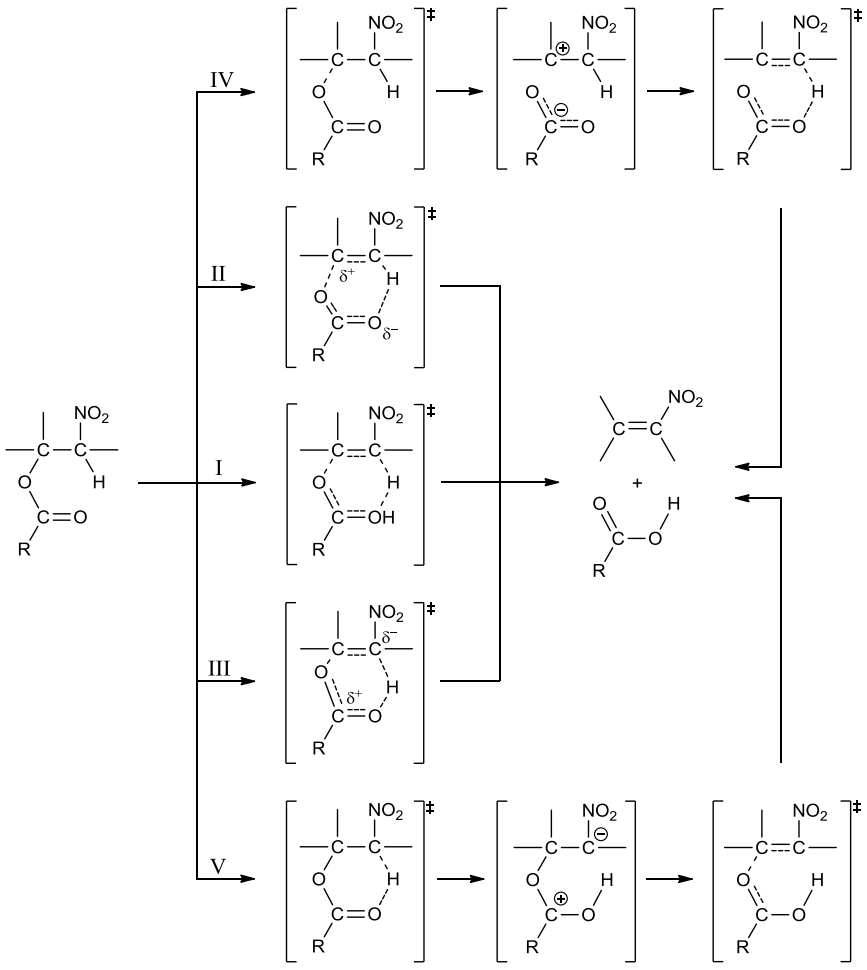

Schemat 2. Teoretycznie możliwe mechanizmy termicznej dekompozycji estrów kwasów karboksylowych i nitroalkoholi.

Pomimo tego, iż reakcje termicznej dekompozycji estrów nitroalkilowych znane są od 1883 roku [145, 146], to ich mechanizm został zaproponowany raczej intuicyjnie, i nie był do tej pory obiektem głębszych badań. Trzeba podkreślić w tym miejscu, że znajomość molekularnego mechanizmu tytułowych reakcji jest istotnym problemem ze względu zarówno teoretycznego jak i praktycznego. Reakcje te pozwalają bowiem na syntezę istotnych w chemii organicznej sprzężonych nitroalkenów (CNA).

Badania teoretyczne w tym obszarze prowadziłam wykorzystując infrastrukturę obliczeniową „Prometheus" i „Zeus" znajdującą się w Akademickim Centrum Komputerowym CYFRONET. Wszystkie obliczenia zostały przeprowadzone w pakiecie GAUSSIAN 09 [147].

W pierwszej kolejności postanowiłam zbadać molekularny mechanizm termicznej dekompozycji benzoesanu nitroetylu, analizując przy tym wpływ podstawników jak również środowiska reakcji na przebieg procesu dekompozycji. W ramach tego studium przeprowadziłam pionierskie w naszym kraju badania z zastosowaniem Teorii Molekularnej Gęstości Elektronowej (*Molecular Electron Density Theory – MEDT*) jak również Teorii Ewolucji Wiązania (*Bonding Evolution Theory – BET*) łączącej w sobie Funkcję Lokalizacji Elektronów (*Electron Localization Function – ELF*) oraz matematyczną Teorię Katastrof (*Catastrophe Theory – CT*). Zagadnienia te zostały szczegółowo przedstawione w pracach **D01**-**D03**. Następnie przeprowadziłam kwantowo-chemiczne obliczenia reakcji dekompozycji estrów kwasów karboksylowych i nitroalkoholi katalizowanych nieorganicznymi kwasami Lewisa. W tej roli zastosowałam borowodór (BH_3) oraz trifluorek boru (BF_3). Zagadnienia te zostały przedstawione w pracy **D04**. Kolejny etap badań obejmował analizę szeregu reakcji dekompozycji estrów kwasów karboksylowych i nitroalkoholi katalizowanych kationami cieczy jonowych. W szczególności były to kationy trietylosulfoniowy (TES), trietylofosfoniowy (TEP), etyloamoniowy (EA) oraz 1,3-dimetyloimidazoliowy (DMIM). Tematyka ta została przedstawiona w pracach **D05**-**D07**. Założyłam że tak sformułowany zakres badań pozwoli na formułowanie wniosków o charakterze ogólnym.

2. Pełne teksty prac stanowiących rozprawę doktorską

D01 Jasiński R., **Kącka A.** IF=1.350
A polar nature of benzoic acids extrusion from nitroalkyl benzoates: DFT mechanistic study.
Journal of Molecular Modeling, **21**, 59-87 (2015).

D02 **Kącka A. (✉)**, Jasiński R. IF=1.221
A density functional theory mechanistic study of thermal decomposition reactions of nitroethyl carboxylates: undermine of pericyclic insight.
Heteroatom Chemistry, **27**, 279-289 (2016).

D03 **Kącka-Zych A. (✉)**, Domingo L.R., Rios- Gutiérrez M., Jasiński R. IF=1.890*
Understanding the mechanism of the decomposition reaction of nitroethyl benzoate through the Molecular Electron Density Theory.
Theoretical Chemistry Accounts, **136**, 129-138 (2017).

D04 **Kącka-Zych A. (✉)**, Domingo L.R., Jasiński R. IF=1.369*
Does a fluorinated Lewis acid catalyst change the molecular mechanism of the decomposition process of nitroethyl carboxylates?
Research on Chemical Intermediates, (2017) – in press – DOI: 10.1007/s11164-017-3106-1.

D05 **Kącka A. (✉)**, Jasiński R. IF=0.809*
Triethylsulfonium and triethylphosphonium cations as novel catalysts for the decomposition process of nitroethyl benzoates.
Phosphorus Sulfur Silicon and the Related Elements, (2017) – in press – DOI: 10.1080/10426507.2017.1290626.

D06 **Kącka A.**, Jasiński R. IF=1.549*
A dramatic change of kinetic conditions and molecular mechanism of decomposition processes of nitroalkyl carboxylates catalyzed by ethylammonium cations.
Computational and Theoretical Chemistry, **1104**, 37-42 (2017).

D07 **Kącka A. (✉)**, Jasiński R. MNiSW=12
DFT study of the decomposition reactions of nitroethyl benzoates catalyzed by the 1,3-dimethylimidazolium cation.
Current Chemistry Letters, **6**, 15-22 (2017).

*Impact Factor podany na rok 2016.

Artykuł D01

R. Jasiński, **A. Kącka**

A polar nature of benzoic acids extrusion from nitroalkyl benzoates: DFT mechanistic study.

Journal of Molecular Modeling, **21**, 59-87 (2015).

J Mol Model (2015) 21: 59
DOI 10.1007/s00894-015-2592-6

ORIGINAL PAPER

A polar nature of benzoic acids extrusion from nitroalkyl benzoates: DFT mechanistic study

Radomir Jasiński · Agnieszka Kącka

Received: 8 December 2014 / Accepted: 26 January 2015 / Published online: 25 February 2015

Abstract Using DFT calculations at various theory levels, quantum-chemical simulations of decomposition paths were performed for a series of nitroalkyl benzoates. It was discovered, that these reactions proceed via polar, but one-step mechanism. It turned out that depending on the nature of the substituent in the ester molecule and on medium polarity, the studied reactions may take place via transition states with varied synchronicity — from E1-like structures, to E1cb-like structures. A purely ionic, two-stage mechanism was not identified in any of the cases.

Keywords DFT study · Mechanism · Nitrocompounds · Thermal elimination

Introduction

Conjugated nitroalkenes are very valuable precursors in organic synthesis. They are used, e.g., in syntheses of many four-, five-, and six-membered carbo- and heterocycles in cycloaddition reactions [1–4]. The presence of a nitro group adjacent to the vinyl moiety activates it strongly in reactions with nucleophilic reagents on one side, and on the other, enables introduction of a nitro group to the final products, characterized by an exceptionally wide spectrum of potential transformation directions [4–8]. In practice, it results in the possibility of further functionalization.

The most universal strategies for their synthesis are based on the decomposition of esters of appropriate β-nitroalcohols [4]. These may be, e.g., benzoic acid esters [9], which are easy to synthesize and isolate (e.g., Scheme 1).

R. Jasiński (✉) · A. Kącka
Institute of Organic Chemistry and Technology, Cracow University of Technology,, Warszawska 24, 31-155 Cracow, Poland
e-mail: radomir@chemia.pk.edu.pl

It is accepted, in general, that esters thermolysis takes place according to a synchronous, "pericyclic" mechanism, via a six-membered transition complex. It should be underlined however, that several atypical mechanisms have been discovered recently about reactions, which earlier without any doubt were considered as synchronous and "pericyclic": zwitterionic, stepwise [2+3] cycloadditions [10–14], extremely asynchronous nitrous acid extrusion [15, 16], thermal decomposition of fluoronitroazoxy compounds [17], as well as multi-step reactions between dienes and ethylenic dienophiles which carry out via [3.3]-sigmatropic shift stage instead of according to typical Diels-Alder mechanism [18–21]. Next, *Domingo* [22] generally undermines "pericyclic" notion for several organic reactions. It is significant that many of these anomalous mechanisms have been implemented in relation to nitrocompounds. In consequence, general examination of mechanistic aspects of nitroalkyl carboxylates decompositions process is necessary. Disturbances in the electron-density redistribution within transition states of benzoic acid extrusion reactions will be certainly stimulated by the electron-withdrawing character of nitrogroup. Therefore, in the case of nitroalkyl benzoates, not one, but five theoretically possible reactions mechanisms should be considered (Scheme 2): (i) ideal "pericyclic" mechanism, (ii) asynchronous E1-like mechanism, (iii) asynchronous E1cb-like mechanism as well as (iv,v) purely ionic mechanisms.

With these concerns in mind, in this work, we have initiated DFT mechanistic studies of model decomposition reactions of selected nitroalkyl benzoates (Scheme 2). In particular, we have performed simulations of reaction paths for processes involving benzoates that contain substituents with various donor-acceptor power in the phenyl ring. We analyzed these reactions both in gaseous phase and in the simulated presence of dielectric media.

Scheme 1 Benzoic acids extrusion from nitroalkyl benzoates

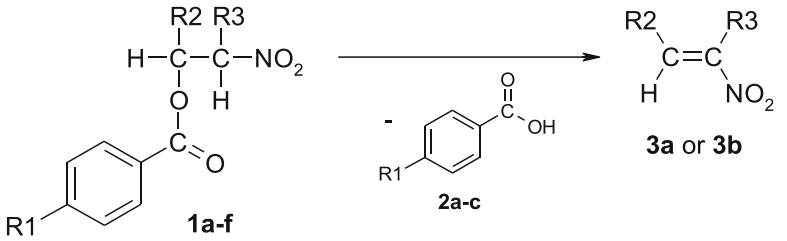

(**a**) R1=H, R2=Me, R3=H, (**b**) R1=H, R2=H, R3=Me, (**c**) R1=NMe_2, R2=Me, R3=H, (**d**) R1=NMe_2, R2=H, R3=Me, (**e**) R1=NO_2, R2=Me, R3=H. (**f**) R1=NO_2, R2=H,R3=Me

Computational methods

All calculations reported in this thesis were performed on an SGI-Altix 3700 computer in the CYFRONET regional computational center in Cracow. Hybrid functional B3LYP with the 6-31G(d) basis set included in the GAUSSIAN 09 package [23] was used. Recently published reports show that the same theoretical level was used, e.g., for the analysis of chemical properties of nitro-functionalized compounds [12, 15, 17, 24, 25] including thermal decomposition process [15, 17]. In addition, similar simulations using more advanced B3LYP/6-31G(d,p), B3LYP/6-31+G(d) as well as B3LYP/6-311G(d) theoretical levels were performed. Optimizations of the stable structures were performed with the Berny algorithm, whereas the transition states were calculated using the QST2 procedure followed by the TS method. Stationary points were characterized by frequency calculations. All reactants, and products had positive Hessian matrices. All transition states showed only one negative eigenvalue in their diagonalized Hessian matrices, and their associated eigenvectors were confirmed to correspond to the motion along the reaction coordinate under consideration. For all reactions, intrinsic reaction coordinate

Scheme 2 Five theoretically possible reactions mechanisms for decomposition of nitroalkyl benzoates

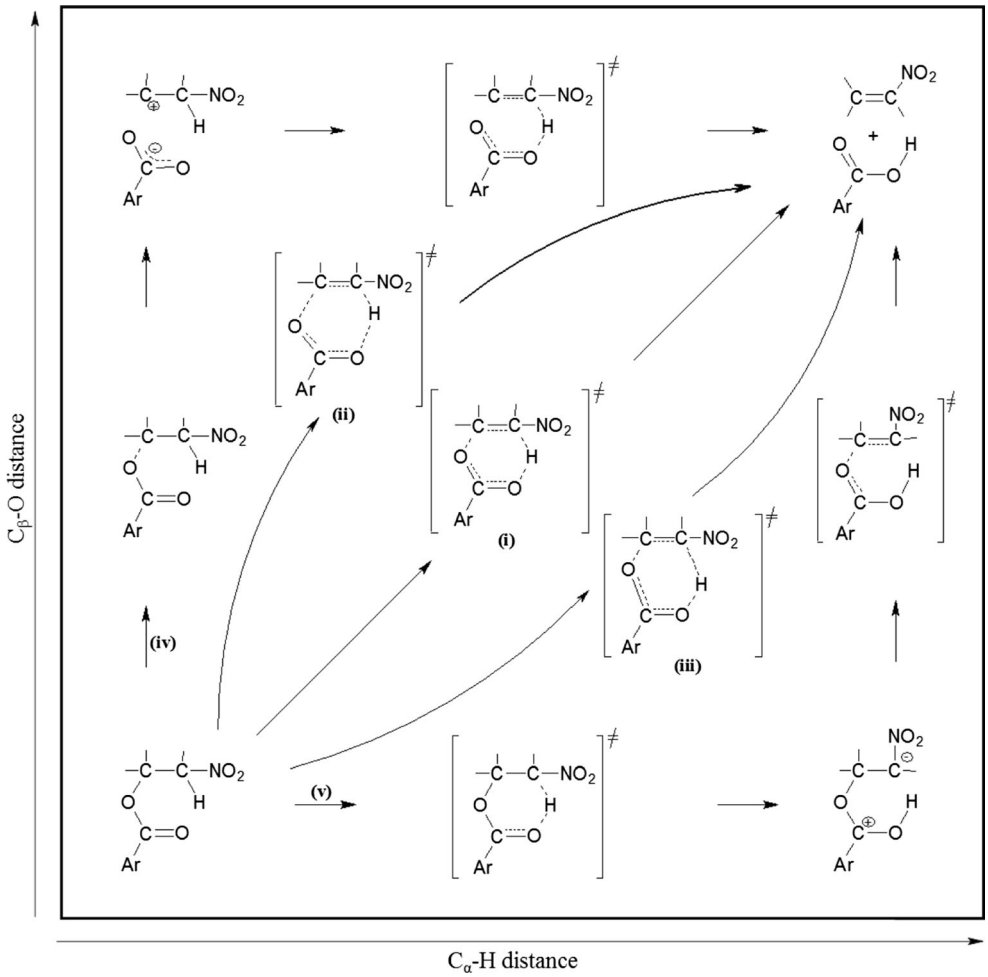

(IRC) calculations were performed to connect previously computed transition structures (TS) with suitable minima. For the calculations of solvent effect on the reaction paths the polarizable continuum model (PCM) [26] in which the cavity is created via a series of overlapping spheres was used. Charge global electron density transfer (GEDT) [22] was calculated according to the formula:

$$GEDT = -\Sigma q_A$$

where q_A is the net charge and the sum is taken over all the atoms of substructure. The same calculation methodology was applied to solutions as to the gas phase. Results are collected in Tables 1, 2, and 3.

Results and discussion

Energy profiles

B3LYP/6-31G(d) calculations showed that conversion of esters 1a and b into respective nitroalkenes in gaseous phase proceeds according to a one-step mechanism. In both cases, between the minima for substrates and respective products (Fig. 1) exists only one transition state (TS). This is confirmed by IRC calculations. All attempts to find the ionic intermediate on reaction paths were not successful.

Table 1 Kinetic and thermodynamic parameters for thermal decomposition of nitroalkyl benzoates 1a–f according to B3LYP/6-31G(d) calculations (T=298 K; ΔH, ΔG in kcal mol^{-1}; ΔS in cal mol^{-1} K^{-1})

Ester	Solvent (ε)	Transition	ΔH	ΔG	ΔS
1a	Gas phase	1a→TS	34.2	35.0	−2.7
	(1.0000)	1a→2a+3a	12.4	0.2	40.9
	Toluene	1a→TS	33.3	34.4	−3.6
	(2.3741)	1a→2a+3a	10.9	−1.0	40.1
	Water	1a→TS	32.3	33.5	−4.2
	(78.3553)	1a→2a+3a	9.5	−2.3	39.6
1b	Gas phase	1b→TS	40.6	41.5	−3.1
	(1.0000)	1b→2a+3b	14.6	2.7	39.9
	Toluene	1b→TS	39.8	40.7	−3.1
	(2.3741)	1b→2a+3b	13.5	1.6	40.0
	Water	1b→TS	38.3	39.0	−2.3
	(78.3553)	1b→2a+3b	12.3	0.4	39.8
1c	Gas phase	1c→TS	33.3	34.5	−4.0
	(1.0000)	1c→2c+3a	12.2	1.6	35.5
1d	Gas phase	1d→TS	39.5	40.9	−4.7
	(1.0000)	1d→2c+3b	14.4	4.1	34.3
1e	Gas phase	1e→TS	34.9	35.4	−1.7
	(1.0000)	1e→2e+3a	12.3	0.0	41.4
1f	Gas phase	1f→TS	41.5	42.5	−3.6
	(1.0000)	1f→2e+3b	14.3	2.8	38.7

Table 2 Kinetic and thermodynamic parameters for thermal decomposition of nitroalkyl benzoates 1a, b according to B3LYP/6-31G(d,p), B3LYP/6-31+G(d) and B3LYP/6-311G(d) calculations (T=298 K; ΔH, ΔG in kcal mol^{-1}; ΔS in cal mol^{-1} K^{-1})

Ester	Theory level	Transition	ΔH	ΔG	ΔS
1a	B3LYP/	1a→TS	31.8	32.5	−2.6
	6-31G(d,p)	1a→2a+3a	9.8	−2.5	41.3
	B3LYP/	1a→TS	33.2	34.1	−3.1
	6-31+G(d)	1a→2a+3a	8.6	−3.5	40.7
	B3LYP/	1a→TS	34.6	35.3	−2.2
	6-311G(d)	1a→2a+3a	10.1	−2.2	41.4
1b	B3LYP/	1b→TS	38.1	39.1	−3.2
	6-31G(d,p)	1b→2a+3b	11.8	0.0	39.8
	B3LYP/	1b→TS	40.3	41.1	−2.7
	6-31+G(d)	1b→2a+3b	11.8	−0.1	40.0
	B3LYP/	1b→TS	41.2	42.0	−2.6
	6-311G(d)	1b→2a+3b	12.7	0.6	40.3

However, reaching this critical point by the reacting system may require a different energy requirement to be met (Table 1). In particular, the decomposition process of nitrobenzoate 1a requires crossing the activation barrier of ΔG=35 kcal mol^{-1}. Fundamentally, it is associated with increasing enthalpy of reaction system. On the other hand, entropy of reaction system only slightly changes. This is typical for elimination reactions which lead via high ordered transition states [27]. In case of an analogous reaction involving nitrobenzoate 1b entropy of activation is also low, but the activation barrier (determined by ΔH value) is greater than 41.5 kcal mol^{-1}. This means that the presence of a substituent in the vicinal position in relation to the nitro group makes extrusion of a molecule of benzoic acid faster. Presumably, this is a result of higher substituents crowd on β carbon atom of nitroalkyl moiety. In consequence, this accelerates dissociation of -O-C(O)-Ph group.

Subsequently, we have performed simulations of theoretically probable paths of nitrous acid extrusion from 1a and b. It was found, that these reactions proceed via one step, Cope-like mechanism similar to described earlier thermal decomposition of the product derived from 3-nitro-2-(trifluoromethyl)-2H-chromene and 2-(1-phenylpropylidene)malononitrile [15]. It should be noted however, that nitrous acid extrusion process should be considered forbidden from kinetic point of view (activation barriers equal 45.7 and 44.9 kcal mol^{-1} for decomposition of 1a and b respectively).

A similar image of these reactions in gaseous phase is supplied by calculation on higher theory levels (B3LYP/6-31G(d,p), B3LYP/6-31+G(d), B3LYP/6-311G(d)). In particular, all performed simulations clearly indicate a one-step reaction

Table 3 Electronic and geometrical characteristics of key structures of thermal decomposition of nitroalkyl benzoates 1a–f according to B3LYP/6-31G(d) calculations

Dielectric constants of reaction environment ε	Reaction	Structure	Interatomic distances [Å]						GEDT [e]	Dipole moment μ [D]
			H1-C2	C2-C3	C3-O4	O4-C5	C5-O6	O6-H1		
1.0000	1a→2a+3a	1a	1.091	1.528	1.450	1.359	1.217	2.398	0.14	3.18
		TS	1.503	1.430	1.810	1.272	1.290	1.128		6.72
		2a+3a		1.333		1.215	1.359	0.975		
1.0000	1b→2a+3b	1b	1.091	1.525	1.434	1.363	1.216	2.547	0.18	2.39
		TS	1.543	1.431	1.750	1.273	1.291	1.107		6.92
		2a+3b		1.332		1.215	1.359	0.975		
1.0000	1c→2c+3a	1c	1.086	1.529	1.445	1.366	1.220	2.381	0.19	4.85
		TS	1.561	1.434	1.764	1.278	1.297	1.094		10.38
		2c+3a		1.333		1.218	1.364	0.975		
1.0000	1d→2c+3b	1d	1.089	1.525	1.430	1.371	1.219	2.690	0.22	4.37
		TS	1.601	1.435	1.714	1.279	1.298	1.076		10.04
		2c+3b		1.332		1.218	1.364	0.975		
1.0000	1e→2e+3a	1e	1.091	1.527	1.454	1.353	1.215	2.493	0.08	5.76
		TS	1.452	1.426	1.865	1.269	1.286	1.164		5.57
		2e+3a		1.333		1.213	1.355	0.975		
1.0000	1f→2e+3b	1f	1.090	1.524	1.438	1.357	1.214	2.730	0.13	5.36
		TS	1.494	1.426	1.793	1.270	1.286	1.137		4.93
		2e+3b		1.332		1.213	1.355	0.975		
2.3741	1a→2a+3a	1a	1.086	1.528	1.451	1.357	1.218	2.409	0.18	3.52
		TS	1.551	1.436	1.771	1.273	1.293	1.100		8.34
		2a+3a		1.334		1.217	1.356	0.975		
2.3741	1b→2a+3b	1b	1.089	1.525	1.436	1.360	1.217	2.729	0.22	2.56
		TS	1.602	1.437	1.714	1.273	1.294	1.077		8.67
		2a+3b		1.332		1.217	1.356	0.975		
78.3553	1a→2a+3a	1a	1.086	1.529	1.454	1.354	1.220	2.427	0.23	3.93
		TS	1.625	1.443	1.726	1.273	1.297	1.066		10.43
		2a+3a		1.336		1.219	1.353	0.976		
78.3553	1b→2a+3b	1b	1.089	1.525	1.438	1.358	1.219	2.740	0.27	2.81
		TS	1.690	1.443	1.679	1.273	1.299	1.044		11.00
		2a+3b		1.333		1.219	1.353	0.976		

mechanism, and activation barriers along individual paths do not differ significantly from those obtained on the basis of B3LYP/6-31G(d) calculations. In every case, ester decomposition 1a takes place much more easily than that of 1b (Table 2).

B3LYP/6-31G(d) calculations also make it possible to shed some light on the influence of the substituent in the leaving group on the course of reaction. It turned out that regardless of the nature of substituent in the benzene ring, esters of both 1-nitropropane-1-ol and 2-nitropropane-1-ol will undergo decomposition according to a one-step mechanism. It must also be noted that electrodonating groups (e.g., NMe_2) will lower the activation barrier of the decomposition process, while electroaccepting groups (e.g., NO_2) will make the process more difficult.

The further course of quantum-chemical studies also included analysis of solvent influence on reaction kinetics. It turned out that a polarity increase of the reaction medium facilitates lowering of the activation barrier. It does not change, however, the mechanism of carboxylic acid cleavage from the parent ester. In all cases (even extremely polar aqueous environment), all attempts to find alternatively, two-step reaction paths were not successful.

Transition structures

Studies on the transition state structure (TS) were started with a reaction involving esters 1a and b. It turned out that both of these TSs have a six-membered structure (Fig. 2). A new bond is formed within both of these structures (H1-O6) and at the

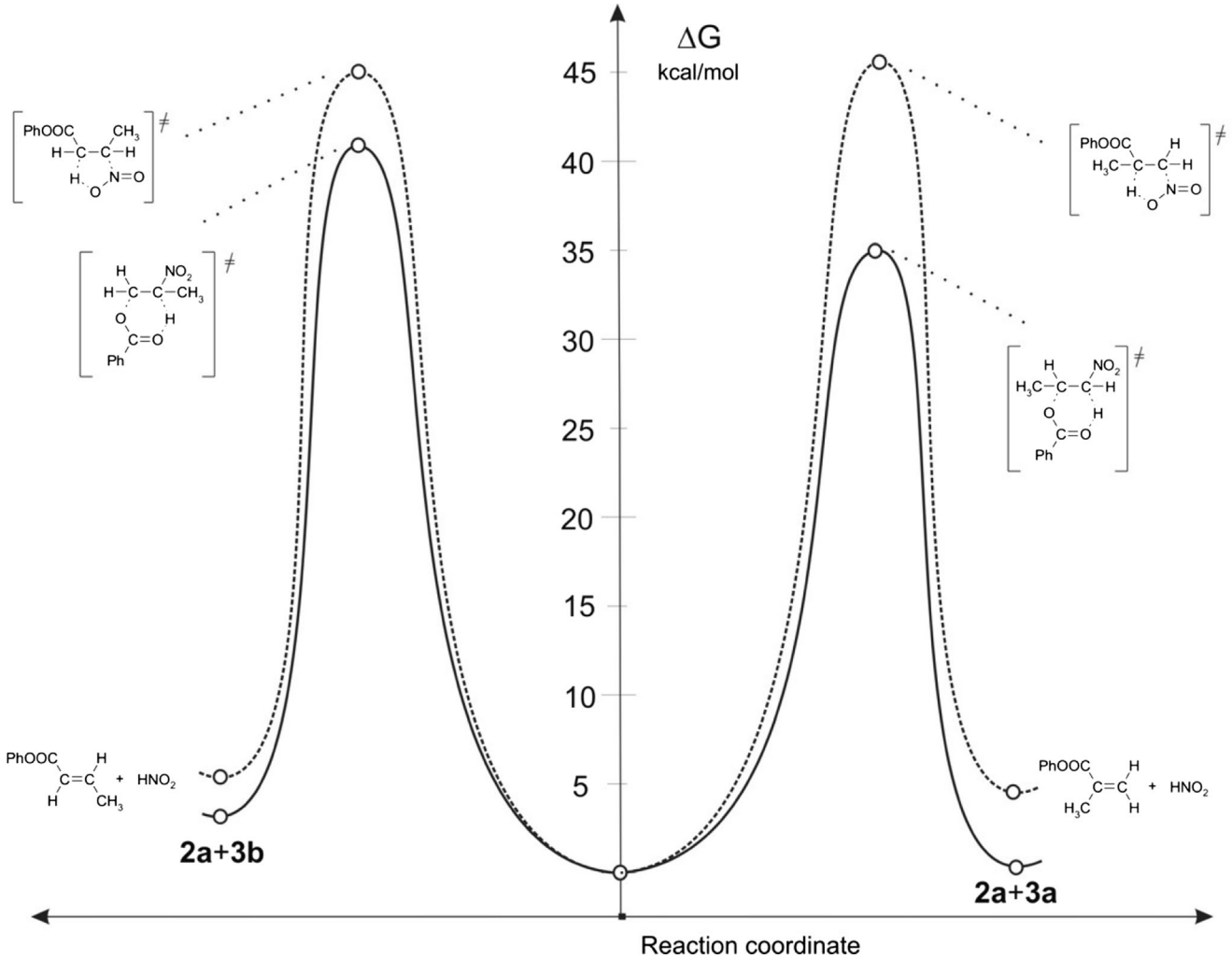

Fig. 1 Gibbs free energy profiles for thermal decomposition of esters 1a and b in gas phase according to B3LYP/6-31G(d) calculations (T=298 K)

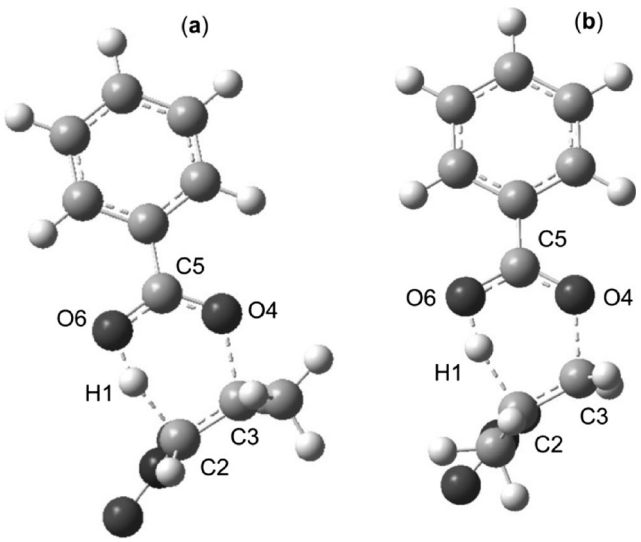

Fig. 2 Transition states for thermal decomposition reactions of esters 1a (**a**) and b (**b**) in gas phase according to B3LYP/6-31G(d) calculations (T=298 K)

same time, the nature of C2-C3 and C5-O4 bonds changes (the bond gains features characteristic for a double bond) and C5-O6 (the bond gains features characteristic for a single bond). Simultaneously, H1-C2 and C3-O4 bonds become broken. Loosening of these bonds is, however, significantly different.

The H1-C2 in the case of reaction of 1a→2a+3a is broken more slowly than in the case of reaction 1b→2a+3b. In turn, the C3-O4 bond of TS of reaction 1a→2a+3a is broken faster than in the case of reaction 1b→2a+3b. This means that the energetically relatively more favorable transition state of the 1a→2a+3a process has a more profound, asynchronous character.

Subsequently to asynchronicity of bonds loosening, asynchronous redistribution of electron density asynchrony is observed. This is evidenced by GEDT index values (see Table 3). Moreover, GEDT values as well as dipole moments confirmed polar nature of TSs. In consequence — according to *Domingo* terminology [22] — they cannot be considered as "pericyclic". Next, we have re-optimized transition state

structures using UB3LYP/6-31G(d) theory level. It was found, that both TSs have non-biradicaloid character. This is confirmed by < S2 > values which in both cases equal 0.00.

It must be noted that the geometric parameters of the studied TSs obtained using higher theory levels (B3LYP/6-31G(d, p), B3LYP/6-31+G(d), B3LYP/6-311G(d)) are practically identical.

B3LYP/6-31G(d) calculations also provided us with information about the influence of the substituent in the leaving group on the TS structure. It turned out that both in the case of 1-nitropropane-1-ol and 2-nitropropane-1-ol esters, the presence of an electrodonating substituent facilitates an increase in TS synchronicity, whilst the presence of an electroaccepting substituent facilitates an increase in TS asynchronicity. The influence of the nature of the substituent on the symmetry of transition complex is in general decidedly too weak to enforce a change of the reaction mechanism to a two-step one. On the other hand, substituent nature stimulated asynchronicity of electron density redistribution. In particular, TSs of reaction involving dimethylamino-substituted esters are characterized by relatively higher GEDT values, whereas TSs of reaction involving nitro-substituted esters — relatively lower. However, in any case this process is ideal synchronous (GEDT≠ 0.00e).

Finally, we have also analyzed the influence of the solvent on the structure of TSs. It turned out that more polar medium facilitates a faster loosening of the H1-C2 bond. At the same time, it makes breaking the C3-C4 bond more difficult. Asynchronicity of TSs increases in an extremely polar, aqueous medium. In consequence, TSs for reactions 1a→2a+3a and reaction 1b→2a+3b under these conditions should be interpreted rather as similar to the E1cb-like type. It should be noted, that increasing of environment polarity stimulated more polar nature of TSs. This is confirmed by GEDT values, which reach even above 0.22e. However, it is not sufficient (even in extremely polar, aqueous solution) to generate evidence of ionic structures.

Conclusions

DFT calculations — regardless of theory level — indicate a one-step mechanism of thermal decomposition of nitroalkyl benzoates. However, depending on the nature of the substituent in the ester molecule and on medium polarity, the studied reactions may take place via transition state structures with varied synchronicity — from E1-like structures, through a rather synchronous model, to E1cb-like structures. It must be noted that a purely ionic, two-stage mechanism was not identified in any of the cases. Reaction kinetics may influence — albeit to a limited extent — the nature of the substituent and polarity of the reaction medium.

Acknowledgments The generous allocation of computing time by the regional computer center "Cyfronet" in Cracow (Grant No. MNiSW/Zeus_lokalnie/PK/009/2013) and financial support from the Polish State Committee (Grant No. C-2/33/2014/DS) are gratefully acknowledged.

References

1. Ono N (2001) The nitro group in organic synthesis. Wiley-VCH, Weinheim
2. Barrett AGM, Graboski GG (1985) Conjugated nitroalkenes: versatile intermediates in organic synthesis. Chem Rev 86:751–762
3. Szczepanek A, Mróz K, Goliasz G, Jasiński R (2011) Trihalonitropropenes in [4 + 2]-π-electron cycloaddition reactions. Chemik 65:1049–1054
4. Perekalin VV, Lipina ES, Berestovitskaya VM, Efremov DA (1994) Nitroalkenes: conjugated nitroalkenes. Wiley, New York
5. Jasiński R (2013) Preparatyka alifatycznych nitrozwiązków. RTN, Radom
6. Belenkii LI (2008) in Nitrile oxides, nitrone and nitronates in orgnanic synthesis (Ed. Feuer H.). Wiley, Noboken
7. Agrawal JP, Hodgson RD (2007) Chemistry of explosives. Wiley, Chichester
8. Boruwa J, Gogoi N, Saikia PP, Barua NC (2006) Catalytic asymmetric Henry reaction. Tetrahedron: Assymetry 17:3315–3326
9. Blomquist AT, Tapp WJ, Johnson JR (1945) Polymerization of nitroolefins. The preparation of 2-nitropropene polymer and of derived vinylamine polymers. J Am Chem Soc 67:1519–1524
10. Khlebnikov AF, Koneva AS, Virtseva AA, Yufit DS, Mlostoń G, Heimgartner H (2014) Concerted vs. non-concerted 1,3-dipolar cycloadditions of azomethine ylides to electron-deficient dialkyl 2,3-dicyanobut-2-enedioates. Helv Chim Acta 97:453–470
11. Krompiec S, Bujak P, Malarz J, Krompiec M, Skórka Ł, Pluta T, Danikiewicz W, Kania M, Kusz J (2012) An isomerization – 1,3-dipolar cycloaddition tandem reaction towards the synthesis of 3-aryl-4-methyl-5-O-substituted isoxazolines from O-allyl compounds. Tetrahedron 68:6018–6031
12. Jasiński R (2013) Competition between the one-step and two-step, zwitterionic mechanisms in the [2 + 3] cycloaddition of gem-dinitroethene with (Z)-C, N-diphenylnitrone: a DFT computational study. Tetrahedron 69:927–932
13. Domingo LR, Picher MT (2004) A DFT study of the huisgen 1,3-dipolar cycloaddition between hidered thiocarbonyl ylides and tetracyanoethylene. Tetrahedron 60:5053–5058
14. Jasiński R (2015) A stepwise, zwitterionic mechanism for the 1,3-dipolar cycloaddition between (Z)-C-4-methoxyphenyl-N-phenylnitrone and gem-chloronitroethene catalyzed by 1-butyl-3-methylimidazolium ionic liquid cations. Tetrahedron Lett 56:532–535
15. Łapczuk-Krygier A, Korotaev VY, Barkov AY, Sosnovskikh VY, Jasińska E, Jasiński R (2014) A DFT computational study on the molecular mechanism of the nitro group migration in the product derived from 3-nitro-2-(trifluoromethyl)-2H-chromene and 2-(1-phenylpropylidene)malononitrile. J Fluor Chem 168:236–239
16. Domingo LR, Aurell MJ, Kneeteman MN, Mancini PM (2008) Mechanistic details of the domino reaction of nitronaphthalenes with the electron-rich dienes. A DFT study. J Mol Struct - TheoChem 853: 68–76

17. Jasiński R (2014) Molecular mechanism of thermal decomposition of fluoronitroazoxy compounds: DFT computational study. J Fluor Chem 169:29–33
18. Jasiński R, Kwiatkowska M, Barański A (2009) A competition between carbo and hetero diels-alder reactions of E-2-phenyl-1-cyano-1-nitroethene to cyclopentadiene in the light of B3LYP/6-31G(d) computational study. J Mol Struct - TheoChem 910:80–87
19. Gómez AV, Aranda AI, Moreno A, Cossio FP, de Cózar A, Diaz-Irtiz Á, de la Hoz A, Prieto P (2009) Microwave-assisted reactions of nitroheterocycles with dienes. Diels–alder and tandem hetero diels–alder/[3,3] sigmatropic shift. Tetrahedron 65:5328–5336
20. Steglenko DV, Kletsky ME, Kurbatov SV, Tatarov AV, Minkin VI, Goumont R, Terrier F (2009) A theoretical and experimental study of the polar diels–alder cycloaddition of cyclopentadiene with nitrobenzodifuroxan. J Phys Org Chem 20:298–307
21. Arroyo P, Picher MT, Domingo LR, Terrier F (2005) A DFT study of the polar diels–alder reaction between 4-aza-6-nitrobenzofuroxan and cyclopentadiene. Tetrahedron 61:7359–7365
22. Domingo LR (2014) A new C-C bond formation model based on the quantum chemical topology of electron density. RSC Adv 4:32415–32428
23. Frisch MJ, Trucks GW, Schlegel HB, Scuseria GE, Robb MA, Cheeseman JR, Montgomery JA, Vreven TJ, Kudin KN, Burant JC, Millam JM, Iyengar SS, Tomasi J, Barone V, Mennucci B, Cossi M, Scalmani G, Rega N, Petersson GA, Nakatsuji H, Hada M, Ehara M, Toyota K, Fukuda R, Hasegawa J, Ishida M, Nakajima Y, Honda O, Kitao O, Nakai H, Klene M, Li X, Knox JE, Hratchian HP, Cross JB, Adamo C, Jaramillo J, Gomperts R, Stratmann RE, Yazyev O, Austin AJ, Cammi R, Pomelli C, Ochterski JW, Ayala PY, Morokuma K, Voth GA, Salvador P, Dannenberg JJ, Zakrzewski VG, Dapprich S, Daniels AD, Strain MC, Farkas MC, Malick DK, Rabuck AD, Raghavachari K, Foresman JB, Ortiz JV, Cui Q, Baboul AG, Clifford S, Cioslowski J, Stefanov BB, Liu G, Liashenko A, Piskorz P, Komaromi I, Martin RL, Fox DJ, Keith T, Al-Laham MA, Peng CY, Nanayakkara A, Challacombe M, Gill PMW, Johnson B, Chen W, Wong MW, Gonzalez C, Pople JA (2009) Gaussian 09 rev A.1. Gaussian Inc, Wallingford
24. Jasiński R (2014) Searching for zwitterionic intermediates in hetero diels–alder reactions between methyl α, p-dinitrocinnamate and vinyl-alkyl ethers. Comput Theor Chem 1046:93–98
25. Szczepanek A, Jasińska E, Kącka A, Jasiński R (2015) An experimental and quantumchemical study of [2+3] cycloaddition between (Z)-C-(m,m,p-trimethoxyphenyl)-N-(p-methyphenyl)-nitrone and (E)-3,3,3-trichloro-1-nitroprop-1-ene: mechanistic aspects. Current Chem Lett 4:33–33
26. Cossi M, Rega N, Scalmani G, Barone V (2003) Energies, structures, and electronic properties of molecules in solution with the C-PCM solvation model. J Comp Chem 24:669–681
27. Schwetlick K (1971) Kinetische metoden zur untersuchung von reaktionsmechanismen. VEB, Berlin

Artykuł D02

A. Kącka, R. Jasiński

A density functional theory mechanistic study of the thermal decomposition reactions of nitroethyl carboxylates: undermine of pericyclic insight.

Heteroatom Chemistry, **27**, 279-289 (2016).

Received: 14 January 2016 | Revised: 15 June 2016

DOI: 10.1002/hc.21326

RESEARCH ARTICLE

WILEY Heteroatom Chemistry

A density functional theory mechanistic study of thermal decomposition reactions of nitroethyl carboxylates: undermine of "pericyclic" insight

Agnieszka B. Kącka | Radomir A. Jasiński

Institute of Organic Chemistry and Technology, Cracow University of Technology, Cracow, Poland

Correspondence
Agnieszka Kącka, Institute of Organic Chemistry and Technology, Cracow University of Technology, Cracow, Poland.
Email: akacka@chemia.pk.edu.pl

Abstract

Quantum chemical study of thermal decomposition reactions of model nitroethyl carboxylates were studied using various density functional theory levels. It was found that conversion esters into nitroalkenes demean according to one-step mechanism. However, it is not an expected "pericyclic" mechanism but a "one-step two-stage" process. Subsequently, nitrous acid extrusion was also analyzed.

1 | INTRODUCTION

Conjugated nitroalkenes (CNA) have proved to be a valuable group of reactants in organic chemistry. Their strong electrophilic character makes them important precursors to a wide variety of target molecules. They are useful compounds applied, e.g., in syntheses of many four-, five- and six-membered compounds in cycloadditions reactions.[1–6] Applications of nitroalkenes in organic synthesis are largely due to their ease of conversion into a variety of functionalities. Moreover, a considerable number of nitroalkenes are exhibit remarkable biological activity.[7–10]

There are many strategies for preparation of CNA. However, most universal method is based on decomposition of corresponding nitroalkyl esters. The thermal decomposition of carboxylic esters to yield an alkene and a carboxylic acid has been studied since 1883.[11,12] The esters that undergo pyrolysis may be divided into two classes: esters with β-hydrogen atom on the alkyl portion of the molecule and esters without β-hydrogen atoms. The pyrolysis of esters without β-hydrogen atoms in the alkyl portion requires higher temperatures and the products are suggestive of a free radical type mechanism.[13] However, if β-hydrogen atoms are accessible and the temperature of pyrolysis is optimum, only the excepted olefins and acids products are formed. Although few scientists[14] believe that all esters decompose by the same mechanism, however, others[15] take care that the mechanism is not the same in different cases.

Only one "pericyclic" variant of the mechanism of the thermal decomposition of esters is generally reproduced in academic books. Nonetheless, recently, several atypical mechanisms for process which were considered earlier as "pericyclic". In these mechanisms, reaction groups were stepwise [2+3] cycloadditions,[16–18] thermal decomposition reactions of fluoronitroazoxy compounds,[19] as well as nitrous acid extrusion.[20–22] Additionally, Domingo generally negates the term "pericyclic process" for the majority as defined reactions.[23] Therefore, mechanistic aspects of nitroalkyl carboxylate decomposition reactions necessarily require a deep re-examination. Our work is part of this new trend.

In the event of nitroalkyl carboxylates, five theoretically possible reaction mechanism should be investigated: (i, v) purely ionic mechanism, (ii) asynchronous E1-like mechanism, (iii) ideal pericyclic mechanism, and (iv) asynchronous E1 cb-like mechanism. All theoretically possible reaction mechanism are presented in Scheme 1.

The aim of this work is a density functional theory (DFT) mechanistic studies of the model decomposition reactions of selected nitroethyl carboxylates (Scheme 2). First, we decide to analyze rotational isomerism in nitroethyl benzoate **1a** as simple, model compounds at variety of theoretical level so as to determine, which forms will undergo rotation. Next, for the better comprehend of the mechanism of thermal decomposition of nitroethyl carboxylates, we have performed

Contract grant sponsor: PL-Grid Infrastructure.

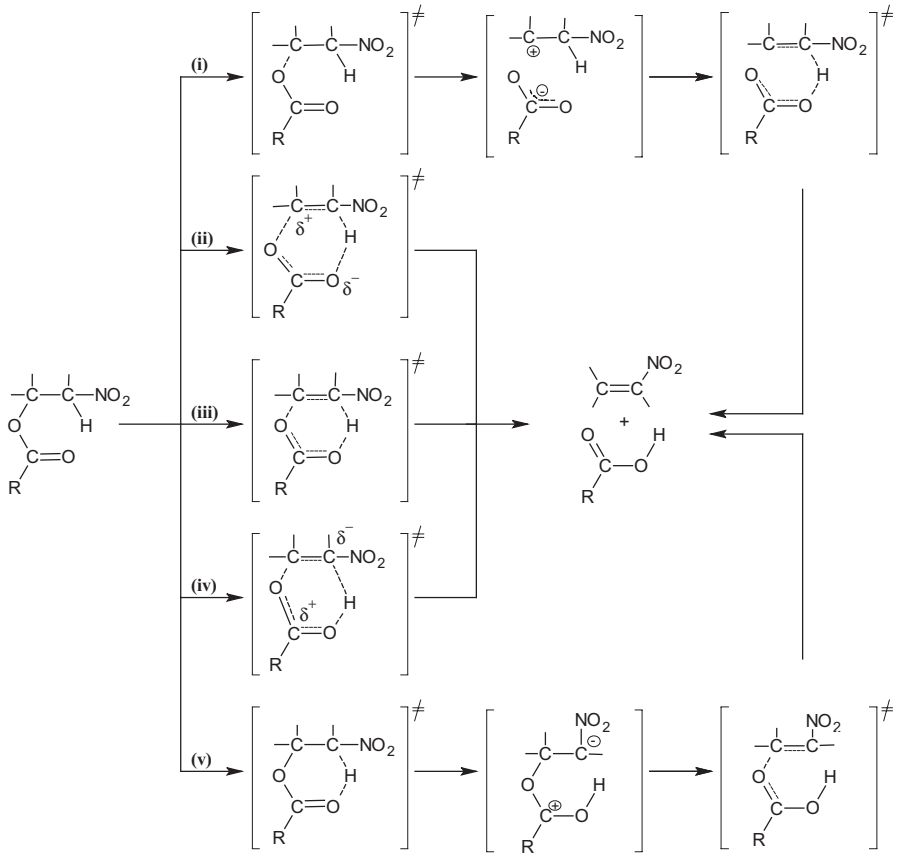

SCHEME 1 Theoretically possible mechanism for the thermal decomposition reaction of nitroethyl carboxylates

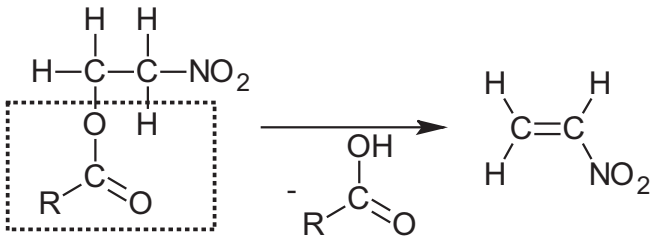

SCHEME 2 General scheme of the thermal decomposition of nitroethyl carboxylates. (a) R=C_6H_5; (b) R=C_6H_4–p–NMe_2; (c) R=C_6H_4–p–OMe; (d) R=C_6H_4–p–CF_3; (e) R=C_6H_4–p–NO_2; (f) R=$C(CH_3)_3$; (g) R=$CH(CH_3)_2$; (h) R=CH_3.

simulations of reaction path for esters that contain various substituents at –C(O)O– group. These reactions were examined in gaseous phase and also in the presence of simulated dielectric media (toluene, water).

2 | RESULTS AND DISCUSSION

2.1 | Computational details

All calculations were carried out using the Zeus cluster of computer in the CYFRONET Regional Computer

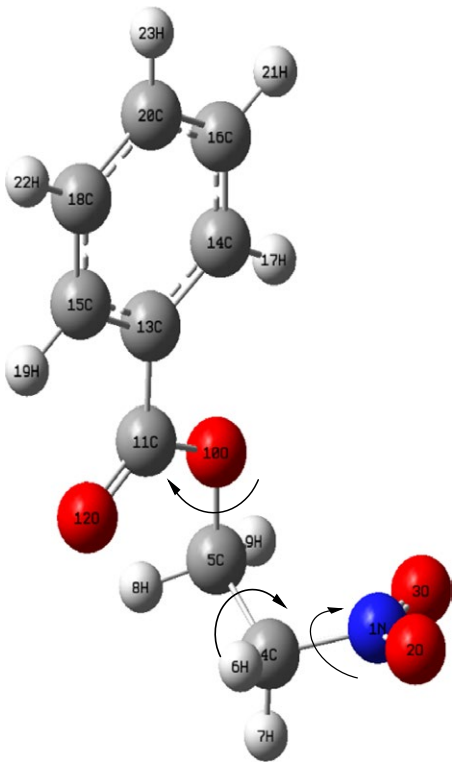

FIGURE 1 Atom numbering in 2-nitroethyl benzoate (**1a**) molecule

TABLE 1 Dihedral angles in structure rotamers (°) for rotation around the C4–C5 bond

Theoretical level	Reaction environment (ε)		Dihedral angle C4–C5–O10–C11	Dihedral angle N1–C4–C5–O10	Dihedral angle C5–C4–N1–O2
B3LYP/6-31G(d)	Gas phase (1.0000)	**1a(I)**	−81.94	−65.66	138.57
		TS1a(I)	−73.14	−120.16	164.90
		1a(II)	−80.08	−171.78	174.85
		TS1a(II)	−75.42	129.50	−154.90
		1a(III)	−101.51	74.34	−98.18
	Toluene (2.3741)	**1a(I)**	−82.74	−64.43	140.24
		TS1a(I)	−73.19	−121.52	163.86
		1a(II)	−81.19	−172.94	175.21
		TS1a(II)	−76.71	132.00	−154.94
		1a(III)	−98.53	74.24	−100.39
	Water (78.3553)	**1a(I)**	−83.11	−63.55	147.39
		TS1a(I)	−74.02	−122.46	163.21
		1a(II)	−82.69	−173.89	172.95
		TS1a(II)	−78.25	135.55	−155.35
		1a(III)	−96.00	73.60	−101.48
B3LYP/6-31+G(d)	Gas phase (1.0000)	**1a(I)**	−84.01	−65.21	130.99
		TS1a(I)	−73.87	−121.03	156.27
		1a(II)	−80.47	−170.10	171.54
		TS1a(II)	−76.94	128.81	−151.93
		1a(III)	174.11	66.12	−134.65
B3LYP/6-31G(d,p)	Gas phase (1.0000)	**1a(I)**	−81.71	−66.18	139.79
		TS1a(I)	−73.44	−120.42	165.52
		1a(II)	−79.69	−171.54	174.80
		TS1a(II)	−75.66	129.50	−155.61
		1a(III)	−103.19	73.90	−97.17

TABLE 2 Dihedral angles in structure rotamers (°) for rotation around the C5–O10 bond

Theoretical level	Reaction environment (ε)		Dihedral angle C4–C5–O10–C11	Dihedral angle N1–C4–C5–O10	Dihedral angle C5–C4–N1–O2
B3LYP/6-31G(d)	Gas phase (1.0000)	**1a(III)**	−101.51	74.34	−98.18
		TS1a(III)	−112.57	72.83	−105.02
		1a(IV)	173.64	66.30	−136.48
		TS1a(IV)	134.89	65.57	−138.57
		1a(V)	81.92	65.65	−138.56
		TS1a(V)	−4.63	73.00	−168.86
	Toluene (2.3741)	**1a(III)**	−98.53	74.24	−100.39
		TS1a(III)	−111.23	72.92	−110.12
		1a(IV)	174.88	65.82	−138.53
		TS1a(IV)	132.29	64.68	−140.86
		1a(V)	82.74	64.43	−140.24
		TS1a(V)	−1.72	70.52	−167.23
	Water (78.3553)	**1a(III)**	−96.00	73.60	−101.48
		TS1a(III)	−109.91	73.22	−119.61
		1a(IV)	177.62	66.40	−148.94
		TS1a(IV)	122.46	63.35	−151.34
		1a(V)	83.16	63.52	−147.35
		TS1a(V)	3.21	66.96	−165.04
B3LYP/6-31+G(d)	Gas phase (1.0000)	**1a(III)**	174.11	66.12	−134.65
		TS1a(III)	174.87	79.67	−53.97
		1a(IV)	174.09	66.13	−134.68
		TS1a(IV)	130.13	64.50	−133.79
		1a(V)	84.09	65.21	−130.99
		TS1a(V)	−3.92	73.45	−168.20
B3LYP/6-31G(d,p)	Gas phase (1.0000)	**1a(III)**	−103.19	73.90	−97.17
		TS1a(III)	−111.92	73.13	−104.16
		1a(IV)	172.53	66.81	−137.80
		TS1a(IV)	134.64	66.07	−140.00
		1a(V)	81.67	66.18	−139.75
		TS1a(V)	−4.49	73.29	−168.95

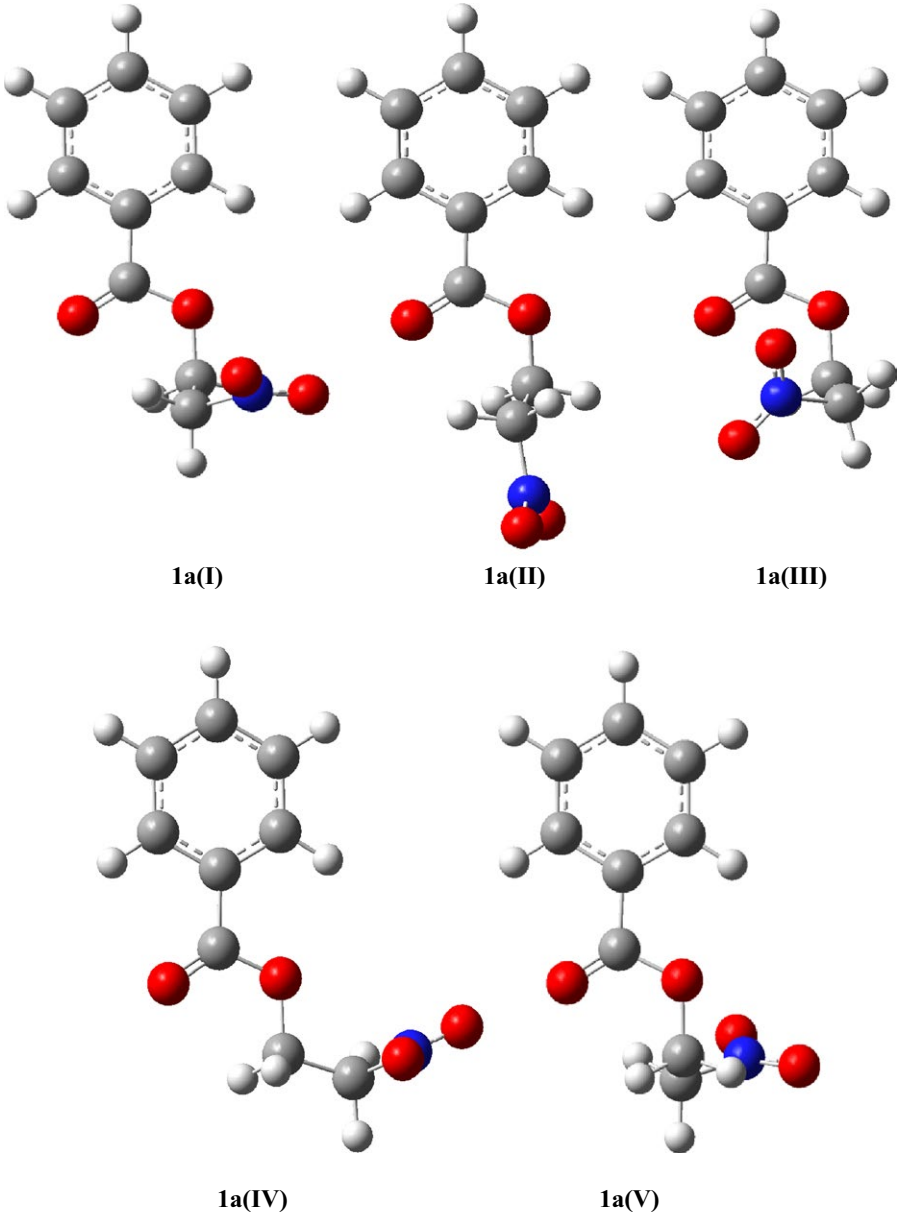

FIGURE 2 Structures of stable conformers of 2-nitroethyl benzoate **1a**

Centre in Cracow. The mechanism of the decomposition of nitroalkyl benzoates have been examined as implemented in the GAUSSIAN 09 package.[24] The geometric parameters for all the reactants, transition states, and products of the reactions studied were fully optimized using the DFT method. The calculations were performed using B3LYP[25] with 6-31G(d) basic set. Additionally, calculations in more advanced 6-31G(d,p), 6-31+G(d), and 6-31++G(d) basis sets were carried out.

Recently published reports[19,20,26–30] show that a similar approach was used successfully for the exploration of a reaction involving several different nitrocompounds. B3LYP is a combination of Becke's three-parameter hybrid exchange functional[31] with the Lee–Yang–Parr-correlated functional.[32] Geometry optimization calculations have been carried out to obtain the global minima for reactant and products, and to locate the saddle point for the transition state. Stationary points were characterized by frequency calculations. All reactants and products had positive Hessian matrices. All transition states showed only one negative eigenvalue in their diagonalized Hessian matrices, and their associated eigenvectors were confirmed to correspond to the motion along the reaction coordinate under consideration. Transition states were located using the (QST2) algorithm. For the optimization process, the Berny analytical gradient was employed. Intrinsic reaction coordinate (IRC) calculations[33] have been made in all events to verify that the localized transition-state structures connect with the corresponding minimum stationary points associated with reactants and products. Solvents effects of toluene and water in the optimizations were taken into account using the polarizable continuum model (PCM) as developed by the Tomasi's group[34] in the framework of

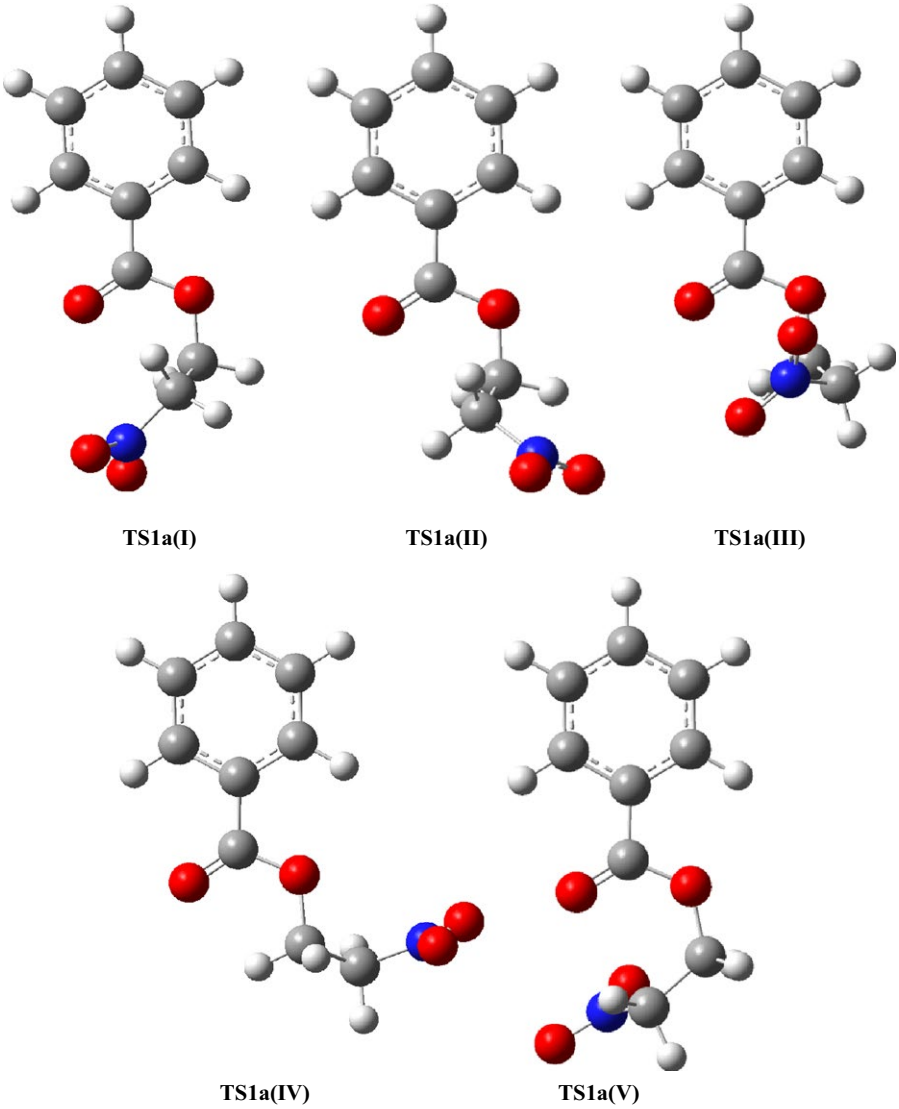

FIGURE 3 Structures of rotation transition states for isomers of 2-nitroethyl benzoate **1a**

the self-consistent reaction field (SCRF).[35] Values of enthalpies, entropies, and free energies in all calculations were calculated with the standard statistical thermodynamics at 25°C and 1 atm.[36]

2.2 | Rotational isomerism in nitroethyl benzoate (1a)

First, we decided to shed light on energetic properties of possible rotamers of 2-nitroethyl benzoate **1a**. Rotational isomerism in 2-nitroethyl benzoate may arise generally by rotating around the C4–C5 and C5–O10 bonds (Fig. 1). Several different orientations of conformers were used as the starting point in the present computations. The geometry was fully optimized in each stable conformer to ensure that a true minimum had been found. The most stable conformation was chosen as a reference for calculating the relative energy of 2-nitroethyl benzoate. Fundamental dihedral angles in the structure rotamers are shown in Tables 1 and 2.

Five optimized structures corresponding to low-lying stationary points and transition states are shown in Figs 2–4, respectively. The Gibbs free energy profile for the rotational transition nitroethyl benzoate **1a** are presented in Figs 5–7.

Kinetic and thermodynamics parameters of 2-nitroethyl benzoate rotamers have been collected in Table 3 and 4. In gas phase, **1a** exist generally in four forms. However, calculations using B3LYP with 6-31G(d) basic set show free rotation around the C4–C5 and C5–O10 bonds, which are possible even in room temperature. The most stable conformer is **1a(IV)**, which has the least Gibbs free energy, regardless of the applied basic set, and in consequence, this isomeric form should be considered as starting structure for the decomposition processes. Similar calculations have also been provided in the presence of dielectric media. In the environment of toluene, rotation also runs freely and the most stable conformer is also **1a(IV)**. The decomposition reaction carried out in water proceeded identically.

Similar picture of rotation isomerism in nitroethyl benzoate **1a** gives calculations on more advanced theory levels (B3LYP/6-31+G(d) and B3LYP/6-31G(d,p)). In particular, the geometries of the conformers are particularly identical to those obtained in B3LYP/6-31G(d) basic set. The Gibbs free energy profile for rotational transition **1a** are also practically the same with those obtained in B3LYP/6-31G(d) basic set.

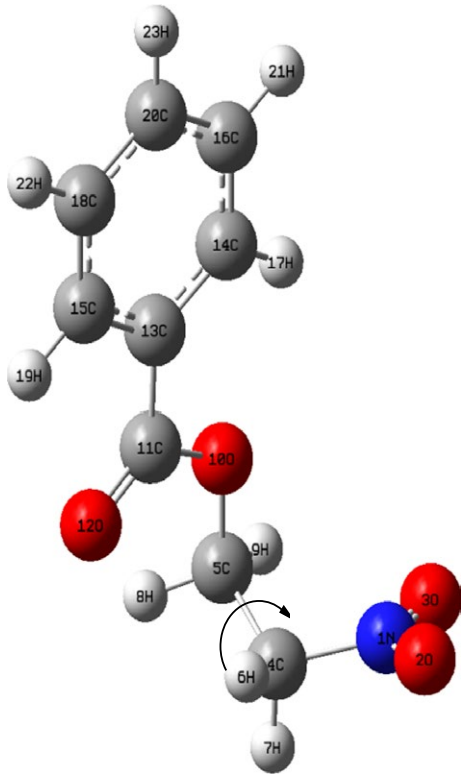

FIGURE 4 Rotational isomerism in 2-nitroethyl benzoate by rotation around the C4–C5 bond

2.3 | Energy profiles of carboxylic acid extrusion

The B3LYP/6-31G(d) calculation proved that conversion of ester **1a** into corresponding nitroalkenes in the gaseous phase demean according to a one-step mechanism. The thermal decomposition of **1a(IV)** proceeded through the transition complex **TS** (Fig. 8). The free Gibbs activation energy for this transition is equal to 39.65 kcal mol^{-1}. A similar image of these reactions in the gaseous phase is provided by calculations on higher theory levels (B3LYP/6-31+G(d), B3LYP/6-31++G(d), B3LYP/6-31G(d,p)). These calculations supplied a bit lower activation barrier for the decomposition process of **1a(IV)** (Table 5). In particular, all performed simulations clearly indicate a one-step mechanism, and activation barriers along individual paths do differ slightly from those obtained in the B3LYP/6-31G(d) calculations. Only one transition state (**TS**) exist between the substrate and products, which was validated by IRC calculations.

Then, we performed simulations of theoretically possible competitive paths of nitrous acids extrusion from **1a(IV)** (Fig. 8). The nitrous acid extrusion from **1a(IV)** takes place via an activation barrier, which is equal to 47.01 kcal mol^{-1}. Therefore, in this case, the nitrous acid extrusion process should be decidedly forbidden form kinetic point of view. In addition, similar simulations using more advanced theory levels were performed and provided a bit lower activation barrier for nitrous acid extrusion of **1a(IV)** (Table 5).

B3LYP/6-31G(d) calculations also make it possible to present the influence of the substituent in the leaving group on the course of reaction. It turned out that regardless of the nature of substituent in benzene ring, esters will undergo decomposition according to a one-step mechanism. The decomposition process of substituted esters with electron-donating groups (EDG; e.g., NMe_2, OMe) will lower the activation barrier

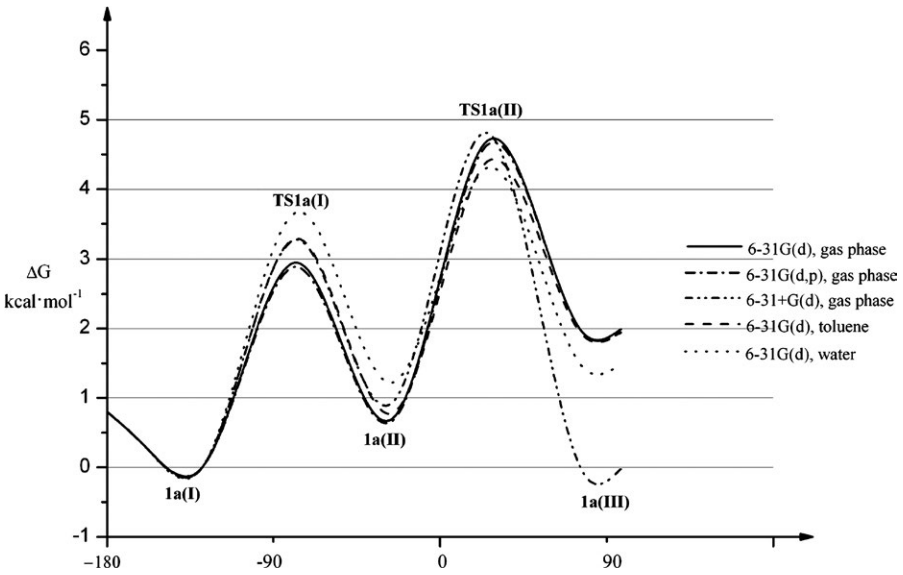

FIGURE 5 Gibbs free energy profile for rotational transition **1a** around the C4–C5 bond

(up to 39.00 kcal mol^{-1}). In turn, the decomposition process of esters with electron-accepting group (e.g., CF_3, NO_2) will make the process more difficult (Table 6).

Next, we also performed calculations by replacing the phenyl group on *tert*-butyl, isopropyl, and methyl group, respectively. B3LYP/6-31G(d) calculations proved that conversion of esters **1f**–**1h** into nitroalkenes proceeded according to a one-step mechanism. Moreover, calculations with mentioned substituents are slightly the same with those obtained for nitroethyl benzoate **1a**. A similar image of these reactions in the gaseous phase are provided by calculations on higher theory levels (B3LYP/6-31+G(d), B3LYP/6-31++G(d), B3LYP/6-31G(d,p)). These calculations supplied a bit lower activation barrier for decomposition process of **1f**–**1h** (Table 7).

Thereafter, the influence of solvent polarity on reaction kinetics decomposition of esters **1a**–**1h** was also analyzed. It was found that the thermal decomposition reaction of **1b** in the gas phase takes place via an activation barrier which is equal 39.00 kcal mol^{-1}, whereas in the presence of water, the same reaction carried out with the activation barrier equal 35.41 kcal mol^{-1}. Similarly, it was assumed that strongly polar medium reduce the activation barrier value and make the decomposition process run faster. Thus, regardless of the polarity of the medium, the reaction proceeds to a one-step mechanism.

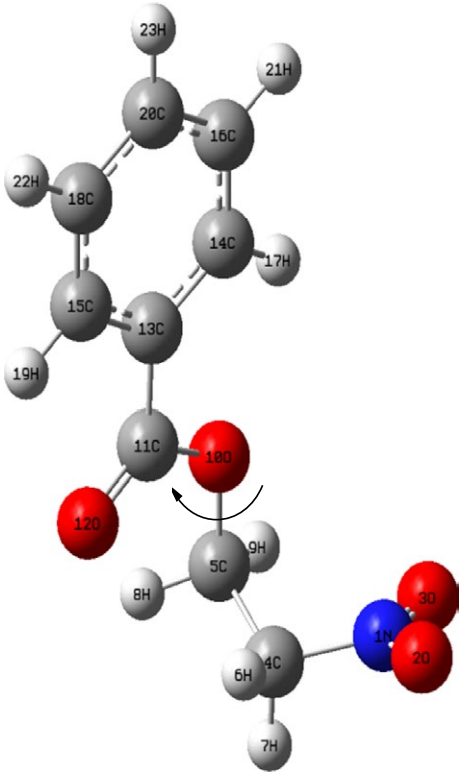

FIGURE 6 Rotational isomerism in 2-nitroethyl benzoate by rotation around the C5–O10 bond

2.4 | Transition structures of thermal decomposition reactions

We then analyzed the transition-state structure (**TS**) of the decomposition process of ester **1a(IV)**. It turned out that **TS** has a six-membered structure (Fig. 9). Simultaneously, a new bond between atoms H6–O12 is formed, between atoms C4–C5 and C11–O10 double bonds are formed, C11–O12 bond changes to a single bond and H6–C4 and C5–O10 bonds are broken. The process of electron density redistribution in the TS area is not ideally synchronized. The H6–C4 bond is not disrupted simultaneously with the creation of a O12–H6 bond. In the TS range, the H6–C4 bond is very week, while a new O12–H6 bond is in the process of formation. Hence, the transition state and reaction should be investigated not as a "pericyclic process" but rather as a E1 cb-like reaction. According to Domingo terminology,[23] formed TS can be defined as typical for a "one-step two-stage" process.

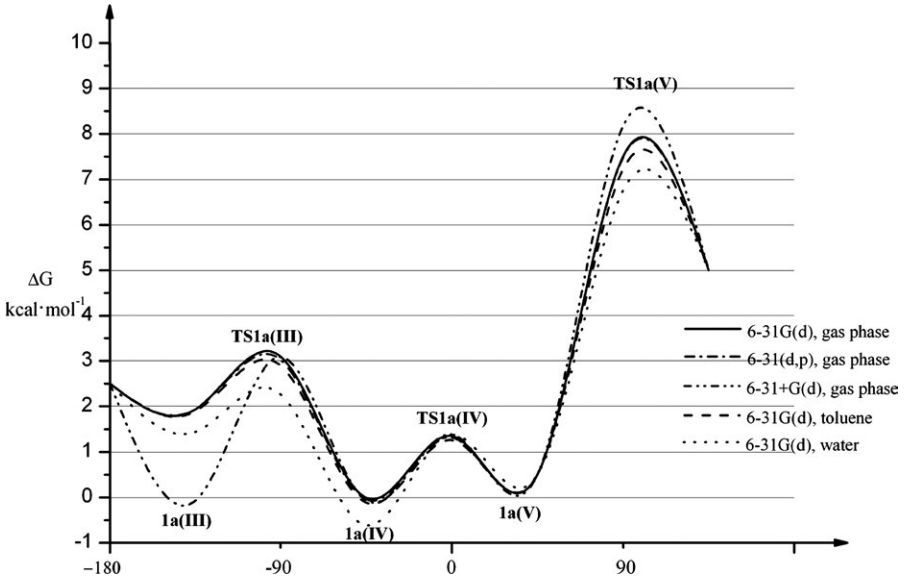

FIGURE 7 Gibbs free energy profile for rotational transition **1a** around the C5–O10 bond

TABLE 3 Kinetic and thermodynamics parameters for rotational isomerism in nitroethyl benzoate **1a**, in line with the C4–C5 bond, according to density functional theory (DFT) calculations (T = 298K; ΔH, ΔG in kcal mol^{-1}; ΔS in cal mol^{-1} K^{-1})

Basic set[a]	Reaction environment (ε)	Energy	ΔH°	ΔG°	ΔS°	Transition state	ΔH‡	ΔG‡	ΔS‡
6-31G(d)	Gas phase (1.0000)	**1a(I)→1a(II)**	0.81	0.70	−0.40	**1a(I)→TS1a(I)→1a(II)**	1.80	2.95	−3.83
		1a(II)→1a(III)	1.54	1.25	0.99	**1a(II)→TS1a(II)→1a(III)**	2.18	3.99	−6.06
	Toluene (2.3741)	**1a(I)→1a(II)**	1.02	0.78	0.50	**1a(I)→TS1a(I)→1a(II)**	2.02	3.26	−4.18
		1a(II)→1a(III)	0.84	1.03	−0.62	**1a(II)→TS1a(II)→1a(III)**	3	3.53	−5.69
	Water (78.3553)	**1a(I)→1a(II)**	1.23	1.22	0.03	**1a(I)→TS1a(I)→1a(II)**	2.32	3.67	−4.56
		1a(II)→1a(III)	−0.36	0.22	−1.93	**1a(II)→TS1a(II)→1a(III)**	1.38	3.09	−5.71
6-31G(d,p)	Gas phase (1.0000)	**1a(I)→1a(II)**	0.83	0.67	0.54	**1a(I)→TS1a(I)→1a(II)**	1.77	2.89	−3.76
		1a(II)→1a(III)	1.55	1.27	0.93	**1a(II)→TS1a(II)→1a(III)**	2.15	3.97	−6.11
6-31+G(d)	Gas phase (1.0000)	**1a(I)→1a(II)**	1.18	0.93	0.85	**1a(I)→TS1a(I)→1a(II)**	1.88	3.28	−4.71
		1a(II)→1a(III)	1.13	−1.00	−0.42	**1a(II)→TS1a(II)→1a(III)**	1.92	3.88	−6.59

[a]DFT calculations were performed by B3LYP level.
‡All values ΔH, ΔG are in kcal mol^{-1} and also all values ΔS are in cal mol^{-1} K^{-1}. This values are containing two meanings, parameters of reactions and parameters of formations TS.

TABLE 4 Kinetic and thermodynamics parameters for rotational isomerism in nitroethyl benzoate **1a**, in line with the C5–O10 bond, according to density functional theory (DFT) calculations (T = 298K; ΔH, ΔG in kcal mol^{-1}; ΔS in cal mol^{-1} K^{-1})

Basic set[a]	Reaction environment (ε)	Energy	ΔH°	ΔG°	ΔS°	Transition state	ΔH‡	ΔG‡	ΔS‡
6-31G(d)	Gas phase (1.0000)	**1a(III)→1a(IV)**	−1.99	−1.95	−0.13	**1a(III)→TS1a(III)→1a(IV)**	−0.55	1.16	−5.76
		1a(IV)→1a(V)	−0.37	−0.01	−1.25	**1a(IV)→TS1a(IV)→1a(V)**	−0.32	1.36	−5.63
						1a(V)→TS1a(V)	5.52	7.51	−6.69
	Toluene (2.3741)	**1a(III)→1a(IV)**	−1.72	−2.02	1.00	**1a(III)→TS1a(III)→1a(IV)**	−0.52	1.00	−5.08
		1a(IV)→1a(V)	−0.14	0.12	−0.88	**1a(IV)→TS1a(IV)→1a(V)**	−0.24	1.38	−5.43
						1a(V)→TS1a(V)	5.21	7.24	−6.80
	Water (78.3553)	**1a(III)→1a(IV)**	−1.09	−2.06	3.23	**1a(III)→TS1a(III)→1a(IV)**	−0.39	0.83	−4.08
		1a(IV)→1a(V)	0.22	0.62	−1.32	**1a(IV)→TS1a(IV)→1a(V)**	−0.04	1.99	−6.79
						1a(V)→TS1a(V)	4.48	6.78	−7.68
6-31G(d,p)	Gas phase (1.0000)	**1a(III)→1a(IV)**	−2.02	−1.99	0.06	**1a(III)→TS1a(III)→1a(IV)**	−0.57	1.09	−5.58
		1a(IV)→1a(V)	−0.37	0.05	−1.42	**1a(IV)→TS1a(IV)→1a(V)**	−0.38	1.37	−5.85
						1a(V)→TS1a(V)	5.25	7.49	−6.61
6-31+G(d)	Gas phase (1.0000)	**1a(III)→1a(IV)**	−0.00	−0.00	−0.01	**1a(III)→TS1a(III)→1a(IV)**	1.71	3.16	−4.88
		1a(IV)→1a(V)	−0.05	0.07	−0.40	**1a(IV)→TS1a(IV)→1a(V)**	0.13	1.45	−5.31
						1a(V)→TS1a(V)	6.11	8.18	−6.91

[a]DFT calculations were performed by B3LYP level.
‡All values ΔH, ΔG are in kcal mol^{-1} and also all values ΔS are in cal mol^{-1} K^{-1}. This values are containing two meanings, parameters of reactions and parameters of formations TS.

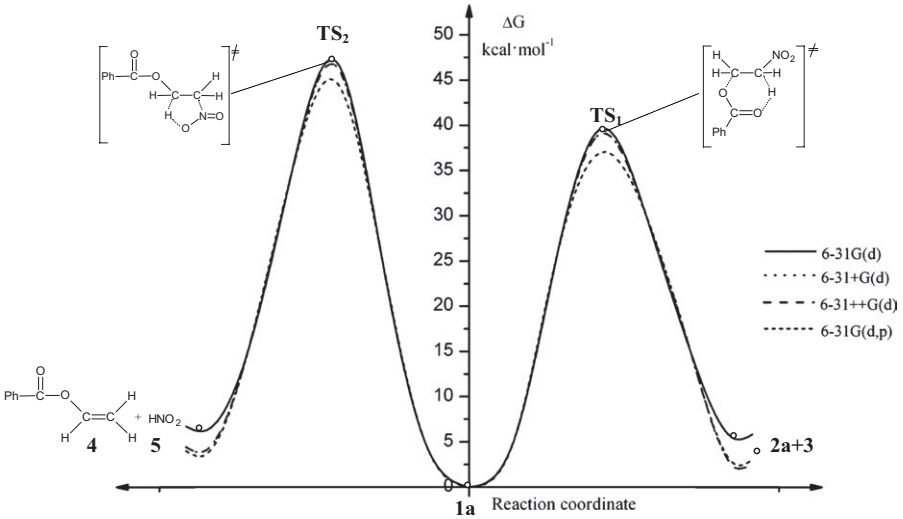

FIGURE 8 Gibbs free energy profiles for benzoic acid as well as nitrous acid extrusion from **1a(IV)** in the gas phase according to density functional theory calculations (T = 298K)

TABLE 5 Kinetic and thermodynamics parameters for the thermal decomposition ester and nitrous acid extrusion from **1a(IV)** according to density functional theory (DFT) calculations (T = 298K; ΔH, ΔG in kcal mol^{-1}; ΔS in cal mol^{-1} K^{-1}).

Basic set[a]	Reaction environment (ε)	Energy	ΔH°	ΔG°	ΔS°	Transition state	ΔH‡	ΔG‡	ΔS‡
6-31G(d)	Gas phase (1.0000)	**1a→2a+3**	17.08	5.33	39.41	**1a→TS$_1$→2a+3**	38.73	39.65	−3.08
		1a→4+5	18.51	6.19	41.35	**1a→TS$_2$→4+5**	47.04	47.01	0.09
6-31+G(d)	Gas phase (1.0000)	**1a→2a+3**	13.77	2.14	38.99	**1a→TS$_1$→2a+3**	37.93	39.12	−3.80
		1a→4+5	16.15	3.90	41.09	**1a→TS$_2$→4+5**	46.59	46.52	0.23
6-31++G(d)	Gas phase (1.0000)	**1a→2a+3**	13.80	2.18	38.97	**1a→TS$_1$→2a+3**	37.93	39.09	−3.92
		1a→4+5	16.18	3.92	41.13	**1a→TS$_2$→4+5**	46.58	46.51	0.21
6-31G(d,p)	Gas phase (1.0000)	**1a→2a+3**	14.28	2.52	39.47	**1a→TS$_1$→2a+3**	36.09	37.01	−3.08
		1a→4+5	15.82	3.47	41.42	**1a→TS$_2$→4+5**	44.84	44.78	0.22

[a]DFT calculations were performed by B3LYP level.
‡All values ΔH, ΔG are in kcal mol^{-1} and also all values ΔS are in cal mol^{-1} K^{-1}. This values are containing two meanings, parameters of reactions and parameters of formations TS.

TABLE 6 Kinetic and thermodynamics parameters for the thermal decomposition of nitroethyl benzoates **1a**–**1h** according to 6-31G(d) calculations (T = 298K; ΔH, ΔG in kcal mol^{-1}; ΔS in cal mol^{-1} K^{-1})

Ester[a]	Reaction environment (ε)	Energy	ΔH°	ΔG°	ΔS°	Transition state	ΔH‡	ΔG‡	ΔS‡
1a	Gas phase (1.0000)	**1a→2a+3**	17.08	5.33	39.41	**1a→TS$_1$→2a+3**	38.73	39.65	−3.08
	Water (78.3553)	**1a→2a+3**	14.84	3.35	38.52	**1a→TS$_1$→2a+3**	36.47	37.74	−4.25
1b	Gas phase (1.0000)	**1b→2b+3**	17.54	5.65	39.86	**1b→TS$_1$→2b+3**	37.52	39.00	−4.98
	Water (78.3553)	**1b→2b+3**	15.00	2.95	40.41	**1b→TS$_1$→2b+3**	34.30	35.41	−3.72
1c	Gas phase (1.0000)	**1c→2c+3**	17.22	5.33	39.84	**1c→TS$_1$→2c+3**	38.18	39.21	−3.48
	Water (78.3553)	**1c→2c+3**	14.92	3.36	38.76	**1c→TS$_1$→2c+3**	35.66	37.00	−4.47
1d	Gas phase (1.0000)	**1d→2d+3**	16.81	4.99	39.62	**1d→TS$_1$→2d+3**	39.29	40.30	−3.37
	Water (78.3553)	**1d→2d+3**	14.75	3.02	39.33	**1d→TS$_1$→2d+3**	37.26	38.25	−3.33
1e	Gas phase (1.0000)	**1e→2e+3**	16.66	5.20	38.44	**1e→TS$_1$→2e+3**	39.65	40.90	−4.19
	Water (78.3553)	**1e→2e+3**	14.72	3.14	38.84	**1e→TS$_1$→2e+3**	37.81	38.96	−3.85
1f	Gas phase (1.0000)	**1f→2f+3**	17.17	6.19	36.83	**1f→TS$_1$→2f+3**	38.64	40.33	−5.68
	Water (78.3553)	**1f→2f+3**	14.94	3.27	39.13	**1f→TS$_1$→2f+3**	36.35	37.06	−2.39
1g	Gas phase (1.0000)	**1g→2g+3**	17.11	5.42	39.22	**1g→TS$_1$→2g+3**	38.82	39.53	−2.36
	Water (78.3553)	**1g→2g+3**	14.99	3.54	38.41	**1g→TS$_1$→2g+3**	36.56	37.79	−4.13
1h	Gas phase (1.0000)	**1h→2h+3**	17.08	5.30	39.51	**1h→TS$_1$→2h+3**	38.79	39.91	−3.75
	Water (78.3553)	**1h→2h+3**	14.95	3.44	38.63	**1h→TS$_1$→2h+3**	36.41	37.80	−4.68

[a]DFT calculations were performed by B3LYP level.
‡All values ΔH, ΔG are in kcal mol^{-1} and also all values ΔS are in cal mol^{-1} K^{-1}. This values are containing two meanings, parameters of reactions and parameters of formations TS.

We then also analyzed the influence of the substituent nature of the TS structure. The H6–C4 bond in the reaction **1e→2e+3** is broken more slowly than in the reaction **1a→2a+3**. In turn, the C5–O10 bond of TS of reaction **1e→2e+3** is broken faster than in the reaction **1a→2a+3** (Table 8). By contrast, the H6–C4 bond in the reaction **1b→2b+3** is broken more faster than in the reaction **1a→2a+3**. In turn, the C5–O10 bond of TS of the reaction **1b→2b+3** is broken slowly than in the reaction **1a→2a+3** (Table 8). Consequently, the EDG in the benzene ring further favored synchronicity, but the electron-withdrawing group (EWG) favored asynchronicity.

Replacement of the phenyl group by the alkyl group in the ester molecule does not significantly impact the synchronicity of the broken H6–C4 bond and the creation of the C5–O10 bond. The obtained results are practically identical with those obtained for 2-nitroethyl benzoate **1a**.

Finally, we analyzed the impact of solvent polarity on the TS structure. It turned out that the breaking of the H6–C4 bond in the event of decomposition of **1a** in the gas phase is slower than in the same reaction conducted in a polar, water environment. However, the C5–O10 bond is broken slowly in the gas phase than when conducted in water. Thus, the TS structure in a tiny polar environment is more similar to that in a "one-step two-stage" model.

3 | CONCLUSIONS

In summary, DFT calculations, regardless of theory levels, prove that the thermal decomposition of nitroethyl carboxylates cannot be considered as a pericyclic process. Detailed analysis of the IRC and geometry of transition states indicate

TABLE 7 Kinetic and thermodynamics parameters for the thermal decomposition of nitroethyl benzoates **1a**–**1h** according to density functional theory (DFT) calculations (T = 298K; ΔH, ΔG in kcal mol^{-1}; ΔS in cal mol^{-1} K^{-1})

Basic set[a]	Ester	Energy	ΔH°	ΔG°	ΔS°	Transition state	ΔH‡	ΔG‡	ΔS‡
6-31+G(d)	**1a**	**1a→2a+3**	13.77	1.91	38.99	**1a→TS$_1$→2a+3**	37.94	38.88	−3.95
	1b	**1b→2b+3**	14.10	2.12	40.15	**1b→TS$_1$→2b+3**	36.52	38.22	−5.69
	1c	**1c→2c+3**	13.84	2.11	39.34	**1c→TS$_1$→2c+3**	37.31	38.51	−4.03
	1d	**1d→2d+3**	13.51	1.79	39.31	**1d→TS$_1$→2d+3**	38.71	39.55	−2.81
	1e	**1e→2e+3**	13.44	1.97	38.47	**1e→TS$_1$→2e+3**	38.99	40.18	−3.99
	1f	**1f→2f+3**	13.72	2.12	38.92	**1f→TS$_1$→2f+3**	37.75	38.85	−3.71
	1g	**1g→2g+3**	13.82	1.87	40.06	**1g→TS$_1$→2g+3**	38.06	39.12	−3.55
	1h	**1h→2h+3**	13.79	2.04	39.42	**1h→TS$_1$→2h+3**	38.22	39.59	−4.58
6-31++G(d)	**1a**	**1a→2a+3**	13.80	2.18	38.96	**1a→TS$_1$→2a+3**	37.93	39.09	−3.89
	1b	**1b→2b+3**	14.15	2.04	40.61	**1b→TS$_1$→2b+3**	36.47	38.19	−5.77
	1c	**1c→2c+3**	13.87	2.12	39.40	**1c→TS$_1$→2c+3**	37.31	38.49	−3.95
	1d	**1d→2d+3**	13.53	1.82	39.27	**1d→TS$_1$→2d+3**	38.70	39.56	−2.90
	1e	**1e→2e+3**	13.44	1.99	38.40	**1e→TS$_1$→2e+3**	38.99	40.20	−4.06
	1f	**1f→2f+3**	13.74	2.15	38.88	**1f→TS$_1$→2f+3**	37.73	38.86	−3.80
	1g	**1g→2g+3**	13.82	1.90	39.98	**1g→TS$_1$→2g+3**	38.04	39.10	−3.56
	1h	**1h→2h+3**	13.80	2.07	39.34	**1h→TS$_1$→2h+3**	38.21	39.53	−4.43
6-31G(d,p)	**1a**	**1a→2a+3**	14.28	2.51	39.46	**1a→TS$_1$→2a+3**	36.09	37.01	−3.08
	1b	**1b→2b+3**	14.76	2.84	39.95	**1b→TS$_1$→2b+3**	34.81	36.33	−5.10
	1c	**1c→2c+3**	14.42	2.55	39.83	**1c→TS$_1$→2c+3**	35.51	36.55	−3.51
	1d	**1d→2d+3**	14.01	2.14	39.79	**1d→TS$_1$→2d+3**	36.68	37.69	−3.41
	1e	**1e→2e+3**	13.86	2.37	38.52	**1e→TS$_1$→2e+3**	37.05	38.31	−4.22
	1f	**1f→2f+3**	14.34	2.78	38.76	**1f→TS$_1$→2f+3**	35.97	37.16	−3.98
	1g	**1g→2g+3**	14.30	2.67	39.01	**1g→TS$_1$→2g+3**	36.20	36.91	−2.37
	1h	**1h→2h+3**	14.27	2.53	39.38	**1h→TS$_1$→2h+3**	36.15	37.30	−3.83

[a]DFT calculations were performed by B3LYP level.
‡All values ΔH, ΔG are in kcal mol^{-1} and also all values ΔS are in cal mol^{-1} K^{-1}. This values are containing two meanings, parameters of reactions and parameters of formations TS.

TABLE 8 Geometrical characteristics of key structures of the thermal decompositions of nitroethyl benzoates **1a**–**1h** according to B3LYP/6-31G(d) calculations

Reaction environment (ε)	Reaction	Structure	Interatomic distances [Å]					
			H6–C4	C4–C5	C5–O10	O10–C11	C11–O12	O12–H6
Gas phase (1.0000)	**1a→2a+3**	**1a**	1.088	1.518	1.435	1.363	1.216	2.707
		TS$_1$	1.569	1.424	1.750	1.273	1.292	1.095
		2a+3		1.327		1.215	1.359	0.975
Water (78.3553)	**1a→2a+3**	**1a**	1.088	1.516	1.439	1.358	1.219	2.754
		TS$_1$	1.707	1.432	1.694	1.272	1.300	1.040
		2a+3		1.328		1.219	1.352	0.976
Gas phase (1.0000)	**1b→2b+3**	**1b**	1.088	1.519	1.431	1.371	1.219	2.698
		TS$_1$	1.621	1.427	1.722	1.278	1.300	1.069
		2b+3		1.327		1.218	1.364	0.975
Gas phase (1.0000)	**1c→2c+3**	**1c**	1.088	1.518	1.433	1.366	1.217	2.706
		TS$_1$	1.591	1.425	1.737	1.275	1.296	1.084
		2c+3		1.327		1.218	1.361	0.975
Gas phase (1.0000)	**1d→2d+3**	**1d**	1.088	1.518	1.437	1.359	1.215	2.723
		TS$_1$	1.542	1.422	1.769	1.271	1.289	1.110
		2d+3		1.327		1.214	1.357	0.975
Gas phase (1.0000)	**1e→2e+3**	**1e**	1.088	1.517	1.439	1.357	1.214	2.741
		TS$_1$	1.524	1.421	1.784	1.270	1.288	1.120
		2e+3		1.327		1.213	1.355	0.975
Gas phase (1.0000)	**1f→2f+3**	**1f**	1.088	1.521	1.434	1.365	1.212	2.683
		TS$_1$	1.574	1.424	1.748	1.268	1.290	1.093
		2f+3		1.327		1.212	1.361	0.976
Gas phase (1.0000)	**1g→2g+3**	**1g**	1.088	1.519	1.436	1.364	1.212	2.702
		TS$_1$	1.574	1.425	1.747	1.268	1.289	1.095
		2g+3		1.327		1.212	1.360	0.976
Gas phase (1.0000)	**1h→2h+3**	**1h**	1.088	1.519	1.436	1.363	1.211	2.704
		TS$_1$	1.561	1.424	1.759	1.267	1.287	1.102
		2h+3		1.327		1.210	1.359	0.976

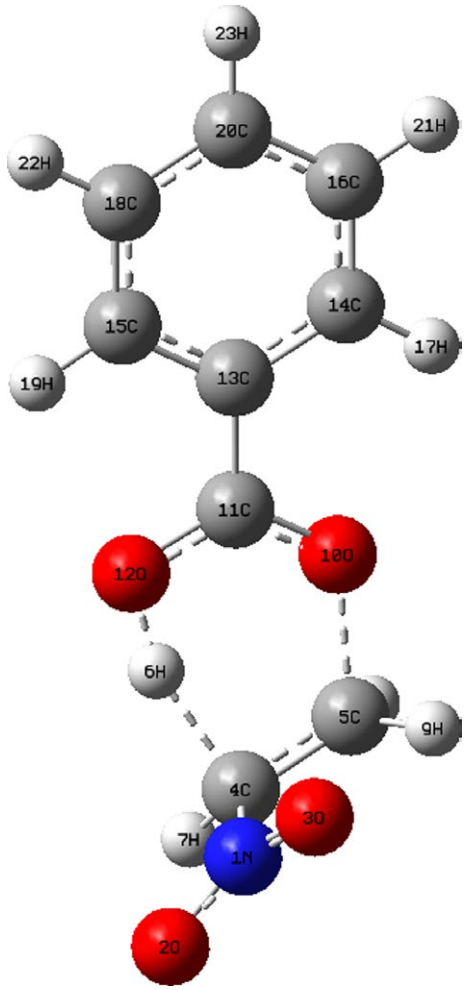

FIGURE 9 Transition states **TS** for the thermal decomposition reaction of ester **1a** in gas phase according to B3LYP/6-31G(d) calculations (T = 298K)

that these processes should be included in the group of "one-step two-stage" reactions. The synchronicity of TS, to a certain extent, can be controlled by changing the electric nature and volume of the substituent in the leaving group, but should be sufficient enough so as not to alter the purely ionic mechanism.

ACKNOWLEDGMENTS

This research was supported in part by PL-Grid Infrastructure.

REFERENCES

[1] A. Barrett, G. Graboski, *Chem. Rev.* **1986**, *86*, 751.
[2] R. Ballini, R. Castagnani, M. Petrini, *J. Org. Chem.* **1992**, *4*, 2160.
[3] E. Jasińska, E. Dresler, A. Łapczuk-Krygier, A. Kącka, E. Nowakowska-Bogdan, R. Jasiński, *Chemik* **2015**, *69*, 395.
[4] V. V. Perekalin, E. S. Lipina, V. M. Berestovitskaya, D. A. Efremov, Nitroalkenes: Conugated Nitroalkenes, Wiley, New York **1994**.
[5] G. W. Kabalka, R. S. Varma, *Org. Prep. Proced. Int.* **1987**, *19*, 283.
[6] R. I. Baichurin, N. I. Aboskalova, E. V. Trukhin, V. M. Berestovitskaya, *Russ. J. Gen. Chem.* **2015**, *85*, 1288.
[7] A. Boguszewska-Czubara, A. Łapczuk-Krygier, K. Rykała, A. Biernasiuk, A. Wnorowski, L. Popiołek, A. Maziarka, A. Hordyjewska, R. Jasiński, *J. Enz. Inhib. Med. Chem.* **2016**. doi:10.3109/14756366.2015.1070264
[8] W. Al-Zereini, I. Schuhmann, H. Laatsh, E. Helmke, H. Anke, *J. Antibiot.* **2007**, *60*, 301.
[9] N. G. Clark, B. Croshaw, B. E. Leggetter, D. F. Spooner, *J. Med. Chem.* **1974**, *17*, 977.
[10] C. Herrera, G. A. Vallejos, R. Loaiza, R. Zeledon, A. Urbina, S. Sepulveda-Boza, *Mem. Inst. Oswaldo Cruz* **2009**, *104*, 980.
[11] E. Fisher, F. Jourdan, *Chem. Ber.* **1883**, *16*, 6.
[12] F. Kraft, *Berichte Deutsch. Chem. Gesell.* **1883**, *16*, 3018.
[13] C. D. Hurd, F. H. Blunck, *J. Am. Chem. Soc.* **1938**, *60*, 2419.
[14] R. T. Arnold, G. G. Smith, R. M. Dodson, *J. Org. Chem.* **1950**, *15*, 1256.
[15] A. M. Silva, *Chem. Phys. Lett.* **2007**, *439*, 8.
[16] S. Krompiec, P. Bujak, J. Malarz, M. Krompiec, Ł. Skórka, T. Pluta, W. Danikiewicz, M. Kania, J. Kusz, *Tetrahedron* **2012**, *68*, 6018.
[17] R. L. Domingo, M. T. Picher, *Tetrahedron* **2004**, *60*, 5053.
[18] R. Jasiński, *RSC Adv.* **2015**, *5*, 101045.
[19] R. Jasiński, *J. Fluor. Chem.* **2014**, *160*, 29.
[20] R. Jasiński, *RSC Adv.* **2015**, *5*, 50070.
[21] R. Jasiński, *J. Fluor. Chem.* **2015**, *176*, 35.
[22] L. R. Domingo, M. J. Aurell, M. N. Kneeteman, P. M. Mancini, *J. Mol. Struct.* **2008**, *853*, 68.
[23] L. R. Domingo, *RSC Adv.* **2014**, *4*, 32415.
[24] M. J. Frisch, G. W. Trucks, H. B. Schlegel, G. E. Scuseria, M. A. Robb, J. R. Cheeseman, J. A. Montgomery, T. J. Vreven, K. N. Kudin, J. C. Burant, J. M. Millam, S. S. Iyengar, J. Tomasi, V. Barone, B. Mennucci, M. Cossi, G. Scalmani, N. Rega, G. A. Petersson, H. Nakatsuji, M. Hada, M. Ehara, K. Toyota, R. Fukuda, J. Hasegawa, M. Ishida, Y. Nakajima, O. Honda, O. Kitao, H. Nakai, M. Klene, X. Li, J. E. Knox, H. P. Hratchian, J. B. Cross, C. Adamo, J. Jaramillo, R. Gomperts, R. E. Stratmann, O. Yazyev, A. J. Austin, R. Cammi, C. Pomelli, J. W. Ochterski, P. Y. Ayala, K. Morokuma, G. A. Voth, P. Salvador, J. J. Dannenberg, V. G. Zakrzewski, S. Dapprich, A. D. Daniels, M. C. Strain, M. C. Farkas, D. K. Malick, A. D. Rabuck, K. Raghavachari, J. B. Foresman, J. V. Ortiz, Q. Cui, A. G. Baboul, S. Clifford, J. Cioslowski, B. B. Stefanov, G. Liu, A. Liashenko, P. Piskorz, I. Komaromi, R. L. Martin, D. J. Fox, T. Keith, M. A. Al-Laham, C. Y. Peng, A. Nanayakkara, M. Challacombe, P. M. W. Gill, B. Johnson, W. Chen, M. W. Wong, C. Gonzalez, J. A. Pople, Gaussian 09 Rev A.1, Gaussian Inc, Wallingford, CT **2009**.
[25] P. Stephens, F. J. Devlin, C. F. Chabalowski, M. J. Frisch, *J. Phys. Chem.* **1994**, *98*, 11623.
[26] R. Jasiński, *Comput. Theor. Chem.* **2014**, *1046*, 93.
[27] A. Szczepanek, E. Jasińska, A. Kącka, R. Jasiński, *Curr. Chem. Lett.* **2015**, *4*, 33.
[28] L. R. Domingo, P. Pérez, R. Contreras, *Tetrahedron* **2004**, *60*, 6585.
[29] L. R. Domingo, M. Arno, J. Andrés, *J. Org. Chem.* **1999**, *64*, 5867.
[30] L. R. Domingo, M. José Aurell, M. N. Kneeteman, P. M. Mancini, *J. Mol. Struct.* **2008**, *853*, 68.
[31] A. D. Becke, *J. Chem. Phys.* **1993**, *5648*, 6.
[32] C. Lee, W. Yang, R. G. Parr, *Phys. Rev. B* **1988**, *37*, 785.
[33] K. Fukui, *J. Phys. Chem.* **1970**, *74*, 4161.
[34] A. D. Becke, K. E. Edgecombe, *J. Chem. Phys.* **1990**, *92*, 5397.
[35] A. Saving, R. Nesper, S. Wengert, T. F. Fassler, *Angew. Chem. Int. Ed. Engl.* **1808**, *1997*, 36.
[36] S. Berski, J. Andres, B. Silvi, L. R. Domingo, *J. Phys. Chem.* **2003**, *107*, 6014.

Artykuł D03

A. Kącka-Zych, L.R. Domingo, M. Rios- Gutiérrez, R. Jasiński

Understanding the mechanism of the decomposition reaction of nitroethyl benzoate through the Molecular Electron Density Theory

Theoretical Chemistry Accounts,**136**, 12-138 (2017).

Theor Chem Acc (2017) 136:129
DOI 10.1007/s00214-017-2161-4

REGULAR ARTICLE

Understanding the mechanism of the decomposition reaction of nitroethyl benzoate through the Molecular Electron Density Theory

Agnieszka Kącka-Zych[1] · Luis R. Domingo[2] · Mar Ríos-Gutiérrez[2] · Radomir Jasiński[1]

Received: 26 July 2017 / Accepted: 9 October 2017

Abstract The molecular mechanism of the decomposition reaction of nitroethyl benzoate (NEB) **1** yielding nitroethylene **2** and benzoic acid **3** has been studied within the Molecular Electron Density Theory (MEDT) using DFT methods at the B3LYP/6-31G(d) computational level. This decomposition reaction takes place through a one-step mechanism. Bonding Evolution Theory (BET) analysis of this reaction provides a complete characterisation of the electron density changes along the reaction. The reaction begins through the synchronous rupture of the O–C and C–H single bonds of NEB **1**. Interestingly, while the rupture of the O–C single bond takes place heterolytically, that of the C5–H6 one takes place homolytically, yielding the formation of a *pseudoradical* hydrogen atom. These changes, which demand a high energy cost of 37.1 kcal mol^{-1}, are responsible for the high activation energy associated with this decomposition reaction. Formation of the C–C double bond present in nitroethylene **2** takes place at the end of the reaction. The six differentiated phases in which the IRC associated with this reaction is divided clearly point out its non-concerted nature, thus ruling out the proposed pericyclic mechanism. This reaction, whose associated TS presents a more or less distorted six-membered cyclic structure in which all atoms may not necessarily be bound, is categorised as a *pseudocyclic* reaction.

Keywords Thermal elimination · Nitroalkenes · Molecular electron density theory · Bonding evolution theory · Electron localisation function · *Pseudocyclic* reactions

1 Introduction

The thermal decomposition of alkyl esters to produce alkenes and carboxylic acids is a well-established process experimentally investigated a great number of times [1–5]. Detailed reviews that report on many studies involving the kinetics and mechanism of the decomposition of esters are available [4, 5].

Conjugated nitroalkenes (CNAs) have proved to be a valuable group of reactants in organic chemistry. Their strong electrophilic character makes them important precursors towards a wide variety of target molecules. They are useful compounds applied, e.g. in syntheses of many four-, five- and six-membered compounds in cycloaddition reactions [6–11]. Applications of nitroalkenes in organic synthesis are largely due to their ease of conversion into a variety of functionalities. Moreover, a considerable number of nitroalkenes exhibits remarkable biological activity [12–15].

There are many strategies for the preparation of CNAs. However, the most universal method is that based on the decomposition of nitroalkyl esters. The thermal decomposition of carboxylic esters to yield an alkene and a carboxylic acid has been studied since 1883 [16, 17]. Recently, we theoretically studied the thermal decomposition of nitroalkyl esters [18, 19]. Thus, for the thermal decomposition of nitroethyl benzoate (NEB) **1** yielding nitroethylene **2** and

✉ Agnieszka Kącka-Zych
akacka@chemia.pk.edu.pl

✉ Mar Ríos-Gutiérrez
rios@utopia.uv.es

[1] Institute of Organic Chemistry and Technology, Cracow University of Technology, Warszawska 24, 31-155 Cracow, Poland

[2] Department of Organic Chemistry, University of Valencia, Dr. Moliner 50, 46100 Burjassot, Valencia, Spain

Published online: 20 October 2017

benzoic acid **3**, we proposed [19] that this process could be characterised by a *one-step two-stage* mechanism [20] (see Scheme 1).

This decomposition reaction presents a high activation energy, 42.5 kcal mol^{-1}, the reaction being endothermic by 16.3 kcal mol^{-1}. The geometry of the transition state structure (**TS**) given in Fig. 1 shows that it presents a distorted six-membered rearrangement in which the length of the breaking O–C single bond is 1.750 Å, while the distances between the H atom and the C and O atoms are 1.569 and 1.095 Å, respectively [19].

Contemporary determination of the principles controlling a reaction mechanism is closely tied with the progress of quantum chemistry. One of the fundamental goals for understanding a given chemical rearrangement is to analyse the changes of quantum mechanical observables such as the electron density along the reaction pathway. This approach enables a comprehensive picture of the chemical reactivity in terms of how and when chemical events, e.g. bond rupture and formation processes, will take place. To this end, the Bonding Evolution Theory (BET) [21], which combines the topological analysis of the electron localisation function (ELF) [22] with the mathematical Catastrophe Theory (CT), was proposed [23–25]. BET has proved to be a useful quantum chemical tool for the study of reaction mechanisms [26–29].

Very recently, Domingo proposed the Molecular Electron Density Theory (MEDT) [30], in which changes in the electron density, but not molecular orbital (MO) interactions such as the Frontier Molecular Orbital (FMO) theory proposed [31], are responsible for the reactivity in organic chemistry. Note that the electron density obtained from the wavefunction is the unique physically observable. Within MEDT, besides an exhaustive exploration and characterisation of the reaction paths associated with the studied reaction, analysis of the CDFT reactivity indices [32, 33], as well as quantum chemical tools based on the topological analysis of the molecular electron density such as the ELF [22], the Quantum Theory of Atoms In Molecules (QTAIM) [34] and Non-Covalent Interactions (NCI) [35], are used in order to study the reactivity in organic chemistry.

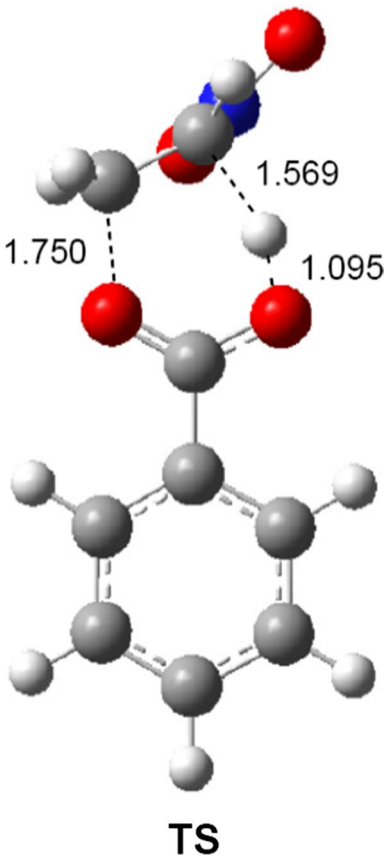

Fig. 1 B3LYP/6-31G(d) geometry of **TS**. Distances are given in angstroms, Å [19]

It is stay accepted that decomposition reactions of alkyl carboxylates are essentially a pericyclic process [36]. Nonetheless, the last reports [37, 38] based on the analysis of the

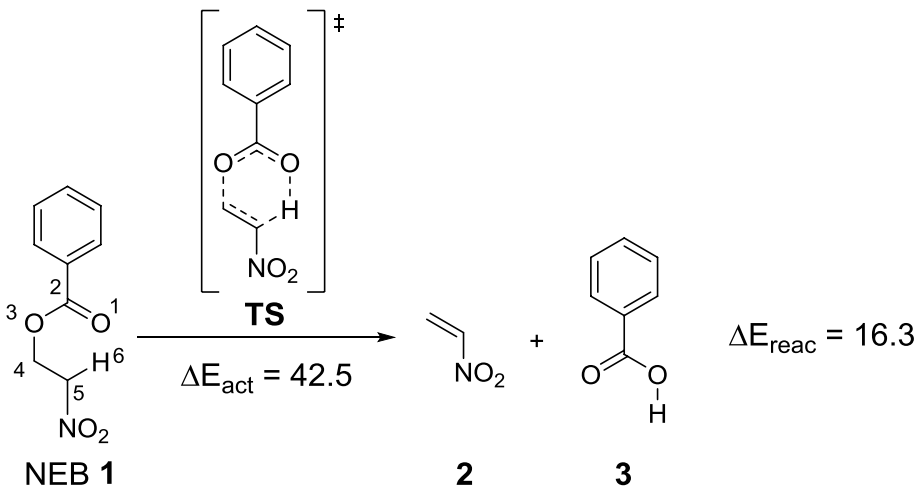

Scheme 1 General scheme of decomposition reaction of nitroethyl benzoate (NEB) **1**. B3LYP/6-31G(d) relative energies with respect to NEB **1** are given in kcal·mol^{-1}. Note that broken lines at **TS** within the breaking and forming regions do not refer to a conjugated cyclic pattern but only indicate the bonds that are going to break or form

evolution of the electron density along a reaction involving a cyclic arrangement of nuclei, i.e. *pseudocyclic* reactions [39], reveal that the pericyclic mechanism does not exist as the bonding changes are not concerted [40]. In this work, as a continuation of the quantum chemical study about the decomposition reaction of nitroethyl carboxylates [18, 19], an MEDT study of the decomposition process of NEB **1** is performed in order to establish the molecular mechanism of this decomposition reaction and the nature of the electronic rearrangement along it.

2 Computational details

Calculations were performed using the Prometheus computer cluster in the CYFRONET regional computer centre in Cracow and the cluster of Domingo's group. All calculations were carried out with the GAUSSIAN 09 package [41]. DFT calculations were performed using the B3LYP [42, 43] functional together with the 6-31G(d) basis set [44]. The stationary points were characterised by frequency calculations in order to verify the number of imaginary frequencies (zero for local minima and one for TSs). The IRC [45] paths, computed using the second order González-Schlegel integration method [46, 47], were traced in order to obtain the energy profiles connecting TS to the two associated minima of the proposed mechanism.

ELF studies were performed with the TopMod [48] programme using the corresponding gas phase B3LYP/6-31G(d) monodeterminantal wavefunctions. For the BET study, the corresponding gas phase reaction channel was followed by performing the topological analysis of the ELF for 855 nuclear configurations along the IRC path. ELF calculations were computed over a grid spacing of 0.1 a.u. for each structure, and ELF localisation domains were obtained for an ELF value of 0.75.

3 Results and discussion

The present theoretical study has been divided into three sections: i) in Sect. 3.1, an ELF topological analysis and a natural population analysis (NPA) of the reagent NEB **1** are performed in order to characterise its electronic structure; ii) in Sect. 3.2, a BET study of the decomposition reaction of NEB **1** is performed in order to characterise the molecular mechanism of this intramolecular process; and finally, iii) in Sect. 3.3, an MEDT study of the decomposition reaction of NEB **1** based, on the one hand, the BET study, and, on the other hand, the analysis of the energies related to the different bonding changes taking place along to the reaction, is given with the aim of providing an explanation of its activation energy.

3.1 ELF and NPA characterisation of the electronic structure of NEB 1

One appealing procedure that provides a straightforward connection between the electron density distribution and the chemical structure is the quantum chemical analysis of Becke and Edgecombe's ELF [22]. Therefore, in order to characterise the electronic structure of NEB **1**, a topological analysis of the ELF was first performed. ELF localisation domains and their attractor positions, together with the most representative valence basin populations, as well as the proposed ELF-based Lewis structure, together with the natural atomic charges, are shown in Fig. 2.

ELF topological analysis of NEB **1** shows the presence of three monosynaptic basins over the O1 and O3 oxygen atoms, V(O1), V′(O1) and V(O3), integrating total electron populations of 5.36e (O1) and 4.60e (O3), four disynaptic basins V(O1, C2), V(C2, O3), V(O3, C4) and V(C4, C5), integrating 2.39e, 1.61e, 1.39e and 1.95e, and one V(C5, H6) protonated basin with a population of 2.07e.

Within the ELF context, monosynaptic basins are associated with non-bonding regions, disynaptic basins are related to bonding regions and protonated basins correspond to bonding regions involving hydrogen atoms [49]. Thus, within the Lewis bonding model [50, 51], the V(O1), V′(O1) and V(O3) monosynaptic basins can be associated with O1 and O3 oxygen lone pairs, the V(O1, C2), V(C2, O3) and V(C5, C4) disynaptic basin with O1–C2, C2–C3 and C4–C5 single bonds, and the V(O3, C4) disynaptic and V(C5,H6) protonated basins with the O3–C4 and C5–H6 bonds that are going to be broken along the decomposition reaction of NEB **1** (see the proposed ELF-based Lewis structure in Fig. 2). Note, however, that the O1 and O3 oxygen "lone pairs" cannot actually be considered so. Interestingly, the V(O1, C2) population, which permits to categorise the O1–C2 bonding region as a single one, and the population of the O1 oxygen monosynaptic basins, ca. 5e, as well as the depopulated O3–C4 single bond, contrast with the common bonding pattern represented for NEB **1** (see the Lewis structures in Fig. 2). It is also worth mentioning that the latter feature may, at first glance, suggest a high feasibility for the rupture of the O3–C4 single bond.

Once the bonding pattern of NEB **1** was established, the charge distribution was analysed through an NPA [47, 48]. Natural atomic charges of the most relevant atoms are shown together with the proposed ELF-based Lewis structure given in Fig. 2. NPA of NEB **1** reveals that while the O1 and O3 oxygen atoms gather the higher negative charges of the six-membered framework involved in the reaction, − 0.61e (O1) and − 0.56e (O3), the C5 carbon is half as negatively charged, − 0.35e, and the C4 carbon only slightly, − 0.14e. On the other hand, while the carbonyl C2 carbon presents a relatively high positive charge, 0.82e, the H6 hydrogen is

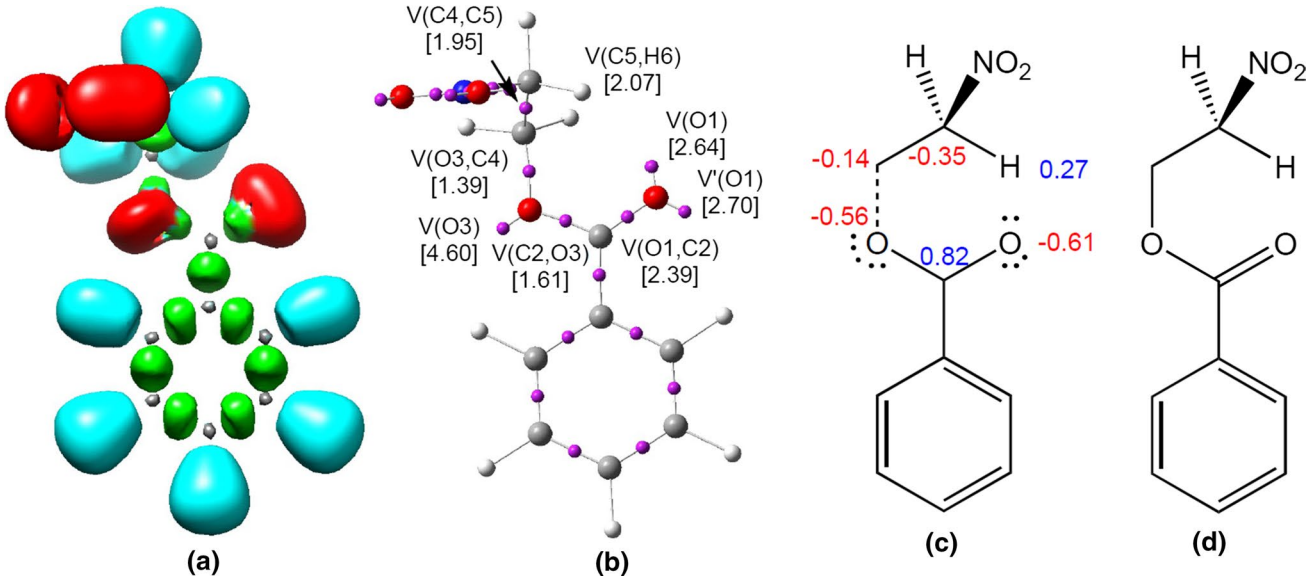

Fig. 2 **a** ELF localisation domains of NEB **1**, represented at an isosurface value of ELF = 0.75; **b** ELF basin attractor positions, together with the most representative valence basin populations; **c** the proposed ELF-based Lewis structures, together with the natural atomic charges, obtained through an NPA; and **d** the commonly used Lewis representation. Negative charges are coloured in red and positive charges are coloured in blue. ELF valence basin population and natural atomic charges are given in average number of electrons, **e**

positively charged by 0.27e. Thus, while the O1, O3, C4 and C5 atoms gather negative charges, only the C2 carbon and the H6 hydrogen are positively charged.

Considering the set of resonance Lewis structures of NEB **1**, neither the O3 oxygen nor the C4 or C5 carbons would never somehow gather negative charges. Consequently, the electronic structure of NEB **1** arising from both the topological analysis of the ELF and the NPA is quite different to that expected (see Fig. 2). Note that the charge distribution obtained through the NPA is the consequence of the asymmetric electron density delocalisation within a molecule resulting from the presence of different nuclei in the molecule, rather than the consequence of the resonance Lewis structures.

3.2 BET study of the decomposition reaction of NEB 1

When trying to achieve a better understanding of the mechanism of organic reactions, the so-called BET [21] has proven to be a very useful methodological tool. This quantum chemical methodology makes it possible to understand the bonding changes along a reaction path and, thus, to establish the nature of the electronic rearrangement associated with a given molecular mechanism [26–29].

The populations, among other relevant parameters, of the most significant ELF valence basins (those associated with the bonding regions directly involved in the reaction) of the selected points of the IRC, **Pi**, defining the different topological phases are gathered in Table 1, while ELF localisation domains and their attractor positions for the points involved in the bond formation processes are shown in Fig. 3.

The long *Phase I* (see Fig. 4), 2.24 Å ≥ d(O1–H6) > 1.52 Å, 1.44 Å ≤ d(O3–C4) < 1.66 Å and 1.09 Å ≤ d(C5–H6) < 1.13 Å, begins at **P0**, which is the discontinue point of the IRC from **TS** towards the isolated reagent NEB **1**. The ELF picture of **P0** usually resembles that of the separated reagents. Thus, ELF topological analysis of **P0** only reveals slight changes in the ELF valence basin electron populations of NEB **1** (see Table 1 and Fig. 2). Along this phase, the population of the V(O1, C2) disynaptic basin progressively decreases, while that of the V(C2, O3) and V(C4, C5) gradually increases, a behaviour maintained until the end of the reaction at **MC**. The V(C5, H6) protonated basin is also slightly depopulated. Note that along this phase, the O1 and H6 atoms remain non-bound.

Phase II, 1.52 Å ≥ d(O1–H6) > 1.35 Å, 1.66 Å ≤ d(O3–C4) < 1.70 Å and 1.13 Å ≤ d(C5–H6) < 1.28 Å, begins at **P1**. At this point, the first most relevant topological change along the reaction path takes place; together with the disappearance of the V(O3, C4) disynaptic basin present in the previous phase by means of a fold *F* catastrophe, a new V′(O3) monosynaptic basin is created with an initial population of 1.04e, strongly increasing the non-bonding total electron density of the O3 oxygen to 5.79e. This significant topological change indicates that the rupture of the O3–C4 single bond begins at an O3–C4 distance of ca. 1.66 Å, resulting in the formation of a O3 *pseudoradical* centre. In this phase, the benzoate framework is formed.

Table 1 ELF valence basin populations, distances of the breaking and forming bonds, relative[a] electronic energies of the IRC points, **P0**–**P5**, defining the six phases characterising the molecular mechanism of the decomposition of NEB **1**. The stationary points **1**, **TS** and **MC** are also included. Distances are given in angstroms, Å, electron populations in average number of electrons, e, and relative energies in kcal mol^{-1}

Points	**1**	**P0**	**P1**	**P2**	**P3**	**P4**	**P5**	**MC**	**TS**
Catastrophes			F	C†	C	F	C†		
Phases			I	II	III	IV	V	VI	
d(O3–C4)	1.435	1.436	1.663	1.696	1.761	1.997	2.006	3.288	1.750
d(C5–H6)	1.088	1.086	1.133	1.283	1.596	1.848	1.856	2.834	1.569
d(O1–H6)	2.707	2.243	1.518	1.353	1.077	0.991	0.990	0.976	1.095
ΔE^{a}	− 5.4	0.0	22.0	30.4	37.1	30.8	30.5	10.9	37.1
V(O1, C2)	2.39	2.37	2.20	2.10	1.95	1.71	1.71	1.64	1.91
V(C2, O3)	1.61	1.59	1.76	1.87	2.07	2.29	2.28	2.37	2.04
V(C4, C5)	1.95	1.99	2.06	2.14	2.51	3.60	1.68	1.74	2.47
V′(C4, C5)							1.92	1.79	
V(O1)	2.64	2.69	2.60	2.20					1.35
V′(O1)	2.70	2.67	2.93	3.32	4.36	4.40	4.39	4.45	4.13
V(O3)	4.60	4.70	4.75	4.62	4.07	3.15	3.14	2.62	4.17
V′(O3)			1.04	1.08	1.41	2.21	2.23	2.71	1.35
V(C5)				1.16	1.15				1.19
V(H6)				0.73					0.58
V(O3, C4)	1.39	1.36							
V(C5, H6)	2.07	2.04	1.96						
V(O1, H6)					1.65	1.79	1.80	1.69	

[a]Relative to the first point of the IRC, **P0**

Phase III, 1.35 Å ≥ d(O1–H6) > 1.08 Å, 1.70 Å ≤ d(O3–C4) < 1.76 Å and 1.28 Å ≤ d(C5–H6) < 1.60 Å, begins at **P2**. At this point, the second most relevant topological change along the reaction path occurs; the V(C5, H6) protonated basin present at the previous phase splits into two new V(C5) and V(H6) monosynaptic basins integrating 1.16e and 0.73e (see **P1** and **TS** in Fig. 3). This significant topological change, associated with a cusp *C* catastrophe, indicates that the rupture of the C5–H6 bond takes place closely after the O3–C4 one, at a C5–H6 distance of ca. 1.28 Å, resulting in the formation of a C5 *pseudoradical* centre and a free *pseudoradical* H6 hydrogen. It should be emphasised that along this phase, the population of the two V(O1) and V′(O1) monosynaptic basins is redistributed between them in such a manner that at the end of this phase both basins end up with 1.30e and 4.15e. In this phase, the TS of the reaction, **TS**, d(O1–H6) = 1.095 Å, d(O3–C4) = 1.750 and d(C5–H6) = 1.569 Å, is found, presenting only slight variations in the ELF basin populations with respect to the topological features of **P2** (see Table 1).

Along *Phases I–III*, the two V(O3, C4) disynaptic and V(C5, H6) protonated basins disappear, while the V(O1, C2) disynaptic basin is being depopulated and those related to the C2–C3 and C4–C5 bonding regions are being populated. Thus, the bonding changes taking place along *Phases I–III*, which are mainly associated with the rupture of the two O3–C4 and C5-H6 bonds, demand a high energy cost (EC) of ca. 37.1 kcal mol^{-1} (see Table 1).

Phase IV, 1.08 Å ≥ d(O1–H6) > 0.99 Å, 1.76 Å ≤ d(O3–C4) < 2.00 Å and 1.60 Å ≤ d(C5–H6) < 1.85 Å, begins at **P3**. At this point, the third most relevant topological change along the reaction path takes place; together with the strong depopulation of the V(O1) and V′(O1) monosynaptic basins by 1.16e, so that both merge into one new V(O1) monosynaptic basin integrating 4.36e, and the disappearance of the V(H6) monosynaptic basin, a new V(O1, H6) protonated basin is created with an initial population of 1.65e through the merger of two V(O1) and V(H6) monosynaptic basins (see **P3** in Fig. 3). This topological change, associated with a cusp *C* catastrophe, reveals that the formation of the new O1-H6 single bond begins at an O1-H6 distance of ca. 1.08 by sharing part of the non-bonding electron density of the O1 oxygen with the *pseudoradical* H6 hydrogen. The V(C5) monosynaptic basin is still present at **P3** with a population of 1.15e, but progressively decreases along *Phase IV* until 0.55e. As a consequence, the population of the adjacent V(C4, C5) disynaptic basin, integrating 2.51e at **P3**, increases in such a manner that the C4–C5 bonding region gradually acquires double bond character (see **P3′**s Lewis structure in Table 2).

Along *Phase IV*, a new V(O1,H6) protonated basin is created and further populated, while the other V(O1, C2), V(C2, O3) and V(C4, C5) disynaptic basins experience the same changes as in previous phases. The electron density of the V(C5) monosynaptic basin gradually decreases, being redistributed into the adjacent V(C4, C5) disynaptic basin provoking its population. Thus, the bonding changes taking place along *Phase IV*, which are mainly associated

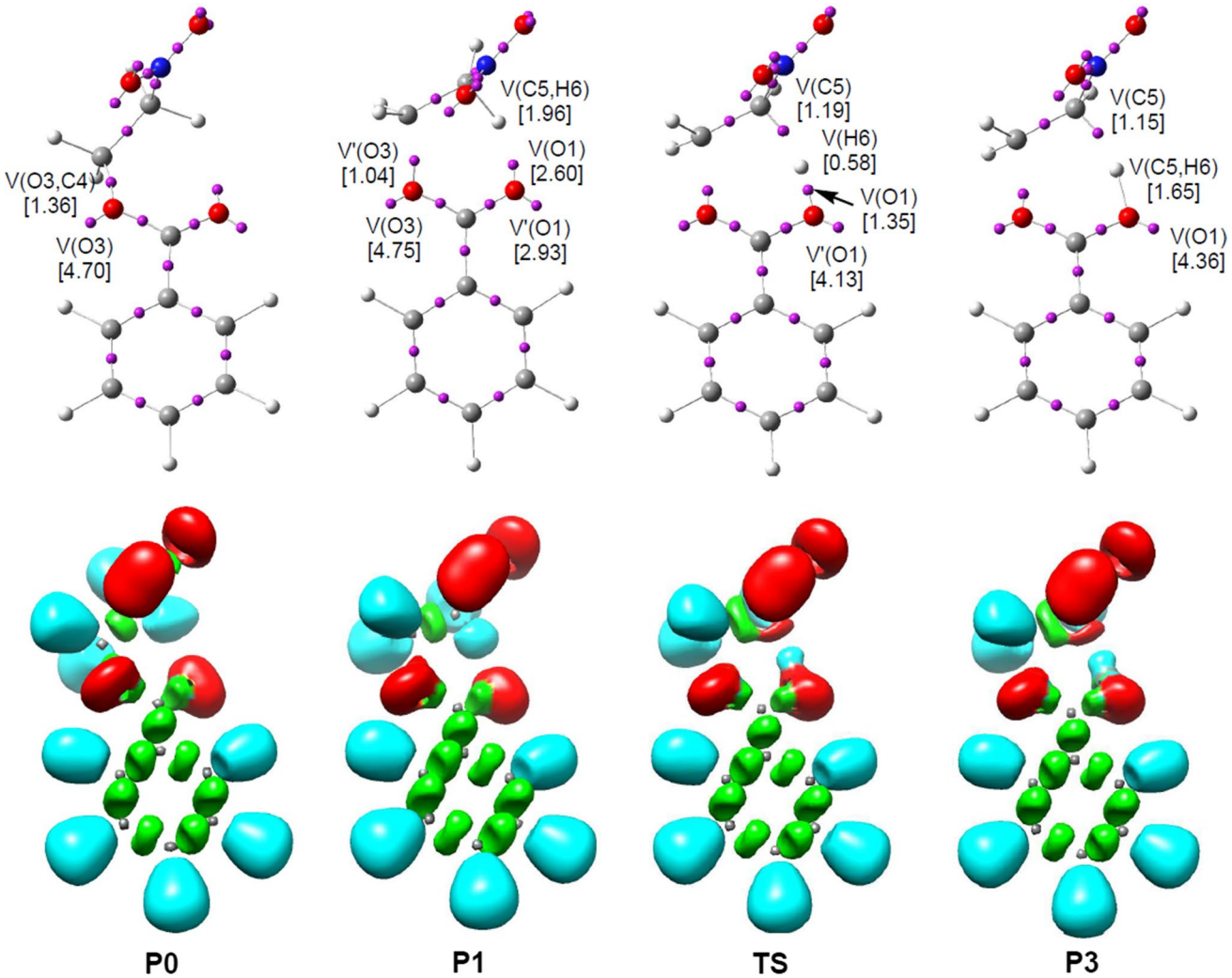

Fig. 3 ELF localisation domains, represented at isosurface values of ELF = 0.75, together with their attractor positions the points of the IRC defining *Phases I* and *II*, involved in the rupture of the O3–C4 and C5–H6 bonds, and **TS** and *Phase IV* involved in the rupture of the C5–H6 bond and the formation of the O1–H6 bond along the decomposition reaction of NEB **1**. The electron populations, in e, are given in brackets

with the formation of the new O1–H6 bond, release a molecular relaxation energy of ca. 6.3 kcal mol^{-1} (see Table 1).

Phase V, 0.991 Å ≥ d(O1–H6) > 0.990 Å, 2.00 Å ≤ d(O3–C4) < 2.01 Å and 1.85 Å ≤ d(C5–H6) < 1.86 Å, begins at **P4**. At this point, established by a fold *F* catastrophe, while the V(C5) monosynaptic basin disappears, the V(C4, C5) disynaptic basin reaches 3.60e as a consequence of the redistribution of the population of the former basin into the latter. This high electron density permits to characterise the C4–C5 bonding region as a double bond at **P4** (see **P4′**s Lewis structure in Table 2). On the other hand, the non-bonding electron density of the O3 oxygen atom is also redistributed between the two V(O3) and V′(O3) monosynaptic basins, integrating 3.15e and 2.21e.

Finally, the long *Phase VI* (see Fig. 4), 0.99 Å ≥ d(O1–H6) ≥ 0.98 Å, 2.01 Å ≤ d(O3–C4) ≤ 3.29 Å and 1.86 Å ≤ d(C5–H6) ≤ 2.83 Å, begins at **P5** and ends at molecular complex **MC**, which is a minimum in the reaction path from **TS** towards the separated products, nitroethylene **2** and benzoic acid **3**. At **P5**, the only notable topological change is the split of the single V(C4, C5) disynaptic basin present in the nitroethylene framework at the previous phase into two new V(C4, C5) and V′(C4, C5) disynaptic basins, integrating 1.68e and 1.92e, by means of a cusp $C^{\dagger}$ catastrophe. This topological change is simply the consequence of an electron density reorganisation within the C4–C5 double bond region, as the total population has not varied.

Along *Phases V* and *VI*, the population of the disynaptic basins corresponding to the C4–C5 bonding region considerably increases, while the population variations of

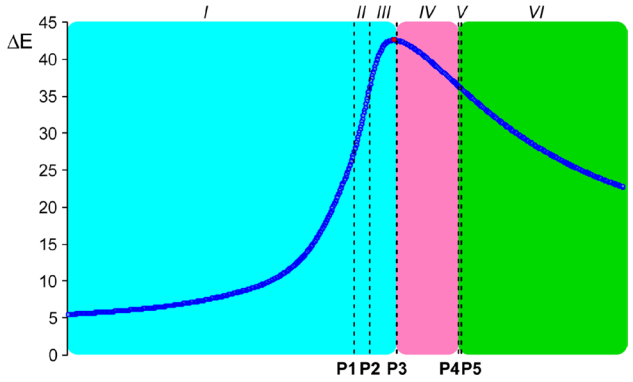

Fig. 4 Phases in which the IRC associated with the decomposition reaction of NEB **1** is topologically divided. The red point indicates the position of **TS**, black broken lines separate the phases defined by points **Pi** along the IRC, while blue, pink and green areas represent the different groups in which the reaction is mechanistically divided. Relative energies (ΔE, in kcal mol^{-1}) are given with respect to the more stable conformational isomer of NEB **1**

the other basins follow the same trend that along previous phases. Consequently, the bonding changes taking place along *Phases V* and *VI*, which are mainly associated with the formation of the C4–C5 double bond of nitroethylene **2** and the complete reorganisation to form the final structures of nitroethylene **2** and benzoic acid **3**, release the maximum MRE along the reaction, ca. 19.9 kcal mol^{-1} (see Table 1).

At **MC**, d(O1–H6) = 0.967, d(O3–C4) = 3.288 Å and d(C5–H6) = 2.834 Å, only slight variations in the ELF basin populations with respect to those calculated at **P5** are observed. After the increase of the population of the monosynaptic basins associated with the O3 oxygen due to the rupture of the O3–C4 single bond, they have been depopulated to 5.33e towards the V(C2, O3) disynaptic basin, which reaches 2.37e. Similarly, the monosynaptic basins associated with the O1 oxygen end up with 4.45e after their early population coming from the V(O1, C2) disynaptic basin and their next depopulation towards the new V(O1, H6) protonated basin, which integrates 1.69e.

From this BET study, the molecular mechanism of the decomposition reaction of NEB **1** can be summarised as follows (see Lewis structures in Table 2): i) this reaction is topologically characterised by six differentiated phases, emphasising the non-concerted nature of the bonding changes taking place along the reaction; ii) the reaction begins with the depopulation of the V(O3, C4) disynaptic and V(C5, H6) protonated basins, associated with the two O3–C4 and C5–H6 bonds that are going to be broken (*Phases I–III*), until they disappear (first the V(O3, C4) disynaptic basins and later the V(C5, H6) protonated one) giving rise to the formation of two V(C5) and V(H6) monosynaptic basins; iii) along *Phases I–III*, no bound six-membered cyclic structure exists. This fact, together with the non-concerted nature of the bonding changes, also allows ruling out the proposed pericyclic mechanism [52, 53] in which the bonding changes take place *"in concert on a closed curve"* assuming a bound cyclic structure; iv) as **TS** is found at the end of *Phase III* (see Fig. 4), the high activation energy associated with this decomposition reaction, 42.5 kcal mol^{-1} (see Table 1), can mainly be related to the disappearance of the mentioned V(O3, C4) and V(C5, H6) basins; v) **TS** consists of three different separated frameworks: the nitroethylene one, the benzoate one and a free *pseudoradical* hydrogen, precluding any conjugation and thus, any aromatic character of the TS [39]; vi) next, a new V(O1, H6) protonated basin, associated with an O1–H6 bond, is formed at *Phase IV* through the merger of two V(O1) and V(H6) monosynaptic basins at $d_{O1\text{-}H6}$ = 1.08 Å, and further populated releasing 6.3 kcal mol^{-1}; and finally, vii) the V(C5) monosynaptic basin disappears towards the V(C4, C5) disynaptic basin, whose population suddenly increases and causes the split into two V(C4, C5) and V′(C4, C5) disynaptic basins associated with the C4–C5 double bond of the nitroethylene framework.

3.3 MEDT study of the decomposition reaction of NEB 1

Within MEDT, the bonding changes are topologically and energetically analysed in order to understand the origin of the activation and the reaction energies associated with an organic reaction. In this section, the bonding changes arising from the BET study and their associated energy changes along the decomposition reaction of NEB **1** are summarised and described in a chemical fashion. Note that BET is a powerful tool to study the bonding changes along a reaction pathway, i.e. the molecular mechanisms, but neither the energies associated with the bonding changes nor energy differences between competitive reaction pathways are analysed within BET.

The sequential bonding changes resulting from the BET study of the decomposition reaction of NEB **1** are summarised in Table 2, together with a simplified representation of the molecular mechanism by ELF-based Lewis structures, while the phases and groups in which the corresponding IRC is topologically divided are represented in Fig. 4. Some appealing conclusions can be drawn from this MEDT study: i) the molecular mechanism of this reaction is topologically characterised by six differentiated phases which, in turn, can be reorganised in three *Groups A–C* associated with significant chemical events (see Table 2 and Fig. 4). This fact clearly allows ruling out the pericyclic mechanism [53] proposed for this reaction; ii) *Group A*, which comprises *Phases I–III* and demands a high EC of ca. 37.1 kcal mol^{-1}, is associated with the rupture of the O3–C4 and C5–H6 bonds of NEB **1**; iii) the rupture of the O3–C4 and C5–H6 bonds, at $d_{O3\text{-}C4}$ = 1.66 Å

Table 2 Sequential bonding changes along the decomposition reaction of NEB **1**, showing the equivalence between the topological characterisation of the different phases and the chemical processes occurring along them. Distances are given in angstroms, Å, while the energies involved in each group, ΔE, are given in kcal mol^{-1}

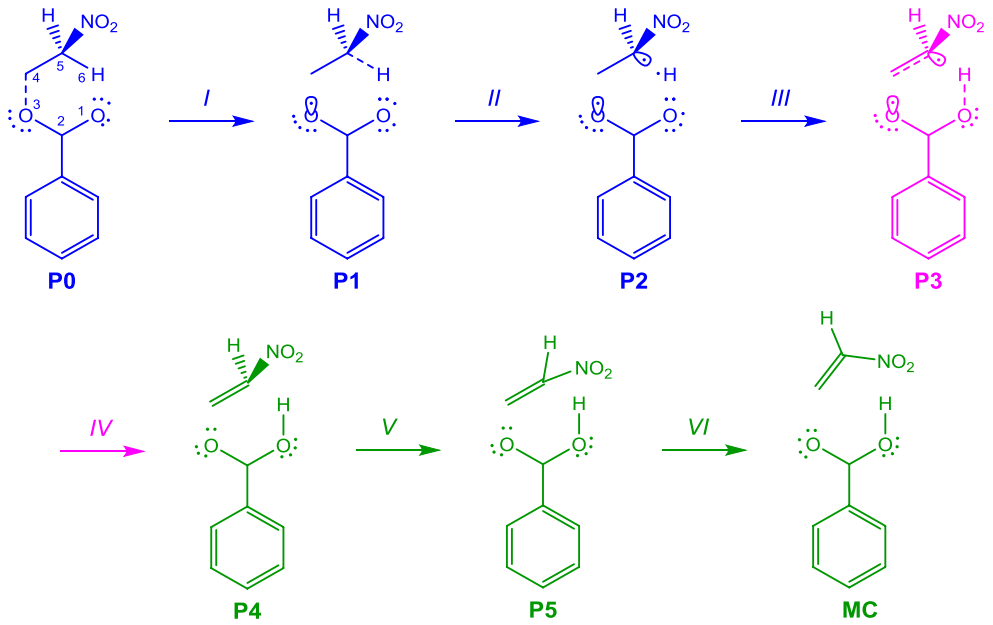

Group	Phases	D_1(O1–H6) d_2(O3–C4) d_3(C5–H6)	ΔE	Topological characterisation	Chemical process
A	*I–III* (**TS**)	$2.24 \geq d_1 > 1.08$ $1.44 \leq d_2 < 1.76$ $1.09 \leq d_3 < 1.60$	37.1	Disappearance of the V(O3, C4) and V(C5, H6) basins	Rupture of the O3–C4 and C5–H6 bonds
B	*IV*	$1.08 \geq d_1 > 0.99$ $1.76 \leq d_2 < 2.00$ $1.60 \leq d_3 < 1.85$	− 6.3	Formation of the V(O1, H6) protonated basin	Formation of the O1–H6 bond
C	*V, VI*	$0.99 \geq d_1 \geq 0.98$ $2.00 \leq d_2 \leq 3.29$ $1.85 \leq d_3 \leq 2.83$	− 19.9	Disappearance of the V(C5) monosynaptic basin and split of the V(C4, C5) disynaptic basin into two V(C4, C5) and V′(C4, C5) disynaptic basins	Formation of the C4–C5 double bond

and $d_{C5\text{-}H6} = 1.28$ Å, is only slightly asynchronous and could be considered a synchronous process ($\Delta d_{O3\text{-}C4} = 0.03$ Å and ($\Delta d_{C5\text{-}H6} = 0.15$ Å); iv) the rupture of these bonds leads to the formation of three O3, C5 and H6 *pseudoradical* centres; v) as **TS** is found at the end of *Phase III*, the high activation energy associated with this decomposition reaction in gas phase, 42.5 kcal mol^{-1}, can mainly be related to the rupture of the O3–C4 (ca. 22.0 kcal mol^{-1}) and C5–H6 (ca. 15.1 kcal mol^{-1}) bonds of NEB **1**, yielding two separated frameworks and a free hydrogen H6 atom stabilised by the C5 *pseudoradical* centre and the non-bonding O1 electron density; vi) the low electron population of the V(O3, C4) disynaptic basin together with the high EC demanded for the rupture of the first O3–C4 single bond suggests that this bond has a strong ionic character; vii) *Group B*, which comprises only *Phase IV* and releases an MRE of 6.3 kcal mol^{-1}, is mainly associated with the formation of the new O1–H6 bond at a O1–H6 distance of ca. 1.1 Å by sharing part of the non-bonding electron density of the O1 oxygen with the free *pseudoradical* H6 hydrogen; and finally, viii) *Group C*, which comprises *Phases V* and *VI* and releases an MRE of 19.9 kcal mol^{-1}, is mainly associated with the formation of the C4–C5 double bond at the nitroethylene framework and to the molecular electronic relaxation associated with the formation of nitroethylene **2** and benzoic acid **3**.

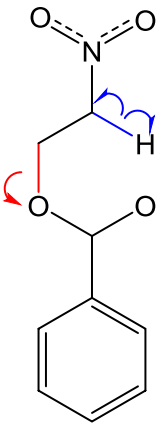

Fig. 5 Main bonding changes on going to **TS**. The rupture of the C–O bond takes place heterolytically (red double-headed arrow), while the rupture of the C–H bond takes place homolytically (two blue single-headed arrows)

4 Conclusions

The molecular mechanism of the decomposition reaction of NEB **1** yielding nitroethylene **2** and benzoic acid **3** has been studied within the MEDT using DFT methods at the B3LYP/6-31G(d) computational level. This decomposition reaction takes place through a one-step mechanism. BET analysis of this reaction provides a complete characterisation of the electron density changes along the reaction. The reaction begins by the synchronous rupture of the O3–C4 and C5–H6 single bonds of NEB **1**. These changes, which demand an energy cost of 37.1 kcal mol^{-1}, are responsible for the high activation energy associated with this decomposition reaction. Interestingly, while the rupture of the first O3–C4 single bond takes place heterolytically, the rupture of the C5–H6 takes place homolytically, leading to the formation of a *pseudoradical* hydrogen atom. Formation of the C4–C5 double bond present in nitroethylene **2** takes place at the end of the reaction. In spite of the fact that this process releases an MRE of 19.9 kcal mol^{-1}, it is not sufficient to overcome the energy demanded for the rupture of the O3–C4 and C5–H6 bonds, and consequently, the overall process is endothermic.

The six differentiated phases in which the IRC associated with this decomposition reaction is divided clearly point out the non-concerted nature of the bonding changes. This behaviour, together with the flux of the electron density on going from the reagent NEB **1** towards **TS1** (see Fig. 5), makes it possible to reject a pericyclic mechanism. These reactions in which the six associated atomic centres are assembled in a more or less distortioned six-membered cyclic rearrangement at the TS but not necessarily bound have recently been categorised as *pseudocyclic* reactions. Consequently, the decomposition reaction of NEB **1** can be considered a non-concerted one-step *pseudocyclic* reaction.

Acknowledgements This research was supported in part by PL-Grid Infrastructure, by the Ministry of Economy and Competitiveness (MINECO) of the Spanish Government (CTQ2016-78669-P). Ríos-Gutiérrez thanks the Spanish MINECO for a pre-doctoral contract co-financed by the European Social Fund (BES-2014-068258).

References

1. Notario R, Quijano J, Sanchez C, Velez E (2005) Theoretical study of the mechanism of thermal decomposition of carbonate esters in the gas phase. J Phys Org Chem 18:134–141
2. Alexander R, Kralert PG, Kagi RI (1992) Kinetics and mechanism of the thermal decomposition of esters in sediments. Org Geochem 19:133–140
3. Saido K, Kuroki T, Ikemura T, Kirisawa M (1983) Studies on the thermal decomposition of phthalate esters. J Anal Appl Pyrol 5:81–87
4. Bailey WJ, Barclay R (1956) Pyrolysis of esters. V. Mechanism of l,4-Elimination. J Org Chem 21(3):328–331
5. Hurd BCh, Blunck FH (1938) The pyrolysis of esters. J Am Chem Soc 60(10):2419–2425
6. Barrett A, Graboski G (1986) Conjugated nitroalkenes: versatile intermediates in organic synthesis. Chem Rev 86:751–762
7. Ballini R, Castagnani R, Petrini M (1992) Chemoselective synthesis of functionalized conjugated nitroalkenes. J Org Chem 4:2160–2162
8. Jasiński R, Kubik M, Łapczuk-Krygier A, Kącka A, Dresler E, Boguszewska-Czubara A (2014) An experimental and theoretical study of the hetero Diels-Alder reactions between (E)-2-aryl-1-cyano-1-nitroethenes and ethyl vinyl ether: one-step or zwitterionic, two-step mechanism? React Kinet Mech Cat 113(2):333–345
9. Perekalin VV, Lipina ES, Berestovitskaya VM, Efremov DA (1994) Nitroalkenes: conugated nitroalkenes. Wiley, New York
10. Kabalka GW, Varma RS (1987) Syntheses and selected reductions of conjugated nitroalkenes. Org Prep Proced Int 19:283–328
11. Jasiński R, Jasińska E, Dresler E (2017) A DFT computational study of the molecular mechanism of [3 + 2] cycloaddition reactions between nitroethene and benzonitrile N-oxides. J Mol Model 23:13–21
12. Boguszewska-Czubara A, Łapczuk-Krygier A, Rykała K, Biernasiuk A, Wnorowski A, Popiołek L, Maziarka A, Hordyjewska A, Jasiński R (2016) Novel synthesis scheme and in vitro antimicrobial evaluation of a panel of (E)-2-aryl-1-cyano-1-nitroethenes. J Enz Inhib Med Chem 31:900–907
13. Al-Zereini W, Schuhmann I, Laatsh H, Helmke E, Anke H (2007) New aromatic nitro compounds from salegentibacter sp. T436, an Arctic Sea Ice Bacterium: taxonomy, fermentation, isolation and biological activities. J Antibiot 60:301–308
14. Clark NG, Croshaw B, Leggetter BE, Spooner DF (1974) Synthesis and antimicrobial activity of aliphatic nitro compounds. J Med Chem 17:977–981

15. Herrera C, Vallejos GA, Loaiza R, Zeledon R, Urbina A, Sepulveda-Boza S (2009) In vitro activity of thienyl-2-nitropropene compounds against trypanosoma cruzi. Mem Inst Oswaldo Cruz 104:980–985
16. Fisher E, Jourdan F (1883) Fischer Indole Synthesis. Chem Ber 16:1069–1075
17. Asinger F, Fell B, Collin G (1963) Über die Doppelbindungsisomerisierung bei höhermolekularen Olefinen, IV. Über den bindungsisomerisierenden Einfluß verschiedener Verbindungen auf n-Undecene. Eur. J Inorg Chem 96(3):716–735
18. Jasiński R, Kącka A (2015) A polar nature of benzoic acids extrusion from nitroalkyl benzoates: DFT mechanistic study. J Mol Model 21:59–65
19. Kącka A, Jasiński R (2016) A density functional theory mechanistic study of thermal decomposition reactions of nitroethyl carboxylates: undermine of "pericyclic" insight. Heteroatom Chem 27:279–289
20. Domingo LR, Saéz JA, Zaragozá RJ, Arnó M (2008) Understanding the participation of quadricyclane as nucleophile in polar $[2\sigma + 2\sigma + 2\pi]$ cycloadditions toward electrophilic π molecules. J Org Chem 73:8791–8799
21. Krokidis X, Noury S, Silvi B (1997) Characterization of elementary chemical processes by catastrophe theory. J Phys Chem A 101:7277–7282
22. Beck AD, Edgecombe KE (1990) A simple measure of electron localization in atomic and molecular systems. J Chem Phys 92:5397–5403
23. Thom R (1976) Structural stability and morphogenesis: an outline of a general theory of models. Inc, Reading, Mass, London-Amsterdam
24. Woodcock AER, Poston T (1974) A geometrical study of elementary catastrophes. Spinger, Berlin
25. Gilmore R (1981) Catastrophe theory for scientists and engineers. Dover, New York
26. Berski S, Andrés J, Silvi B, Domingo LR (2003) The joint use of catastrophe theory and electron localization function to characterize molecular mechanisms. A density functional study of the diels–Alder reaction between ethylene and 1,3-butadiene. J Phys Chem A 107:6014–6024
27. Polo V, Andrés J, Berski S, Domingo LR (2008) Understanding reaction mechanisms in organic chemistry from catastrophe theory applied to the electron localization function topology. J Phys Chem A 112:7128–7136
28. Andrés J, Berski S, Domingo LR, Polo V, Silvi B (2011) Describing the molecular mechanism of organic reactions by using topological analysis of electronic localization function. Curr Org Chem 15:3566–3575
29. Andrés J, González-Navarrete P, Safont V (2014) Unraveling reaction mechanisms by means of quantum chemical topology analysis. Int J Quantum Chem 114:1239–1252
30. Domingo LR (2016) Molecular electron density theory: a modern view of reactivity in organic chemistry. Molecules 21(10):1319–1333
31. Fukui K (1964) Molecular orbitals in Chemistry, Physics and Biology. Academic Press, New York, p 513
32. Geerlings P, De Proft F, Langenaeker W (2003) Conceptual density functional theory. Chem Rev 103:1793–1874
33. Domingo LR, Rios-Gutierrez M, Perez P (2016) Applications of the conceptual density functional theory indices to organic chemistry reactivity. Molecules 21(6):748–769
34. Bader RFW (1990) Atoms in molecules, a quantum theory. Claredon Press, Oxford
35. Johnson ER, Keinan S, Mori-Sanchez P, Contreras-Garcia J, Cohen J, Yang AW (2010) Revealing noncovalent interaction. J Am Chem Soc 132:6498–6506
36. Arnold RT, Smith GG, Dodson RM (1950) Mechanism of the pyrolysis of esters. J Org Chem 15(6):1256–1260
37. Domingo LR, Aurell MJ, Pérez P (2014) Understanding the polar mechanism of the ene reaction. A DFT study. Org Biomol Chem 12:7581–7590
38. Pérez P, Domingo LR (2015) A DFT study of inter- and intramolecular Aryne Ene reactions. Eur J Org Chem 13:2826–2834
39. Domingo LR, Rios-Gutierrez M, Chamorro E, Pérez P (2016) Aromaticity in pericyclic transition state structures? A critical rationalisation based on the topological analysis of electron density. Chem Sel 1(18):6026–6039
40. Domingo LR (2014) Why Diels-Alder reactions are non-concerted processes. J Chil Chem Soc 59:2615
41. Frisch MJ, Trucks GW, Schlegel HB, Scuseria GE, Robb MA, Cheeseman JR, Montgomery JA, Vreven TJ, Kudin KN, Burant JC, Millam JM, Iyengar SS, Tomasi J, Barone V, Mennucci B, Cossi M, Scalmani G, Rega N, Petersson GA, Nakatsuji H, Hada M, Ehara M, Toyota K, Fukuda R, Hasegawa J, Ishida M, Nakajima Y, Honda O, Kitao O, Nakai H, Klene M, Li X, Knox JE, Hratchian HP, Cross JB, Adamo C, Jaramillo J, Gomperts R, Stratmann RE, Yazyev O, Austin AJ, Cammi R, Pomelli C, Ochterski JW, Ayala PY, Morokuma K, Voth GA, Salvador P, Dannenberg JJ, Zakrzewski VG, Dapprich S, Daniels AD, Strain MC, Farkas MC, Malick DK, Rabuck AD, Raghavachari K, Foresman JB, Ortiz JV, Cui Q, Baboul AG, Clifford S, Cioslowski J, Stefanov BB, Liu G, Liashenko A, Piskorz P, Komaromi I, Martin RL, Fox DJ, Keith T, Al-Laham MA, Peng CY, Nanayakkara A, Challacombe M, Gill PMW, Johnson B, Chen W, Wong MW, Gonzalez C, Pople JA (2009) Gaussian 09 rev A.1 Gaussian Inc. Wallingford CT
42. Becke AD (1993) Density-functional thermochemistry. III. The role of exact exchange. J Chem Phys 98:5648–5652
43. Lee WY, Parr RG (1988) Development of the Colle-Salvetti correlation-energy formula into a functional of the electron density. Phys Rev B 37:785–789
44. Hehre WJ, Radom L, Schleyer PVR, Pople JA (1986) Ab initio molecular orbital theory. Wiley, New York
45. Fukui K (1970) Formulation of the reaction coordinate. J Phys Chem 74:4161–4163
46. González C, Schlegel HB (1990) Reaction path following in mass-weighted internal coordinates. J Phys Chem 94:5523–5527
47. González C, Schlegel HB (1991) Improved algorithms for recation path following: higher-order implicit algorithms. J Chem Phys 95:5853–5860
48. Noury S, Krokidis K, Fuster F, Silvi B (1999) Computational tools for the electron localization function topological analysis. Comput Chem 23:597–604
49. Silvi B (2002) The synaptic order: a key concept to understand multicenter bonding. J Mol Struct 614:3–10
50. Lewis GN (1916) The atom and the molecule. J Am Chem Soc 38:762–785
51. Reed AE, Weinstock RB, Weinhold F (1985) Natural population analysis. J Chem Phys 83:735–746
52. Reed AE, Curtiss LA, Weinhold F (1988) Intermolecular interactions from a natural bond orbital, donor-acceptor viewpoint. Chem Rev 88(6):899–926
53. Woodward RB, Hoffmann R (1969) The conservation of orbital symmetry. Angew Chem Int Ed Engl 8:781–853

Artykuł D04

A. Kącka-Zych, L.R. Domingo, R. Jasiński

Does a fluorinated Lewis acid catalyst change the molecular mechanism of the decomposition process of nitroethyl carboxylates?

Research on Chemical Intermediates,

DOI: 10.1007/s11164-017-3106-1 (2017).

Res Chem Intermed
DOI 10.1007/s11164-017-3106-1

Does a fluorinated Lewis acid catalyst change the molecular mechanism of the decomposition process of nitroethyl carboxylates?

Agnieszka Kącka[1] · Luis R. Domingo[2] · Radomir Jasiński[1]

Received: 8 May 2017 / Accepted: 10 August 2017

Abstract The molecular mechanism of the decomposition reaction of nitroethyl benzoates catalyzed by Lewis acids based on boron element—BH_3 and BF_3—was studied using density functional theory methods. These reactions take place much faster than the uncatalyzed process. However, the presence of fluorinated Lewis acids has a unique influence on the molecular mechanism. In the case of BF_3, a change from a one-step mechanism to a two-step one involving a zwitterionic intermediate is observed.

Keywords Thermal elimination · DFT study · Nitroalkene · Fluorine effect

Introduction

Conjugated nitroalkenes (CNAs) are valuable precursors for a wide variety of building blocks and intermediates in organic synthesis [1–3]. These compounds are found to be important because of their biological activities, such as insecticidal [4, 5], fungicidal [5–8], bactericidal [9, 10], and antitumor effects [11], including pharmacologically valuable substances [6–9]. They have proved to be valuable precursors for a wide variety of target molecules. The versatility of the nitro group enables its transformation into many compounds with diverse functionalities [12–14]. Furthermore, CNAs are strong electrophilic ethylenes participating in polar

✉ Agnieszka Kącka
akacka@chemia.pk.edu.pl

[1] Institute of Organic Chemistry and Technology, Cracow University of Technology, Warszawska 24, 31-155 Cracow, Poland

[2] Departamento de Química Orgánica, Universidad de Valencia, Dr. Moliner 50, Burjassot, 46100 Valencia, Spain

Published online: 31 August 2017

Diels–Alder reactions, and alternatively these electrophilic species readily undergo addition reactions with various nucleophiles, thus providing an array of valuable products [11].

Thermal decomposition of alkyl esters to produce alkenes and carboxylic acids is a well-established process that has been studied for over a century [15, 16]. Although some of the decomposition reactions for preparation of nitroalkenes are productive, many of them require strict reaction conditions, are expensive, and lead to low yield of nitroalkenes. Examples include elimination of carboxylic acid from nitroalkyl benzoates carried out at temperature of 180–190 °C [17], and decomposition of nitroalkyl phthalates, which proceeds at 170–185 °C [18]. Additionally, highly reactive nitroalkenes rapidly polymerize under these conditions [19]. Research in this field to identify benign conditions for obtaining conjugated nitroalkenes is therefore essential.

This work is a continuation of our extensive study on the synthesis and fundamental properties of CNAs. Previously [20, 21], we analyzed mechanistic aspects of the decomposition of nitroalkyl carboxylates under thermal conditions. We demonstrated that thermal decomposition of nitroethyl carboxylates should not be recognized as a pericyclic but rather as a two-stage one-step process [22]. We also performed quantum-chemical calculations on the decomposition of nitroalkyl carboxylates catalyzed by triethylsulfonium (TES), triethylphosphonium (TEP) [23], and 1,3-dimethylimidazolium (DMIM) [24] cations. We proved that, in presence of TES, TEP, and DMIM cations, the decomposition process of nitroethyl benzoates takes place much faster than in the same process without catalyst.

It is well known that use of Lewis acids can lead to significant changes in the nature of the molecular mechanism in comparison with the uncatalyzed process [25]. The aim of this work is a quantum-chemical study on the molecular mechanism of the decomposition reactions of model nitroethyl benzoates, without or in presence of inorganic Lewis acid (LA) catalysts, viz. borane (BH_3) and boron trifluoride (BF_3) (Scheme 1).

These catalysts have also been applied for other types of fundamental reaction, for instance, polar Diels–Alder [26–28] or [3 + 2]-cycloaddition reactions [29]. The decomposition process of nitroethyl carboxylates is carried out in dichloromethane environment, because it is a good solvent for LAs [26, 27, 30, 31].

Results and discussion

As shown by M06-2X/6-31 + G(d) calculations, the first step of the decomposition reaction of nitroethyl benzoate (**1a**) is formation of a prereaction complex (**1a[BH$_3$]**) between the ester and the LA- BH_3. Electron-deficient molecules, such as BF_3 and BH_3, contain less than an octet of electrons around one atom, showing a strong tendency to gain an additional pair of electrons by reacting with substances that possess a lone pair of electrons. As a result, a bond is formed. The bond formed between a Lewis acid (BH_3) and nitroethyl benzoate (**1a**) is a coordinate covalent bond, because both electrons are provided by only one of the atoms. After it is formed, however, a coordinate covalent bond behaves like any other covalent single

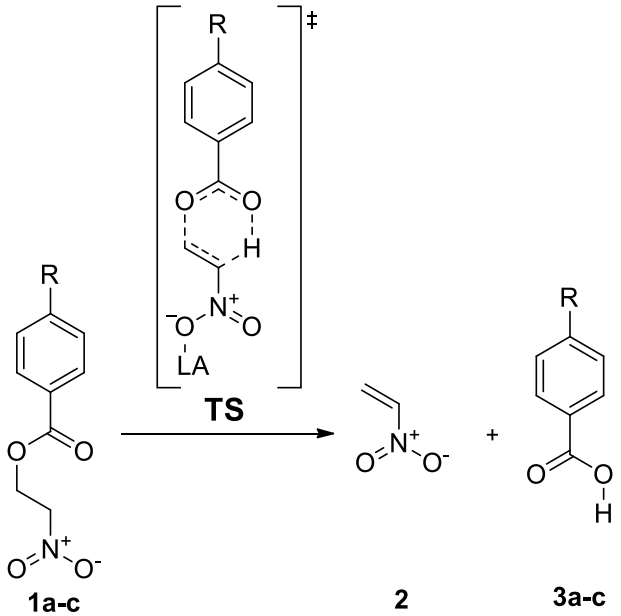

R = a – H, **b** – NO_2, **c** – NMe_2; LA= BH_3 or BF_3

Scheme 1 Mechanism of LA-catalyzed decomposition reaction of nitroethyl benzoates **1a–c**

bond. Consequently, the creation of a prereaction complex entails a drop in reaction enthalpy by 15.0 kcal mol^{-1} (Fig. 1, Table 1). The LA catalyst—BH_3—is located near to the oxygen atom of the nitro group. We also analyzed many other orientations of the LA BH_3 catalyst to the ester molecule. For subsequent research, we chose the most stable form.

Further conversion of the reacting system along the reaction coordinate leads to the transition state structure (**TS**). As these data from M06-2X/6-31 + G(d) calculations show, this is related to an enthalpy increase of over 31.9 kcal mol^{-1} for the reaction catalyzed by the LA BH_3. This barrier, however, is much smaller than suggested by the DFT calculations for a similar decomposition reaction without LA catalysis (about 39.5 kcal mol^{-1}) (Fig. 1, Table 2). Afterwards, the **TS** is converted to products **2** and **3a** (Figs. 1, 2).

In the structure of transition states, a C–H single bond between O5 and H6 atoms is formed. Two double bonds are formed between the C1–C2 and O3–C4 atoms, the C4–O5 bond is changed to a single bond, and the H6–C1 bond becomes broken (Fig. 3, Table 3).

On the basis of the calculations performed, we also analyzed the influence of the LA BH_3 catalyst in the structure of **TS**. It turned out that the H6–C1 bond in the reaction catalyzed by the LA BH_3 is broken earlier than in the uncatalyzed process. In **TS**, the rupture of the O5–H6 single bond is in any case very advanced. The global electron density transfer (GEDT) value for the transition state for the

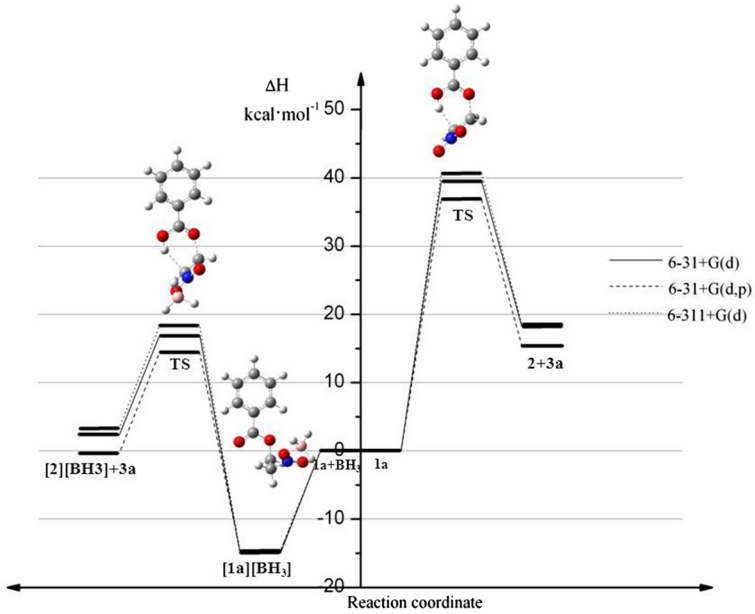

Fig. 1 M06-2X/6-31 + G(d) enthalpy profiles for decomposition of nitroethyl benzoate **1a**, catalyzed by BH_3 and without catalyst

Table 1 M06-2X/6-31 + G(d) kinetic and thermodynamic parameters for decomposition of nitroethyl benzoates catalyzed by BH_3 according to M06-2X calculations ($T = 298$ K; ΔH, ΔG in kcal mol^{-1}, ΔS in cal mol^{-1} K^{-1}; **1a** R = H, **1b** R = NO_2, **1c** R = NMe_2)

Ester	Transition	ΔH	ΔG	ΔS
1a	**1a** + BH_3 → **[1a][BH$_3$]**	−15.0	−4.2	−36.1
	[1a][BH$_3$] → **TS**	31.9	32.2	−1.0
	[1a][BH$_3$] → **[2][BH$_3$]** + **3a**	17.3	5.2	40.6
1b	**1b** + BH_3 → **[1b][BH$_3$]**	−14.9	−3.1	−39.5
	[1b][BH$_3$] → **TS**	34.1	33.8	0.4
	[1b][BH$_3$] → **[2][BH$_3$]** + **3b**	17.3	4.3	43.6
1c	**1c** + BH_3 → **[1c][BH$_3$]**	−15.3	−4.2	−37.5
	[1c][BH$_3$] → **TS**	29.2	30.3	−3.9
	[1c][BH$_3$] → **[2][BH$_3$]** + **3c**	17.8	5.6	40.7

decomposition reaction catalyzed by the Lewis acid BH_3 is 0.40[e]. This value is comparable to the GEDT value for the transition state of similar noncatalytic processes. **TS** structures have a polar nature, as proved by the values of GEDT indices and their dipole moments (Table 3).

The nature of the substituent on the benzene ring also has an impact on the TS, in the case of catalytic reactions and those carried out without presence of catalyst. In the case of the reactions **[1b][BH$_3$]** → **[2][BH$_3$]** + **3b**, the H6–C1 and C2–O3 bonds are broken more slowly than the same bonds in the reaction **[1a][BH$_3$]** → **[2][BH$_3$]** + **3a**. In turn, the H6–C1 and C2–O3 bonds in the case

Table 2 M06-2X/6-31 + G(d) kinetic and thermodynamic parameters for decomposition of nitroethyl benzoates according to M06-2X calculations (T = 298 K; ΔH, ΔG in kcal mol^{-1}, ΔS in cal mol^{-1} K^{-1}; **1a** R = H, **1b** R = NO_2, **1c** R = NMe_2)

Ester	Transition	ΔH	ΔG	ΔS
1a	**1a → TS**	39.5	40.2	−2.2
	1a → 2 + 3a	18.2	6.4	39.8
1b	**1b → TS**	41.4	42.6	−4.2
	1b → 2 + 3b	18.3	6.6	39.3
1c	**1c → TS**	37.4	38.3	−2.9
	1c → 2 + 3c	18.4	6.6	39.5

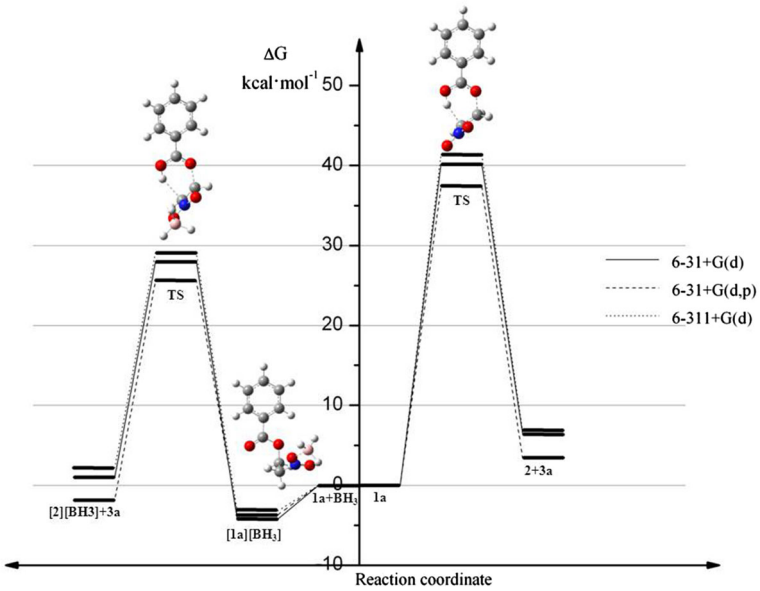

Fig. 2 M06-2X/6-31 + G(d) Gibbs free energy profiles for decomposition of nitroethyl benzoate **1a**, catalyzed by BH_3 and without catalyst

of the reaction **[1c][BH$_3$]** → **[2][BH$_3$]** + **3c** are broken faster than in the case of the reaction **[1a][BH$_3$]** → **[2][BH$_3$]** + **3a** (Table 3).

It should also be mentioned that DFT study using the same M06-2X functional but with larger 6-31 + G(d,p) and 6-311 + G(d) basis sets gives a similar representation of these reactions. These calculations show that the mechanism of the decomposition reaction of nitroalkyl carboxylates catalyzed by the LA BH_3 and without catalyst are also suggestive of a one-step mechanism. In the case of calculations based on M06-2X/6-31 + G(d,p) theory level, we observed a decrease in the activation enthalpy (Figs. 1, 2).

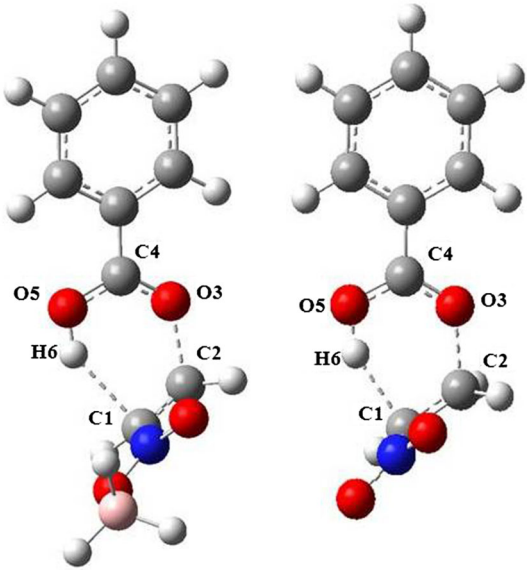

Fig. 3 M06-2X/6-31 + G(d) geometry of **TS**s of decomposition of nitroethyl benzoate **1a**, catalyzed by BH_3 and without catalyst

The situation is quite different in the case of the decomposition reaction of nitroethyl carboxylate catalyzed by the LA BF_3. The results of M06-2X/6-31 + G(d) calculations showed that the first step of the decomposition of nitroethyl benzoate (**1a**) is also formation of a prereaction complex (**1a[BF$_3$]**). Consequently, the creation of a prereaction complex entails a drop of reaction enthalpy by 10.5 kcal mol^{-1} (Fig. 4). Nonetheless, the Gibbs free energy for this transition is equal to 1.0 kcal mol^{-1} (Fig. 4). This is a consequence of large negative entropy changes, linked to an increase in the ordering of the reaction system. The BF_3 molecule is also located near to the oxygen atom of the nitro group, but is bonded to an oxygen atom other than the BH_3 molecule. We analyzed many other orientations of the BF_3 catalyst to the ester molecule, but for further research we chose the most stable form.

Thereafter, the prereaction complex is recast to **TS$_1$**. This transition requires an activation enthalpy which is more than 22 kcal mol^{-1} (Fig. 4, Table 4). However, it is significantly less than in the case of the decomposition process of **1a** without presence of the LA BF_3 (about 39.5 kcal mol^{-1}).

In **TS$_1$**, one single bond breaks (Fig. 5, Table 5). It is the bond between the C1 and H6 atoms. Subsequently, a new single bond between atoms H6 and O5 is formed. It should be mentioned that, in contrast to the LA- BH_3-catalyzed decomposition reaction of **1a** and to the uncatalyzed process, the second single bond C2–O3 is not broken at this reaction stage. **TS$_1$** has an evidently polar, "zwitterionic-like" nature. This is substantiated by the value of the global electron density transfer (GEDT), which is equal to 0.43[e].

Further advance of the reaction leads to intermediate **I**. **I** has a polar, zwitterionic nature, as confirmed by the GEDT value (0.46[e]) and dipole moment (15.67[D]). Decomposition of this intermediate proceeds via **TS$_2$**. This step requires energy of

Table 3 Key parameters for structures in decomposition of nitroethyl benzoates **1a–c**, catalyzed by BH_3 and without catalyst, according to M06-2X/6-31 + G(d) data (**1a** R = H, **1b** R = NO_2, **1c** R = NMe_2)

Reaction	Structure	Interatomic distances (Å)						GEDT [e]	$\bar{\nu}$	Dipole moment, μ (D)
		H6–C1	C1–C2	C2–O3	O3–C4	C4–O5	O5–H6			
1a → 2 + 3a	**1a**	1.088	1.516	1.429	1.349	1.212	2.640			
	TS	1.840	1.418	1.709	1.258	1.300	1.007	0.39	−374.01	11.33
	2 + 3a		1.325		1.213	1.343	0.974			
1b → 2 + 3b	**1b**	1.088	1.517	1.431	1.344	1.210	2.659			
	TS	1.784	1.421	1.705	1.255	1.293	1.019	0.36	−396.25	7.70
	2 + 3b		1.325		1.210	1.339	0.974			
1c → 2 + 3c	**1c**	1.088	1.518	1.425	1.357	1.216	2.632			
	TS	1.920	1.412	1.731	1.262	1.312	0.993	0.40	−355.19	15.83
	2 + 3c		1.325		1.218	1.350	0.973			
[1a][BH_3] → [2][BH_3] + 3a	**[1a][BH_3]**	1.088	1.519	1.425	1.353	1.212	2.605			
	TS	2.090	1.405	1.780	1.249	1.309	0.981	0.40	−319.72	16.40
	[2][BH_3] + 3a		1.327		1.213	1.343	0.974			
[1b][BH_3] → [2][BH_3] + 3b	**[1b][BH_3]**	1.088	1.531	1.425	1.348	1.209	2.549			
	TS	2.059	1.411	1.748	1.248	1.302	0.985	0.39	−317.02	13.61
	[2][BH_3] + 3b		1.327		1.210	1.339	0.974			
[1c][BH_3] → [2][BH_3] + 3c	**[1c][BH_3]**	1.088	1.527	1.420	1.362	1.216	2.567			
	TS	2.479	1.402	1.786	1.265	1.322	0.974	0.43	−376.68	15.45
	[2][BH_3] + 3c		1.327		1.218	1.350	0.973			

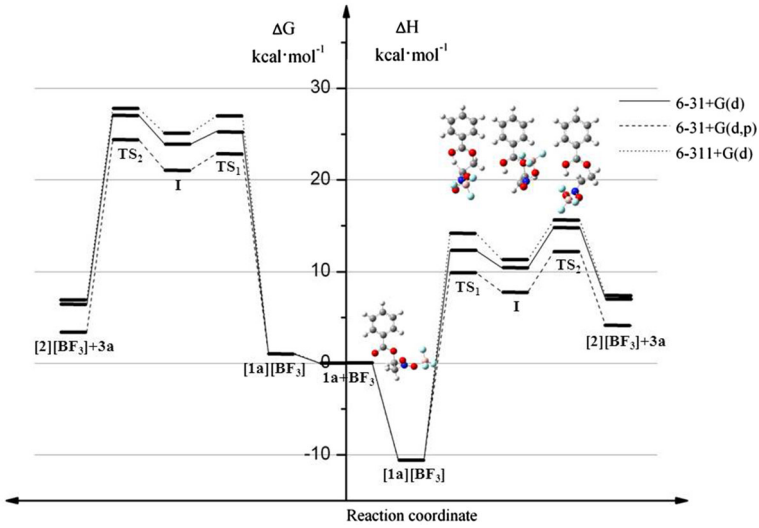

Fig. 4 M06-2X/6-31 + G(d) enthalpy and Gibbs free energy profiles for decomposition of nitroethyl benzoate **1a** catalyzed by BF_3

Table 4 M06-2X/6-31 + G(d) kinetic and thermodynamic parameters for LA BF_3-catalyzed decomposition of nitroethyl benzoates according to M06-2X calculations ($T = 298$ K; ΔH, ΔG in kcal mol^{-1}, ΔS in cal mol^{-1} K^{-1}; **1a** R = H, **1b** R = NO_2, **1c** R = NMe_2)

Ester	Transition	ΔH	ΔG	ΔS
1a	**1a** + BF_3 → **[1a][BF$_3$]**	−10.5	1.0	−38.6
	[1a][BF$_3$] → **TS$_1$**	22.8	24.3	−5.1
	[1a][BF$_3$] → **I**	20.9	22.9	−6.7
	[1a][BF$_3$] → **TS$_2$**	25.3	26.1	−2.5
	[1a][BF$_3$] → **[2][BF$_3$]** + **3a**	17.5	5.4	40.7
1b	**1b** + BF_3 → **[1b][BF$_3$]**	−10.1	1.8	−39.9
	[1b][BF$_3$] → **TS$_1$**	24.9	26.0	−3.5
	[1b][BF$_3$] → **I**	23.5	24.0	−1.8
	[1b][BF$_3$] → **TS$_2$**	26.8	27.6	−3.0
	[1b][BF$_3$] → **[2][BF$_3$]** + **3b**	17.2	4.8	41.7
1c	**1c** + BF_3 → **[1c][BF$_3$]**	−11.1	−0.3	−35.6
	[1c][BF$_3$] → **TS$_1$**	20.1	22.4	−7.8
	[1c][BF$_3$] → **I**	16.2	19.0	−9.4
	[1c][BF$_3$] → **TS$_2$**	23.1	25.6	−8.2
	[1c][BF$_3$] → **[2][BF$_3$]** + **3c**	18.1	7.2	36.5

25.3 kcal mol^{-1} (Fig. 4, Table 4). In the structure of **TS$_2$**, the C2–O3 single bond breaks (Fig. 5, Table 5).

We also performed quantum-chemical study on the decomposition of the other nitroethyl benzoates **1b** and **1c**. In the reaction **[1b][BF$_3$]** → **[2][BF$_3$]** + **3b**, it was found that the H6–C1 and C2–O3 single bonds are broken more slowly (2.798 Å and 1.845 Å) than in the reaction **[1a][BF$_3$]** → **[2][BF$_3$]** + **3a**. In turn, the H6–C1

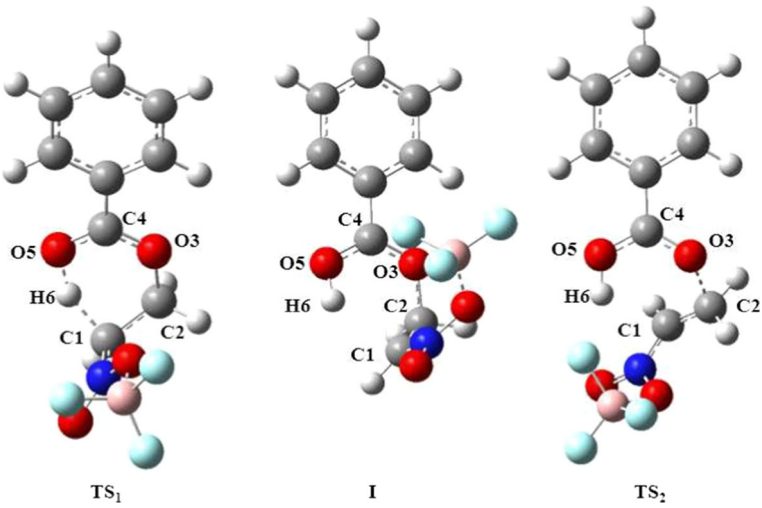

Fig. 5 M06-2X/6-31 + G(d) geometries of the **TS**s and intermediate associated with LA- BF_3-catalyzed decomposition of nitroethyl benzoate **1a**

and C2–O3 single bonds are broken faster (2.952 Å and 1.938 Å) in the reaction **[1c][BF_3] → [2][BF_3] + 3c** than in the case of the reaction **[1a][BF_3] → [2][BF_3] + 3a**.

The decompositions of the nitroethyl benzoates **1a–c** proceed according to a similar mechanistic scheme at the higher theory levels of M06-2X/6-31 + G(d,p) and M06-2X/6-311 + G(d). Calculations at M06-2X/6-31 + G(d,p) level gave slightly lower activation enthalpy (Fig. 4).

On the grounds of the quantum-chemical calculations, we propose the mechanisms of the decomposition reactions of nitroethyl benzoates **1a–c** catalyzed by the LAs BH_3 and BF_3 shown in Scheme 2. It turned out that the LA BH_3-catalyzed decomposition reactions of nitroethyl carboxylates proceed via a polar one-step mechanism. In turn, the decomposition of nitroethyl carboxylates catalyzed by the fluorinated LA BF_3 proceeds via a two-step mechanism involving a zwitterionic intermediate.

Computational details

All calculations reported in this paper were performed on the "Prometheus" computer cluster in the CYFRONET regional computer center in Cracow. The mechanism of decomposition of nitroalkyl benzoates catalyzed by LAs was examined as implemented in the GAUSSIAN 09 package [32]. The geometric parameters for all the reactants, **TS**s, and products of the reactions studied were fully optimized using the density functional theory (DFT) method. The calculations were performed at M06-2X level with the 6-31 + G(d) basis set. The B3LYP functional was replaced by M06-2X because of its increased accuracy. Additionally,

Table 5 Key parameters for structures in decomposition of nitroethyl benzoates catalyzed by BF_3 according to M06-2X/6-31 + G(d) data (**1a** R = H, **1b** R = NO_2, **1c** R = NMe_2)

Reaction	Structure	Interatomic distances (Å)						GEDT [e]	$\bar{\nu}$	Dipole moment, μ (D)
		H6–C1	C1–C2	C2–O3	O3–C4	C4–O5	O5–H6			
[1a][BF$_3$] → [2][BF$_3$] + 3a	**[1a][BF$_3$]**	1.088	1.524	1.423	1.355	1.211	2.640			
	TS$_1$	1.452	1.504	1.464	1.298	1.265	1.157	0.43	−1159.63	15.43
	I	2.122	1.484	1.478	1.279	1.291	0.983	0.46		15.67
	TS$_2$	2.811	1.396	1.876	1.249	1.307	0.987	0.34	−339.19	14.77
	[2][BF$_3$] + 3a		1.328		1.213	1.343	0.974			
[1b][BF$_3$] → [2][BF$_3$] + 3b	**[1b][BF$_3$]**	1.089	1.525	1.426	1.349	1.208	2.676			
	TS$_1$	1.487	1.500	1.472	1.290	1.264	1.136	0.43	−1024.06	14.47
	I	2.124	1.482	1.486	1.273	1.287	0.983	0.40		15.26
	TS$_2$	2.798	1.400	1.845	1.246	1.300	0.990	0.34	−323.39	9.95
	[2][BF$_3$] + 3b		1.328		1.210	1.339	0.974			
[1c][BF$_3$] → [2][BF$_3$] + 3c	**[1c][BF$_3$]**	1.088	1.526	1.420	1.363	1.216	2.584			
	TS$_1$	1.400	1.508	1.453	1.314	1.269	1.195	0.39	−1243.81	18.29
	I	2.105	1.489	1.464	1.295	1.305	0.981	0.50		19.71
	TS$_2$	2.952	1.387	1.938	1.258	1.319	0.985	0.31	−370.46	20.52
	[2][BF$_3$] + 3c		1.328		1.218	1.350	0.973			

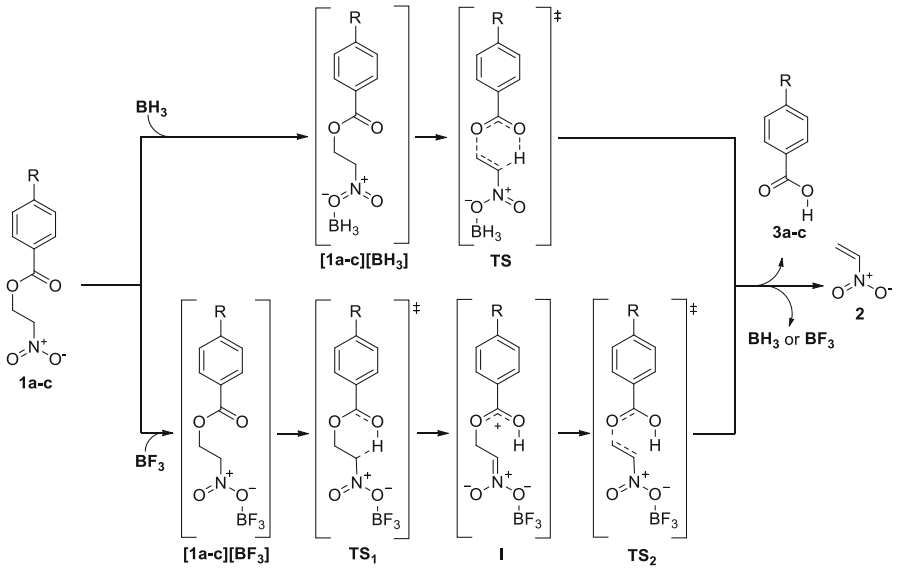

Scheme 2 Mechanisms of decomposition reaction of nitroethyl benzoates **1a–c** catalyzed by LAs BH_3 and BF_3

calculations using the more advanced 6-31 + G(d,p) and 6-311 + G(d) basis sets were carried out.

Published reports show that a similar approach was used successfully to explore a reaction involving several different nitro and other compounds [33–35]. M06-2X is a hybrid meta exchange–correlation functional developed recently [36], parameterized to include short-range dispersion energy. Geometry optimization calculations were carried out to obtain the global minima for the reactants and products, and to locate the saddle point for the **TS**. Stationary points were characterized by frequency calculations. All reactants and products had positive Hessian matrices. All **TS**s had only one negative eigenvalue in their diagonalized Hessian matrices, and their associated eigenvectors were confirmed to correspond to motion along the reaction coordinate under consideration. **TS**s were located using the (QST2) algorithm. Intrinsic reaction coordinate (IRC) calculations [37] were carried out for all events to verify that the localized **TS**s connected with the corresponding minimum stationary points associated with reactants, products, and intermediates.

The reaction environment polarity was simulated using a relatively simple self-consistent reaction field (SCRF) [38–40] based on the polarizable continuum model (PCM) of Tomasi's group [41–43]. Since the solvent used is usually dichloromethane, we used a dielectric constant at 298.0 K of $\varepsilon = 8.93$.

Charge global electron density transfer (GEDT) [44] was calculated according to the formula

$$\mathrm{GEDT} = -\Sigma q_{\mathrm{A}},$$

where q_{A} is the net charge and the sum is taken over all the atoms of the substructure.

The values of enthalpies, entropies, and free energies in all calculations were calculated using standard statistical thermodynamics at 25 °C and 1 atm [45].

Conclusions

This quantum-chemical DFT study demonstrates that the LA BH_3-catalyzed decomposition reactions of nitroethyl benzoates proceed via a polar one-step mechanism. By contrast, the decomposition reaction of nitroethyl benzoates catalyzed by the fluorinated LA BF_3 proceeds via a two-step mechanism involving formation of a zwitterionic intermediate. These decomposition reactions, catalyzed by the LAs BH_3 and BF_3, take place much faster than the same reactions without catalyst.

Acknowledgements Partial support of this research by PL-Grid Infrastructure and financial support from the Polish State Committee (Grant No. C-2/88/2016/DS) are gratefully acknowledged.

References

1. R. Ballini, R. Castagnani, M. Petrini, J. Org. Chem. **4**, 2160 (1992)
2. V.V. Perekalin, E.S. Lipina, V.M. Berestovitskaya, D.A. Efremov, *Nitroalkenes: Conjugated Nitroalkenes* (Wiley, New York, 1994)
3. S.H. Lee, Y.J. Park, ChM Yoon, Org. Biomol. Chem. **1**, 1099 (2003)
4. P.W. Brian, M. Jamieson, J.C. McGowan, Nature **162**, 780 (1948)
5. F.C. Bocobo, A.C. Curtis, W.D. Block, E.R. Harrell, E.E. Evans, R.F. Haines, Antibiot. Chemother. **6**, 385 (1956)
6. P.W. Brian, J.F. Grove, J.C. McGowan, Nature **158**, 876 (1946)
7. J.C. McGowan, P.W. Brian, H.G. Hemming, Ann. Appl. Biol. **35**, 25 (1948)
8. Y. Hoashi, T. Yabuta, Y. Takemoto, Tetrahedron Lett. **45**, 9185 (2004)
9. O. Schales, H.A. Graefe, J. Am. Chem. Soc. **74**, 4486 (1952)
10. S. Kaap, I. Quentin, D. Tamiru, M. Shaheen, K. Eger, H.J. Steinfelder, Biochem. Pharmacol. **65**, 603 (2003)
11. K. Zee-Cheng, C. Cheng, J. Med. Chem. **12**, 157 (1969)
12. R. Ballini, G. Bosica, Synthesis **7**, 723 (1994)
13. A.G.M. Barrent, Chem. Soc. Rev. **20**, 95–127 (1991)
14. B.P. Bandgar, L.S. Uppalla, Synth. Commun. **30**, 2071 (2000)
15. V.V. Perekalin, E.S. Lipina, V.M. Berestovitskaya, D.A. Efremov, *Nitroalkenes: Conjugated Nitroalkenes* (Wiley, New York, 1994)
16. R. Alexander, P.G. Kralert, R.I. Kagi, Org. Geochem. **19**, 133 (1992)
17. L. Leseticky, V. Fidler, M. Prochazka, Collect. Czechoslov. Chem. Commun. **38**, 459 (1973)

18. G.D. Buckley, C.W. Scaife, J. Chem. Soc. **280**, 1471 (1947)
19. B.A.T. Blomquist, W.J. Tapp, J.R. Johnson, J. Am. Chem. Soc. **67**, 1519 (1945)
20. R. Jasiński, A. Kącka, J. Mol. Mod. **21**, 59 (2015)
21. A. Kącka, R. Jasiński, Heteroatom Chem. **27**, 279–289 (2016)
22. L.R. Domingo, J.A. Saéz, R.J. Zaragozá, M. Arnó, J. Org. Chem. **73**, 8791–8799 (2008)
23. A. Kącka, R. Jasiński, Phosphorus Sulfur Silicon Relat. Elem. (2017). doi:10.1080/10426507.2017.1290626
24. A. Kącka, R. Jasiński, Curr. Chem. Lett. **6**, 15 (2017)
25. I.H. Sanches, R. Yanez, R. Enriquez, P. Joseph-Nathan, J. Org. Chem. **46**, 2818 (1981)
26. L.R. Domingo, M. Arnó, J. Andrés, J. Org. Chem. **64**, 5867 (1999)
27. L.R. Domingo, A. Asensio, J. Org. Chem. **65**, 1076 (2000)
28. L.R. Domingo, A. Asensio, P. Arroyo, J. Phys. Org. Chem. **15**, 660 (2002)
29. J. Tanakap, Sh Kanemasa, Tetrahedron **57**, 899 (2001)
30. L.R. Domingo, M.J. Aurell, R. Jalal, M. Esseffar, Comput. Theor. Chem. **986**, 6 (2012)
31. L.R. Domingo, P. Perez, D.E. Ortega, J. Org. Chem. **78**, 2462–2471 (2013)
32. M.J. Frisch, G.W. Trucks, H.B. Schlegel, G.E. Scuseria, M.A. Robb, J.R. Cheeseman, J.A. Montgomery, T.J. Vreven, K.N. Kudin, J.C. Burant, J.M. Millam, S.S. Iyengar, J. Tomasi, V. Barone, B. Mennucci, M. Cossi, G. Scalmani, N. Rega, G.A. Petersson, H. Nakatsuji, M. Hada, M. Ehara, K. Toyota, R. Fukuda, J. Hasegawa, M. Ishida, Y. Nakajima, O. Honda, O. Kitao, H. Nakai, M. Klene, X. Li, J.E. Knox, H.P. Hratchian, J.B. Cross, C. Adamo, J. Jaramillo, R. Gomperts, R.E. Stratmann, O. Yazyev, A.J. Austin, R. Cammi, C. Pomelli, J.W. Ochterski, P.Y. Ayala, K. Morokuma, G.A. Voth, P. Salvador, J.J. Dannenberg, V.G Zakrzewski, S. Dapprich, A.D. Daniels, M.C. Strain, M.C. Farkas, D.K. Malick, A.D. Rabuck, K. Raghavachari, J.B. Foresman, J.V. Ortiz, Q. Cui, A.G. Baboul, S. Clifford, J. Cioslowski, B.B. Stefanov, G. Liu, A. Liashenko, P. Piskorz, I. Komaromi, R.L. Martin, D.J. Fox, T. Keith, M.A. Al-Laham, C.Y. Peng, A. Nanayakkara, M. Challacombe, P.M.W. Gill, B. Johnson, W. Chen, M.W. Wong, C. Gonzalez, J.A. Pople, Gaussian 09 rev A.1 Gaussian Inc, Wallingford CT, (2009)
33. L. Rhyman, P. Ramasami, J.A. Joule, J.A. Saez, L.R. Domingo, RSC Adv. **3**, 447 (2013)
34. D. Rayenne, A.Y. Ouassila, K. Djameleddine, Can. J. Chem. **93**, 1115 (2015)
35. Y. Qiao, X. Chen, D. Wei, J. Chang, Sci. Rep. **6**, 38200 (2016)
36. Y. Zhao, N.E. Schultz, D.G. Truhlar, J. Chem. Theory Comput. **2**, 364 (2016)
37. K. Fukui, J. Phys. Chem. **74**, 4161–4163 (1970)
38. O. Tapia, J. Math. Chem. **10**, 139 (1992)
39. J. Tomasi, M. Persico, Chem. Rev. **94**, 2027 (1994)
40. B.Y. Simkin, I. Sheikhet, *Quantum Chemical and Statistical Theory of Solutions—a Computational Approach* (Ellis Horwood, Chichester, 1995)
41. M.T. Cances, V. Mennunci, J. Tomasi, J. Chem. Phys. **107**, 3032 (1997)
42. M. Cossi, V. Barone, R. Cammi, J. Tomasi, Chem. Phys. Lett. **255**, 327 (1996)
43. V. Barone, M. Cossi, J. Tomasi, Comput. Chem. **19**, 404 (1998)
44. L.R. Domingo, RSC Adv. **4**, 32415 (2014)
45. S. Berski, J. Andres, B. Silvi, L.R. Domingo, J. Phys. Chem. **107**, 6014 (2003)

Artykuł D05

A. Kącka, R. Jasiński

Triethylsulfonium and triethylphosphonium cations as novel catalyst for the decomposition process of nitroethyl benzoates.

Phosphorous, Sulfur, and Silion and the Related Elements,

DOI: 10.1080/10426507.2017.1290626 (2017).

PHOSPHORUS, SULFUR, AND SILICON
http://dx.doi.org/10.1080/10426507.2017.1290626

Taylor & Francis
Taylor & Francis Group

Triethylsulfonium and triethylphosphonium cations as novel catalysts for the decomposition process of nitroethyl benzoates

Agnieszka Kącka and Radomir Jasiński

Institute of Organic Chemistry and Technology, Cracow University of Technology, Cracow, Poland

ABSTRACT

A quantum chemical study of the decomposition reactions of nitroethyl benzoates catalyzed by triethylsulfonium and triethylphosphonium cations was carried out using various DFT theory levels. It was found that these reactions take place according to a one-step but polar mechanism, and much faster than the uncatalyzed process.

ARTICLE HISTORY
Received 17 November 2016
Accepted 31 January 2017

KEYWORDS
Thermal elimination; DFT study; nitroalkene; triethylsulfonium cation; triethylphosphonium cation

GRAPHICAL ABSTRACT

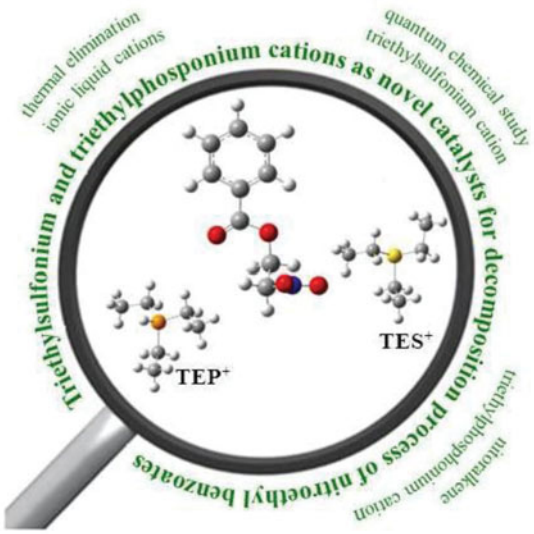

Introduction

The synthesis of conjugated nitroalkenes (CNA) has been a challenge for many years because of their importance in terms of their application as either biologically or pharmacologically active substances.[1–6,7] As stated, some nitroalkene motifs have also been reported as pro-apoptotic anticancer[8] and antibacterial agents.[9] Nitroalkenes are also valuable precursors to a wide variety of building blocks, and in organic synthesis as key intermediates in the construction of more complex molecules.[10–13] The synthetic versatility of these derivatives arises from the powerful electron-withdrawing effect of the nitro substituent that makes them hard electrophiles and, therefore, good Michael acceptors[14–16] as well as efficient dienophiles in Diels-Alder reactions[17–20] and dipolarophiles in 1,3-dipolar cycloadditions.[21–25] The versatility in organic synthesis is largely due to the ease with which they are transformed in to various functionalities.[26] For example, they provide access to useful synthetic precursors such as amines,[27] nitroalkanes,[28] ketones,[29] oximes,[30] or N-substituted hydroxylamines.[31]

The most common method for the preparation of nitroalkenes involves the decomposition of nitroalkyl esters.[32] The thermal decomposition of alkyl esters to produce alkenes and carboxylic acids is a well-established process that has been studied for over a century.[33] Although some of the decomposition reactions for the preparation of nitroalkenes are efficient, they are provided in strict reaction conditions, are expensive, and lead with a low yield to nitroalkenes. For example, decompositions of nitroalkyl phthalates proceed at 170–185°C.[34] As similar elimination of carboxylic acid from nitroalkyl benzoates is carried out at a temperature 180–190°C.[35] Unfortunately,

CONTACT Agnieszka Kącka akacka@chemia.pk.edu.pl Institute of Organic Chemistry and Technology, Cracow University of Technology, Warszawska 24, 31-155 Cracow, Poland.
Color versions of one or more of the figures in the article can be found online at www.tandfonline.com/gpss.

simple, high reactive nitroalkenes such as nitroethene, nitropropenes, and many others, rapidly polymerize under these conditions.[36] Therefore, research undertaken in the field on looking for mild conditions of obtained CNA are necessary and justified.

This present work is a continuation of our comprehensive study on the decomposition process of nitroalkyl carboxylates.[22,37] Previously, we performed a DFT mechanistic study of the decomposition reaction of selected nitroalkyl benzoates. We demonstrated that the thermal decomposition of nitroethyl carboxylates cannot be considered as a pericyclic process. Detailed analysis indicated that these process should be included in the group of "one-step two-stage" reactions.[22]

Ionic liquids, in different ways, have been applied in catalysis: as the catalyst itself, as a co-catalyst or catalyst activator, as the source of a new ligand for a catalytic metal centre, or just as the solvent for the reaction. In the literature we find many examples of applications of ionic liquids in catalysis.[38–43] For example, phosphonium and sulfonium ionic liquids are applied as catalysts in the thermal decomposition of cyclic organic peroxides[44] and hydrothermal decomposition reactions of cellulose, glucose and fructose.[45]

The potentially powerful way in which an ionic liquid can be used in catalysis is as a combination of both solvent and catalyst. However, changing the solvent leads to a faster reaction, and the new solvent can be viewed as being a catalyst. After all, the reaction has been accelerated and the solvent has remained unchanged by the process.[46]

The aim of this work is a quantum chemical study of the molecular mechanism of the decomposition reaction of model nitroethyl benzoates in the presence of Et_3PH^+ and Et_3S^+ cations. The cations may be obtained from ionic liquids, which have been generating interest over the last decade due to their properties. Ionic liquids with these cations have been tested in practice as reaction mediums for several organic reactions.[38,47–49]

Results and discussion

Computational details

All calculations were carried out using the Prometheus computer cluster in the CYFRONET regional computer centre in Cracow. The mechanism of the decomposition of nitroalkyl benzoates catalyzed by the triethylsulfonium and the triethylphosphonium cations have been examined as implemented in GAUSSIAN 09 package.[50] The geometric parameters for all the reactants, transition states and products of the reactions studied were fully optimized using the density functional theory (DFT) method. The calculations were performed using the B3LYP[51] with 6–31G(d) basic set. Additionally, calculations in more advanced 6-31G(d,p), 6-31+G(d), and 6-31++G(d) basis sets, were carry out.

Recently published reports[52–58] show that a similar approach was used successfully for the exploration of a reaction involving several different nitro compounds. B3LYP is a combination of Becke's three parameter hybrid exchange functional[59] with the Lee, Yang and Parr correlated functional.[60] Geometry optimization calculations have been carried out to obtain the global minima for the reactant and products, and to locate the saddle point for the transition state. Stationary points were characterised by frequency calculations. All reactants, and products had positive Hessian matrices. All transition states showed only one negative eigenvalue in their diagonalized Hessian matrices, and their associated eigenvectors were confirmed to correspond to the motion along the reaction coordinate under consideration. Transition states were located using the (QST2) algorithm. For the optimization process, the Berny analytical gradient was employed. Intrinsic reaction coordinate (IRC) calculations[61] have been made in all events to verify that the localized transition state structures connect with the corresponding minimum stationary points associated with reactants and products.

The reaction environment polarity was simulated using Polarizable Continuum Model (PCM).[62] It was assumed that the reaction environment has dielectric constant, $\varepsilon = 14.1$, for reaction catalyzed by triethylsulfonium cation, and $\varepsilon = 10.1$ for the reaction catalyzed by triethylphosphonium cation (the most typical triethylsulfonium ionic liquids have $\varepsilon = \sim 13.2–15.8$[63,64] and the triethylphosphonium ionic liquid have $\varepsilon = \sim 8–12$[65]).

Charge global electron density transfer (GEDT)[66] was calculated according to the formula:

$$\mathrm{GEDT} = -\Sigma q_A$$

where q_A is the net charge and the sum is taken over all the atoms of the substructure.

The values of enthalpies, entropies and free energies in all calculations were calculated with the standard statistical thermodynamics at 25°C and 1 atm.[67]

Energetical aspects of the decomposition reactions catalyzed by the TES and the TEP cations

Results of the B3LYP/6–31G(d) calculations showed, that the first step of the decomposition of nitroethyl benzoate (**1a**) is the formation of a pre-reaction complex (**[1][TES]** and **[1][TEP]**) between the molecule of the ester and the triethylsulfonium and the triethylphosphonium cations, respectively (Scheme 1). A formation pre-reaction complex is associated with the reduction enthalpy of the reaction of about 2.31 kcal·mol^{-1} for **[1][TES]** complex and 2.78 kcal·mol^{-1} for **[1][TEP]** complex. Optimally, from the energetic point of view the orientation of these cations is situated nearby the oxygen atoms of the nitro group.

Next, the pre-reaction complex is converted to the transition state (**TS[TES]** and **TS[TEP]**, respectively) (Scheme 1, Figure 1 and 2). It results in the enthalpy of activation increase of over 22 kcal·mol^{-1} for the reaction catalyzed by both cations (Table 1 and 2). This barrier, however, is significantly smaller than shown by DFT calculations for a similar reaction provide without ionic liquid cations (about 38 kcal·mol^{-1}).[37] Further conversion of the transition state leads to products **2** and **3** (Scheme 1).

We have also performed B3LYP/6-31G(d) calculations, which present the influence of the substituent in the leaving

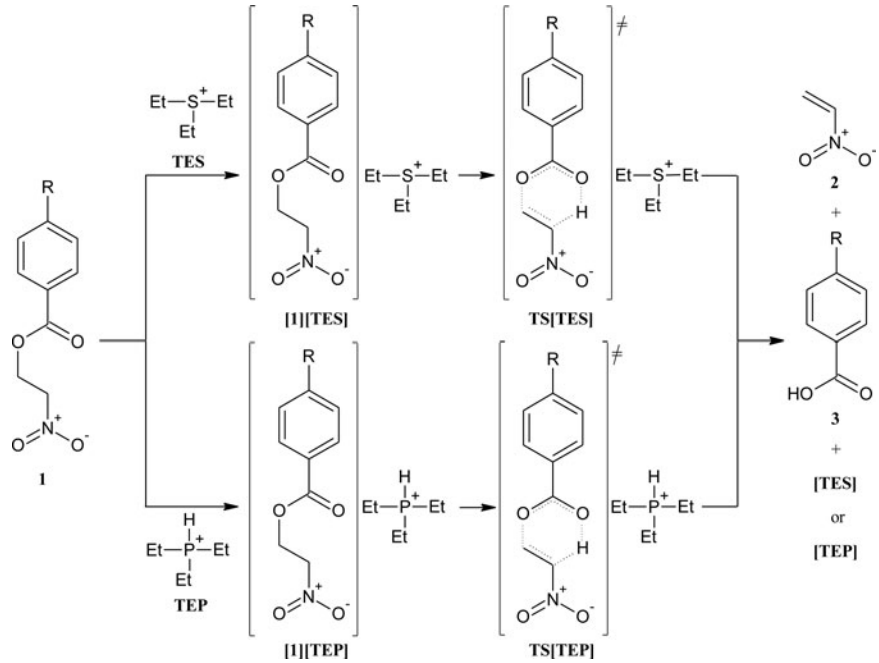

Scheme 1. Mechanism of the decomposition reaction of nitroethyl benzoates catalyzed by the triethylsulfonium (TES) and the triethylphosphonium (TEP) cations.

group. Regardless of the nature of the substituent in the benzene ring, esters will undergo the decomposition according to a one-step mechanism. In the event of the reaction catalyzed by the triethylphosphonium cation, the decomposition process of substituted esters with the electrodonating group (**1b** – NMe_2) will lower the enthalpy of the activation barrier (19.64 kcal·mol^{-1}). Then, the decomposition process of esters with the electroaccepting group (**1c** – NO_2) will make the process tougher (24.70 kcal·mol^{-1}) (Table 2). Calculations obtained for the decomposition process of substituted esters in uncatalyzed conditions give similar results (NMe_2 – 37.52 kcal·mol^{-1}, NO_2 – 39.65 kcal·mol^{-1}).[38] The situation is the same, in the case of the reaction catalyzed by the triethylsulfonium cation. In the presence of the electrodonating group the process runs faster (18.44 kcal·mol^{-1}), but electroaccepting groups make the increase in the enthalpy of the activation and process proceed with more difficulty (23.14 kcal·mol^{-1}) (Table 1).

It should also be mentioned that calculations at higher theory levels B3LYP/6-31+G(d), B3LYP/6-31++G(d), and B3LYP/6-31G(d,p) give a similar image of these reactions. These calculations supplied slightly lower enthalpy of activation (Table 1 and 2). In the event of the uncatalyzed decomposition, we also observed a decrease in the enthalpy of activation.[38]

Transition structures of the decomposition reactions

The transition states (**TS[TES]** and **TS[TEP]**) have a six-membered structure (Figure 3). Simultaneously, new bonds are

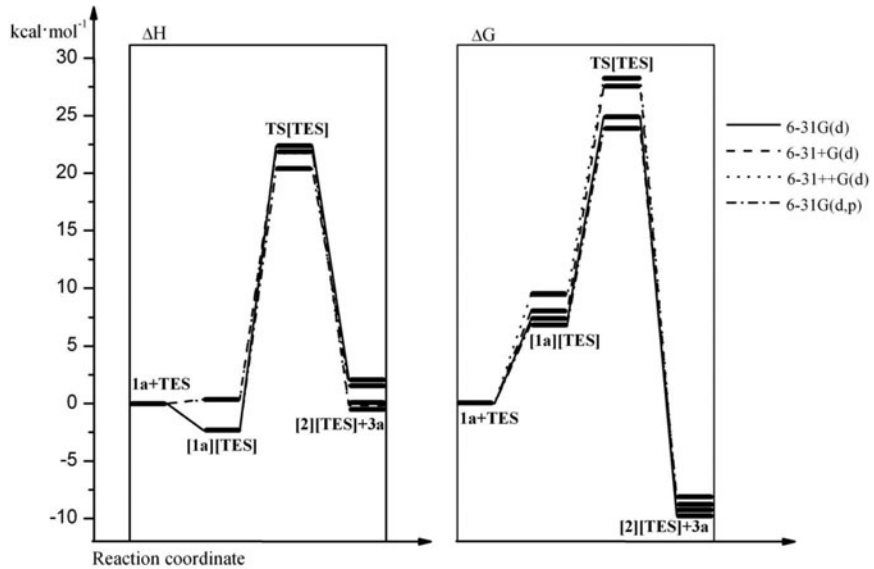

Figure 1. Energy profiles for the decomposition of nitroethyl benzoate 1a catalyzed by the triethylsulfonium cation.

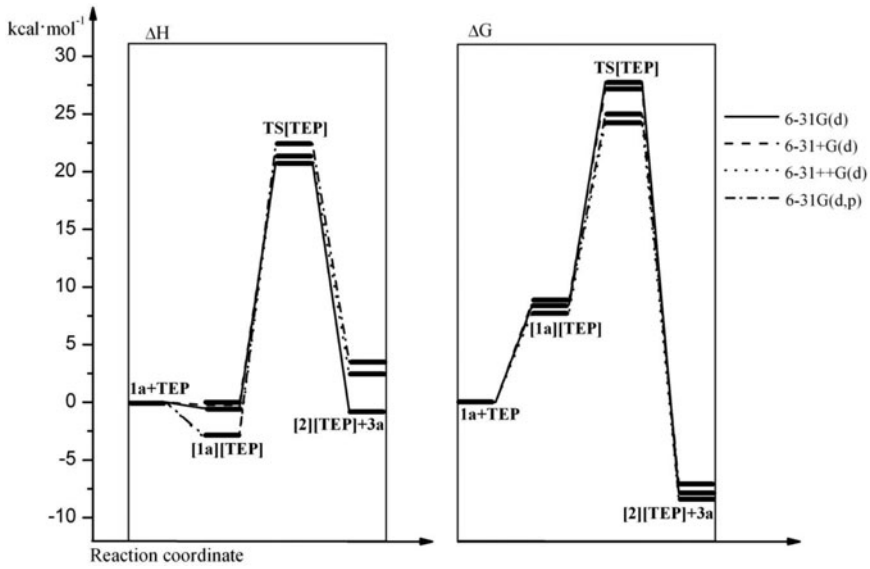

Figure 2. Energy profiles for the decomposition of nitroethyl benzoate 1a catalyzed by the triethylphosphonium cation.

formed: between atoms H6-O5 and between atoms C1-C2 and C4-O3 double bonds. The C4-O5 bond is changed to a single bond. H6-C1 and C2-O3 bonds become broken (Table 4).

Thereafter, we also analysed the influence of the TES and the TEP cations of structure TS. It was found that the H6-C1 bond in the case of reactions catalyzed by the TES and the TEP cations are created faster than in the case of the uncatalyzed reaction. In turn, the C2-O3 bond of TS of reactions catalyzed by both cations are broken more slowly than in the case of the uncatalyzed process.[38] In the reaction catalyzed by the

Table 1. Kinetic and thermodynamics parameters for the decomposition of nitroethyl benzoates catalyzed by the triethylsulfonium cation (T = 298 K; ΔH, ΔG in kcal·mol^{-1}, ΔS in cal·mol^{-1}·K^{-1}; 1a - R = H, 1b - R = NMe_2, 1c - R = NO_2).

Ester	Theoretical level	Transition	ΔH	ΔG	ΔS
1a	6-31G(d)	**1a+TES→[1a][TES]**	− 2.31	7.33	− 32.33
		[1a][TES]→TS[TES]	22.33	24.92	− 8.70
		[1a][TES]→[2][TES]+3a	2.01	− 9.74	39.43
	6-31+G(d)	**1a+TES→[1a][TES]**	0.37	8.07	− 25.83
		[1a][TES]→ TS[TES]	21.94	27.53	− 18.60
		[1a][TES]→[2][TES]+3a	− 0.17	− 9.16	30.15
	6-31++G(d)	**1a+TES→[1a][TES]**	0.30	9.46	− 30.71
		[1a][TES]→ TS[TES]	21.72	28.28	− 21.98
		[1a][TES]→[2][TES]+3a	− 0.38	− 8.79	28.22
	6-31G(d,p)	**1a+TES→[1a][TES]**	− 2.31	6.97	− 31.16
		[1a][TES]→ TS[TES]	20.34	23.87	− 11.82
		[1a][TES]→[2][TES]+3a	1.52	− 8.11	32.32
1b	6-31G(d)	**1b+TES→[1b][TES]**	− 2.40	7.80	− 34.22
		[1b][TES]→ TS[TES]	18.44	22.03	− 12.06
		[1b][TES]→[2][TES]+3b	2.47	− 9.17	39.05
	6-31+G(d)	**1b+TES→[1b][TES]**	0.09	7.46	− 24.72
		[1b][TES]→ TS[TES]	18.90	26.46	− 25.39
		[1b][TES]→[2][TES]+3b	− 0.41	− 7.98	25.38
	6-31++G(d)	**1b+TES→[1b][TES]**	0.01	7.37	− 24.69
		[1b][TES]→ TS[TES]	18.91	26.42	− 25.19
		[1b][TES]→[2][TES]+3b	− 0.31	− 7.97	25.70
	6-31G(d,p)	**1b+TES→[1b][TES]**	− 2.48	7.73	− 34.24
		[1b][TES]→ TS[TES]	17.74	23.82	− 20.38
		[1b][TES]→[2][TES]+3b	1.92	− 7.16	30.47
1c	6-31G(d)	**1c+TES→[1c][TES]**	− 2.05	7.47	− 31.95
		[1c][TES]→ TS[TES]	23.14	27.04	− 13.07
		[1c][TES]→[2][TES]+3c	− 1.76	− 8.62	34.80
	6-31+G(d)	**1c+TES→[1c][TES]**	0.59	9.92	− 40.28
		[1c][TES]→ TS[TES]	23.58	29.69	− 20.47
		[1c][TES]→[2][TES]+3c	− 0.76	− 8.99	27.63
	6-31++G(d)	**1c+TES→[1c][TES]**	0.50	9.16	− 29.04
		[1c][TES]→ TS[TES]	23.79	30.89	− 23.80
		[1c][TES]→[2][TES]+3c	− 0.55	− 7.81	24.33
	6-31G(d,p)	**1c+TES→[1c][TES]**	− 2.13	7.29	− 31.59
		[1c][TES]→ TS[TES]	23.09	26.48	− 11.38
		[1c][TES]→[2][TES]+3c	1.76	− 9.01	36.12

Table 2. Kinetic and thermodynamics parameters for the decomposition of nitroethyl benzoates catalyzed by the triethylphosphonium cation (T = 298 K; ΔH, ΔG in kcal·mol^{-1}, ΔS in cal·mol^{-1}·K^{-1}; 1a - R = H, 1b - R = NMe_2, 1c - R = NO_2).

Ester	Theoretical level	Transition	ΔH	ΔG	ΔS
1a	6-31G(d)	**1a+TEP→[1a][TEP]**	−2.78	8.35	−37.33
		[1a][TEP]→TS[TEP]	22.44	24.92	−8.31
		[1a][TEP]→[2][TEP]+3a	3.51	−7.05	35.41
	6-31+G(d)	**1a+TEP→[1a][TEP]**	−0.51	8.45	−30.05
		[1a][TEP]→ TS[TEP]	20.84	27.80	−23.32
		[1a][TEP]→[2][TEP]+3a	−0.77	−7.88	23.85
	6-31++G(d)	**1a+TEP→[1a][TEP]**	−0.23	8.75	−30.13
		[1a][TEP]→ TS[TEP]	20.84	27.19	−21.32
		[1a][TEP]→[2][TEP]+3a	−0.75	−8.27	25.25
	6-31G(d,p)	**1a+TEP→[1a][TEP]**	−2.95	7.76	−35.90
		[1a][TEP]→ TS[TEP]	21.30	24.23	−9.82
		[1a][TEP]→[2][TEP]+3a	2.47	−8.43	36.57
1b	6-31G(d)	**1b+TEP→[1b][TEP]**	−3.01	7.86	−36.47
		[1b][TEP]→ TS[TEP]	19.64	23.84	−14.10
		[1b][TEP]→[2][TEP]+3b	4.05	−6.41	35.11
	6-31+G(d)	**1b+TEP→[1b][TEP]**	−0.68	8.56	−31.00
		[1b][TEP]→ TS[TEP]	20.03	24.66	−15.54
		[1b][TEP]→[2][TEP]+3b	1.51	−10.35	39.76
	6-31++G(d)	**1b+TEP→[1b][TEP]**	−0.41	8.13	−28.65
		[1b][TEP]→ TS[TEP]	20.70	23.26	−8.61
		[1b][TEP]→[2][TEP]+3b	1.67	−8.55	34.29
	6-31G(d,p)	**1b+TEP→[1b][TEP]**	−3.20	6.62	−32.94
		[1b][TEP]→ TS[TEP]	19.32	23.78	−14.96
		[1b][TEP]→[2][TEP]+3b	3.99	−6.18	34.12
1c	6-31G(d)	**1c+TEP→[1c][TEP]**	−2.47	8.20	−35.79
		[1c][TEP]→ TS[TEP]	24.70	27.97	−10.99
		[1c][TEP]→[2][TEP]+3c	3.66	−6.44	33.90
	6-31+G(d)	**1c+TEP→[1c][TEP]**	−0.20	10.01	−34.26
		[1c][TEP]→ TS[TEP]	25.75	31.63	−19.75
		[1c][TEP]→[2][TEP]+3c	1.77	−8.27	33.70
	6-31++G(d)	**1c+TEP→[1c][TEP]**	0.17	10.91	−36.00
		[1c][TEP]→ TS[TEP]	25.87	32.47	−22.14
		[1c][TEP]→[2][TEP]+3c	1.23	−5.03	21.01
	6-31G(d,p)	**1c+TEP→[1c][TEP]**	−2.63	8.21	−36.37
		[1c][TEP]→ TS[TEP]	24.56	28.33	−12.63
		[1c][TEP]→[2][TEP]+3c	3.56	−6.66	34.29

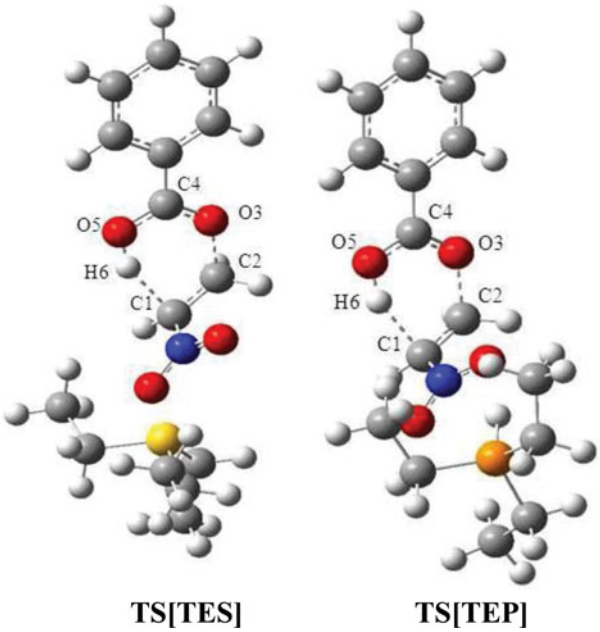

Figure 3. Transition state **TS** structures for the decomposition of nitroethyl benzoates **1a** catalyzed by the TES and the TEP cations according to B3LYP/6-31G(d) data.

TES cation, it was found that the H6-C1 bond is broken faster (1.793 Å) than in the reaction catalyzed by the TEP cation. In turn, the C2-O3 bond of TS is broken more slowly (1.665 Å) in the case of reaction catalyzed by the TES cation than in the case of the reaction catalyzed by the TEP cation. In turn, the H6-C1 and C2-O3 bonds are broken faster in the case of reactions **[1b][TES]→[2][TES]+3b** and **[1b][TEP]→[2][TEP]+3b** than in reactions **[1c][TES]→[2][TES]+3c** and **[1c][TEP]→[2][TEP]+3c**. In turn, the compound **1c**, the H6-C1 bonds are created more slowly than in the reaction proceeding without substituents (Table 4).

Additionally, the analysis of key bond orders within the transition states showed that the process of rehybridization of reaction sites are very similar (Table 3).

For comparison, the GEDT value for the transition states of similar non-catalytic processes is half as large as the GEDT value for the decomposition reaction catalyzed by TES and TEP cations (Table 4).[37]

Table 3. Key Wiberg bond orders for transition states structures of the decomposition of nitroethyl benzoates catalyzed by the TES and the TEP cations according to B3LYP/6-31G(d) data.

	Wiberg bond orders		
Structure	C1-C2	O3-C4	C4-O5
TS[TES]	1.2229	1.3498	1.2265
TS[TEP]	1.2251	1.3470	1.2188

Table 4. Key parameters for structures of the decomposition of nitroethyl benzoates catalyzed by the TES and the TEP cations according to B3LYP/6-31G(d) data (1a - R = H, 1b - R = NMe_2, 1c - R = NO_2).

Reaction	Structure	Interatomic distances [Å]						GEDT [e]
		H6-C1	C1-C2	C2-O3	O3-C4	C4-O5	O5-H6	
[1a][TES]→[2][TES]+3a	**[1a][TES]**	1.088	1.518	1.437	1.360	1.218	2.708	
	TS[TES]	1.793	1.439	1.665	1.273	1.305	1.019	0.30
	[2][TES]+3a		1.329		1.219	1.353	0.976	
[1b][TES]→[2][TES]+3b	**[1b][TES]**	1.088	1.518	1.433	1.369	1.222	2.697	
	TS[TES]	1.855	1.424	1.714	1.276	1.317	1.004	0.32
	[2][TES]+3b		1.329		1.224	1.361	0.975	
[1c][TES]→[2][TES]+3c	**[1c][TES]**	1.088	1.516	1.441	1.353	1.216	2.759	
	TS[TES]	1.703	1.435	1.687	1.269	1.295	1.043	0.27
	[2][TES]+3c		1.329		1.216	1.348	0.976	
[1a][TEP]→[2][TEP]+3a	**[1a][TEP]**	1.088	1.518	1.437	1.360	1.218	2.705	
	TS[TEP]	1.789	1.432	1.690	1.270	1.304	1.019	0.30
	[2][TEP]+3a		1.329		1.219	1.353	0.976	
[1b][TEP]→[2][TEP]+3b	**[1b][TEP]**	1.088	1.518	1.433	1.37	1.222	2.674	
	TS[TEP]	1.878	1.423	1.717	1.276	1.318	1.000	0.33
	[2][TEP]+3b		1.329		1.223	1.361	0.975	
[1c][TEP]→[2][TEP]+3c	**[1c][TEP]**	1.088	1.516	1.440	1.353	1.216	2.740	
	TS[TEP]	1.720	1.436	1.682	1.269	1.296	1.038	0.28
	[2][TEP]+3c		1.329		1.216	1.348	0.976	

Conclusions

In summary, DFT calculations of the decomposition reaction of nitroethyl benzoates catalyzed by the triethylsulfonium and the triethylphosphonium cations proceeds according to the polar one – step mechanism. For comparison, B3LYP/6-31G(d) calculations suggests that, in the presence of the TES and the TEP cations of ionic liquids, the decomposition process of nitroethyl benzoates should take place much faster than in the same process without the catalyst.

Furthermore, both types of cations, in a similar manner, accelerate the process of the decomposition of nitroethyl benzoates. These cations are characterized by approximate, high global electrophilicity (for the TES cation – 4.3eV, for TEP cation 3.7eV). Using the scale proposed by Domingo[68,69], these cations should be classified as belonging to the group of strong electrophiles.

Funding

This research was supported in part by PL-Grid Infrastructure. There was also financial support from the Polish State Committee (Grant no. C-2/88/2016/DS). Their support is gratefully acknowledged.

References

1. Fioravanti, S.; Pellacani, L.; Vergari, M. C. *Org. Biomol. Chem.* **2012**, 10, 524-528.
2. Barrett, A. G. M.; Graboski, G. G. *Chem. Rev.* **1986**, 86, 751-762.
3. Alston, T. A.; Porter, D. J. T.; Bright, H. *J. Bioorg. Chem.* **1985**, 13, 375-403.
4. Barrett, A. G. M. *Chem. Soc. Rev.* **1991**, 20, 95-127.
5. Rastogi, N.; Mohan, R.; Panda, D.; Mobinc, S. M.; Namboothiri, I. N. N. *Org. Biomol. Chem.* **2006**, 4, 3211-3214.
6. Hoashi, Y.; Yabuta, T.; Takemoto, Y. *Tetrahedron Lett.* **2004**, 45, 9185-9188.
7. Boguszewska-Czubara, A.; Łapczuk-Krygier, A.; Rykała, K.; Biernasiuk, A.; Wnorowski, A.; Popiołek, Ł.; Maziarka, A.; Hordyjewska, A.; Jasiński, R. *J. Enzyme Inhib. Med. Chem.* **2016**, 31, 900-907.
8. Pettit, R. K.; Pettit, G. R.; Hamel, E.; Hogan, F.; Moser, B. R.; Wolf, S.; Pon, S.; Chapuis, J. C.; Schmidt, J. M. *Bioorg. Med. Chem.* **2009**, 17, 6606-6612.
9. Kaap, S.; Quentin, I.; Tamiru, D.; Shaheen, M.; Eger, K.; Steinfelder, H. *J. Biochem. Pharmacol.* **2003**, 65, 603-610.
10. Barrett, A. G. M. *Tetrahedron* **1990**, 46, 7313-7316.
11. Dornow, A.; Jordan, H. D.; Muller, A. *Chem. Ber.* **1961**, 94, 67-76.
12. Chaudhuri, T.; Banerjee, M. *J. Lumin.* **2012**, 132, 1456-1461.
13. Das, P.; Chaudhuri, T.; Mukhopadhyay, Ch. *ACS Comb. Sci.* **2014**, 16, 606-613.
14. Baer, H. H.; Urbas, L. *The Chemistry of Amino, Nitroso and Nitro Compounds and their Derivatives*, part 2, ed.; Patai, S., John Wiley & Sons: New York, **1982**, pp. 105-159.
15. Coombes, R. G. *Comprehensive Organic Chemistry*, part 7, ed.; Barton, D. S.; Ollis, W. D., Ed., Pergamon Press: United Kingdom, **1979**, pp. 239-277.
16. Chen, F. X.; Shao, C.; Wang, Q.; Gong, P.; Zhang, D. Y.; Zhanga, B. Z.; Wanga, R. *Tetrahedron Lett.* **2007**, 48, 8456-8459.
17. Ranganathan, D.; Rao, C. B.; Ranganathan, S.; Mehrotra, A. K.; Iyengar, R. *J. Org. Chem.* **1980**, 45, 1185-1189.
18. Jasiński, R. *Monatsh. Chem.* **2016**, 147, 1207-1213.
19. Jasiński, R.; Kubik, M.; Łapczuk-Krygier, A.; Kącka, A.; Dresler, E.; Boguszewska-Czubara, A. *React. Kinet. Mech. Catal.* **2014**, 113, 333-345.
20. Łapczuk-Krygier, A.; Ponikiewski, Ł.; Jasiński, R. *Crystallogr. Rep.* **2014**, 59, 961-963.
21. Jasiński, R.; Jasińska, E.; Dresler, E. *J. Mol. Model.* **2017**, 23, 13-21.
22. Kącka, A.; Jasiński, R. *Heteroatom Chem.* **2016**, 27, 279-289.
23. Jasiński, R. *Tetrahedron Lett.* **2015**, 56, 532-535.
24. Jasiński, R.; Mróz, K. *React. Kinet. Mech. Catal.* **2015**, 116, 35-41.
25. Jasiński, R.; Ziółkowska, M.; Demchuk, O. M.; Maziarka, A. *Centr. Eur. J. Chem.* **2014**, 12, 586-593.
26. Kabalka, G. W.; Varma, R. S., *Syntheses and Selected Reductions of Conjugated Nitroalkenes. A Review, Organic Preparations and Procedures Int.*, Taylor & Francis: United States, **1987**, pp. 283-328.
27. Varma, R. S.; Kabalka, G. W. *Synth. Commun.* **1985**, 15, 843-847.
28. Varma, R. S.; Kabalka, G. W. *Synth. Commun.* **1985**, 15, 151-155.
29. Varma, R. S.; Varma, M.; Kabalka, G. W. *Tetrahedron Lett.* **1985**, 26, 3777-3778.
30. Vanna, R. S.; Varma, M.; Kabalka, G. W. *Synth. Commun.* **1986**, 16, 91-96.
31. Maurad, M. S.; Varm, R. S.; Kabalka, G. W. *J. Org. Chem.* **1985**, 50, 133-135.
32. Perekalin, V. V.; Lipina, E. S.; Berestovitskaya, V. M.; Efremov, D. A. *Nitroalkenes: Conjugated Nitroalkenes*, Wiley: New York, **1994**.
33. Alexander, R.; Kralert, P. G.; Kagi, R. I. *Org. Geochem.* **1992**, 19, 133-140.

34. Buckley, G. D.; Scaife, C. W. *J. Chem. Soc.* **1947**, 1471-1472.
35. Leseticky, L.; Fidler, V.; Prochazka, M. *Collect. Czech. Chem. Commun.* **1973**, 38, 459-464.
36. Blomquist, B. A. T.; Tapp, W. J.; Johnson, J. R. *J. Am. Chem. Soc.* **1945**, 67(9), 1519-1524.
37. Jasiński, R.; Kącka, A. *J. Mol. Mod.* **2015**, 21, 59-65.
38. Olivier-Bourbigou, H.; Magna, L. *J. Mol. Cat. A* **2002**, 182, 419-437.
39. Wasserchеid, P.; Keim, W. *Angew. Chem. Int. Ed.* **2000**, 39, 3772-3789.
40. Sheldon, R. *Chem. Commun.* **2001**, 23, 2399-2407.
41. Gordon, C. M. *Appl. Catal. A* **2001**, 222, 101-117.
42. Zhao, D.; Wu, M.; Kou, Y.; Min, E. *Catal. Today* **2002**, 74, 157-189.
43. Dupont, J.; de Souza, R. F.; Suarez, P. A. Z. *Chem. Rev.* **2002**, 102, 3667-3692.
44. Barreto, G. P.; Rodríguez, K. D.; Morales, G. E.; Enríquez, J.; Cañizoa, A. I.; Eyler, G. N. *Arab J Chem.* **2016**, DOI: 10.1016/j.arabjc.2016.05.016
45. Fu, J.; Xu, X.; Lu, X.; Lu, X. *Ind. Eng. Chem. Res.* **2016**, 55, 11044-11051.
46. Welton, T. *Ionic Liquids in Catalysis*, South Kensington: London, **2008**.
47. McNulty, J.; Dyck, J.; Larichev, V.; Capretta, A.; Robertson, A. *J. Lett. Org. Chem.* **2004**, 1(2), 137-139.
48. Welton, T. *Chem. Rev.* **1999**, 99, 2071-2083.
49. Cheekoori, S. *Phosphonium Salt Ionic Liquids in Organic Synthesis*, McMaster University: Canada, **2008**, pp. 45-88.
50. Frisch, M. J.; Trucks, G. W.; Schlegel, H. B.; Scuseria, G. E.; Robb, M. A.; Cheeseman, J. R.; Montgomery, J. A.; Vreven, T. J.; Kudin, K. N.; Burant, J. C.; Millam, J. M.; Iyengar, S. S.; Tomasi, J.; Barone, V.; Mennucci, B.; Cossi, M.; Scalmani, G.; Rega, N.; Petersson, G. A.; Nakatsuji, H.; Hada, M.; Ehara, M.; Toyota, K.; Fukuda, R.; Hasegawa, J.; Ishida, M.; Nakajima, Y.; Honda, O.; Kitao, O.; Nakai, H.; Klene, M.; Li, X.; Knox, J. E.; Hratchian, H. P.; Cross, J. B.; Adamo, C.; Jaramillo, J.; Gomperts, R.; Stratmann, R. E.; Yazyev, O.; Austin, A. J.; Cammi, R.; Pomelli, C.; Ochterski, J. W.; Ayala, P. Y.; Morokuma, K.; Voth, G. A.; Salvador, P.; Dannenberg, J. J.; Zakrzewski, V. G.; Dapprich, S.; Daniels, A. D.; Strain, M. C.; Farkas, M. C.; Malick, D. K.; Rabuck, A. D.; Raghavachari, K.; Foresman, J. B.; Ortiz, J. V.; Cui, Q.; Baboul, A. G.; Clifford, S.; Cioslowski, J.; Stefanov, B. B.; Liu, G.; Liashenko, A.; Piskorz, P.; Komaromi, I.; Martin, R. L.; Fox, D. J.; Keith, T.; Al-Laham, M. A.; Peng, C. Y.; Nanayakkara, A.; Challacombe, M.; Gill, P. M. W.; Johnson, B.; Chen, W.; Wong, M. W.; Gonzalez, C.; Pople, J. A. *Gaussian 09 rev A.1*, Gaussian Inc: Wallingford CT, **2009**.
51. Stephens, P.; Devlin, F. J.; Chabalowski, C. F.; Frisch, M. J. *J. Phys. Chem.* **1994**, 98, 11623-11627.
52. Jasiński, R. *J. Fluorine Chem.* **2014**, 160, 29-33.
53. Jasiński, R. *RSC Adv.* **2015**, 5, 50070-50072.
54. Jasiński, R. *Comput. Theor. Chem.* **2014**, 1046, 93-98.
55. Szczepanek, A.; Jasińska, E.; Kącka, A.; Jasiński, R. *Curr. Chem. Lett.* **2015**, 4, 33-44.
56. Domingo, L. R.; Perez, P.; Contreras, R. *Tetrahedron* **2004**, 60, 6585-6591.
57. Domingo, L. R.; Arno, M.; Andres, J. *J. Org. Chem.* **1999**, 64, 5867-5875.
58. Domingo, L. R.; Jose Aurell, M.; Kneeteman, M. N.; Mancini, P. M. *J. Mol. Struct.* **2008**, 853, 68-76.
59. Becke, A. D. *J. Chem. Phys.* **1993**, 5648, 6-11.
60. Lee, C.; Yang, W.; Parr, R. G. *Phys. Rev. B* **1988**, 37, 785-789.
61. Fukui, K. *J. Phys. Chem.* **1970**, 74, 4161-4163.
62. Cossi, M.; Rega, N.; Scalmani, G.; Barone, V. *J. Comp. Chem.* **2003**, 24, 669-681.
63. Weinga1rtner, H.; Sasisanker, P.; Daguenet, C.; Dyson, P. J.; Krossing, I.; Slattery, J. M.; Schubert, T. *J. Phys. Chem. B* **2007**, 111, 4775-4780.
64. Weingärtner, H. *J. Mol. Liq.* **2014**, 192, 185-190.
65. Chen, H.; Kwait, D. C.; Gonen, Z. S.; Weslowski, B. T.; Abdallah, D. J.; Weiss, R. D. *Chem. Mater.* **2002**, 14, 4063-4072.
66. Domingo, L. R. *RSC Adv.* **2014**, 4, 32415-32428.
67. Berski, S.; Andres, J.; Silvi, B.; Domingo, L. R. *J. Phys. Chem.* **2003**, 107, 6014-6024.
68. Domingo, L. R.; Aurell, M. J.; Perez, P.; Contreras, R. *Tetrahedron* **2002**, 58, 4417-4423.
69. Domingo, L. R. *Molecules* **2016**, 21, 1319-1332.

Artykuł D06

A. Kącka, R. Jasiński

A dramatic change of kinetic conditions and molecular mechanism of decomposition processes of nitroalkyl carboxylates catalyzed by ethylammonium cations.
Computational and Theoretical Chemistry, **1104**, 37-42 (2017).

Computational and Theoretical Chemistry 1104 (2017) 37–42

Contents lists available at ScienceDirect

Computational and Theoretical Chemistry

journal homepage: www.elsevier.com/locate/comptc

A dramatic change of kinetic conditions and molecular mechanism of decomposition processes of nitroalkyl carboxylates catalyzed by ethylammonium cations

Agnieszka Kącka, Radomir Jasiński *

Institute of Organic Chemistry and Technology, Cracow University of Technology, Warszawska 24, 31-155 Cracow, Poland

ARTICLE INFO

Article history:
Received 16 November 2016
Received in revised form 9 February 2017
Accepted 9 February 2017
Available online 12 February 2017

Keywords:
Thermal elimination
Stepwise mechanism
Nitroalkene
DFT study

ABSTRACT

DFT calculations at different theory levels, indicate consistently, that in the presence of ethylammonium cation, a nitroethyl benzoates decomposition process is expected to take place much faster than under "conventional" (non-catalyzed) conditions. The one-step mechanism being replaced by a two-step mechanism involving a zwitterionic intermediate.

1. Introduction

Conjugated nitroalkenes (CNA) are valuable building blocks for the synthesis of many interesting compounds, which are difficult to obtain in an alternative, synthetic way. In particular, based on reactions involving CNA three-, four-, five- and six-membered carbo- and heterocycles may be prepared [1–3], via cycloaddition or cyclocondensation processes. The presence of a nitro group in the molecule makes them highly reactive components in reaction with nucleophilic reagents [4,5]. Additionally, the introduction of a nitro group to target compounds provides many opportunities for further functionalization due to the possibilities for the transformation of nitro compounds into carbonyl compounds (Nef reaction) [3,6,7] nitrile N-oxides (Mukaiyama reaction) [8], hydroxylamines [9,10] aminoalcohols (via a Henry reaction/reduction sequence) [3,11–13], esters and nitronic acid salts [3,14] and many others.

The most universal strategy for the preparation of CNA is decomposition of the appropriate nitroalkyl carboxylates [15]. Unfortunately, many of these processes require relatively dramatic conditions. For example, decompositions of nitroalkyl phthalates proceed at 180–200 °C [16]. Similar elimination of carboxylic acid from nitroalkyl benzoates are carried out at temperatures higher than 185 °C [17]. Alternatively, some CNA may be obtained via base-catalyzed E1cb elimination in boiling benzene [18]. Unfortunately, simple, high reactive nitroalkenes such as nitroethene, nitropropenes, halonitroethenes and many others, rapidly polymerize under these conditions [15,19] Therefore, research aimed at searching for relatively mild conditions for a universal methodology for preparation of CNA from nitroalkyl carboxylates is justified.

This work is a continuation of our comprehensive study about the synthesis and fundamental properties of CNA [5,20–26]. Previously [26], we analyzed in detail mechanistic aspects of the decomposition of nitroalkyl carboxylates under thermal (non-catalyzed) conditions. Our DFT calculations suggest, that these processes proceed via a one-step reaction. However, this is not a "pericyclic" mechanism, but rather strong a asynchronous one-step, two-stage mechanism. In presented work, we decided to shed light on a theoretically possible decomposition of model nitroalkyl carboxylates catalyzed by ethylammonium cation (**EA+**). In practice, the source of ethylammonium cation under reaction conditions may be, for example ionic liquid, which has been tested in practice as a reaction medium for several organic reactions [27,28]. It is possible that in the presence of this catalyst, one-step mechanism decomposition of starting molecules may be competed with a two-step, ionic mechanism (Scheme 1). It should be noted at this point, that our recent studies show that some nitroalkene-cycloaddition reactions catalyzed by ammonium cations proceed via a multi-step, zwitterionic mechanism [20,29], instead of the one-step

* Corresponding author.
E-mail address: radomir@chemia.pk.edu.pl (R. Jasiński).

http://dx.doi.org/10.1016/j.comptc.2017.02.008
2210-271X/

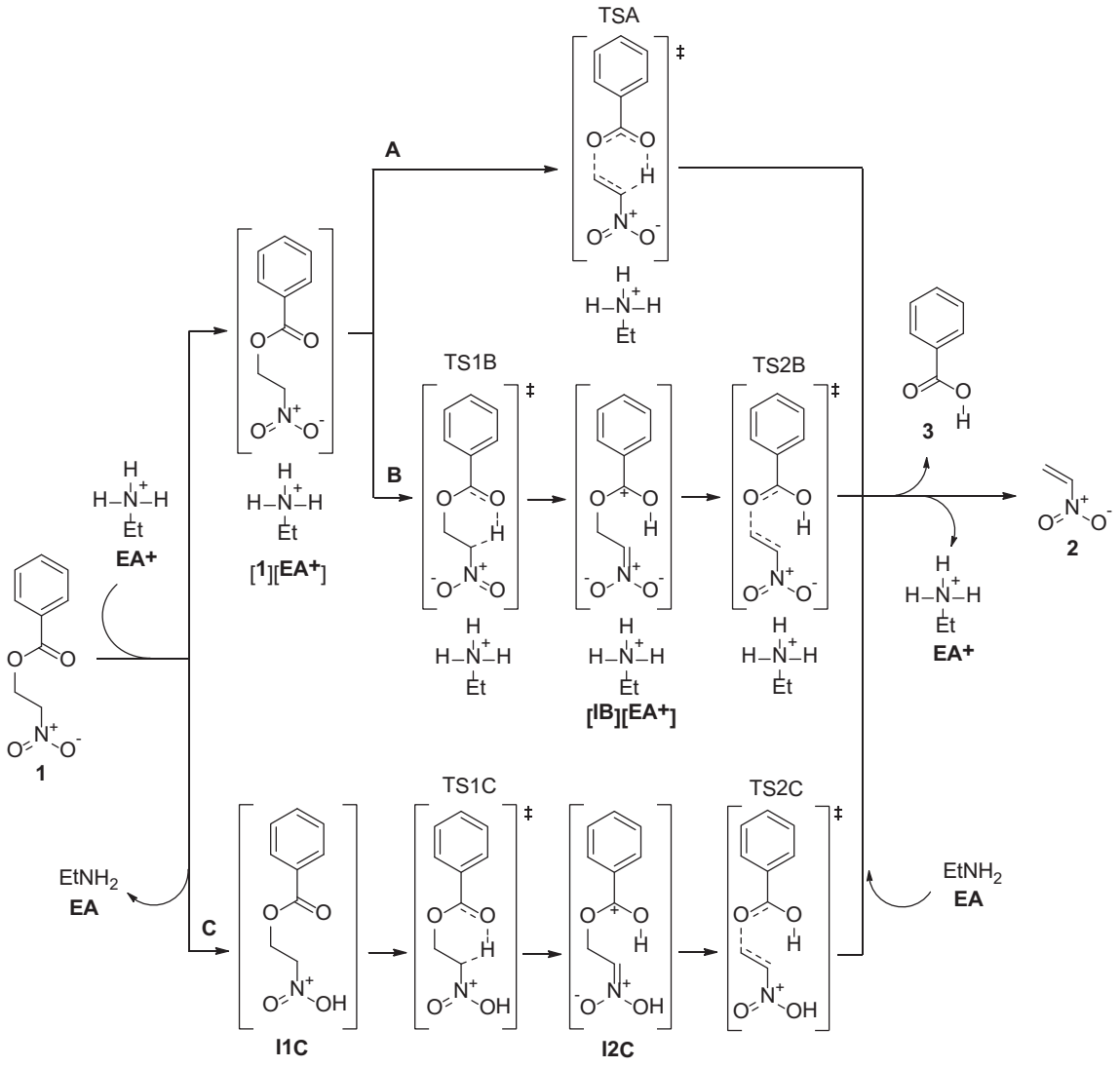

Scheme 1. Theoretically possible mechanisms for nitroethene formation process in the presence of the ethylammonium cation.

mechanism, which was observed under non-catalytic conditions [30–32].

2. Computational details

All calculations reported in this thesis were performed on SGI-Altix 3700 computer in the CYFRONET regional computational centre in Cracow. Hybrid functional B3LYP with the 6-31+G(d, p) basis set included in the GAUSSIAN 09 package [33] was used. Recently published reports show that the same functional was used e.g. for the analysis of chemical properties of nitro-functionalized compounds [20–22,26,34] including thermal decomposition process [23,35–37]. In addition, similar simulations using more advanced B3LYP/6-31++G(d, p) as well as B3LYP/6-311+G(d, p) theoretical levels were performed. Optimizations of the stable structures were performed with the Berny algorithm, whereas the transition states were calculated using the QST2 procedure followed by the TS method. Stationary points were characterised by frequency calculations. All reactants, and products had positive Hessian matrices. All transition states showed only one negative eigenvalue in their diagonalized Hessian matrices, and their associated eigenvectors were confirmed to correspond to the motion along the reaction coordinate under consideration. For all reactions, intrinsic reaction coordinate (IRC) calculations were performed to connect previously computed transition structures (**TS**) with suitable minima. The reaction environment polarity were simulated using PCM [38]. It was assumed that the reaction environment has dielectric constant, $\varepsilon = 28$, because most typical ethylammonium ionic liquids have $\varepsilon \approx 26–30$ [39]. Similar approach has been successfully used by the Domingo group for the analysis of Diels-Alder reaction between N-tosylpyrroles and isoprene in the presence of dialkylimidazolium ionic liquids [40]. Charge global electron density transfer (GEDT) [41] was calculated according to the formula:

$$GEDT = -\Sigma qA$$

where q_A is the net charge and the sum is taken over all the atoms of substructure.

3. Results and discussion

In particular, we performed a quantum chemical study about the elimination of benzoic acids from nitroethyl benzoates in the presence of $EtNH_3^+$ cation. These studies will be the first stage of a comprehensive research project under new, highly effective strategies for the preparation of CNA. Additionally, our studies will

help toward better understanding of the mechanistic aspects of organic reactions which earlier (and wrongly!) were considered as "pericyclic".

B3LYP/6-31+G(d, p) calculations showed that the first stage of the decomposition of nitroethyl benzoate (**1**) is a formation of a pre-reaction complex (**[1][EA+]**) between the ester molecule and ethylammonium cation. It is connected with the reduction of the enthalpy of the reaction system (ΔH) about 3 kcal·mol^{-1} (Table 1). However, Gibbs free energy (ΔG) for this transition is equal to 6.26 kcal·mol^{-1}. This is a consequence of large negative entropy changes (ΔS), which are linked with an increase in the ordering of the reaction system. Within the **[1][EA+]**, the ethylammonium cation is located near the oxygen atoms of the nitro group. However, any σ-bonds at this stage are not formed. Similar complexes between CNA and imidazolium cations were recently described [20,29].

Firstly we decide to explored the reaction path which is associated with one-step (channel **A** on Scheme 1) decomposition of nitroethyl benzoate (**1**). Unfortunately, all attempts to find transition state on the reaction path proceeding via one step decomposition of the nitroethyl benzoates were failed.

Our calculations showed, that conversion of **1** must be proceed via alternative molecular mechanism. The first stage of this transformation is formation of the transition state **TS1B**. This transition required Gibbs free energy of activation which is more than 28 kcal·mol^{-1} (Fig. 1, Table 1). However, this is significantly less than in the case of the thermal decomposition process of **1** without the presence of the ethylammonium cation (more than 39 kcal·mol^{-1}) [26]. So, the catalytic presence of **EA+** in the reaction environment significantly reduces the barrier of reaction, although it is rather still too high to occur at room temperature. It should be noted that entropy of the reaction system is changed only slightly at this stage.

Due to issues mentioned above, simple thermal elimination of benzoic acid (described previously in work [26]) in the presence of **EA+** should be considered as formally forbidden.

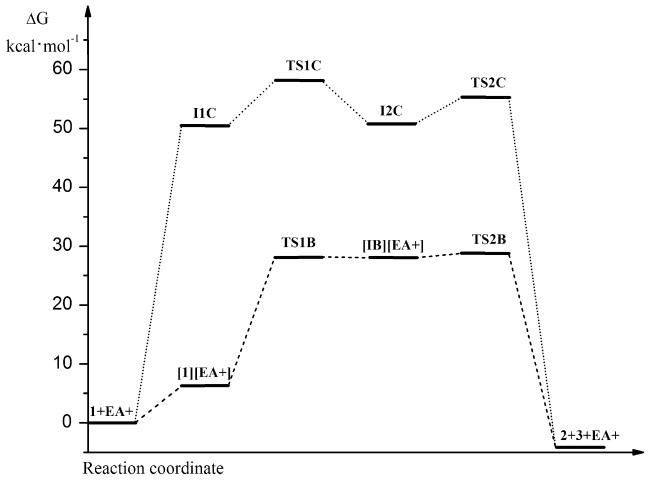

Fig. 1. Energy profiles for decomposition of nitroethyl benzoate **1** catalyzed by (**EA+**) according to data of B3LYP/6-31+G(d, p) calculations.

In **TS1B** one σ-bond is breaking (Fig. 2, Table 2). It is a bond between atoms C1 an H6 of nitroethyl moiety. Subsequently, a new σ-bond between H6 and the oxygen atom from the carbonyl group (O5) is formed. It should be underscored, that in contrast to the uncatalyzed process of **1** decomposition [26], the second σ-bond C2—O3 is not breaking at this reaction stage. Next, **TS1B** has an evidently polar, "zwitterionic-like" nature. This is confirmed by the value of global electron density transfer between substructures (GEDT), which is equal 0.37e.

Further conversion of **TS1B** leads to intermediate (**[IB][EA+]**), in which a new σ-bond O5—H6 is practically fully formed. **[IB][EA+]** have polar, zwitterionic nature (GEDT = 0.38e). Decomposition of this zwitterion proceeds via **TS2B**, and requires a small amount of Gibbs free energy (Fig. 1, Table 1). Subsequently, the entropic factor is practically unchanged in comparison to **[IB][EA+]**.

Table 1
Energetical parameters for decomposition of nitroethyl benzoate **1** catalyzed by (**EA+**) according to data of B3LYP calculations (T = 298 K; ΔH, ΔG in kcal·mol^{-1}, ΔS in cal·mol^{-1}·K^{-1}).

Basis set	Path	Transition	ΔH	ΔG	ΔS
6-31+G(d, p)	**B**	**1 + EA+ → [1][EA+]**	−3.00	6.28	−31.15
		[1][EA+] → TS1B	25.75	28.17	−8.14
		[1][EA+] → [IB][EA+]	26.71	28.03	−4.41
		[1][EA+] → TS2B	27.08	28.77	−5.66
		[1][EA+] → 2 + 3 + EA+	7.98	−4.11	40.52
	C	**1 + EA+ → I1C**	49.57	50.52	−3.17
		1 + EA+ → TS1C	6.55	7.59	−3.50
		1 + EA+ → I2C	0.39	0.27	0.41
		1 + EA+ → TS2C	5.75	4.75	3.37
6-31++G(d, p)	**B**	**1 + EA+ → [1][EA+]**	−2.28	6.40	−29.11
		[1][EA+] → TS1B	25.72	28.02	−7.69
		[1][EA+] → [IB][EA+]	26.73	27.38	−2.18
		[1][EA+] → TS2B	27.07	28.75	−5.48
		[1][EA+] → 2 + 3 + EA+	8.01	−4.05	40.45
	C	**1 + EA+ → I1C**	49.54	50.50	−3.20
		1 + EA+ → TS1C	6.58	7.61	−3.49
		1 + EA+ → I2C	0.41	0.29	0.41
		1 + EA+ → TS2C	5.77	4.60	3.92
6-311+G(d, p)	**B**	**1 + EA+ → [1][EA+]**	−3.11	6.39	−31.75
		[1][EA+] → TS1B	26.78	29.20	−8.23
		[1][EA+] → [IB][EA+]	28.14	29.31	−4.04
		[1][EA+] → TS2B	27.69	28.83	−3.92
		[1][EA+] → 2 + 3 + EA+	6.84	−4.87	39.18
	C	**1 + EA+ → I1C**	49.13	49.86	−2.55
		1 + EA+ → TS1C	7.70	8.83	−3.78
		1 + EA+ → I2C	1.26	1.38	−0.40
		1 + EA+ → TS2C	5.18	3.63	5.20

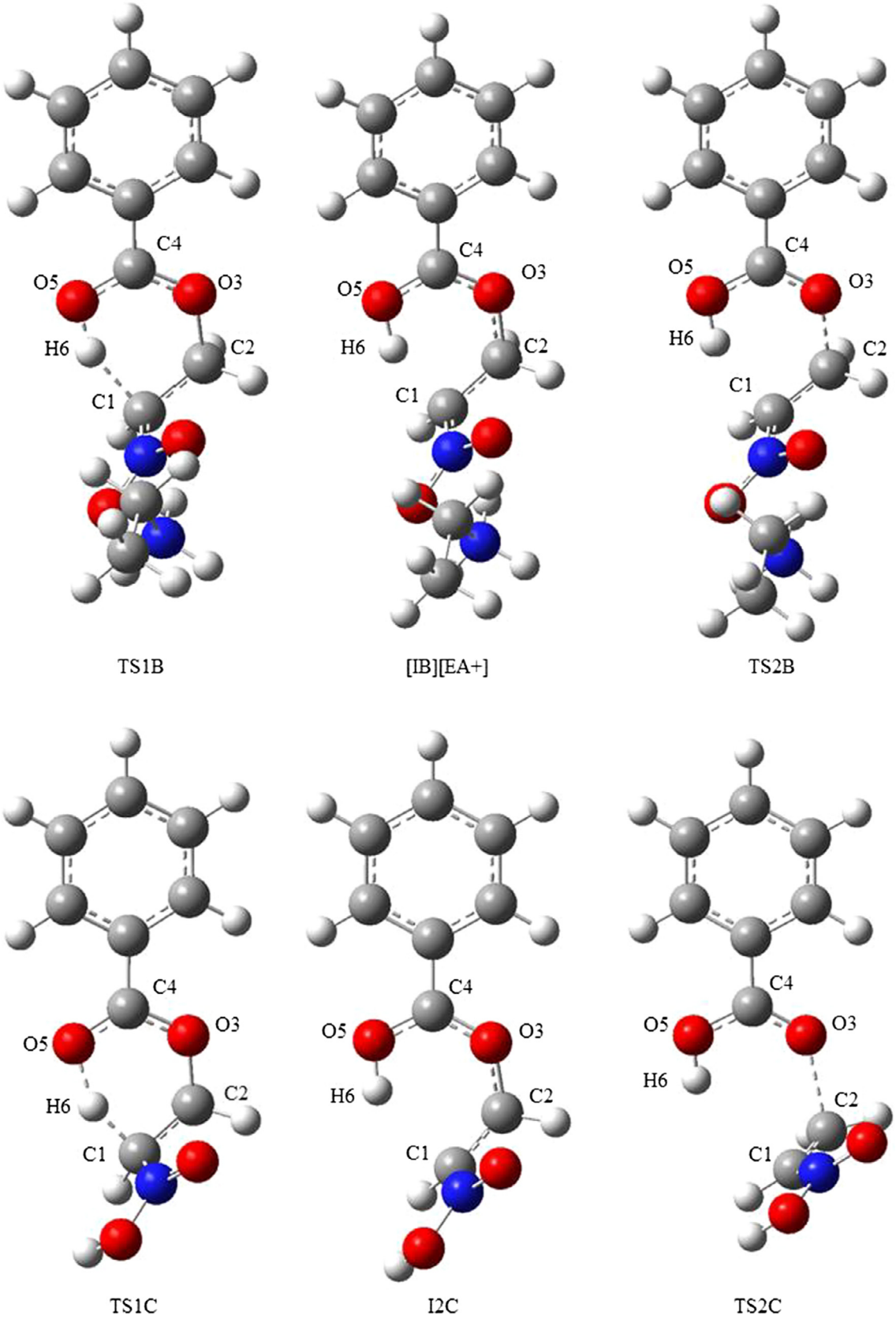

Fig. 2. Key structures of decomposition of nitroethyl benzoate **1** catalyzed by (**EA+**) according to data of B3LYP/6-31+G(d, p) calculations.

In **TS2B** the C2—O3 σ-bond is breaking (Fig. 2, Table 2). IRC calculations confirmed, that this structure is linked with the valley of **[IB][EA+]**, and the valley of final products (Scheme 1). It should be underscored at this point that under the considered conditions, the thermodynamic equilibrium of the overall process is completely shifted into products ($\Delta G = -4.11$ kcal·mol^{-1}). At this stage,

Table 2
Key parameters for structures of decomposition of nitroethyl benzoate **1** catalyzed by (**EA+**) according to data of B3LYP/6-31+G(d, p) calculations.

Reaction	Structure	Interatomic distances [Å]						GEDT[a] [e]
		H6—C1	C1—C2	C2—O3	O3—C4	C4—O5	O5—H6	
B	**[1][EA+]**	1.088	1.517	1.440	1.359	1.221	2.853	
	TS1B	1.611	1.484	1.520	1.293	1.287	1.067	0.37
	[IB][EA+]	1.700	1.476	1.535	1.288	1.293	1.036	0.38
	TS2B	1.913	1.432	1.692	1.269	1.308	0.995	0.33
C	**I1C**	1.090	1.536	1.429	1.365	1.220	2.654	
	TS1C	1.304	1.518	1.460	1.323	1.262	1.293	0.31
	I2C	2.137	1.483	1.500	1.290	1.302	0.980	0.49
	TS2C	2.856	1.393	1.983	1.250	1.326	0.970	0.25

[a] Global electron density transfer: GEDT = $-\Sigma q_A$; where q_A is the net charge and the sum is taken over all the atoms of substructure.

entropy of the reaction system significantly increases, which is linked with a decrease in the ordering of the reaction system.

Next, we considered an alternative reaction mechanism, in which ethylammonium cation **EA+** is capable of acting as a proton donor (path **C** on Scheme 1). For this purpose, we tested many possibilities of protonation of the starting ester. From all of the attempts only one was successful. In this way we obtained the structure **I1C** (Scheme 1), in which the proton moved from **EA+** is linked with the oxygen atom of the NO_2 group.

Decomposition of **I1C** proceeds via a stepwise mechanism, with a zwitterionic intermediate **I2C** (Table 2). This process requires a relatively lower energy of activation (Table 1), as in the case of reaction **B** (Scheme 1). Unfortunately, under reaction conditions it is reaction channel **C** that must be considered as forbidden from an energetic point of view, because the Gibbs free energy of formation of **I1C** intermediate is more than 20 kcal·mol^{-1} (!) higher than the key activation barrier for process **1** + **EA+** → **[1][EA+]** → **2** + **3** + **EA+**.

It should be also noted that a similar picture of title reactions is provided by calculations at higher theory levels B3LYP/6-31++G(d, p) as well as B3LYP/6-311+G(d, p). In particular, independent of the theory level, the geometric parameters of critical structures are practically identical. Some small differences appear only at energetic description of the critical points. These differences do not however influence the picture of energetic aspects of transformation described. Thus, it may be assumed that applications of B3LYP/6-31G(d, p) theory level is completely sufficient for resolving this type of problems.

4. Conclusion

In conclusion, DFT calculations indicate consistently that a nitroethyl benzoates decomposition process catalyzed by ethylammonium cations proceeds a via two-step mechanism involving a zwitterionic intermediate. All attempts to find transition state on the reaction path proceeding via one step decomposition of the nitroethyl benzoates were failed. This is dramatic change of mechanistic scheme in comparison to an uncatalyzed process.

Acknowledgements

The regional computer center "Cyfronet" in Cracow (Grant No. MNiSW/Zeus_lokalnie/PK/009/2013) is thanked for the allocation of computing time.

References

[1] A.Z. Halimehjani, I.N.N. Namboothiri, S.E. Hooshmanda, Nitroalkenes in the synthesis of carboxylic compounds, RSC Adv. 4 (2014), pp. 31261–31261.
[2] I. Mierina, M. Jure, Nitroolefins as starting materials for 5-membered N-heterocycles, Heterocycl. Compd. 52 (2016) 10–12.
[3] N. Ono, The Nitro Group in Organic Synthesis, Wiley-VCH, Weinheim, 2001.
[4] P. Perez, L.R. Domingo, A. Aizman, R. Contreras, The electrophilicity index in organic chemistry, in: A. Toto-Labbe (Ed.), Theoretical Aspects of Chemical Reactivity, Elsevier, New York, 2007, pp. 139–201.
[5] R. Jasiński, M. Ziółkowska, O.M. Demchuk, A. Maziarka, Regio- and stereoselectivity of polar [2 + 3] cycloaddition reactions between (Z)-C-(3,4,5-trimethoxyphenyl)-N-methylnitrone ans selected (E)-2-substituted nitroethenes, Centr. Eur. J. Chem. 12 (2014) 586–593.
[6] A.G.M. Barrett, G.G. Graboski, Conjugated nitroalkenes: versatile intermediates in organic synthesis, Chem. Rev. 86 (1985) 751–762.
[7] R. Ballini, M. Petrini, Recent synthetic developments in the nitro to carbonyl conversion (Nef reaction), Tetrahedron 60 (2004) 1017–1047.
[8] L.I. Belenkii, in: H. Feuer (Ed.), Nitrile Oxides, Nitrones, and Nitronates in Organic Synthesis, Wiley, 2007.
[9] Sh. Liu, Y. Wang, X. Yang, J. Jiang, Selective reduction of nitroarenes to N-arylhydroxylamines by use of Zn in CO_2-H_2O system, promoted by ultrasound, Res. Chem. Intermed. 38 (2012) 2471–2478.
[10] A.G. Beirakhov, I.M. Orlova, E.G. Il'in, S.G. Sakharov, L.V. Goeva, A.V. Churakov, M.D. Surazhskaya, Y.N. Mikhailov, Molybdenum(VI) complex with N-substituted hydroxylamines, Russ. J. Inorg. Chem. 58 (2013) 1446–1451.
[11] J. Boruwa, N. Gogoi, P.P. Saikia, N.C. Barua, Catalytic asymmetric Henry reaction, Tetrahedron: Assymet. 17 (2006) 3315–3326.
[12] J.P. Agrawal, R.D. Hodgson, Organic Chemistry of Explosives, Wiley, 2007.
[13] S.C. Bergmeier, The synthesis of vicinal amino alcohols, Tetrahedron 56 (2000) 2561–2576.
[14] S.E. Denmark, J.J. Cottell, in: A. Padwa, W.H. Pearson (Eds.), The Chemistry of Heterocyclic Compounds, New York, 2002.
[15] V.V. Perekalin, E.S. Lipina, V.M. Berestovitskaya, D.A. Efremov, Nitroalkenes: Conjugated Nitroalkenes, Wiley, New York, 1994.
[16] G.D. Buckley, C.W. Scaife, Aliphatic nitro-compounds. Part I. Preparation of nitro-olefins by dehydration of 2-nitro-alcohils, J. Chem. Soc. (1947) 1471–1472.
[17] L. Lešeticky, V. Fidler, M. Procházka, Isomerisation of nitroolefines. II. Isomerisation recations of nitroethylene, Coll. Czech Chem. Commun. 38 (1973) 459–464.
[18] M. Compton, H. Higgins, L. MacBeth, J. Osborn, H. Burkett, Trichloroaminoalcohols. I. 1,1,1-Trichloro-3-aminopropanol-2 and derivatives, J. Am. Chem. Soc. 71 (1949) 3229–3231.
[19] A.T. Blomquist, T.H. Shelley, Preparation of 2-nitro-1-alkenes from Nitro amines, J. Am. Chem. Soc. 70 (1948) 147–149.
[20] R. Jasiński, A stepwise, zwitterionic mechanism for the 1,3-dipolar cycloaddition between (Z)-C-4-methoxyphenyl-N-nitrone and gem-chloronitroethene catalysed by 1-butyl-3-methylimidazolium ionic liquid cations, Tetrahedron Lett. 56 (2015) 532–535.
[21] R. Jasiński, Searching for zwitterionic intermediates in Hetero Diels-Alder reactions between methyl a, p-dinitrocinnamate and vinyl-alkyl ethers, Comput. Theor. Chem. 1046 (2014) 93–98.
[22] R. Jasiński, Regio- and stereoselectivity of [2 + 3]cycloaddition of nitroethene to (Z)-N-aryl-C-phenylnitrones, Coll. Czech Chem. Commun. 74 (2009) 1341–1349.
[23] R. Jasiński, Nitroacetylene as dipolarophile in [2 + 3] cycloaddition reactions with allenyl-type three-atom components: DFT computational study, Monatsh. Chem. 146 (2015) 591–599.
[24] R. Jasiński, Molecular mechanism of thermal decomposition of fluoronitroazoxy compounds: DFT computational study, J. Fluor. Chem. 160 (2014) 29–33.
[25] R. Jasiński, A. Kącka, A polar nature of benzoic acids extrusion from nitroalkyl benzoates: DFT mechanistic study, J. Mol. Mod. 21 (2015) 59–65.
[26] A. Kącka, R. Jasiński, A DFT mechanistic study of the thermal decomposition reactions of nitroethyl carboxylates: undermine of pericyclic insight, Heteroatom Chem. 27 (2016) 279–289.
[27] R.V. Hangarge, D.V. Jarikote, M.S. Shingare, Knoevenagel condensation recations in an ionic liquid, Green Chem. 4 (2002) 266–268.
[28] A. Aggarwal, N.L. Lancaster, A.R. Sethi, T. Welton, The role of hydrogen bending in controlling the selectivity of Diels-Alder reactions in room-temperature ionic liquid, Green Chem. 4 (2002) 517–520.

[29] R. Jasiński, First example of stepwise, zwitterionic mechanism for bicycle [2.2.1]hept-5-ene (norbornene) formation process catalyzed by the 1-butyl-3-methylimidazolium cations, Monatsh. Chem. 147 (2016) 1207–1213.
[30] R. Jasiński, M. Mikulska, O. Koifman, A. Barański, Conjugated nitroalkenes in cycloaddition reactions 18*. Regio- and stereoselectivity of (2 + 3) cycloaddition recations between gem-chloronitroethene and (Z)-C,N-diarylnitrones, Chem. Heterocycl. Compd. 49 (2013) 1188–1194.
[31] R. Jasiński, M. Rzyman, A. Barański, Conjugated nitroalkenes in cycloaddition reactions. Part 2. Diels-Alder reactions of E-2-aryl-1-cyano-1-nitroethenes with cyclopentadiene, Coll. Czech, Chem. Commun. 75 (2010) 919–929.
[32] A. Łapczuk-Krygier, Ł. Ponikiewski, R. Jasiński, The crystal structure of (1RS, 4RS, 5RS, 6SR)-5-Cyano-5-nitro-6-phenyl-bicyclo[2.2.1]hept-2-ene, Crystal Rep. 59 (2014) 961–963.
[33] M.J. Frisch, G.W. Trucks, H.B. Schlegel, G.E. Scuseria, M.A. Robb, J.R. Cheeseman, J.A. Montgomery Jr., T. Vreven, K.N. Kudin, J.C. Burant, J.M. Millam, S.S. Iyengar, J. Tomasi, V. Barone, B. Mennucci, M. Cossi, G. Scalmani, N. Rega, G.A. Petersson, H. Nakatsuji, M. Hada, M. Ehara, K. Toyota, R. Fukuda, J. Hasegawa, M. Ishida, Y. Nakajima, O. Honda, O. Kitao, H. Nakai, M. Klene, X. Li, J.E. Knox, H. P. Hratchian, J.B. Cross, C. Adamo, J. Jaramillo, R. Gomperts, R.E. Stratmann, O. Yazyev, A.J. Austin, R. Cammi, C. Pomelli, J.W. Ochterski, P.Y. Ayala, K. Morokuma, G.A. Voth, P. Salvador, J.J. Dannenberg, V.G. Zakrzewski, S. Dapprich, A.D. Daniels, M.C. Strain, M.C. Farkas, D.K. Malick, A.D. Rabuck, K. Raghavachari, J.B. Foresman, J.V. Ortiz, Q. Cui, A.G. Baboul, S. Clifford, J. Cioslowski, B.B. Stefanov, G. Liu, A. Liashenko, P. Piskorz, I. Komaromi, R.L. Martin, D.J. Fox, T. Keith, M.A. Al-Laham, C.Y. Peng, A. Nanayakkara, M. Challacombe, P.M.W. Gill, B. Johnson, W. Chen, M.W. Wong, C. Gonzalez, J.A. Pople, Gaussian 09 Rev A.1, Gaussian, Inc., Wallingford CT, 2009.
[34] R. Jasiński, M. Kubik, A. Łapczuk-Krygier, A. Kącka, E. Dresler, A. Boguszewska-Czubara, An experimental and theoretical study of the hetero Diels-Alder reactions between (E)-2-aryl-1-cyano-1-nitroethenes and ethyl vinyl ether: one-step or zwitterionic, two-step mechanism?, React Kinet. Mech. Catal. 113 (2014) 333–345.
[35] A. Łapczuk-Krygier, V.Y. Korotaev, A.Y. Barkov, V.Y. Sosnovskikh, E. Jasińska, R. Jasiński, A DFT computational study on the molecular mechanism of the nitro group migration in the product derived from 3-nitro-2-(trifluoromethyl)-2H-chromene and 2-(1-phenylpropylidene)malononitrile, J. Fluor. Chem. 168 (2014) 236–239.
[36] R. Jasiński, E. Dresler, A desulfonylation process as easy route for synthesis of 1,4-dinitro-1,3-dienes: mechanistic study, Phosph. Sulf. Silic. Relat. Elem. 191 (2016) 311–315.
[37] R. Jasiński, A new mechanistic insight on beta-lactam systems formation from 5-nitroisoxazolidines, RSC Adv. 5 (2015) 50070–50072.
[38] M. Cossi, N. Rega, G. Scalmani, V. Barone, Energies, structures, and electronic properties of molecules in solution with the C-PCM solvation model, J. Comput. Chem. 24 (2003) 669–681.
[39] M.M. Huang, Y. Jiang, P. Sasisanker, G.W. Driver, H. Weingärtner, Static relative dielectric permittivities of ionic liquids at 25C, J. Chem. Eng. Data 5 (2011) 1494–1496.
[40] P.M. Mancini, C.M. Ormachea, C.D. Della Rosa, M.N. Kneeteman, A.G. Suarez, L. R. Domingo, Ionic liquids and microwave irradiation as synergistic combination for polar Diels-Alder recations using properly substituted heterocycles as dienophiles. A DFT study related, Tetrahedron Lett. 53 (2012) 6508–6511.
[41] L.R. Domingo, A new C—C bond formation model based on the quantum chemical topology of electron density, RSC Adv. 4 (2014) 32415–32428.

Artykuł D07

A. Kącka, R. Jasiński

DFT study of the decomposition reactions of nitroethyl benzoates catalyzed by the 1,3-dimethylimidazolium cation.

Current Chemistry Letters, **6**, 15-22 (2017).

Current Chemistry Letters 6 (2017) 15–22

Contents lists available at GrowingScience

Current Chemistry Letters

homepage: www.GrowingScience.com

DFT study of the decomposition reactions of nitroethyl benzoates catalyzed by the 1,3-dimethylimidazolium cation

Agnieszka Kącka[a*] and Radomir Jasiński[a]

[a]*Institute of Organic Chemistry and Technology, Cracow University of Technology, Warszawska Str. 24, 31-155 Cracow, Poland*

C H R O N I C L E

Article history:
Received August 21, 2016
Received in revised form
October 24, 2016
Accepted 8 November 2016
Available online
9 November 2016

Keywords:
Thermal elimination
Quantum chemical study
Nitroalkenes

A B S T R A C T

DFT calculations indicate that the decomposition reaction of nitroethyl benzoates in the presence of 1,3-dimethylimidazolium cation takes place much faster than in the case of the non-catalyzed process. Additionally, our calculations suggest one-step polar mechanism of title reactions.

1. Introduction

The synthesis of nitroalkenes is very significant in organic chemistry. Conjugated nitroalkenes (CNA) have been recognized as versatile synthetic intermediates in various organic syntheses because of their easy conversion to a variety of diverse functionalities.[1-5] They react as dienophiles, heterodienes, 1,3-dipoles and, above all, as Michael acceptors.[6-8] Conjugated nitroalkenes are also distinguished by their biological properties.[9-11] Among various biological properties, the anticancer activity of nitroalkenes and their novel MBH adducts with other activated alkenes has highlighted the enormous potential of nitroalkene derivatives as bioactive molecules.[12-14] Furthermore, nitroalkenes are important precursors of many insecticides,[15] fungicides[16] and pharmaceuticals.[13]

Several methods are available for the preparation of nitroalkenes.[1,17-20] However, a great demand still exists for a method to prepare nitroolefins in a convenient and effective way. The present work is a continuation of our comprehensive study about the synthesis and fundamental properties of CNA.[21-28] Our previous works[27,28] present the decomposition of nitroalkyl carboxylates under thermal conditions. DFT calculations confirmed that these processes proceed via the one step mechanism, not "pericyclic", but quite a strong asynchronous one-step, two-stage mechanism.

* Corresponding author.
E-mail address: akacka@chemia.pk.edu.pl (A. Kącka)

doi: 10.5267/j.ccl.2016.11.001

This work is a continuation of our quantum chemical study of the decomposition reaction of nitroethyl benzoates in the presence of the 1,3-dimethylimidazolium (DMIM) cation. It should be mentioned, that our recent studies show that some nitroalkene cycloaddition reactions catalyzed by the imidazolium cation proceed via a stepwise, zwitterionic mechanism,[29,30] instead of the one step mechanism, which was noted in the case of non-catalytic conditions. This cation can be introduced for reaction as an ionic liquid. Such ionic liquid was used in organic reactions.[31-34]

2. Results and Discussion

2.1 Computational details

All calculations were carried out using the Prometheus computer cluster in the CYFRONET regional computer centre in Cracow. The mechanism of the decomposition of nitroalkyl benzoates catalyzed by the 1,3-dimethylimidazolium cation have been examined as implemented in the GAUSSIAN 09 package.[35] The geometric parameters for all the reactants, transition states and products of the reactions studied were fully optimized using the density functional theory (DFT) method. The calculations were performed using the B3LYP[36] with 6-31G(d) basic set. Additionally, calculations in more advanced 6-31+G(d) and 6-31G(d,p) basis sets, were carry out.

B3LYP is a combination of Becke's three parameter hybrid exchange functional[37] with the Lee, Yang and Parr correlated functional.[38] Geometry optimization calculations have been carried out to obtain the global minima for the reactant and products, and to locate the saddle point for the transition state. Stationary points were characterised by frequency calculations. All reactants, and products had positive Hessian matrices. All transition states showed only one negative eigenvalue in their diagonalized Hessian matrices, and their associated eigenvectors were confirmed to correspond to the motion along the reaction coordinate under consideration. Transition states were located using the (QST2) algorithm. For the optimization process, the Berny analytical gradient was employed. Intrinsic reaction coordinate (IRC) calculations[39] have been made in all events to verify that the localized transition state structures connect with the corresponding minimum stationary points associated with reactants and products. The reaction environment polarity was simulated using PCM.[40] It was assumed that the reaction environment has dielectric constant, ε= 13, for the reaction catalyzed by the 1,3-dimethylimidazolium cation (the most typical 1,3-dimethylimidazolium ionic liquids have ε=~11,6-15,1[41]).

Charge global electron density transfer (GEDT)[42] was calculated according to the formula:

$$GEDT=-\Sigma q_A, \quad (1)$$

where q_A is the net charge and the sum is taken over all the atoms of the substructure.

The values of enthalpies, entropies and free energies in all calculations were calculated with the standard statistical thermodynamics at 25ºC and 1 atm.[43]

2.2 Energetical aspects of the decomposition reaction catalyzed by the DMIM cation

The reaction pathway of the decomposition reaction was studied using the B3LYP/6-31G(d) theoretical level. Recently published reports[26,44-48], indicate that a similar approach was used successfully for the exploration of a reaction involving several different nitrocompounds. These calculations proved that the first step of the decomposition of nitroethyl benzoate (**1a**) is the establishment of a pre-reaction complex (**[1][DMIM]**) between the ester molecule and the 1,3-dimethylimidazolium cation. Consequently, the creation of a pre-reaction complex entails the drop of reaction enthalpy by 3.54 kcal·mol^{-1} (**Fig. 1** and **Fig. 2**). The DMIM cation is located near to the oxygen atom of the nitro group. We also analyzed many other orientations of the DMIM cation to the ester molecule. For further research we chose the most stable form.

Thereafter, the pre-reaction complex is recast to **TS**, which is associated with an increase in the enthalpy of activation over 33.31 kcal·mol^{-1} (**Fig. 2**). The decomposition reaction of nitroethyl benzoate **1a** catalyzed by the DMIM cation proceeded faster than the same reaction without the catalyst. The enthalpy of the activation of the uncatalyzed process is equal to 38.73 kcal·mol^{-1}.[28] Subsequently, the **TS** is converted to products **2** and **3** (**Scheme 1**).

Similar studies have been performed for the decomposition reactions of other nitroethyl benzoates which are substituted by NMe_2 (**1b**) and NO_2 (**1c**) functional groups. The decomposition process of substituted ester with the electrodonationg group (NMe_2) will lower the activation barrier. In particular, for the decomposition of compound **1b**, the activation barrier is 30.61 kcal·mol^{-1}. The decomposition process of the **1c** compound with an NO_2 group has an activation barrier of 35.13 kcal·mol^{-1}. Therefore, as could be expected, the presence of an electroaccepting group will make the process more difficult (**Table 1**). For comparison, the uncatalyzed process give similar results (NMe_2 – 37.52 kcal·mol^{-1} , NO_2 – 39.65 kcal·mol^{-1}).[28] It turned out that, regardless of the nature of the substituent in the benzene ring, the decomposition process always followed the same mechanism (**Scheme 1**).

We have also performed similar a DFT study using more advanced B3LYP/6-31+G(d) and B3LYP/6-31G(d,p) theory levels. These calculations show that the mechanism of the decomposition reaction of nitroalkyl carboxylates also indicate one-step mechanism and makes that process proceed more mildly. The value of the enthalpy of activation for compound **1a** are 30.07 kcal·mol^{-1} and 30.47 kcal·mol^{-1}, respectively (**Table 1**).

Table 1. Kinetic and thermodynamic parameters for the decomposition of nitroethyl benzoates catalyzed by 1,3-dimethylimidazolium cation (T=298 K; ΔH, ΔG in kcal·mol^{-1}, ΔS in cal·mol^{-1}·K^{-1}; **1a** - R=H, **1b** - R=NMe_2, **1c** - R=NO_2)

Ester	Theoretical level	Transition	ΔH	ΔG	ΔS
1a	6-31G(d)	**1a+DMIM→[1a][DMIM]**	-3.54	3.99	-25.24
		[1a][DMIM]→TS	33.31	34.31	-2.86
		[1a][DMIM]→[2][DMIM]+3a	3.54	-3.99	26.00
	6-31+G(d)	**1a+DMIM→[1a][DMIM]**	-0.47	6.43	-23.14
		[1a][DMIM]→TS	30.07	32.20	-3.02
		[1a][DMIM]→[2][DMIM]+3a	-20.54	-28.29	26.00
	6-31G(d,p)	**1a+DMIM→[1a][DMIM]**	-4.22	4.88	-30.51
		[1a][DMIM]→TS	30.47	31.98	-5.09
		[1a][DMIM]→[2][DMIM]+3a	4.22	-4.88	30.51
1b	6-31G(d)	**1b+DMIM→[1b][DMIM]**	-3.74	3.54	-24.44
		[1b][DMIM]→TS	30.61	31.23	-2.06
		[1b][DMIM]→[2][DMIM]+3b	14.94	1.05	46.59
	6-31+G(d)	**1b+DMIM→[1b][DMIM]**	-0.66	6.09	-22.64
		[1b][DMIM]→TS	29.38	30.98	-5.36
		[1b][DMIM]→[2][DMIM]+3b	11.14	-1.97	43.97
	6-31G(d,p)	**1b+DMIM→[1b][DMIM]**	-3.86	3.28	-23.95
		[1b][DMIM]→TS	27.78	28.60	-2.76
		[1b][DMIM]→[2][DMIM]+3b	11.61	-1.33	45.51
1c	6-31G(d)	**1c+DMIM→[1c][DMIM]**	-3.24	3.66	-23.15
		[1c][DMIM]→TS	35.13	36.56	-4.80
		[1c][DMIM]→[2][DMIM]+3c	14.09	1.11	43.56
	6-31+G(d)	**1c+DMIM→[1c][DMIM]**	12.30	7.29	-25.28
		[1c][DMIM]→TS	31.80	35.61	-4.24
		[1c][DMIM]→[2][DMIM]+3c	-1.80	-2.60	43.65
	6-31G(d,p)	**1c+DMIM→[1c][DMIM]**	-3.32	3.4	-22.52
		[1c][DMIM]→TS	34.28	34.28	-6.67
		[1c][DMIM]→[2][DMIM]+3c	-1.23	-1.23	42.11

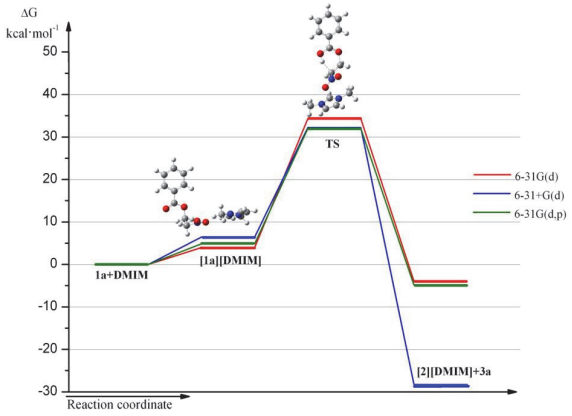

Fig. 1. Gibbs free energy profiles for the decomposition of nitroethyl benzoate **1a** catalyzed by the 1,3-dimethylimidazolium cation

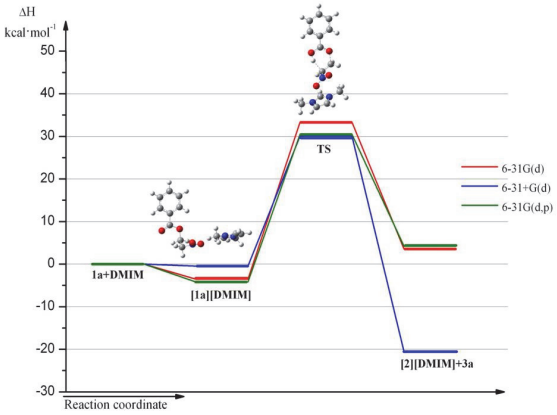

Fig. 2. Enthalpy profiles for the decomposition of nitroethyl benzoate **1a** catalyzed by the 1,3-dimethylimidazolium cation

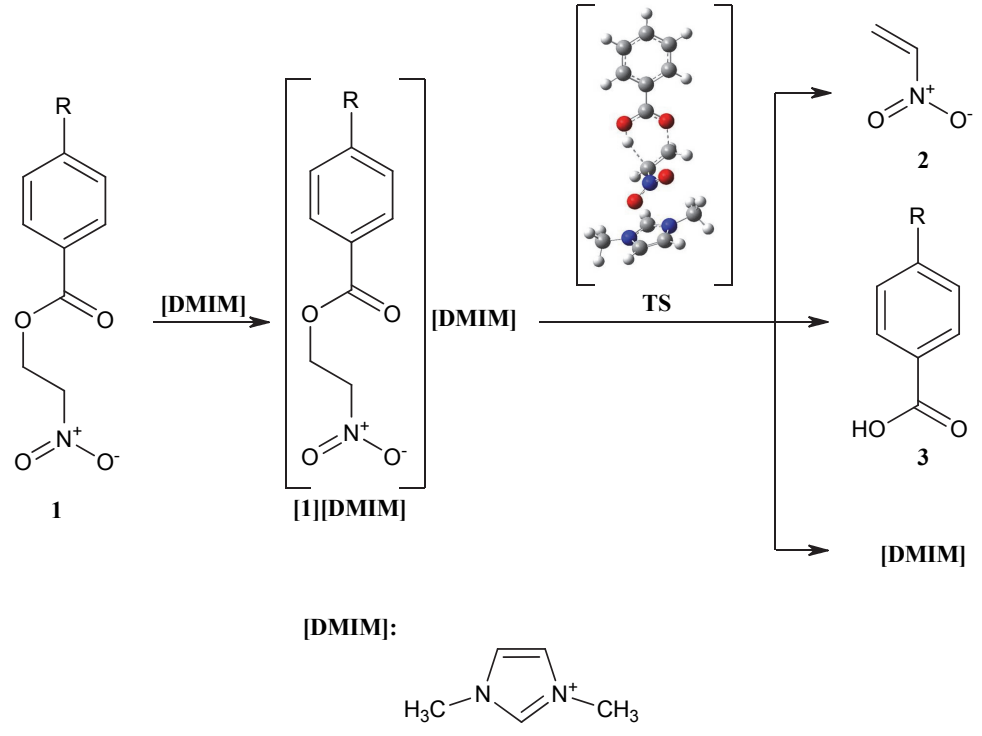

Scheme 1. Mechanism of the decomposition reaction of nitroethyl benzoates catalyzed by the 1,3-dimethylimidazolium cation

2.3 Transition structure of the decomposition reaction

The **TS**, also in the decomposition reaction catalyzed by the 1,3-dimethylimidazolium cation, has a six-membered structure (**Fig. 3**). Simultaneously, new bonds are formed: between atoms O5-H6 and between atoms C1-C2 and O3-C4 double bonds. The C4-O5 bond is change to a single bond, and H6-C1 and C2-O3 bonds become broken (**Table 2**).

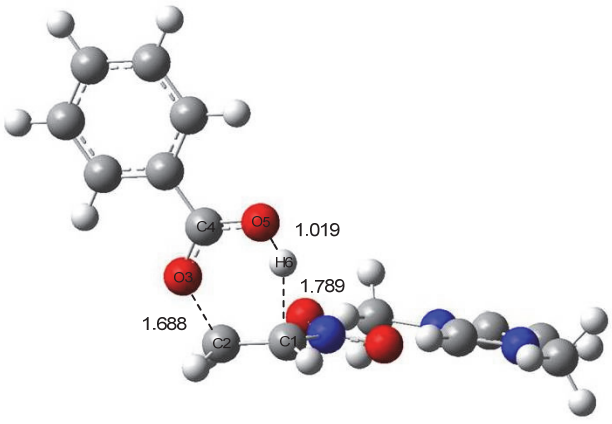

Fig. 3. Transition state **TS** structure for the decomposition of nitroethyl benzoates **1a** catalyzed by the DMIM cation

Table 2. Key parameters for structures of the decomposition of nitroethyl benzoates catalyzed by the DMIM cation according to B3LYP/6-31G(d) data (**1a** - R=H, **1b** - R=NMe_2, **1c** - R=NO_2)

Reaction	Structure	Interatomic distances [Å]						GEDT [e]
		H6-C1	C1-C2	C2-O3	O3-C4	C4-O5	O5-H6	
[1a][DMIM]→[2][DMIM]+3a	**[1a][DMIM]**	1.088	1.517	1.437	1.360	1.218	2.727	0.30
	TS	1.789	1.432	1.688	1.270	1.304	1.019	
	[2][DMIM]+3a		1.329		1.219	1.353	0.976	
[1b][DMIM]→[2][DMIM]+3b	**[1b][DMIM]**	1.088	1.517	1.434	1.368	1.223	2.752	0.35
	TS	1.885	1.422	1.721	1.276	1.318	1.000	
	[2][DMIM]+3b		1.329		1.224	1.361	0.976	
[1c][DMIM]→[2][DMIM]+3c	**[1c][DMIM]**	1.088	1.516	1.440	1.353	1.216	2.744	0.28
	TS	1.730	1.436	1.682	1.268	1.296	1.036	
	[2][DMIM]+3c		1.329		1.216	1.348	0.976	

Finally, we analysed the influence of the DMIM cation of structure TS. It was found that the H6-C1 bond in the reaction catalyzed by the DMIM cation is broken faster than in the uncatalyzed process. In turn, the C2-O3 bond of the TS of reaction with the ionic liquid cation is broken more slowly than in the case of the uncatalyzed reaction.[28] The nature of the substituent in benzene ring also has an impact on the transition structure. In the case of reaction **[1b][DMIM]→[2][DMIM]+3b**, the H6-C1 and C2-O3 bonds are broken faster than the same bonds in reaction **[1a][DMIM]→[2][DMIM]+3a**. By contrast, the H6-C1 and C2-O3 bonds in the case of reaction **[1c][DMIM]→[2][DMIM]+3c** are broken more slowly than in the case of reaction **[1a][DMIM]→[2][DMIM]+3a** (**Table 2**).

The GEDT value for the transition state for the decomposition reaction catalyzed by the 1,3-dimethylimidazolium cation is 0.30. This value is bigger than the same GEDT value for the transition states of similar non-catalytic processes.

3. Conclusions

Our quantum chemical study proved that the decomposition reaction of nitroethyl benzoates catalyzed by the 1,3-dimethylimidazolium cation proceeded via a polar one-step mechanism. Compared to the uncatalyzed process, the decomposition reaction in the presence of the 1,3-dimethylimidazolium cation proceed faster. All other research for the localization of different reaction channels lead via the ionic intermediate failed.

Acknowledgements

This research was supported in part by PL-Grid Infrastructure and financial support from the Polish State Committee (Grant no. C-2/88/2016/DS) are gratefully acknowledged.

References

1 Corey E. J., and Estreicher H. (**1978**) A new synthesis of conjugated nitro cyclo olefins, unusually versatile synthetic intermediates. *J. Am. Chem. Soc*., 100 (19) 6294-6295.
2 Varma R. S., and Kabalka G. W. (**1986**) Nitroalkenes in the synthesis of heterocyclic compounds. *Heterocycles*, 24 (9) 2645-2677.
3 Barrett A. G. M. (**1991**) Heterosubstituted nitroalkenes in synthesis. *Chem. Soc. Rev.*, 20 (1) 95-127.
4 Tso H. H., Gilbert B. A., and Hwu J. R. (**1993**) Novel double functional group transformation: 'one-flask' conversion of 1-nitrocycloalkenes to terminally unsaturated nitriles. *J. Chem. Soc., Chem. Commun.*, 18 669-670.
5 Perekalin V. V. **(1994)** *Nitroalkenes: conjugated nitro compounds*, Wiley, New York.
6 Berner O. M., Tedeschi L., and Enders D. (**2002**) Asymmetric Michael additions to nitroalkenes. *Eur. J. Org. Chem.*, 2002 (12) 1877-1894.
7 Kranse N., and Hoffmann-Röder A. (**2001**) Recent advances in catalytic enantioselective Michael additions. *Synthesis*, 2001 (2) 171-196.
8 Tietze L. F., and Kettschau G. (**1997**) Hetero Diels-Alder reactions in organic synthesis, in: Metz P. (Eds) *Stereoselective Heterocyclic Synthesis I.* Springer Berlin Heidelberg, Berlin, 1-120.
9 Kabalka G. W., and Varma R. S. (**1987**) Syntheses and selected reductions of conjugated nitroalkenes – a review. *Org. Prep. Proc. Int.*, 19 (4-5) 283-328.
10 Blades K., Butt A. H., Cockerill G. S., Easterfield H. J., Lequeux T. P., and Percy J. M. (**1997**) Phosphorus(III) ligands with fluorous ponytails. *J. Chem. Soc.*, Perkin Trans. 1, 1997 (24) 3609-3612.
11 Hoashi Y., Yabuta T., and Takemoto Y. (**2004**) Bifunctional thiourea—catalyzed enantioselective double Michael reaction of γ,δ-unsaturated β-ketoester to nitroalkene: asymmetric synthesis of (-)-epibatidine. *Tetrahedron Lett.*, 45 (50) 9185-9188.
12 Latif N., Asaad F. M., and Hosni H. (**1986**) N-Unsubstituted (carbamoyloxy)nitrostyrenes: a new series of aryl-β-nitroalkenes with fungicidal properties. *Liebigs Ann. Chem.*, 1987 (6) 495-498.
13 Zee-Cheng K.-Y., and Cheng C.-C. (**1969**) Experimental tumor inhibitors. Antitumor activity of esters of ω-aryl-ψ-nitro-ψ-alken-1-ol and related compounds. *J. Med. Chem.*, 12 (1) 157-161.
14 Dadwal M., Mohan R., Panda D., Mobin S. M., and Namboothiri I. N. N. (**2006**) The Morita-Baylis-Hilman adducts of β-aryl nitroethylenes with other activated alkenes: synthesis and anticancer activity studies. *Chem. Commun.*, 2006 (3) 338-340.
15 Brian P. W., Jamieson M., and McGowan J. C. (**1948**) Toxicity of Sulphydryl Compounds to Seeds. *Nature*, 162 (13) 780.
16 Bocobo F. C., Curtis A.C., Block W. D., Harrell E. R., Evans E. E., and Haines R. F. (**1956**) Evaluation of nitrostyrenes as antifungal agents. I. In vitro studies. *Antibiot. Chemother.*, 6 (6) 385-390.
17 Hwu J. R., Chen K.-L., and Ananthan S. J. (**1994**) A new method for nitration of alkenes to α,β-unsaturated nitroalkenes. *J. Chem. Soc., Chem. Commun.*, 12 1425-1426.
18 Kunai A., Yanagi Y., and Sasaki K. (**1983**) A convenient preparation of conjugated nitro olefins by electrochemical method. *Tetrahedron Lett.*, 24 (41) 4443-4444.
19 Sy W. W., and By A. W. (**1985**) Nitration of substituted styrenes aith nitryl iodide. *Tetrahedron Lett.*, 26 (9) 1193-1196.
20 Jew S. S., Kim H. D., Cho Y. S., Cook C. H. (**1986**) A practical preparations of conjugated nitroalkenes. *Chem. Lett.*, 15 (10) 1747-1748.

21 Jasiński R., Ziółkowska M., Demchuk O. M., and Maziarka A. (**2014**) Regio- and stereoselectivity of polar [2+3] cycloaddition reactions between (Z)-C-(3,4,5-trimethoxyphenyl)-N-methylnitrone and selected (E)-2-sybstituted nitroethenes. *Central. Eur. J. Chem.*, 12 (5) 586-593.
22 Jasiński R. (**2015**) A stepwise, zwitterionic mechanism for the 1,3-dipolar cycloaddition between (Z)-C-4-methoxyphenyl-N-phenylnitrone and gem-chloronitroethene catalysed by 1-butyl-3-methylimidazolium ionic liquid cations. *Tetrahedron Lett.*, 56 (3) 532-535.
23 Jasiński R. (**2014**) Searching for zwitterionic intermediates in Hetero Diels-Alder reactions between methyl a,p-dinitrocinnamate and vinyl-alkyl ethers. *Comput. Theor. Chem.*, 1046 (15) 93-98.
24 Jasiński R. (**2009**) Regio- and stereoselectivity of [2+3]cycloaddition of nitroethene to (Z)- N-aryl-C-phenylnitrones. *Coll. Czech. Chem. Commun.*, 74 (9) 1341-1349.
25 Jasiński R. (**2015**) Nitroacetylene as dipolarophile in [2 + 3] cycloaddition reactions with allenyl-type three-atom components: DFT computational study. *Monatsh. Chem.*, 146 (4) 591–599.
26 Jasiński R. (**2014**) Molecular mechanism of thermal decomposition of fluoronitroazoxy compounds: DFT computational study. *J. Fluor. Chem.*, 160 29-33.
27 Jasiński R., and Kącka A. (**2015**) A polar nature of benzoic acids extrusion from nitroalkyl benzoates: DFT mechanistic study. *J. Mol. Mod.*, 21 (3) 59-65.
28 Kącka A., and Jasiński R. (**2016**) A density functional theory mechanistic study of thermal decomposition reactions of nitroethyl carboxylates: undermine of "pericyclic" insight. *Heteroatom Chem.*, 27 (5) 279-289.
29 Jasiński R. (**2016**) First example of stepwise, zwitterionic mechanism for bicycle[2.2.1]hept-5-ene (norbornene) formation process catalyzed by the 1-butyl-3-methylimidazolium cations. *Monatsh. Chem.*, 147 (7) 1207-1213.
30 Jasiński R. (**2015**) A stepwise, zwitterionic mechanism for the 1,3-dipolar cycloaddition between (Z)-C-4-methoxyphenyl-N-phenylnitrone and gem-chloronitroethene catalyzed by 1-butyl-3-methylimidazolium ionic liquid cations. *Tetrahedron Lett.*, 56 (3) 532-535.
31 Feng D., Li L., Yang F., Tan W., Zhao G., Zou H., Xian M., and Zhang Y. (**2011**) Separation of ionic liquid [Mmim][DMP] and glucose from enzymatic hydrolysis mixture of cellulose using alumina column chromatography. *Appl. Microbiol. Biotechnol.*, 91 (2) 399-405.
32 Park S., and Kazlauskas R. J. (**2003**) Biocatalysis in ionic liquids - advantages beyond green technology. *Curr. Opin. Biotechnol.*, 14 (4) 432-437.
33 Dommert F., and Holm Ch. (**2013**) Refining classical force fields for ionic liquids: theory and application to [MMIM][Cl]. *Phys. Chem. Chem. Phys.*, 15 (6) 2037-2049.
34 Kragl U., Eckstein M., and Kaftzik N. (**2002**) Enzyme catalysis in ionic liquids. *Curr. Opin. Biotechnol.*, 13 (6) 565-571.
35 Frisch M. J., Trucks G. W., Schlegel H. B., Scuseria G. E., Robb M. A., Cheeseman J. R., Montgomery J. A., Vreven T. J., Kudin K. N., Burant J. C., Millam J. M., Iyengar S. S., Tomasi J., Barone V., Mennucci B., Cossi M., Scalmani G., Rega N., Petersson G. A., Nakatsuji H., Hada M., Ehara M., Toyota K., Fukuda R., Hasegawa J., Ishida M., Nakajima Y., Honda O., Kitao O., Nakai H., Klene M., Li X., Knox J. E., Hratchian H. P., Cross J. B., Adamo C., Jaramillo J., Gomperts R., Stratmann R. E., Yazyev O., Austin A. J., Cammi R., Pomelli C., Ochterski J. W., Ayala P. Y., Morokuma K., Voth G. A., Salvador P., Dannenberg J. J., Zakrzewski V. G., Dapprich S., Daniels A. D., Strain M. C., Farkas M. C., Malick D. K., Rabuck A. D., Raghavachari K., Foresman J. B., Ortiz J. V., Cui Q., Baboul A. G., Clifford S., Cioslowski J., Stefanov B. B., Liu G., Liashenko A., Piskorz P., Komaromi I., Martin R. L., Fox D. J., Keith T., Al-Laham M. A., Peng C. Y., Nanayakkara A., Challacombe M., Gill P. M. W., Johnson B., Chen W., Wong M. W., Gonzalez C., and Pople J. A. (**2009**) Gaussian 09 rev A.1 Gaussian Inc. Wallingford CT.
36 Stephens P., Devlin F. J., Chabalowski C. F., and Frisch M. J. (**1994**) Ab Initio Calculation of Vibrational Absorption and Circular Dichroism Spectra Using Density Functional Force Fields. *J. Phys. Chem.*, 98 (45) 11623-11627.
37 Becke A. D. (**1993**) Density-functional thermochemistry. III. The role of exact exchange. *J. Chem. Phys.*, 98 (7) 5648-5658.

38 Lee C., Yang W., and Parr R. G. (**1988**) Development of the Colle-Salvetti correlation-energy formula into a functional of the electron density. *Phys. Rev. B*, 37 (2) 785-789.
39 Fukui K. (**1970**) Formulation of the reaction coordinate. *J. Phys. Chem.*, 74 (23) 4161-4163.
40 Cossi M., Rega N., Scalmani G., and Barone V. (**2003**) Energies, structures, and electronic properties of molecules in solution with the C-PCM solvation model. *J. Comp. Chem.*, 24 (6) 669-681.
41 Wasserscheid P., and Welton T. (**2007**) *Ionic Liquid in Synthesis*, 2nd Ed, Wiley-VCH Verlag GmbH, Weinheim.
42 Domingo L. R. (**2014**) A new C–C bond formation model based on the quantum chemical topology of electron density. *RSC Adv.*, 4 (61) 32415-32428.
43 Berski S., Andres J., Silvi B., and Domingo L. R. (**2003**) The Joint Use of Catastrophe Theory and Electron Localization Function to Characterize Molecular Mechanisms. A Density Functional Study of the Diels−Alder Reaction between Ethylene and 1,3-Butadiene. *J. Phys. Chem.*, 107 (31) 6014-6024.
44 Jasiński R. (**2015**) A new mechanistic insight on beta-lactam systems formation from 5-nitroisoxazolidines. *RSC Adv.*, 5 (62) 50070-50072.
45 Szczepanek A., Jasińska E., Kącka A., and Jasiński R. (**2015**) An experimental and quantumchemical study of [2+3] cycloaddition between (Z)-C-(m,m,p-trimethoxyphenyl)-N-(p-methyphenyl)-nitrone and (E)-3,3,3-trichloro-1-nitroprop-1-ene: mechanistic aspects. *Curr. Chem. Lett.*, 4 (1) 33-44
46 Domingo L. R., Perez P., and Contreras R. (**2004**) Reactivity of the carbon–carbon double bond towards nucleophilic additions. A DFT analysis. *Tetrahedron*, 60 (31) 6585-6591.
47 Domingo L. R., Arno M., and Andres J. (**1999**) Influence of reactant polarity on the course of the inverse-electron-demand Diels−Alder reaction. A DFT study of regio- and stereoselectivity, presence of Lewis Acid catalyst, and inclusion of solvent effects in the reaction between nitroethene and substituted ethenes. *J. Org. Chem.*, 64 (16) 5867-5875.
48 Domingo L. R., Jose Aurell M., Kneeteman M. N., and Mancini P. M. (**2008**) Mechanistic details of the domino reaction of nitronaphthalenes with the electron-rich dienes. A DFT study. *J. Mol. Struct.*, 853 (1-3) 68-76.

IV. WNIOSKI

Na podstawie przeprowadzonych badań teoretycznych można sformułować następujące wnioski:

1. Obliczenia kwantowo-chemiczne niezależnie od poziomu teorii wskazują, iż mechanizm dekompozycji estrów kwasów karboksylowych i nitroalkoholi nie może być traktowany jako mechanizm pericykliczny.
2. Szczegółowe analizy trajektorii IRC oraz geometrii stanów przejściowych wskazują, że procesy te powinny być zaliczane do grupy procesów „one-step – two-stage".
3. Analizy wykonane techniką BET wskazują, że proces dekompozycji benzoesanu nitroetylowego rozpoczyna się od synchronicznego rozluźnienia wiązań O-C i C-H. Podczas heterolitycznego rozerwania wiązania O-C, zachodzi homolityczne oddziaływanie atomów C5-H6, powodując utworzenie pseudorodników. Formowanie wiązania podwójnego obecnego w nitroetylenie dokonuje się w ostatniej fazie reakcji.
4. Na kinetykę reakcji dekompozycji estrów kwasów karboksylowych i nitroalkoholi w pewnym zakresie wpływ ma charakter podstawnika oraz polarność medium reakcyjnego.
5. Reakcje dekompozycji estrów kwasów karboksylowych i nitroalkoholi w obecności BH_3 przebiegają według polarnego, jednostopniowego mechanizmu. Z kolei dekompozycja tych samych estrów katalizowana przez BF_3 dokonuje się według mechanizmu dwustopniowego przechodzącego przez jonowy intermediat. Oba te procesy realizują się szybciej, niż analogiczne procesy niekatalityczne.
6. W obecności kationów cieczy jonowych (trietylosulfoniowego, trietylofosfoniowego, 1,3-dimetyloimidazoliowego oraz etyloamoniowego) – reakcje rozkładu estrów kwasów karboksylowych i nitroalkoholi przebiegają szybciej, niż w warunkach bez katalitycznych. Spośród testowanych kationów najefektowniejszymi okazały się być kationy trietylosulfoniowy (TES) oraz trietylofosfoniowy (TEP).
7. Proces dekompozycji estrów kwasów karboksylowych i nitroalkoholi w obecności kationu etyloamoniowego (EA) realizuje się według mechanizmu dwustopniowego, przechodzącego poprzez jonowy intermediat.

V. STRESZCZENIE

W ramach pracy przeprowadzono kwantowo-chemiczne studia nad molekularnym mechanizmem reakcji dekompozycji estrów kwasów karboksylowych i nitroalkoholi. Symulacje te wykonano dla reakcji realizujących się w warunkach termicznych jak również katalitycznych. W roli katalizatorów zastosowano kwasy Lewisa (BH_3 i BF_3) oraz kationy cieczy jonowych (trietylosulfoniowy, trietylofosfoniowy, 1,3-dimetyloimidazoliowy i etyloamoniowy).

W pierwszym etapie tych studiów zbadano mechanizm procesu termicznej dekompozycji estrów kwasów karboksylowych i nitroalkoholi. Okazało się, iż reakcje te powinny być zaliczane do grupy procesów „one-step – two-stage". Szczegółowa analiza MEDT ukazuje, iż tytułowe procesy, rozpoczynają się od synchronicznego rozluźnienia wiązań O-C oraz C-H (przy czym podczas heterolitycznego rozerwania wiązania O-C, zachodzi homolityczne oddziaływanie atomów C5-H6, powodując utworzenie pseudorodników), podczas gdy formowanie wiązania podwójnego dokonuje się w ostatniej fazie reakcji.

Kolejny etap badań obejmował studia reakcji dekompozycji estrów kwasów karboksylowych i nitroalkoholi katalizowane nieorganicznymi kwasami Lewisa. Okazało się, iż procesy te realizują się szybciej niż procesy bez obecności katalizatora. W szczególności reakcje w obecności BH_3 przebiegają według polarnego, jednostopniowego mechanizmu, podczas gdy przy obecności BF_3 realizują się według mechanizmu dwustopniowego przebiegającego przez jonowy intermediat.

Ostatni etap badań obejmował reakcjie dekompozycji estrów kwasów karboksylowych i nitroalkoholi w obecności kationów cieczy jonowych. Okazało się, że procesy te realizują się znacznie szybciej niż w warunkach bezkatalitycznych (najszybciej w obecności kationów trietylosulfoniowego i trietylofosfoniowego). Należy w tym miejscu zaznaczyć, że proces katalizowany przez kation etyloamoniowy realizuje się według mechanizmu dwustopniowego, przechodzącego poprzez jonowy intermediat.

VI. ABSTRACT

The study involved quantum-chemical analysis of the molecular mechanism of decomposition of carboxylic esters of nitroalcohols. Simulations were performed for reactions proceeding in thermal as well as catalytic conditions. Lewis acids (BH_3, BF_3) and ionic liquid cations (triethylsulfonium, triethylphosponium, 1,3-dimethylimidazolium, and ethylammonium) were used as catalysts.

The first step consisted in the analysis of the mechanism of thermal decomposition of carboxylic esters of nitroalcohols. The reactions were found to fall within the category of "one-step – two-stage" processes. As demonstrated by detailed MEDT analysis, the title processes begin with synchronous loosening of O-C and C-H bonds (with homolytic interaction occurring between C5 and H6 atoms upon heterolytic cleavage of the O-C bond, thus generating a pseudoradical) whereas the formation of the double bond takes place at the last stage of the process.

The next step consisted in the analysis of the mechanism of decomposition of carboxylic esters of nitroalcohols catalyzed by inorganic Lewis acids. The processes were observed to proceed faster than non-catalyzed processes. In particular, reactions catalyzed by BH_3 proceed along a polar, single-stage mechanism while reactions catalyzed by BF_3 proceed along a two-stage mechanism via an ionic intermediate.

The last step of the study consisted in the analysis of the mechanism of decomposition of carboxylic esters of nitroalcohols catalyzed by ionic liquid cations. The processes were shown to proceed much faster than in non-catalytic conditions (with reaction rates being the highest in the presence of triethylsulfonium or triethylphosphonium ions). It should be noted that the process catalyzed by the ethylammonium cation proceeds along a two-step mechanism via an ionic intermediate.

VII. ZUSAMMENFASSUNG

Im Rahmen der Arbeit wurde das quantenchemische Studium über molekularen Mechanismus der Zersetzungsreaktion der Ester von Carbonsäuren und Nitroalkoholen durchgeführt. Diese Simulation wurde für Reaktionen durchgeführt, die sich sowohl in thermischen aus auch katalytischen Bedingungen realisieren. Als Katalysatoren wurden Lewis-Säuren (BH_3 und BF_3) und Kationen der ionischen Flüssigkeiten (Triethylosulfonium, Triethylofosfonium, 1,3-Dimethyloimidazolium und Ethyloammonium) verwendet.

Auf der ersten Etappe dieses Studiums wurde Mechanismus des Prozesses der thermischen Zersetzung der Ester von Carbonsäuren und Nitroalkoholen geprüft. Es hat sich erwiesen, dass diese Reaktionen zur Prozessgruppe „one-step – two-stage" gezählt werden sollen. Die ausführliche MEDT-Analyse zeigt, dass die Titelprozesse mit einer synchronischen Lockerung der Bindungen O-C und C-H beginnen (wobei während der heterolytischen Bindungsprengung O-C eine homolytische Wirkung der Atome C5-H6 stattfindet und Bildung von Pseudoradikalen verursacht), während die Formung der Doppelbindung in der letzten Phase der Reaktion zustande kommt.

Die nächste Etappe der Untersuchungen umfasste das Studium von Zersetzungsreaktion der Ester von Carbonsäuren und Nitroalkoholen, mit anorganischen Lewis-Säuren katalysiert. Es hat sich erwiesen, dass sich diese Prozesse schneller realisieren als die Prozesse ohne Katalysator. Insbesondere verlaufen die Reaktionen in Anwesenheit von BH_3 nach polarem, einstufigem Mechanismus, während sie sich in Anwesenheit von BF_3 nach zweistufigem Mechanismus realisieren, der durch ionischen Intermediat verläuft.

Die letzte Etappe des Studiums umfasste das Studium von Zersetzungsreaktion der Ester von Carbonsäuren und Nitroalkoholen in Anwesenheit von Kationen der ionischen Flüssigkeiten. Es hat sich bewiesen, dass sich diese Prozesse bedeutend schneller realisieren, als in Bedingungen ohne Katalysator (am schnellsten in Anwesenheit von Kationen: Triethylosulfonium und Triethylofosfonium). Es ist dabei zu bemerken, dass sich der Prozess, der durch Ethyloammonium-Kation katalysiert wird, nach zweistufigem Mechanismus realisiert, der durch ionischen Intermediat verläuft.

VIII. АВТОРЕФЕРАТ

В рамках работы проведены квантово-химические исследования молекулярного механизма реакции разложения сложных эфиров карбоновых кислот и нитроспиртов. Моделирование было выполнено для реакций, которые проводились как в термических, так и в каталитических условиях. В качестве катализаторов использовались кислоты Льюиса (BH3 и BF3) и катионы ионных жидкостей (триэтилсульфоний, триэтилфосфоний, 1,3-диметилимидазолий и этиламмоний).

На первом этапе этих исследований был рассмотрен механизм процесса термического разложения сложных эфиров карбоновых кислот и нитроспиртов. Оказалось, что эти реакции должны быть включены в группу процессов „one-step – two-stage". Детальный анализ MEDT показывает, что заглавные процессы начинаются с синхронного ослабления связей O-C и C-H (причем во время гетеролитического расщепления связи O-C происходит гомолитическое взаимодействие атомов C5-H6, что приводит к образованию псевдорадикалов), тогда как образование двойной связи происходит в заключительной фазе реакции.

Следующий этап исследований включал изучение реакций разложения сложных эфиров карбоновых кислот и нитроспиртов, катализируемых неорганическими кислотами Льюиса. Оказалось, что эти процессы происходят быстрее, чем без присутствия катализатора. В частности, реакции в присутствии BH3 протекают в соответствии с полярным одностадийным механизмом, а в присутствии BF3 – с двухстадийным механизмом, протекающим путем создания ионного нтермедиата.

Последний этап исследований касался изучения реакций разложения сложных эфиров карбоновых кислот и нитроспиртов в присутствии катионов ионных жидкостей. Оказалось, что эти процессы протекают намного быстрее, чем при некаталитических условиях (быстрее всего в присутствии катионов триэтилсульфония и триэтилфосфония). Здесь следует отметить, что процесс, катализируемый катионом этиламмония, осуществляется в соответствии с двухстадийным механизмом, проходящим путем создания ионного нтермедиата.

IX. SPIS CYTOWANEJ LITERATURY

[1] Berner O.M., Tedeschi L., Enders D., *Eur. J. Org. Chem.*, 1877 (2002).

[2] Kranse N., Hoffmann-Röder A., *Synthesis*, 171 (2001).

[3] Barrett A.G.M., *Chem. Soc. Rev.*, **20**, 95 (1991).

[4] Barrett A.G.M., Graboski G.G., *Chem. Rev.*, **86**, 751 (1990).

[5] Denmark S.E., Thorarensen A., *Chem. Rev.*, **96**, 137 (1996).

[6] Yoshikoshi A., Miyashita M., *Acc. Chem. Res.*, **18**, 284 (1985).

[7] Tietze L.F., Kettschau G., *Top. Curr. Chem.*, **189**, 1 (1997).

[8] Rajappa S., *Tetrahedron*, **37**, 1453 (1981).

[9] Kabalka G.W., Varma R.S., *Org. Prep. Proc. Int.*, **19**, 283 (1987).

[10] Schales O., Graefe H.A., *J. Am. Chem. Soc.*, **74**, 4486 (1952).

[11] Dann O., Holler E.F., *Chem. Ber.*, **82**, 76 (1949).

[12] Bousquet E.W., Kirby J.E., Searle N.E., *U. S. Patent, 2,335,384* (1943).

[13] Bousquet E.W., Kirby J.E., Searle N.E., *Chem. Abstr.*, **38**, 2834 (1944).

[14] Brown A.W.A., Robinson D.B.W., Hurtig H., Wenner B.J., *Can. J. Res.*, **26D**, 177 (1948).

[15] Delmastro-Greenwood M., Hughan K.S., Vitturi D.A., Salvatore S.R., Grimes G., Potti G., Shiva S., Schopfer F.J., Gladwin M.T., Freeman B.A., Gelhaus-Wendell S., *Free. Radic. Biol. Med.*, **89**, 333 (2015).

[16] Perekalin V.V., Lipina E.S., Berestovitskaya V.M., Efremov D.A., *Nitroalkenes: conjugated nitroalkenes*, Wiley, New York (1994).

[17] Alexander R., Kralert P.G., Kagi R.J., *Org. Geochem.*, **19**, 133 (1992).

[18] Scheer J.C., Kooyman E.C., Sixma F.L.J., *Recl. Trav. Chim. Pays-Bas*, **82**, 1123 (1963).

[19] Taylor R., *The Chemistry of Functional Groups*, Supplement B, Ed. Patai S., Wiley, New York (1949).

[20] Richardson W. H., O'Neale H.E., *Comprehensive Chemical Kinetics*, Ed. Bamford C. H., Tipper C. F. H., American Elsevier, New York (1972).

[21] Lakhdar S., Terrier F., Vichard D., Berionni G., Guesmi N.E., Goumont R., Boubaker T., *Chem. Eur. J.*, **16**, 5681 (2010).

[22] Grebennikov V.N., Manelis G.B., Nazin G.M., Studney Y.N., Fokin A.V., *Russ. Chem. Bull.*, 1573 (1985).

[23] Jasiński R., *J. Fluor. Chem.*, **160**, 29 (2014).

[24] Corey E.J., Estreicher H., *J. Am. Chem. Soc.*, **100**, 6294 (1987).

[25] Seebach D., Colvin E.W., Lehr F., Weller T., *Chimia*, **33**, 1 (1979).

[26] Rosini G., Ballini R., *Synthesis*, 833 (1988).

[27] Dornow A., Jordan H.D., Muller A., *Chem. Ber.*, **94**, 67 (1961).

[28] Ono N., *The nitro group in organic synthesis*, New York, Wiley-VCH (2001).

[29] Ballini R., Petrini M., *Tetrahedron*, **60**, 1017 (2004).

[30] Li J.J., Corey E., *Name reactions of homologation*, Part I, Ed. Hoboken N.J., John Wiley (2009).

[31] Halimehjani A.Z., Namboothini I.N.N., Hooshmand S.E., *RSC Adv.*, **4**, 31261 (2014).

[32] Sibi M.P., Manyem S., *Tetrahedron*, **56**, 8033 (2000).

[33] Corey E., Estreicher H., *Tetrahedron Lett.*, **21**, 1113 (1980).

[34] Dampawan P., *Tetrahedron Lett.*, **23**, 135 (1982).

[35] Noland W.E., *Chem. Rev.*, **55**, 137 (1955).

[36] Chen F., Ren H.X., Yang Y., Ji Sh.P., Zhang Z.B., Tian F., Peng L., Wang L.X., *Chirality*, **29(7)**, 369 (2017).

[37] Okino T., Hoashi Y., Takemoto Y., *J. Am. Chem. Soc.*, **125**, 12672 (2003).

[38] Takenaka N., Chen. J., Captain B., Sarangthem R.S., Chandrakumar A., *J. Am. Chem. Soc.*, **132**, 4536 (2010).

[39] Wu J., Li X., Wu F., Wan B., *J. Am. Chem. Soc.*, **13**, 4834 (2011).

[40] Kurth M.J., O'Brien M.J., Hope H., Yanuck M., *J. Org. Chem.*, **50**, 2626 (1985).

[41] Varma R.S., Kabalka G.W., *Heterocycles*, **24**, 2645 (1986).

[42] Boyer J.H., Nitroazoles: *The C-nitro Derivatives of Five-membered N- and N,O-Heterocycles*, VCH, Berlin (1986).

[43] Rudchenko V.F., *Chem. Rev.*, **93**, 725 (1993).

[44] Fringualli F., Taticchi A., *The Diels-Alder Reaction: Selected Practical Methods*. Wiley, New York (2002).

[45] Jasiński R., *Comp. Theor. Chem.*, **1046**, 93 (2014).

[46] Jasiński R., Kubik M., Łapczuk-Krygier A., Kącka A., Dresler E., *React. Kinet., Mech., Cat.*, **113**, 333 (2014).

[47] Korotaev V.Y., Barkov A.Y., Slepukhin P.A., Kodess M.I., Sosnovskikh V.Y., *Tetrahedron Lett.*, **52**, 5764 (2011).

[48] Itoh K., Kitoh K., Kishimoto Sh., *Canad. J. Chem.*, **84(3)**, 392 (2006).

[49] He F., Bo Y., Altom J.D., Corey J., *J. Am. Chem. Soc.*, **121**, 6771 (1999).

[50] Yamabe S., Kuwata K., Minato T., *Theor. Chem. Acc.*, 139 (1999).

[51] Huisgen R., Angew. *Chem. Int. Ed.*, **2(10)**, 565 (1963).

[52] Smith I., *Chem. Rev.*, **23(2)**, 193 (1938).

[53] Padwa A., *Synthetic Applications of 1,3-Dipolar Cycloaddition Chemistry Toward Heterocycles and Natural Products*, Ed. Pearson W.H., New York, USA, John Wiley & Sons Inc. (2002).

[54] Moulay S., Touati A., *Compt. Rend. Chim.*, **13(12)**, 1474 (2010).

[55] Ioffe S.L., *Nitrile oxides, Nitrones and nitronates in organic synthesis*, Wiley, Interscience, New Yersey (2007).

[56] Nicolaou K.C., Snyder S.A., Montagnon T., Vassilikogiannakis G., *Angew. Chem., Int. Ed.*, **41**, 1668 (2002).

[57] Łapczuk-Krygier A., Ponikiewski Ł., Jasiński R., *Crystallogr. Reports*, **59(7)**, 961 (2014).

[58] Fuji K., Node M., Nagasawa H., Nanima Y., Terada S., *J. Am. Chem. Soc.*, **108**, 3855 (1986).

[59] Novellino L., d'Ischina M., Prota G., *Synthesis*, 793 (1999).

[60] Buckley G.D., Scaife C.W., *J. Chem. Soc.*, 1471 (1947).

[61] Blomquist A.T., Tapp W.J., Johnson J.R., *J. Am. Chem. Soc.*, **67**, 1519 (1945).

[62] Agrawal J.P., Hodgson R.D., *Organic Chemistry of Explosives*, John Wiley & Sons, England (2007).

[63] Kaap S., Quentin I., Tamiru D., Shaheen M., Eger K., Steinfelder H.J., *Biochem. Pharmacol.*, **65**, 603 (2003).

[64] Zee-Cheng K., Cheng C., *J. Med. Chem.*, **12**, 157 (1969).

[65] Pettit R.K., Pettit G.R., Hamel E., Hogan F., Moser B.R., Wolf S., Pon S., Chapuis J.C., Schmidt J.M., *Bioorg. Med. Chem.*, **17**, 6606 (2009).

[66] Zee-Cheng K., Cheng C., *J. Med. Chem.*, **2**, 157 (1969).

[67] Boelle J., Schneider R., Gerardin P., Loubinoux B., Maienfisch P., Rindlisbacher A., *Pestic. Sci.*, **54**, 304 (1998).

[68] Brian P.W., Grove J.F., McGowan J.C., *Nature*, **158**, 876 (1946).

[69] Bocobo F.C., Curtis A.C., Block W.D., Harrell E.R., Evans E.E., Haines R.F., *Antibiol. Chemother.*, **6**, 385 (1956).

[70] McGawan J.C., Brian P.W., Hming H.G., *Ann. Applied Biol.*, **35**, 25 (1948).

[71] Bouis J., *Ann. Chim. Phys.*, **44**, 77 (1855).

[72] Konovalov M., *Zh. Obshch. Khim.*, **25**, 472 (1893).

[73] Gupta A., Ahmad F., Siddiqui M.S., *Indian J. Chem.*, **26**, 870 (1987).

[74] McMurray J.E., Musser J.H., Fleming I., Fortunek J., Nubline C., *Org. Synth. Coll.*, **6**, 799 (1988).

[75] Andrews M.A., Kelly K.P., *J. Am. Chem. Soc.*, **103**, 2894 (1981).

[76] Pecunioso A., Menicagli R., *J. Org. Chem.*, **53**, 2614 (1988).

[77] Hwu J.R., Chen K.L., Ananthan S., *J. Chem. Soc. Chem. Commun.*, 1425 (1994).

[78] Maity S., Naveen T., Sharma U., Maiti D., *Org. Lett.*, **15(3)**, 3384 (2013).

[79] Hasche R.J., *Pat. U.S. 2 298375* (1942).

[80] Bachman G.B., Standisch N.W., *J. Org. Chem.*, **26**, 1474 (1961).

[81] Abbott R.L., *Pat. U.S. 3255263* (1966).

[82] Chattaway F.D., Witherington P., *J. Chem. Soc.*, 1178 (1935).

[83] Chattaway F.D., Drewitt J.G.N., Parkes G.D., *J. Chem. Soc.*, 1294 (1936).

[84] Ballini R., Castagnani R., Petrini M., *J. Org. Chem.*, **57(7)**, 2160 (1992).

[85] Sopova A.S., Perekalin V.V., Lebedeva W.M., Yurchenko O.I., *Zh. Obsch. Khim.*, **34**, 1185 (1964).

[86] Wilkendorf R., Trenel M., *Chem. Ber.*, **57**, 306 (1924).

[87] Molteni M., Consonni R., Giovenzana T., Malpezzi L., Zanda M., *J. Fluor. Chem*,, **127(7)**, 901 (2006).

[88] Melton J., McMurry J.E., *J. Org. Chem.*, **40(14)**, 2138 (1975).

[89] Buckley G.D., Scaife C.W., *J. Chem. Soc.*, 1471 (1947).

[90] Blumquist A.T., Tapp W.J., Johnson J.R., *J. Am. Chem. Soc.*, **67**, 1519 (1945).

[91] Saikia A.K., Barua N.C., Sharma R.P., Ghosh A.C., *Synthesis*, 685 (1994).

[92] Rokhum L., Bez G., *Tetrahedron Lett.*, **54**, 5500 (2013).

[93] Knochel P., Seebach D., *Synthesis*, 1017 (1982).

[94] Karaoglu E., Baykal A., Senel M., Sozeri H., Toprak M.S., *Mater. Res. Bull.*, **47**, 2480 (2012).

[95] Anbazhagan M., Kumaran G., Sasidharan M., *J. Chem. Research*, 336 (1997).

[96] Thangaraj B., Jayaraj Ch., Srinivasan R., *J. Mol. Catal. A-Chem.*, **409**, 11 (2015).

[97] Dougnier F., Patarin J., Guth J.L., Anglerot D., *Zeolites*, **12**, 160 (1992).

[98] Sreekumar R., Padmakumar R., Rugmini P., *Tetrahedron Lett.*, **39**, 2695 (1998).

[99] Hoff H., Capaul M., *Helv. Chim. Acta.*, **1898**, 232 (1960).

[100] Leseticky L., Fidler V., Prochizka M., *Coll. Czech. Chem. Commun.*, **38**, 459 (1973).
[101] Tsivasov W.P., Petrovic W.F., *Khim. Khim. Tekhnol.*, **5**, 942 (1962).
[102] Sovish R.C., Boettcher W., *J. Polym. Sci. A.*, **2**, 5247 (1964).
[103] Noland W.E., *Org. Synth.*, **5**, 833 (1973).
[104] Miyashita M., Yanami T., Yoshikoshi A., *Org. Synth.*, **7**, 396 (1990).
[105] Payne G.B., *Org. Synth.*, **5**, 805 (1973).
[106] Gold M.H., *J. Am. Chem. Soc.*, **68**, 2544 (1946).
[107] Hass H.B., Susie A.G., Heider R.L., *J. Org. Chem.*, **15**, 8 (1949).
[108] Carroll F.I., White J.D., Wall M.E., *J. Org. Chem.*, **28**, 1236 (1963).
[109] Feuer H., Miller R., Lawyer C.B., *J. Org. Chem.*, **26**, 1357 (1961).
[110] Schwarz H., Nelles J., *Pat. U.S. 2 257980* (1941).
[111] Kędzierski B., Piotrowska H., *Roczniki Chem.*, **46**, 1421 (1972).
[112] Lampe K.F., Mende T.J., Mills A.P., *J. Chem. Eng. Data*, **7(1)**, 85 (1962).
[113] Eremenko L.T., Oreshko G.V., *Bull. Acad. Sci. USSR, Div. Chem. Sci. (Engl Transl.)*, **18(3)**, 660 (1969).
[114] Ferrand J.C., Schneider R., Gerardin P., Loubinoux B., *Synth. Commun.*, **26(33)**, 4329 (1996).
[115] Larkin J.M., Cummings W.M., Kreuz K.L., *J. Org. Chem.*, **39(5)**, 714 (1974).
[116] Wilkendorf R., Trenel M., *Chem. Ber.*, **57**, 306 (1924).
[117] Gold M.H., Pat. *U.S. 2414595* (1947).
[118] Verbruggen R., Viehe H.G., *Chimia*, **29**, 350 (1975).
[119] Viehe H.G., Verbruggen R., *Chimia*, **29**, 352 (1975).
[120] Shechter H., Conrad F., Daulton A.L., Kaplan R.B., *J. Am. Chem. Soc.*, **74(12)**, 3052 (1952).
[121] Pietrov A.A., Rail K.B., Vildovskaya A.J., *Zh. Obsch. Khim.*, **34**, 3513 (1964).
[122] Obenland C.O., *Preparation of alfa, bet unsaturated nitroalkenes and their reactions*, Facsinule Publisher (1950).
[123] Blomquist A.T., Shelley T.H., *J. Am. Chem. Soc.*, **70**, 147 (1948).
[124] Emmons W.D., Cannon W.N., Dawson J.W., Ross R.M., *J. Am. Chem. Soc.*, **75**, 1993 (1953).
[125] Ranaganathan S., Ranaganathan D., Singh S.K., *Tetrahedron Lett.*, **28(25)**, 2893 (1987).
[126] Barton D.H.R., Togo H., Zard S.Z., *Tetrahedron*, **41**, 5507 (1985).

[127] Jang Y.J., Lin W.W., Shin Y.K., Liu J.T., Hwang M.H., Yao Ch.F., *Tetrahedron*, **59**, 4979 (2003).

[128] Lee K., Oh D.Y., *Synth. Commun.*, **19(17)**, 3055 (1989).

[129] Kunetsky R.A., Dilman A.D., Struchkova M.I., Tartakovsky V.A., Ioffe S.L., *Tetrahedron Lett.*, **46**, 5203 (2005).

[130] Jaishankar M., Tseten T., Anbalagan N., Mathew B.B., Beeregowda K.N., *Interdiscip. Toxicol.*, **7(2)**, 60 (2014).

[131] Rim K.T., Koo K.H., Park J.S., *Saf. Health. Work.*, **4**, 12 (2013).

[132] Sobek J.M., Talburt D.E., *J. Bacteriol.*, **95**, 47 (1968).

[133] Emsley J., *J. Clin. Invest.*, **116(5)**, 1132 (2006).

[134] Leśniewska E., Szynkowska M.I., Paryjczak T., *Główne źródła rtęci w organizmach ludzi nie narażonych zakładowo*, Środkowo-Pomorskie Towarzystwo Naukowe Ochrony Środowiska, **11(28)**, 403 (2009).

[135] Mahajan V.K., Sharma N.L., *Austral. J. Derm.*, **52(4)**, 5 (2011).

[136] Semczuk W., *Toksykologia współczesna*, PZWL, Warszawa (2012).

[137] Zalups R.K., *Pharmacological Reviews*, **52(1)**, 113 (2000).

[138] Tchounwou P.B., Yedjou C.G., Patlolla A.K., Sutton D.J., *EXS*, **101**, 133 (2012).

[139] Chang L.W., Magos L., Suzuki T., *Toxicology of Metals*, Boca Raton, FL., USA, CRC Press (1996).

[140] Wood J.M., *Science*, **183**, 1049 (1974).

[141] Alexander R., Kralert P.G., Kagi R.J., *Org. Geochem.*, **19**, 133 (1992).

[142] Scheer J.C., Kooyman E.C., Sixma F.L.J., *Recl. Trav. Chim. Pays-Bas*, **82**, 1123 (1963).

[143] Taylor R., *The Chemistry of Functional Groups, Supplement B*, Ed. Patai S.,Wiley, New York (1949).

[144] Richardson W.H., O'Neale H.E., *Comprehensive Chemical Kinetics*, Ed. Bamford C. H., Tipper C.F.H., American Elsevier, New York (1972).

[145] Fisher E., Jourdan F., *Chem. Ber.*, **16**, 67 (1883).

[146] Kraft F., *Berichte Deutsch. Chem. Geseu.*, **16**, 3018 (1883).

[147] Frisch M.J., Trucks G.W., Schlegel H.B., Scuseria G.E., Robb M.A., Cheeseman J.R., Montgomery J.A., Vreven T.J., Kudin K.N., Burant J.C., Millam J.M., Iyengar S.S., Tomasi J., Barone V., Mennucci B., Cossi M., Scalmani G., Rega N., Petersson G.A., Nakatsuji H., Hada M., Ehara M., Toyota K., Fukuda R., Hasegawa J., Ishida M., Nakajima Y., Honda O.,

Kitao O., Nakai H., Klene M., Li X., Knox J.E., Hratchian H.P., Cross J.B., Adamo C., Jaramillo J., Gomperts R., Stratmann R.E., Yazyev O., Austin A.J., Cammi R., Pomelli C., Ochterski J.W., Ayala P.Y., Morokuma K., Voth G.A., Salvador P., Dannenberg J.J., Zakrzewski V.G., Dapprich S., Daniels A.D., Strain M.C., Farkas M.C., Malick D.K., Rabuck A.D., Raghavachari K., Foresman J.B., Ortiz J.V., Cui Q., Baboul A.G., Clifford S., Cioslowski J., Stefanov B.B., Liu G., Liashenko A., Piskorz P., Komaromi I., Martin R.L., Fox D.J., Keith T., Al-Laham M.A., Peng C.Y., Nanayakkara A., Challacombe M., Gill P.M.W., Johnson B., Chen W., Wong M.W., Gonzalez C., Pople J. A. *Gaussian 09* rev A.1 Gaussian Inc., Wallingford CT (2009).

X. ANEKS – WYKAZ DOROBKU NAUKOWEGO

1. Oryginalne publikacje (indeksowane na tzw. liście filadelfijskiej)

[1] **Kącka-Zych A.**, Domingo L.R., Rios-Gutiérrez M., Jasiński R.
Understanding the mechanism of the decomposition reaction of nitroethyl benzoate through the Molecular Electron Density Theory.
Theoretical Chemistry Accounts, **136**, 129 (2017) (IF=1.890)*.

[2] **Kącka-Zych A.**, Domingo L.R., Jasiński R.
Does a fluorinated Lewis acid catalyst change the molecular mechanism of the decomposition process of nitroethyl carboxylates?
Research on Chemical Intermediates, (2017) – in press – DOI: 10.1007/s11164-017-3106-1, (IF=1.369)*.

[3] **Kącka A.**, Jasiński R.
A dramatic change of kinetic conditions and molecular mechanism of decomposition processes of nitroalkyl carboxylates catalyzed by ethylammonium cations.
Computational and Theoretical Chemistry, **1104**, 37 (2017) (IF=1.549)*.

[4] **Kącka A.**, Jasiński R.
Triethylsulfonium and triethylphosphonium cations as novel catalysts for the decomposition process of nitroethyl benzoates.
Phosphorus Sulfur Silicon and the Related Elements, (2017) – in press – DOI: 10.1080/10426507.2017.1290626, (IF=0.809)*.

[5] Jasiński R., Kula K., **Kącka A.**, Mirosław B.
Unexpected course of reaction between (E)-2-aryl-1-cyano-1-nitroethenes and diazafluorene: why is there no 1,3-dipolar cycloaddition?
Monatshefte für Chemie , **148**, 909 (2017) (IF=1.282)*.

[6] **Kącka A.**, Jasiński R.
A density functional theory mechanistic study of thermal decomposition reactions of nitroethyl carboxylates: undermine of pericyclic insight.
Heteroatom Chemistry, **27**, 279 (2016) (IF=1.221).

[7] Jasiński R., Mróz K., **Kącka A.**
Experimental and theoretical DFT study on synthesis of sterically crowded 2,3,3,(4)5-tetrasubstituted-4-nitroisoxazolidines via 1,3-dipolar cycloaddition reactions between ketonitrones and conjugated nitroalkenes.
Journal of Heterocyclic Chemistry, **53**, 1424 (2016) (IF=0.893).

*Impact Factor podany na rok 2016

[9] Jasiński R., Kubik M., Łapczuk-Krygier A., **Kącka A.**, Dresler E., Boguszewska-Czubara A.
An experimental and theoretical study of the hetero Diels-Alder reactions between (E)-2-aryl-1-cyano-1-nitroethenes and ethyl vinyl ether: one-step or zwitterionic, two-step mechanism?
Reaction Kinetics, Mechanisms and Catalysis, **113**, 333 (2014) (IF=1.170).

2. Oryginalne publikacje (pozostałe)

[1] **Kącka A.**, Jasiński R.
DFT study of the decomposition reactions of nitroethyl benzoates catalyzed by the 1,3-dimethylimidazolium cation.
Current Chemistry Letters, **6**, 15 (2017) (MNiSW=12).

[2] Szczepanek A., Jasińska E., **Kącka A.**, Jasiński R.
An experimental and quantumchemical study of [2+3] cycloaddition between (Z)-C-(m,m,p-trimethoxyphenyl)-N-(p-methyphenyl)-nitrone and (E)-3,3,3-trichloro-1-nitroprop-1-ene: mechanistic aspects.
Current Chemistry Letters, **4**, 33 (2015) (MNiSW =12).

3. Publikacje przeglądowe

[1] Demchuk O.M., Kapłon K., **Kącka A.**, Pietrusiewicz K.M.
Utilisation of chiral phosphorus ligands in atroposelective cross-coupling reactions.
Phosphorus Sulfur and Silicon and the Related Elements, **191**, 180 (2016) (IF=0.809).

[2] **Kącka A.**, Dresler E., Jasiński R.
Nowe realizacje procesu Meyera.
Przemysł Chemiczny, **95**, 2334 (2016) (MNiSW =15).

[3] Dresler E., Jasińska E., Łapczuk-Krygier A., **Kącka A.**, Nowakowska-Bogdan E., Jasiński R.
Sprzężone nitroalkeny jako komponenty nieuzgodnionych reakcji Dielsa-Aldera – najnowsze doniesienia.
Chemik, **69** (7) 645 (2015) (MNiSW =8).

4. Książki, monografie

[1] Jasiński R., Łapczuk-Krygier A., **Kącka A.**, Kula K., Demchuk O.M.
Elementy preparatyki organicznej.
ISBN: 978-83-88100-78-9, RTN, Radom (2016).

5. Patenty i zgłoszenia patentowe

[1] Łapczuk-Krygier A., Dresler E., Jasiński R., Kulesza R., **Kącka A.**, Fiszer R.
Sposób otrzymywania (E)-2-(4-dimetyloamino)-fenylo-1-cyjano-1-nitroetenu.
Zgłoszenia patentowe PL412703
Data pierwszeństwa: 2015-06-12
Data publikacji: 2016-12-19

6. Konferencje międzynarodowe i krajowe (komunikaty)

[1] Kula K., **Kącka A.**, Mirosław B., Jasiński R.
Pochodne hydrazyny jako nieoczekiwany produkt reakcji diazafluorenu z wybranymi komponentami elektrofilowymi.
VI Ogólnopolska konferencja "Pomiędzy naukami".
mat. str. 48, Chorzów (2017).

[2] Łapczuk-Krygier A., **Kącka A.**, Jasiński R.
Czy ciecze jonowe mają przyszłość?
XVII Konferencja naukowa „Pierwiastki chemiczne a jakość życia".
mat. str. 80, Lublin (2014).

7. Konferencje międzynarodowe i krajowe (prezentacje posterowe)

[1] **Kącka-Zych A.**, Domingo L.R., Rios- Gutiérrez M., Jasiński R.
A modern view on decomposition reaction of 2-nitroethyl benzoate using ELF and MEDT theory.
XX International conference "Advances in chemistry of heterorganic compounds". Łódź (2017).

[2] **Kącka A.**, Jasiński R.
Non-pericyclic nature of thermal decomposition of nitroethyl carboxylates.
XIX International conference "Advances in chemistry of heterorganic compounds".
mat. P-012, Łódź (2016).

[3] Kula K., **Kącka A.**, Mirosław B., Jasiński R.
Diazafluorene as 1,3-dipole in reactions with conjugated nitroalkenes.
XIX International conference "Advances in chemistry of heterorganic compounds".
mat. P-014, Łódź (2016).

[4] Jasiński R., Mróz K., **Kącka A.**
1,3-Dipolar cycloaddition of selected ketonitrones with 2-EWG-substituted nitroethenes.
XVIII International conference "Advances in chemistry of heterorganic compounds".

mat. P-003, Łódź (2015).

[5] Łapczuk-Krygier A., **Kącka A.**, Rykała K., Kula K., Jasiński R.
Some examples of nitroaldol reactions catalyzed by ionic liquids.
XVII International conference "Advances in chemistry of heterorganic compounds".
mat. P-021, Łódź (2014).

[6] Jasiński R., Kubik M., Łapczuk-Krygier A., **Kącka A.**, Dresler E., Boguszewska-Czubara A.
Experimental and theoretical study of the polar D-A reaction between (E)-2-aryl-1-cyano-1-nitroethenes and vinyl-ethyl ether: mechanistic aspects.
XVII International conference "Advances in chemistry of heterorganic compounds".
mat. P-019, Łódź (2014).

[7] Hordyjewska A., Bernasiuk A., Jasiński R., Horecka A., Popiołek Ł., Boguszewska-Czubara A., Łapczuk-Krygier A., **Kącka A.**, Malm A., Kurzepa J.
The antimicrobial activity of novel compounds from nitroalkeny and norbornene group.
XVII Konferencja naukowa „Pierwiastki a zdrowie".
mat. str. 35, Lublin (2014).

[8] Jasiński R., Łapczuk-Krygier A., **Kącka A.**, Kubik M., Barański A.
Indeksy globalnej elektrofilowości – nowe narzędzie prognozowania reaktywności sprzężonych nitroalkenów w procesach [4+2] cykloaddycji do sprzężonych dienów.
XVII Sympozjum 'Kinetyczne metody badania mechanizmów reakcji w roztworach'.
mat. P-5, Poznań (2013).

XI. DEKLARACJE WSPÓŁAUTORÓW

Kraków, 18.10.2017

Oświadczenie o udziale w publikacjach i pracach realizowanych wspólnie z mgr inż. Agnieszką Kącką-Zych

Oświadczamy, że udział w pracy opublikowanej wspólnie z mgr inż. Agnieszką Kącką-Zych jest zgodny z opisem przedstawionym poniżej:

Publikacja:

R. Jasiński, **A. Kącka**
A polar nature of benzoic acids extrusion from nitroalkyl benzoates: DFT mechanistic study.
Journal of Molecular Modeling, **21**, 59-87 (2015).

Udział:

- mgr inż. Agnieszka Kącka-Zych
  współudział w sformułowaniu problemu naukowego, opracowanie koncepcji badań, wybór metodyki badań, prowadzenie badań i analiza wyników, opracowanie tekstu i przygotowanie do druku.
  (udział 85%)

- dr hab. inż. Radomir Jasiński, prof. PK
  współudział w sformułowaniu koncepcji badań, konsultacja naukowa, korespondencja z edytorem, przygotowanie odpowiedzi na recenzje.
  (udział 15%)

Agnieszka Kącka-Zych *Radomir Jasiński*

Kraków, 18.10.2017

Oświadczenie o udziale w publikacjach i pracach realizowanych wspólnie z mgr inż. Agnieszką Kącką-Zych

Oświadczamy, że udział w pracy opublikowanej wspólnie z mgr inż. Agnieszką Kącką-Zych jest zgodny z opisem przedstawionym poniżej:

Publikacja:

A. Kącka, R. Jasiński
A DFT mechanistic study of the thermal decomposition reactions of nitroethyl carboxylates: undermine of pericyclic insight.
Heteroatom Chemistry, **27**, 279-289 (2016).

Udział:

- mgr inż. Agnieszka Kącka-Zych:
  współudział w sformułowaniu problemu naukowego, opracowanie koncepcji badań, wybór metodyki badań, prowadzenie badań i analiza wyników, opracowanie tekstu i przygotowanie do druku, przygotowanie odpowiedzi na recenzje.
  (udział 90%)
- dr hab. inż. Radomir Jasiński, prof. PK
  współudział w sformułowaniu problemu naukowego, konsultacja naukowa.
  (udział 10%)

Agnieszka Kącka-Zych *Radomir Jasiński*

Kraków, 18.10.2017

Oświadczenie o udziale w publikacjach i pracach realizowanych wspólnie z mgr inż. Agnieszką Kącką-Zych

Oświadczamy, że udział w pracy opublikowanej wspólnie z mgr inż. Agnieszką Kącką-Zych jest zgodny z opisem przedstawionym poniżej:

Publikacja:

A. Kącka, R. Jasiński
Triethylsulfonium and triethylphosphonium cations as novel catalyst for the decomposition process of nitroethyl benzoates.
Phosphorous, Sulfur, and Silion and the Related Elements,
DOI: 10.1080/10426507.2017.1290626 (2017).

Udział:

- mgr inż. Agnieszka Kącka-Zych
  współudział w sformułowaniu problemu naukowego, opracowanie koncepcji badań, wybór metodyki badań, prowadzenie badań i analiza wyników, opracowanie tekstu i przygotowanie do druku, przygotowanie odpowiedzi na recenzje.
  (udział 90%)

- dr hab. inż. Radomir Jasiński, prof. PK
  współudział w sformułowaniu problemu naukowego, konsultacja naukowa.
  (udział 10%)

Kącka-Zych
Agnieszka Kącka-Zych

Radomir Jasiński

Kraków, 18.10.2017

Oświadczenie o udziale w publikacjach i pracach realizowanych wspólnie z mgr inż. Agnieszką Kącką-Zych

Oświadczamy, że udział w pracy opublikowanej wspólnie z mgr inż. Agnieszką Kącką-Zych jest zgodny z opisem przedstawionym poniżej:

Publikacja:

A. Kącka, R. Jasiński
A dramatic change of kinetic conditions and molecular mechanism of decomposition processes of nitroalkyl carboxylates catalyzed by ethylammonium cations.
Computational and Theoretical Chemistry, **1104**, 37-42 (2017).

Udział:

- mgr inż. Agnieszka Kącka-Zych
  współudział w sformułowaniu problemu naukowego, opracowanie koncepcji badań, wybór metodyki badań, prowadzenie badań i analiza wyników, opracowanie tekstu i przygotowanie do druku.
  (udział 85%)
- dr hab. inż. Radomir Jasiński, prof. PK
  współudział w sformułowaniu koncepcji badań, konsultacja naukowa, korespondencja z edytorem, przygotowanie odpowiedzi na recenzje.
  (udział 15%)

Agnieszka Kącka-Zych *Radomir Jasiński*

Kraków, 18.10.2017

Oświadczenie o udziale w publikacjach i pracach realizowanych wspólnie z mgr inż. Agnieszką Kącką-Zych

Oświadczamy, że udział w pracy opublikowanej wspólnie z mgr inż. Agnieszką Kącką-Zych jest zgodny z opisem przedstawionym poniżej:

Publikacja:

A. Kącka-Zych, L.R. Domingo, M. Ríos-Gutiérrez, R. Jasiński
Understanding the mechanism of the decomposition reaction of nitroethyl benzoate through the Molecular Electron Density Theory
Theoretical Chemistry Accounts, DOI: 10.1007/s00214-017-2161-4 (2017).

Udział:

- mgr inż. Agnieszka Kącka-Zych
  współudział w sformułowaniu problemu naukowego, opracowanie koncepcji badań, wybór metodyki badań, współudział w prowadzeniu badań i analizie wyników, opracowanie tekstu i przygotowanie do druku, przygotowanie odpowiedzi na recenzje.
  (udział 50%)

- prof. Luis R. Domingo
  współudział w sformułowaniu problemu naukowego, konsultacja naukowa.
  (udział 10%)

- M.Sc. Mar Ríos-Gutiérrez, PhD student
  współudział w sformułowaniu problemu naukowego, współudział w prowadzeniu badań i analizie wyników, konsultacja naukowa.
  (udział 30%)

- dr hab. inż. Radomir Jasiński, prof. PK
  współudział w sformułowaniu problemu naukowego, konsultacja naukowa.
  (udział 10%)

A Kącka-Zych
Agnieszka Kącka-Zych *Luis R. Domingo* *Mar Ríos-Gutiérrez* *Radomir Jasiński*

Kraków, 18.10.2017

Oświadczenie o udziale w publikacjach i pracach realizowanych wspólnie z mgr inż. Agnieszką Kącką-Zych

Oświadczamy, że udział w pracy opublikowanej wspólnie z mgr inż. Agnieszką Kącką-Zych jest zgodny z opisem przedstawionym poniżej:

Publikacja:

A. Kącka-Zych, L.R. Domingo, R. Jasiński
Does a fluorinated Lewis acid catalyst change the molecular mechanism of the decomposition process of nitroethyl carboxylates?
Research on Chemical Intermediates, DOI: 10.1007/s11164-017-3106-1 (2017).

Udział:

- mgr inż. Agnieszka Kącka-Zych
  współudział w sformułowaniu problemu naukowego, opracowanie koncepcji badań, wybór metodyki badań, prowadzenie badań i analiza wyników, opracowanie tekstu i przygotowanie do druku, przygotowanie odpowiedzi na recenzje.
  (udział 80%)
- prof. Luis R. Domingo
  współudział w sformułowaniu problemu naukowego, konsultacja naukowa.
  (udział 10%)
- dr hab. inż. Radomir Jasiński, prof. PK
  współudział w sformułowaniu problemu naukowego, konsultacja naukowa.
  (udział 10%)

A. Kącka-Zych
Agnieszka Kącka-Zych

Luis R. Domingo

Radomir Jasiński

Kraków, 18.10.2017

Oświadczenie o udziale w publikacjach i pracach realizowanych wspólnie z mgr inż. Agnieszką Kącką-Zych

Oświadczamy, że udział w pracy opublikowanej wspólnie z mgr inż. Agnieszką Kącką-Zych jest zgodny z opisem przedstawionym poniżej:

Publikacja:

A. Kącka, R. Jasiński

DFT study of the decomposition reactions of nitroethyl benzoates catalyzed by the 1,3-dimethylimidazolium cation.

Current Chemistry Letters, **6**, 15-22 (2017).

Udział:

- mgr inż. Agnieszka Kącka-Zych
  współudział w sformułowaniu problemu naukowego, opracowanie koncepcji badań, wybór metodyki badań, prowadzenie badań i analiza wyników, opracowanie tekstu i przygotowanie do druku, przygotowanie odpowiedzi na recenzje.
  (udział 90%)
- dr hab. inż. Radomir Jasiński, prof. PK:
  współudział w sformułowaniu problemu naukowego, konsultacja naukowa.
  (udział 10%)

Kącka-Zych
Agnieszka Kącka-Zych

Radomir Jasiński

XII. SPISY

Spis tabel

Spis schematów